



저작자표시-비영리-변경금지 2.0 대한민국

이용자는 아래의 조건을 따르는 경우에 한하여 자유롭게

- 이 저작물을 복제, 배포, 전송, 전시, 공연 및 방송할 수 있습니다.

다음과 같은 조건을 따라야 합니다:



저작자표시. 귀하는 원저작자를 표시하여야 합니다.



비영리. 귀하는 이 저작물을 영리 목적으로 이용할 수 없습니다.



변경금지. 귀하는 이 저작물을 개작, 변형 또는 가공할 수 없습니다.

- 귀하는, 이 저작물의 재이용이나 배포의 경우, 이 저작물에 적용된 이용허락조건을 명확하게 나타내어야 합니다.
- 저작권자로부터 별도의 허가를 받으면 이러한 조건들은 적용되지 않습니다.

저작권법에 따른 이용자의 권리는 위의 내용에 의하여 영향을 받지 않습니다.

이것은 [이용허락규약\(Legal Code\)](#)을 이해하기 쉽게 요약한 것입니다.

[Disclaimer](#)

**A THESIS FOR THE DEGREE OF DOCTOR OF  
PHILOSOPHY**

**New Molecular and Pharmacological  
Mechanisms of Camptothecin  
in Cell Death and Cell Division**

**RAJAPAKSHA GEDARA PRASAD THARANGA  
JAYASOORIYA**

Department of Marine Life Sciences  
SCHOOL OF BIOMEDICAL SCIENCE  
JEJU NATIONAL UNIVERSITY  
REPUBLIC OF KOREA

February 2016

# New Molecular and Pharmacological Mechanisms of Camptothecin in Cell Death and Cell Division

**Rajapaksha Gedara Prasad Tharanga Jayasooriya**  
(Supervised by Professor Kim Gi-Young)

A thesis submitted in partial fulfillment of the requirement for the degree of

## DOCTOR OF PHILOSOPHY

**November 2015**

The thesis has been examined and approved by

.....  
The thesis directors,  
**Yung Hyun Choi**, Professor of Biochemistry, Department of Biochemistry,  
College of Oriental Medicine, Dong-Eui University  
.....  
**Moon-Soo Heo**, Professor of Microbiology, School of Biomedical Science, Jeju  
National University  
.....  
**Seungheon Lee**, Professor of Pharmacology, School of Biomedical Sciences,  
Jeju National University  
.....  
**Sang-Rul Park**, Professor of Ecology, School of Biomedical Sciences, Jeju  
National University  
.....  
**Kim Gi-Young**, Professor of Immunology, School of Biomedical Sciences, Jeju  
National University

30.11.2015

**Date**

**Department of Marine Life Science  
SCHOOL OF BIOMEDICAL SCIENCE  
JEJU NATIONAL UNIVERSITY  
REPUBLIC OF KOREA**



## Acknowledgments

Though the following dissertation is an individual work, I could never have researched the heights or explored the depths without the help, support, guidance and efforts lot of people.

First I would like express my deepest appreciation to Professor Kim Gi-Young, who has the attitude and the substance of a genius: he continually and convincingly conveyed a spirit of adventure in regard to this research and an excitement in regard to teaching. Without his guidance and persistent help this dissertation would not have been possible.

I would like to thank to all of the staff members in department of Marine Life Sciences in Jeju National University, Prof. Choon-bok song, Prof. Moon-Soo Heo, Prof. Jehee Lee, Prof. Kyeong-Jun Lee, Prof. Kwang-Sik Choi, Prof. You-Jin Jeon, Prof, In-Kyu Yeo, Prof. Joon-Bom Lee, Prof. Young Dong Lee, Prof. Jung Suk-Geun, Prof. Seunghoon Lee, Prof. Sang-Rul Park who gave me the possibility to complete this thesis. In addition, specially thank to Professor Yung Hyun Choi, Professor Moon-Soo, Professor Seunghoon Lee and Professor Sang-Rul Park for being the members of supervising committee in my thesis.

Then I would like to thank to all of my lab members Chang-Hee Kang, Sang-Hyuck Kang, Hee-Ju Kim, those who always encourage and help me to be successful of my research. I also express my gratitude to the Prof. Mahanama De Zoysa and other Srilankan and all other friends who support me to success my work. Finally, I dedicated to my wonderful parents, R.G. Jayasooriya and R.A. Seela, sister, K.K. Keshila and my wife M.G. Dilshara for supporting my studies and urging me on. All of your continued support and urging after moving to JNU is deeply appreciated. Thanks for making me finish this thing. It's about time! Remember, it's ok to stress just not to stress out. To all of you, thanks for always being there for me.

## Table of Contents

Acknowledgments.....	i
Table of Contents.....	ii
한글요약.....	vi
Summary.....	x
List of figures.....	xiv
Chapter 1	
An introduction to anti-cancer mechanisms <i>invitro</i> .....	1
1.1    Camptothecin as anticancer drug.....	2
1.2    Cell cycle and check point control as anticancer target.....	4
1.3    Autophagy as a cell death and tumor suppressor mechanism .....	5
1.4    Regulation of the telomerase hTERT gene as a target for cellular oncogenic mechanisms .....	7
1.5    Anti-invasive mechanism of cancer cells .....	9
1.6    TRAIL-induced apoptosis: a relevant tool for anticancer therapy .....	10
1.7    Aims of this study.....	13
Chapter 2	
Camptothecin induces G <sub>2</sub> /M phase cell cycle arrest resulting from autophagy-mediated cytoprotection: Implication of reactive oxygen species.....	14
Abstract .....	15
2.1 Introduction .....	16
2.2 Materials and methods .....	18
2.3 Results.....	22
2.3.1 CPT irreversibly induces G <sub>2</sub> /M phase arrest in various cancer cell lines.....	22
2.3.2 ROS are potential initiators of CPT-induced G <sub>2</sub> /M phase arrest.....	24
2.3.3 CPT-induced Nrf2 in the early stage delays cell cycle at the S phase.....	25
2.3.4 ATM-mediated Chk2 is a key checkpoint in CPT-induced G <sub>2</sub> /M phase arrest.....	28
2.3.5 CPT-induced Cdc25C degradation requires the proteasome pathway in G <sub>2</sub> /M phase arrest .....	31

2.3.6 ERK and JNK regulate Cdc25C-mediated cyclin B and p21 expression in CPT-induced G <sub>2</sub> /M phase arrest.....	35
2.3.7 CPT decreases cell viability, but not induces cell death.....	37
2.3.8 CPT-induced autophagy blocks cell death and leads to G <sub>2</sub> /M phase arrest .....	39
2.4 Discussion.....	42
2.5 Conclusion.....	46

### Chapter 3

Camptothecin induces mitotic arrest in LNCaP cells, resulting from Mad2-mediated cyclin B1 and Cdk1 expression: Implication of tubulin polymerization .....	47
Abstract .....	48
3.1 Introduction .....	49
3.2 Materials and method.....	51
3.3 Results.....	57
3.3.1 Mad2 is a key M phase check point in CPT-induced cell cycle arrest.....	57
3.3.2 CPT-induced Mad2 regulates cyclin B1 and Cdk1 .....	60
3.3.3 CPT increases Mad2 expression by inducing JNK-mediated Sp1 activation .....	62
3.3.4 CPT-induced phosphorylation of p21 promotes Mad2 expression .....	64
3.3.5 CPT stimulates Mad2 expression resulting from tubulin polymerization.....	66
3.3.6 Accumulation of procaspase-9 and autophagy regulates CPT-induced M phase arrest .....	69
3.4 Discussion.....	72
3.5 Conclusion.....	76

### Chapter 4

Camptothecin enhances c-Myc-mediated endoplasmic reticulum stress, leading to autophagy .....	77
Abstract .....	78
4.1 Introduction .....	79
4.2 Materials and methods .....	82
4.3 Results.....	86
4.3.1 CPT induces c-Myc-mediated ROS generation, accompanied by CHOP expression .....	86

4.3.2 c-Myc regulates CPT-induced ER stress by inducing ROS generation .....	88
4.3.3 CPT promotes autophagy formation, resulting from ER stress.....	91
4.3.4 CPT promotes autophagy by increasing intracellular Ca <sup>2+</sup> release .....	93
4.3.5 CPT induces JNK-dependent autophagy by enhancing AP-1 activity .....	96
4.4 Discussion.....	99
4.5 Conclusion.....	101

## Chapter 5

CPT induces c-Myc- and Sp1-mediated hTERT expression in LNCaP cells: involvement of reactive oxygen species and PI3K/Akt .....	102
Abstract .....	103
5.1 Introduction .....	104
5.2 Materials and method.....	107
5.3 Results.....	112
5.3.1 CPT increases hTERT expression and activity, which is not associated with G <sub>2</sub> /M phase arrest .....	112
5.3.2 ROS regulate CPT-induced hTERT expression .....	115
5.3.3 CPT regulates c-Myc- and Sp1-dependent hTERT expression.....	117
5.3.4 CPT induces PI3K/Akt signaling involved in hTERT expression .....	120
5.3.5 CPT induces apoptosis in human leukemia cells.....	122
5.4 Discussion.....	124
5.5 Conclusion.....	127

## Chapter 6

Camptothecin suppresses matrix metalloproteinase-9 and vascular endothelial growth factor in DU145 cells through Nrf2-dependent HO-1 induction .....	128
Abstract .....	129
6.1 Introduction .....	130
6.2 Materials and methods .....	132
6.3 Results.....	137
6.3.1 CPT has no influence on cell viability.....	137
6.3.2 CPT suppresses MMP-9 expression and activity .....	139

6.3.3 CPT inhibits VEGF expression and production .....	141
6.3.4 CPTdownregulates NF-κB activity .....	143
6.3.5 HO-1 induces CPT-induced MMP9 and VEGF inhibition.....	145
6.3.6 Nrf2 regulates CPT-induced MMP-9 and VEGF expression by inducing HO-1 expression .....	147
6.4 Discussion.....	150
6.5 Conclusion.....	152
Chapter 7	
Camptothecin sensitizes human hepatoma Hep3B cells to TRAIL-mediated apoptosis via ROS-dependent death receptor 5 upregulation with the involvement of MAPKs.....	153
Abastract.....	154
7.1 Introduction .....	155
7.2 Materials and methods .....	157
7.3 Results.....	160
7.3.1 CPT sensitizes various types of cancer cells to TRAIL-mediated cell death .....	160
7.3.2 CPT/TRAIL activates apoptotic signals via the extrinsic and intrinsic pathways	161
7.3.3 DR5 upregulation is required for CPT/TRAIL-induced apoptosis .....	164
7.3.4 Reactive oxygen species (ROS) mediate CPT/TRAIL-induced upregulation of DR5 .....	166
7.3.5 ERK and p38 potentiate CPT/TRAIL-mediated DR5 expression.....	168
7.4 Discussion.....	170
7.5 Conclusion.....	172
Bibliography .....	173

## 한글요약

Camptothecin(CPT)은 항암, 항균 효능을 갖는 단일화합물로서, 중국과 티베트의 원주민들이 정통적으로 널리 약초로 쓰이던 희수나무에서 유래하였다. CPT는 1966년 처음으로 보고 되었으며, pentacyclic alkaloid적 성질을 가지고 있다. 현재까지 CPT와 이의 유도체들은 전임상 단계까지의 연구가 성공적으로 진행되어있다. 초기 세포를 대상으로 한 CPT의 type I topoisomerase (topo) 활성 변화 연구는 의약품 개발 부분에 새로운 흥미를 이끌어 내었다. 의약품로서 CPT는 췌장암과 난소암 치료에 사용되는 topotecan과 irinotecan의 반합성 물질로서 재개발되었다. 거기에 더하여 기초연구에 있어서 CPT는 방사선치료와 병행하여 치료하는 것으로 연구가 진행되었다.

이 학위논문에서는 CPT가 갖는 서로 다른 암세포주에서의 항암효과에 대한 *in vitro* 연구를 진행하였다. 이 학위논문에는 CPT의 활성에 대해서 6가지의 다른 챕터로 나눠 항암효과에 대한 신호전달 과정을 진행하였다. 첫 번째 단계는, CPT가 전립선암 세포주인 LNCaP세포에서 cyclin B1, Cdk1, 및 다양한 단백질의 조절을 통해 G<sub>2</sub>/M arrest 유도한다는 내용이다. 더 나아가 CPT에 의한 G<sub>2</sub>/M arrest 는 활성산소와 Cdc25c의 인산화 활성의 변화로 인한 것임을 확인하였다. 그리고, 우리는 Nrf2가 ROS를 조절함으로써 G<sub>2</sub>/M 세포의 비율을 조절하는 것을 찾아내었다. 이번 연구에서 Nrf2를 억제하자 산화스트레스에 의하여 DNA가 손상을 입고 G<sub>2</sub>/M arrest가 유도 되는 것을 확실하게 보여주었다. 추가적으로, 이러한 활성은 MAPK인 ERK와 JNK의 활성화와 공동으로 일어나는 것이 확인되었다. 마지막으로 우리는 CPT가 autophagy의 활성을 통하여 G<sub>2</sub>/M arrest로 인한 apoptosis를 억제함으로써 세포 보호효과를 갖는 것을 보여주었다.

두 번째 챕터에서는 LNCaP 세포를 이용하여 CPT의 세포주기 조절 과정을 분자세포학적으로 이해할 수 있도록 연구를 진행하였다. 우리는 CPT가 유도하는 G<sub>2</sub>/M phase arrest에서 Mad2의 역할을 조사하였다. CPT가 JNK의존적인 Sp1의 활성을 통하여 Mad2의 발현증가를 확인하였으며, mitotic arrest가 발생하는 과정에서 Mad2에 의해 cyclin B1과 Cdk1의 발현이 증가함으로 Mad2의 결핍이 prometaphase arrest를 유도하는 것을 확인하였다. 추가적으로 siRNA를 이용한 p21결핍은 CPT가 유도한 G<sub>2</sub>/M단계의 세포 비율은 감소하였지만, p21이 소모된 조건에서 sub-G<sub>1</sub>의 증가는 유도하지 못하였다. 하지만, caspase-9억제제와 autophagy억제제를 전처리 한 조건에서는 apoptosis가 일어나는 것을 방해하였다. 이러한 결과들은 CPT가 항암제 개발에 있어서 희귀하게도 세포주기와 microtubule 조절을 하는 좋은 잠재력을 가진 것이다.

세 번째로 우리 연구의 목적은 서로 다른 암세포주에서 CPT가 autophagy를 통해 세포의 생존에 관여하는지 죽음에 관여하는지를 연구하는 것이다. c-Myc의 결핍은 LNCaP 세포에서 PERK, eIF2 $\alpha$ 와 ATF의 인산화를 제거하였는데, 이것은 c-Myc이 유도한 UPR의 활성은 CPT에 의한 활성산소의존적임을 규명하였다. 우리는 CPT가 LNCaP 세포에서 c-Myc의 발현을 유도하는 것을 추가적으로 확인하였고, 이것은 autophagy와 JNK의 활성을 통해 생성된 활성산소에 매개되는 UPR 시그널을 유도한다. 추가적으로, 3MA를 통해 CPT가 유도한 autophagy를 억제하면, LNCaP의 세포죽음이 증가한다. 우리의 연구결과는 AMPK의 인산화가 다른 조절인자들을 억제하는 것을 보여 준다. 칼슘의 세포질 내 축적은 APMK의 인산화와 autophagy를 유도하는데 필수적이다. 그럼으로 이 결과들은 CPT가 유도한 autophagy가 LNCaP세포에서 보호 작용을 하는 것을 증명한다.

네 번째로 우리는 hTERT의 promoter가 포함된 luciferase 유전자 발현 실험 방법을 사용하여 CPT가 hTERT의 전사인자들을 조절하는 기전에 대하여 규명하였다. CPT는 농도 의존적으로 hTERT의 promoter 활성을 강하게 증가시켰다. 또한, CPT는 활성산소의 생산을 유도하여 항산화 활성을 저해 하여 LNCaP세포에서 활성산소의 발현을 증가시켰다. TRAP-ELISA kit을 사용하여 CPT가 유도한 telomerase의 활성이 항산화제의 전처리를 하자 감소하는 것을 확인하였다. CPT의 처리는 LNCaP세포에서 c-Myc과 Sp1가 DNA와의 결합 활성을 증가시킴으로써 hTERT의 발현을 크게 증가 시켰다. 이 결과들은 CPT가 hTERT의 인산화를 증가시키고 Akt의 인산화를 통해 핵 안으로의 이동을 방해한다는 것으로 추정된다.

다섯 번째로, CPT가 MMP-9과 VEGF의 발현과 활성에 대한 연구를 진행하였다. CPT는 PMA와 TNF- $\alpha$ 에 의해 유도된 MMP-9의 mRNA와 단백질발현을 강하게 억제하였다. 추가적으로, CPT는 유방암 세포주인 MDA-MB-231과 방광암 세포주인 T24세포에서 PMA 자극에 의해 발현된 MMP-9의 mRNA 발현을 강하게 감소 시켰는데, 이것은 CPT가 서로 다른 암 세포주에서도 MMP-9의 발현을 조절 할 수 있다는 것을 의미한다. 더 나아가, CPT의 전처리는 유방암세포주인 MDA-MB-231과 방광암 세포주인 T24세포에서 PMA와 TNF- $\alpha$ 에 의해 유도된 VEGF의 mRNA 과발현을 강하게 억제하였다. 우리는 CPT가 DU145 세포에서 NF- $\kappa$ B의 억제를 통하여 MMP-9과 VEGF의 발현 억제를 통하여 세포의 침윤작용을 방해하는 것을 추가적으로 확인하였다. 이것은 CPT가 암세포의 전이와 침윤을 억제할 수 있는 항암제로서 좋은 후보가 될 수 있음을 의미한다. 이번 연구에서 우리는 HO-1의 유도체인 CoPP가 PMA가 유도한 MMP-9과 VEGF의 발현을 억제 하는 것을 확인 하였는데, 이것은 CPT에 의해 발현된 HO-1가 MMP-9과 VEGF

의 발현을 억제하는 것을 의미한다. 우리는 CPT에 의해 활성화된 Nrf2 의존적으로 발현된 HO-1이 PMA가 유도한 MMP-9과 VEGF의 발현을 억제한다는 것을 증명하였다. 이것은 Nrf2를 억제한다면 HO-1에 의해 억제되는 MMP-9과 VEGF의 발현을 증가 시킬 수 있다는 것을 의미한다.

마지막으로, 우리는 CPT와 TRAIL의 병행 처리가 간암세포주인 Hep3B 세포에서 세포죽음을 유도하는 것을 연구하였다. CPT와 TRAIL은 TRAIL에 저항성을 획득한 세포에서도 세포의 증식을 억제하였다. Caspase-8의 억제제인 z-IETD-fmk는 CPT와 TRAIL에 의해 강하게 증가된 sub-G<sub>1</sub> phase, annexin-V 염색된 세포비율, DNA 절편화를 강하게 억제하였고, 이것은 CPT와 TRAIL의 병행 처리가 caspase 의존적인 apoptosis를 유도하는 것을 의미한다. 그리고 우리는 CPT와 TRAIL의 병행 처리에 의해 증가된 세포 죽음이 DR5의 발현 증가에 의한 것임을 찾아 내었고, DR5는 ROS와 MAPK인 ERK와 p38의 활성화에 의한 것임을 증명하였다.

## Summary

Camptothecin (CPT) is a potent antitumor antibiotic isolated from extracts of *Camptotheca acuminata*, a tree native to China and Tibet which has been extensively used in traditional Chinese medicine. The structure was determined to be that of a pentacyclic alkaloid and was first reported in 1966. The success of CPT in preclinical studies led to clinical investigations. Due to the negligible water solubility of CPT, these trials were initiated using the water-soluble sodium salt. The discovery that the primary cellular target of CPT is type I DNA topoisomerase (topo) created renewed interest in the drug. Advances in the medicinal chemistry of CPT resulted in the semi-synthetic, more water-soluble analogues topotecan and irinotecan which are used clinically for the treatment of colon and ovarian cancers, respectively. Additional CPT analogues are under investigation, and are also of interest in combination regimens as radiation sensitizers.

This dissertation is mainly focused on anti-cancer effect of CPT in different cancer cell lines *in vitro* studies. This dissertation is divided in to six chapters based on the different phases of signaling cascade in which the CPT activity is involved. In the first phase, we investigated that CPT-induced an irreversible G<sub>2</sub>/M phase cell cycle arrest in LNCaP cells which is associated with a marked decrease in the expression of G<sub>2</sub>/M regulating proteins such as cyclin B, cell division cycle 25C (Cdc25C) at Ser<sup>216</sup>. Further we reported that cell cycle arrest caused by the generation of reactive oxygen species and ataxia telangiectasia mutated check point kinase 2-mediated phosphorylation of Cdc25C. Our finding demonstrates that depletion of siNrf2 further induce the CPT induce S phase to G<sub>2</sub>/M phase cell population mean that Nrf2 regulate the G<sub>2</sub>/M arrest at S phase. Thus present study opens a clear view that inhibition of Nrf2 induces the oxidative stress lead to advanced DNA

damage and prominent G<sub>2</sub>/M arrest. These events are coordinated with the activation of mitogen-activated protein kinases specially, extracellular-signal regulated kinase and c-jun-N-terminal kinase. Finally, we showed that CPT protects cells from apoptosis through autophagy, direct to the G<sub>2</sub>/M phase cell cycle arrest.

Second chapter illustrated that the molecular mechanisms underline the cell cycle regulation activities of CPT in LNCaP cells. We analyze the role of Mad2 in CPT induce M phase arrest. We report that CPT induces Mad2 expression through JNK dependent Sp1 activity. Also our data show the Mad2 knockdown produced clear suppression of prometaphase arrest, the important of Mad2 in up-regulation of cyclin B1 and Cdk1 protein levels and the development of mitotic arrest. In addition to that transient transfection of LNCaP cells with sip21 decreased the CPT-induced G<sub>2</sub>/M phase cell population but depletion of p21 didn't induce the sub G<sub>1</sub> population. However, pretreatment of caspase 9 inhibitor and autophagy inhibitor increased the apoptosis cell percentage combine treatment with CPT. Importantly CPT has good potential as a novel class of cell cycle and microtubule pathway for cancer therapy.

Next phase our aim to investigate the effect of CPT on autophagy for the cell survival or death mechanism in different cancer cell lines. Depletion of c-Myc abrogated the level of phosphorylation eIF2 $\alpha$ , PERK and also ATF4 in LNCaP cells suggest that cMyc-induced UPR activation is ROS dependent in CPT-treated LNCaP cells. We found that CPT induced c-Myc expression in LNCaP cells, which was induced UPR signaling mediated by ROS leading to activation of JNK cascade as well as autophagy. Further CPT-induced autophagy inhibited by the 3MA, a autophagy inhibitor increased the cell death in LNCaP cells. Our data also showed phosphorylation of AMPK downregulated with the presence of those regulators. Ca<sup>2+</sup> accumulation in the cytosol was required for phosphorylation of AMPK and induction

of autophagy. Therefore, these data confirmed that CPT-induced autophagy as cytoprotection mechanism in LNCaP cells.

Fourth phase we revealed the underlying mechanisms involved in CPT-induced transcriptional control of hTERT using the luciferase gene expression system containing hTERT gene promoter region. CPT significantly increased the promoter activities of hTERT dose-dependent manner. CPT significantly induces the ROS formation in LNCaP cells whereas pretreatment of antioxidant abolished the CPT-induced ROS production. Using TRAP-ELISA kit, we found that CPT-induced telomerase activity was decreased in pretreatment of antioxidant. CPT treatment resulted in a significant increase of c-Myc and Sp1 DNA binding activity in LNCaP cells and also CPT increases hTERT gene expression through enhance of c-Myc- and Sp1-binding on the regulatory regions of hTERT. These results suggest that CPT increases phosphorylation of hTERT and thereby possibly inhibit its translocation to the nucleus through the phosphorylation of Akt.

We, in the fifth phase, evaluated the effects of CPT on MMP-9 and VEGF expression and activity. CPT significantly downregulates PMA- and TNF- $\alpha$ -induced MMP-9 mRNA and protein expression. Additionally, CPT substantially downregulated the expression of PMA-stimulated *MMP-9* mRNA in human breast carcinoma MDA-MB-231 cells and bladder carcinoma T24 cells, indicating that CPT suppresses MMP-9 expression in many different types of cancer cells. Moreover, pretreatment with CPT significantly inhibited PMA- and TNF- $\alpha$ -induced *VEGF* upregulation at the mRNA level in breast carcinoma MDA-MB-231 cells and bladder carcinoma T24 cells. We found that CPT reduces invasion of DU145 cells accompanying with downregulation of MMP-9 and VEGF via NF- $\kappa$ B inhibition, which indicates that CPT may be a good candidate to regulate cancer invasion. In this study, we found that CPT increases the expression of HO-1 and CoPP, an HO-1 inducer inhibits PMA-

induced MMP9 and VEGF expression, while the suppressive effect of those gene expression due to CPT is significantly reversed by potent HO-1 inhibitor ZnPP, which indicates that CPT-induced HO-1 expression is intimately associated with the downregulation of PMA-induced MMP-9 and VEGF. We demonstrated that CPT leads induction of Nrf2 by a mechanism dependent on HO-1 expression assuming that CPT reverses PMA-induced MMP-9 and VEGF expression via Nrf2 dependent HO-1 expression. It is confirmed by silencing of Nrf2 increases the *MMP9* and *VEGF* expression accompanying with induction of HO-1.

Final chapter, we examined whether combined treatment with a sublethal dose of CPT and TRAIL (CPT/TRAIL) induces cell death in human hepatocarcinoma Hep3B cells. CPT/TRAIL effectively inhibits cell proliferation in TRAIL-resistant cells in a cell-type-nonspecific manner, although the combined treatment induces different antiproliferation rates. pretreatment with a caspase-8 inhibitor z-IETD-fmk significantly blocked apoptotic characteristics, such as DNA fragmentation, the presence of an annexin-V<sup>+</sup> population, and the sub-G<sub>1</sub> phase induced by CPT/TRAIL, indicating that CPT sensitizes Hep3B cells to TRAIL-induced apoptosis in a caspase-dependent manner. We found that CPT/TRAIL increases cell death via upregulation of DR5 expression through the generation of reactive oxygen species (ROS) and the activation of extracellular signal-regulated protein kinase (ERK) and of p38 mitogen-activated protein kinases (MAPKs).

## List of figures

Fig. 1. Chemical structure of Camptothecin .....	2
Fig. 2. Camptothecin (CPT)-induced G <sub>2</sub> /M phase arrest. ....	23
Fig. 3. Camptothecin (CPT)-induced ROS mediates G <sub>2</sub> /M phase cell cycle arrest. ....	25
Fig. 4. Camptothecin (CPT)-induced the expression of Nrf2 level. ....	27
Fig. 5. Effect of camptothecin (CPT) on ATM and Chks activation in LNCaP cells. ....	30
Fig. 6. Camptothecin (CPT)-induced Cdc25C degradation is mediated by a ubiquitin- proteasome pathway.....	33
Fig. 7. Camptothecin (CPT)-induced G <sub>2</sub> /M phase arrest through JNK and ERK activity. ....	36
Fig. 8. Camptothecin (CPT)-decreased the cell proliferation in prostate cancer cells. ....	38
Fig. 9. Camptothecin (CPT)-induced autophagy as cytoprotection mechanism. ....	40
Fig. 10. Scheme of Camptothecin (CPT)-induced G <sub>2</sub> /M phase cell cycle arrest.....	41
Fig. 11. Camptothecin (CPT)-induced Mad2 expression in LNCaP cells. ....	59
Fig. 12. Effect of camptothecin (CPT) on cyclin B1 and Cdk1.....	61
Fig. 13. Effect of camptothecin (CPT) on JNK dependent-Sp1 activation. ....	63
Fig. 14. Effect of camptothecin (CPT) on phosphorylation of p21 in LNCaP cells.....	65
Fig. 15. Effect of camptothecin (CPT) on tubulin polymerization. ....	68
Fig. 16. Effect of camptothecin (CPT) on accumulation of caspase-9 and autophagy.....	70
Fig. 17. Schematic explanation of camptothecin (CPT)-induced mitotic arrest.....	71
Fig. 18. Effect of camptothecin (CPT) on c-Myc dependent ROS production.....	87
Fig. 19. Effect of camptothecin (CPT) on endoplasmic reticulum (ER) stress. ....	90
Fig. 20. Effect of camptothecin (CPT) on autophagy formation. ....	92
Fig. 21. Effect of camptothecin (CPT) for intracellular Ca <sup>2+</sup> release. ....	95
Fig. 22. Effect of camptothecin (CPT) on JNK-dependent AP1 activity. ....	97
Fig. 23. CPT-induced unfolded protein response (UPR) signal pathways. ....	98

Fig. 24. Camptothecin (CPT)-induced telomerase activity and hTERT expression.....	114
Fig. 25. Nrf2 is essential for camptothecin-induced hTERT expression. ....	116
Fig. 26. Upregulation of c-Myc and Sp1 by camptothecin (CPT).....	119
Fig. 27. Camptothecin (CPT)-induced phosphorylation of Akt in LNCaP cell.....	121
Fig. 28. Camptothecin (CPT) decreases cell viability and proliferation.....	123
Fig. 29. Schematic explanation of camptothecin (CPT) in controlling hTERT. ....	124
Fig. 30 Effect of CPT on the viability of prostate cancer DU145 and LNCaP cells. ....	138
Fig. 31. Effect of CPT on MMP-9 activity and expression. ....	140
Fig. 32. Effects of CPT on VEGF expression.....	142
Fig. 33. Effect of CPT on NF- $\kappa$ B DNA binding activity.....	144
Fig. 34. Effect of CPT on the expression of HO-1 in DU145 cells. ....	146
Fig. 35. Effect of CPT on the expression of Nrf-2 in DU145 cells. ....	148
Fig. 36. A schematic model of CPT-induced downregulation of MMP-9 and VEGF expression in PMA/TNF- $\alpha$ -stimulated DU145 cells. ....	149
Fig. 37. CPT sensitizes TRAIL-induced cell death regardless of cell-type specificity. ....	161
Fig. 38. Effect of CPT and/or TRAIL on the expression of caspases and various intracellular regulators of apoptosis. ....	163
Fig. 39. Effect of CPT and/or TRAIL on DR5 expression. ....	165
Fig. 40. CPT and/or TRAIL induce ROS-mediated DR5 expression.....	167
Fig. 41. Transcription of the DR5 promoter requires ERK and p38 activation.....	169

# Chapter 1

## **An introduction to anti-cancer mechanisms *in vitro***

## 1.1 Camptothecin as anticancer drug

Camptothecin (CPT), a naturally occurring cytotoxic alkaloid and novel effective anticancer drug, was originally isolated from *Camptotheca acuminata* [Zhou et al., 2010] as a strong inhibitor of the DNA-replicating enzyme topoisomerase I [Stewart and Schütz1987]. CPT has a planar pentacyclic ring structure, that includes a pyrrolo [3,4-β]-quinoline moiety, conjugated pyridone moiety and one chiral center at position 20 within the alpha-hydroxy lactone ring with (S) configuration (Fig. 1). Initially, it was discovered that CPT potentially targets topoisomerase I activity by inhibiting the rejoining step during the cleavage and relegation of DNA, resulting in topoisomerase I-induced DNA single-strand break repair pathways, ultimately leading to cell death [Pan et al., 2013; Strumberq et al., 2000]. Research also suggests that CPT possesses promising antitumor activities against a broad spectrum of cancer cell lines, such as those for melanoma, breast, colon, lung, and ovarian cancers, because many cancer cells are defective in the downregulation of topoisomerase I activity [Liu et al., 2010; Wang et al., 2008].

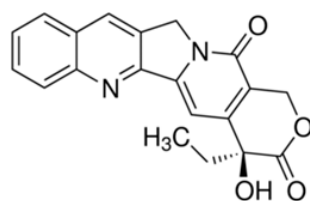


**Fig. 1.** Chemical structure of Camptothecin

Zeng *et al.*, showed CPT induced apoptosis in cancer cells through targeting to the 3'UTR regions of Bak1, p53 and Mcl1 by miR-125b mediated mitochondrial pathways [Zeng et al., 2012]. Park *et al.*, report indicated the CPT induces Cdk1 and cyclin E-associated kinase activities in response to DNA-damaging [Park et al., 1997]. Nevertheless, no reports

emphasize the CPT induce G<sub>2</sub>/M phase cell cycle arrest corresponding to the ROS/Nrf-2 signaling and MAPK cascades. Xiao reported that CPT induced s phase arrest which activate Chk1 and cause the rapid proteolysis of Cdc25A whereas elimination of Chk1 expression through knockdown abrogate s phase and protect Cdc25A degradation [Xiao et al., 2003]. It is also documented that CDK-602, a synthetic water-soluble CPT derivative and topoisomerase I inhibitor that has been shown to exert clinical anticancer effect on various types of tumor [Kim et al., 2015].

Kalpper reported that treatment of topoisomerase II inhibitor increases telomerase activity in HL60 cells and telosome reacts after DNA damage by upregulating telomerase activity and TRF2 expression [Kalpper et al., 2003]. It is further mention that activation of telomere increased the accumulation in the G<sub>2</sub>/M phase cells. Despite Murofushi discussed the highest levels of hTERT expression and telomerase activity, seen in the G<sub>1</sub>- and S-phases in HepG2 cells which were 2-3-fold higher than the lowest levels in G<sub>0</sub>-phase and during asynchronization [Murofushi et al., 2006]. According to Zeng data Camptothecin potentially inhibited DNA synthesis, followed the same kinetics as DNA-PK activation and RPA2 phosphorylation [Zeng et al., 2012].

CPT exposure in LoVo cells resulted c-Myc overexpression and elevation of p53 protein levels, suggesting a role of p53 in the c-Myc-imposed sensitization to the apoptotic effects of CPT [Babcock et al., 2013]. Camptothecin also inhibited DNA synthesis, followed the same kinetics as DNA-PK activation and RPA2 phosphorylation [Arango et al., 2003]. However, there is no report that CPT-induced c-Myc increase the UPR, resulted in induction of autophagy.

## 1.2 Cell cycle and check point control as anticancer target

The mitosis phase in normal human cells is initiated by the Cdk1/cyclin B1 complex through regulation of Cdc25C, however in cancer cells, these proteins are deregulated, so that normal growth control and checkpoints are evaded. Increased Cdc25C phosphatase activity could lead to the activation of Cdk1/cyclin B, which results from the dephosphorylation of Cdk1 by Cdc25C [Stanford et al., 2005]. In contrast, phosphorylation of Cdc25C on Ser-216 decreases its phosphatase activity through the cytoplasmic translocation of Cdc25C with 14-3-3 from the nucleus [Stanford et al., 2005]. This is known to be an important regulatory protein inducing delay or blocking mitotic entry.

The function of microtubules, other cytoskeletal components, has been frequently studied in the G<sub>2</sub>/M cell cycle phase. For example, treatment with microtubulin-interfering agents, such as nocodazole and taxol, induces tetraploidy arrest because sister chromatid segregation is interrupted [Kim et al., 2008]. This mitotic failure state could result in an excessive endoreduplication by prolonged exposure to microtubule-interfering agents. Additionally, Topo II inhibitors such as etoposide, amsacrine, and merbarone can induce endoreduplication by preventing the decatenation of replicated chromosomes, which subsequently fail to complete normal segregation at mitosis [Cortes et al., 2003].

All aerobic organisms experience physiological oxidant stress as a consequence of aerobic metabolism. In generating ATP, aerobic respiration releases the superoxide anion radical as a byproduct. Once produced, superoxide anion can form other ROS, such as hydrogen peroxide (H<sub>2</sub>O<sub>2</sub>) or the highly reactive hydroxyl radical (OH<sup>-</sup>) [Uttara et al., 2009]. In normal physiological states, these are produced through electron leakage and uncoupling when molecular oxygen is consumed in the electron transport chain, although ROS can also be generated in response to various exogenous stimuli, such as radiation, surgery, or

chemicals. It is well established that ROS are mediators of intracellular signaling cascades. Excessive ROS generation can induce redox-signaling pathways, including those involved in oxidative stress, loss of cell function, cell cycle arrest, and apoptosis [Liou et al., 2010]. An accumulation of ROS can severely damage cellular macromolecules, especially DNA, and induce G<sub>2</sub>/M phase arrest through ataxia telangiectasia mutant (ATM) activation [Newshean et al., 2012]. Cytotoxic ROS signaling also induces mitochondrial-dependent apoptosis; this occurs through the activation of apoptosis signal-regulating kinase 1 (ASK1)/mitogen-activated protein kinase (MAPK) pathways, and of the proapoptotic Bcl-2 proteins Bax or Bak, with the subsequent effects of mitochondrial membrane permeabilization and cell death [Kim et al., 2012].

Many cytotoxic agents and/or DNA-damaging agents arrest cell cycling at G<sub>1</sub>, S or G<sub>2</sub>/M phase. Progression from G<sub>2</sub> to M phase is regulated by a number of the cyclin family members, in particular cyclin B1 and Cdk1. cyclin B1, together with cyclin A, promotes the G<sub>2</sub>/M transition. Meanwhile, Cdk1 is essential for the G<sub>1</sub>/S and G<sub>2</sub>/M phase transitions of the eukaryotic cell cycle. The phosphorylation and dephosphorylation of Cdk1 have important regulatory roles in the control of the cell cycle [Asghar et al., 2015]. Moreover, the phosphatase activity of Cdc25C is also implicated in the regulation of the progression of G<sub>2</sub>/M phase [Tyagi et al., 2005]. Nevertheless, no reports emphasize the CPT induce G<sub>2</sub>/M phase cell cycle arrest corresponding to the ROS/Nrf-2 signaling and MAPK cascades.

### **1.3 Autophagy as a cell death and tumor suppressor mechanism**

Autophagy is a homeostatic and evolutionarily conserved process that degrades cellular organelles and proteins, and maintains cellular biosynthesis during nutrient deprivation or metabolic stress [Leone et al., 2013]. Autophagy begins with the formation of double-

membrane vesicles, known as autophagosomes, that engulf cytoplasmic constituents. The autophagosomes then fuse with lysosomes, where the sequestered contents undergo degradation and recycling [Leone, et al., 2013]. Autophagy is important in all cells for the removal of damaged or long-lived proteins and organelles. Autophagy defects are associated with susceptibility to metabolic stress, genomic damage, and tumorigenesis in mice, indicating a role for autophagy in tumor suppression [Yang, et al., 2011]. Monoallelic loss of the essential autophagy gene, *Beclin 1*, has been found in 40 to 75% of human breast, prostate, and ovarian cancers [Laddha et al., 2014], suggesting that autophagy may play a role in preventing these tumors. Although autophagy is a mechanism of tumor suppression, it also confers stress tolerance that enables tumor cells to survive under adverse conditions. Stress in tumor cells is compounded by the high metabolic demand associated with rapid cell proliferation [Phan et al., 2014]. Autophagy is induced in tumor cells within hypoxic tumor regions. Stress-induced autophagy in tumor cells can lead to treatment resistance and tumor dormancy, with eventual tumor regrowth and progression [Yang et al., 2011]. In preclinical models, inhibition of prosurvival autophagy by genetic or pharmacological means was shown to kill tumor cells and trigger apoptotic cell death [Sui et al., 2013]. However, autophagy has been referred to as a double-edged sword because in certain cellular contexts, excessive or sustained tumor cell autophagy may be prodeath, particularly in apoptosis-defective cells [Kimmelman et al., 2011]. Understanding the role of autophagy in cancer treatment is critical, because many anticancer therapies have been shown to activate autophagy, although the consequences of autophagy activation in this context are unclear. The complex role of autophagy in cancer continues to emerge, and it is important to elucidate the mechanisms by which autophagy influences tumorigenesis as well as treatment response [Sui et al., 2013]. Analysis of autophagic signaling may identify novel therapeutic targets for modulation and

therapeutic advantage.

Consistent with previous reports, c-Myc activated the expression of genes involved in multiple physiological functions, including control of cell cycle progression, apoptosis, nucleotide biosynthesis and basal metabolism. c-Myc promote DNA damage correlated with induction of reactive oxygen species without induction of apoptosis in human fibroblasts [Lu et al., 2007]. In peculiar, deregulation of c-Myc controlled the p53-mediated DNA damage response, enabling cells with damaged genomes to enter the cycle, resulting in poor colonogenic survival [Cui et al., 2015]. Despite, c-Myc induces DNA double strand breaks independent of ROS production of murine lymphocytes *in vivo* as well as normal foreskin fibroblasts *in vitro* [Vafa et al., 2002]. Rapamycin treatment decreased bortezomib-induced expression of c-Myc protein in Elt3 cells where exogenous expression of c-Myc overcome the suppressive effect on ATF4/CHOP expression by c-Myc bound to ATF4 promoter [Ray et al., 2006]. Camptothecin exposure in LoVo cells resulted c-Myc overexpression and elevation of p53 protein levels, suggesting a role of p53 in the c-Myc-imposed sensitization to the apoptotic effects of CPT [Babcock et al., 2013]. Camptothecin also inhibited DNA synthesis, followed the same kinetics as DNA-PK activation and RPA2 phosphorylation [Arango et al., 2003]. However, there is no report that CPT-induced c-Myc increase the UPR, resulted in induction of autophagy.

#### **1.4 Regulation of the telomerase hTERT gene as a target for cellular oncogenic mechanisms**

Telomeres are localized in the physical ends of eukaryotic chromosomes in a nucleic acid-protein complex. Disruption of the telomere structure, by telomeric DNA cleavage or loss of telomere binding protein functions, is associated with senescence and cell death, whereas telomere dysfunction also induces a state of constant cell proliferation [Oulton et al.,

2000]. Telomerase is a ribonucleoprotein complex with specialized reverse transcriptase activity which plays a crucial role in sustainment of telomere length and inducing cell immortalization, as found in many cancers [Hahn et al., 2001]. Therefore, telomerase activity regulation has been considered as a strategy for control of senescence and cell death. Telomerase is structurally composed of an RNA subunit known as human telomerase RNA (hTR) and a protein subunit known as human telomerase reverse transcriptase (hTERT), which plays an important enzymatic role in telomerase activity. Previous studies revealed that knockdown of hTERT completely suppress cancer cell growth by telomerase inactivation, while overexpression of hTERT results in a significant decrease of flavonoid-mediated sensitivity in cancer cells [Janknecht et al., 2004]. There have been numerous studies focused on hTERT regulation in inducing cancer cell apoptosis [Moon et al., 2010], because cancer cells specifically express hTERT at much higher concentrations than normal cells.

Most cancer cells exhibit pronounced activation of telomerase which prevents telomere shortening and subsequently leads to immortal cell characteristics and tumorigenesis [Hahn et al., 2001]. This finding suggests that telomerase activity inhibition can act as a cancer treatment strategy. Due to their biological activity, it has been demonstrated that natural compounds possess chemotherapeutic functions including cell cycle arrest and induction of apoptosis [Ramos et al., 2007]. In addition, published studies indicated that many flavonoids target downregulation of telomerase in the apoptosis mechanism of cancer cells, without concurrent cytotoxicity in normal cells [Kale et al., 2008]. These results demonstrate that natural agents are good candidates for diminishing the occurrence of tumorigenesis by telomerase activity suppression.

## 1.5 Anti-invasive mechanism of cancer cells

Tumor metastasis is a multistep process by which a subset of individual cancer cells disseminates from a primary tumor initiation to distant secondary organs or tissues [Spano *et al.*, 2012]. Previous studies have shown that most of cancer cells have high metastatic ability because of the constitutive expression of several angiogenic genes including vascular endothelial growth factor (VEGF) and matrix metalloproteinase-9 (MMP-9) [Sharma *et al.*, 2011]. In especial, VEGF is an interesting inducer of metastasis and invasion both *in vivo* and *in vitro*, because it is a highly specific mitogen from endothelial cells to induce vascularization and angiogenesis in a malignant tissue [Chen *et al.*, 2012]. MMP-9 is also a key effector molecule that promotes tumor cell invasion through type-IV collagen degradation-dependent extracellular matrix remodeling [Deryugina and Quigley, 2006]. MMP-9 expression has been observed in tumors of various organs, including the prostate, bladder, breast, brain, liver, and pancreatic carcinoma. Growing evidence shows that cancer cells secrete high levels of growth factors and matrix-degrading proteases and thus attributed to metastasis to distant organs including the liver, lungs, spine, bladder, bone, and lymph node [Dasgupta *et al.*, 2012]. Therefore, it is good strategy to reduce cancer angiogenesis by inhibiting expression of VEGF and to suppress invasion by downregulate MMP-9 for treatment of several cancers.

NF- $\kappa$ B is maintained in the cytoplasm as an inactive heterodimer form between p50 and p65 bound to its inhibitory factor  $\kappa$ B (I $\kappa$ B) [DiDonato *et al.*, 2012]. Upon stimulation, I $\kappa$ B results in a rapid phosphorylation by I $\kappa$ B kinase  $\alpha/\beta$ , and subsequent ubiquitination as well as degradation by proteasome complex [Magnani *et al.*, 2000]. In consequence, free NF- $\kappa$ B subunits move into the nucleus and bind their specific promoter regions to regulate gene expression such as MMP-9 and VEGF. Pahl *et al.*, (1999) showed obvious evidence that the

NF- $\kappa$ B pathway is closely involved in the expression of MMP-9 and VEGF in several types of cancer cells. A recent study also showed that the inhibition of NF- $\kappa$ B activity in human cancer cells decreases their tumorigenic and metastatic abilities by suppressing angiogenesis and invasion by suppression of MMP-9 and VEGF. These studies suggest that NF- $\kappa$ B-mediated VEGF and MMP-9 play important roles in the regulation of cell proliferation, invasion, and angiogenesis. Therefore, NF- $\kappa$ B is considered a good target to suppress NF- $\kappa$ B-dependent VEGF and MMP-9 expression to inhibit the invasion and metastasis.

### **1.6 TRAIL-induced apoptosis: a relevant tool for anticancer therapy**

Apoptosis plays critical roles in a wide variety of physiological processes during fetal development and in adult tissues, and the characteristics of the apoptotic cells represent chromatin condensation and nuclear fragmentation, plasma membrane blebbing, and cell shrinkage [Reed ET AL., 2000]. The molecular machinery responsible for apoptosis has been elucidated, revealing a family of intracellular proteases and effector caspases, which are directly or indirectly responsible for the morphological and biochemical changes that characterize the phenomenon of apoptosis. TRAIL initiates apoptosis, upon binding to its death ligand DR4 or/and DR5 with a homotrimeric structures by inducing the recruitment of specific cytoplasmic proteins such as FADD to the intracellular DD of the receptors, which form DISC [Srivastava et al., 2001]. In addition to their carboxy-terminal DD, FADD contains an amino terminal death effect or domain (DED), which recruits DED-containing apoptosis initiating proteases, caspase-8, and caspase-10 to the receptors for the complete formation of DISC [Hellwig et al., 2012]. Both FADD and procaspase-8 contain these DED, and it is likely that aggregation of procaspase-8 molecules results in enzymatic conversion to active caspase-8 and further activation of the caspase cascade of enzymes. The recruitment of

caspase-8 can be inhibited by another DED containing protein called FADD-like IL-1 $\beta$ -converting enzyme (FLICE) inhibitory protein (c-FLIP) [Srivastava et al., 2001]. The cellular homologue c-FLIP can also inhibit apoptosis by preventing the recruitment and activation of proximal caspases. In the DISC, caspase-8 and -10 are cleaved through autoproteolysis and thus become enzymatically active and therefore initiate apoptotic cell death through cleavage of downstream effector caspase-3 and -7 [Festjens et al., 2006]. In contrary, DcRs could prevent apoptosis signaling via complex formation with TRAIL-R1 and/or TRAIL-R2, resulting in an ineffective DISC [Munoz-Pinedo et al., 2006]. Nevertheless, activation of caspase-8 is sufficient for subsequent activation of the effector caspase-3 to execute cellular apoptosis in some cell type (known as the intrinsic pathway or the type I apoptotic pathway). Additionally, cells move to the intrinsic pathway (mitochondria-dependent pathway) by causing changes in the inner mitochondrial membrane that results in a loss of the mitochondrial transmembrane potential and release of cytochrome *c*, Smac/DIABLO, and the serine protease HtrA2/Omi pro-apoptotic proteins from the intermembrane space into the cytosol [Shiozaki et al., 2002]. It is initiated by cleavage of Bcl-2 inhibitory BH3-domain-containing protein Bid by caspase-8, is required for cellular apoptosis [Bansal H., et al., 2012]. The truncated Bid (tBid) in turn interacts with Bax and Bak, and induces the oligomerization of Bax and Bak in mitochondrial membrane, which leads to the change of the mitochondrial membrane potential and release above molecules to the cytoplasm [Munoz-Pinedo et al., 2006]. Cytochrome *c* facilitates the interaction of apoptotic protease activating factor 1 (Apaf-1) with caspase-9 as an initiator caspase resulting in the formation of apoptosome in which caspase-9 is activated [Shiozaki et al., 2002]. In a parallel, Smac interacts with X-linked inhibitor of apoptosis protein (XIAP), releases caspase-3 cleavage and thereby allows encountering the TRAIL-induced extrinsic pathway. Activation of caspase-9, -

3, and -7 can be blocked by inhibitor of apoptosis proteins (IAP), an evolutionarily conserved family of caspase inhibitory protein such as XIAP, c-IAP1, c-IAP2, and survivin. Proapoptotic members of the Bcl-2 family such as Bax, or its homologue Bak, which contain three Bcl-2 homology domains (BH3), are counteracted by the anti-apoptotic family members Bcl-2 or Bcl-xL, which contain an additional BH4 domain [Munoz-Pinedo, et al., 2006]. In previous, ectopic Bcl-xL overexpression conferred to acquire resistance against TRAIL in pancreatic cancer cell lines [Shiozaki, et al., 2002]. Hepatocytes also provide an example of cells that become resistant to Fas-induced apoptosis *in vivo* when Bid, or both Bax and Bak, are deleted [Chen et al., 2007]. Thus, the intrinsic pathway was required for TRAIL-mediated apoptosis through activation of proapoptotic Bcl-2 family such as Bid, Bax, and Bak which being essential for induction of the mitochondrial events.

Natural products have played a highly significant role as sources new drugs in recent decades. Therefore, natural products with strong synergistic activity with TRAIL, but minimal toxicity in normal cells are thought to be sources for new chemotherapeutic tools for TRAIL-based cancer therapy [Roberts et al., 2011]. Initially, it was discovered that CPT potentially targets topoisomerase I activity by inhibiting the rejoining step during the cleavage and relegation of DNA, resulting in topoisomerase I-induced DNA single-strand break repair pathways, ultimately leading to cell death [Strumberq et al., 2000; Pan et al., 2013]. To date, most studies have been focused on topoisomerase I activity in CPT-induced cancer cell death. However, the anticancer mechanisms of CPT in TRAIL-mediated cell death remain unclear.

## 1.7 Aims of this study

The principal goal of this thesis was to establish molecular evidence for the anti cancer mechanism and signaling pathway in human cancer cells upon the CPT treatment. The consecutive signaling molecules involved in anticancer mechanism are investigated from the transcription and translation levels. The main objectives of the study were

- To characterized the molecules involved in cell cycle pathways to response CPT in prostate cancer cells
- To identify the autophagy as cytoproctive mechanism under genomic stress condition
- To investigate the role of telomerase activity in CPT-induced cancer cells
- To identify the CPT as anti-invasive agent in prostate cancer cells
- To identify the CPT as sensitizer for various cancer cells to TRAIL-mediated cell death
- To develop the CPT as anticancer drug for the cancer patient

## **Chapter 2**

**Camptothecin induces G<sub>2</sub>/M phase cell cycle arrest resulting from autophagy-mediated cytoprotection: Implication of reactive oxygen species**

## Abstract

Camptothecin (CPT) is a quinolone alkaloid which inhibits DNA topoisomerase I that induces cytotoxicity in a variety of cancer cell lines. We previously showed that CPT effectively inhibited invasion of prostate cancer cells and also combined treatment with subtoxic doses of CPT and TNF-related apoptosis-inducing ligand (TRAIL) potentially enhanced apoptosis in a caspase-dependent manner in hepatoma cancer cells. Here, we found that treatment with CPT caused an irreversible cell cycle arrest in the G<sub>2</sub>/M phase. CPT-induced cell cycle arrest was associated with a decrease in protein levels of cell division cycle 25C (Cdc25C) and increased the level of cyclin B and p21. The CPT-induced decrease in Cdc25C was blocked in the presence of proteasome inhibitor MG132, thus reversed the cell cycle arrest. In addition to that treatment of CPT-increased phosphorylation of Cdc25C was the result of activation of checkpoint kinase 2 (Chk2), which was associated with phosphorylation of ataxia telangiectasia-mutated. Interestingly CPT induce G<sub>2</sub>/M phase of the cell cycle arrest is reactive oxygen species (ROS) dependent where ROS inhibitors NAC and GSH reversed the CPT-induced cell cycle arrest. These results further confirm by using transient knockdown of nuclear factor-erythroid 2-related factor 2 (Nrf2) since it regulates the production of ROS. Our data reveal that treatment of siNrf2 increased the ROS level as well as further increased the CPT induce G<sub>2</sub>/M phase cell cycle arrest. Our data also indicate CPT-enhanced cell cycle arrest through the extracellular signal-regulated kinase (ERK) and the c-Jun N-terminal kinase (JNK) pathway. Inhibitors of ERK and JNK more decreased the Cdc25C expression and protein expression of p21 and cyclin B. These findings indicate that Chk2-mediated phosphorylation of Cdc25C plays a major role in G<sub>2</sub>/M arrest by CPT.

## 2.1 Introduction

Cell cycle checkpoints are important machineries in eukaryotic cells which accurately serve intact cell division by monitoring defects in the cell cycle [Bertoli et al., 2014]. Thus, the checkpoints permit uncontrolled cells to repair DNA damage or to consequently die by blocking cell division after DNA damage [Hartwell et al., 1989]. In particular, ataxia telangiectasia mutated (ATM), and ATM and Rad3 related (ATR) protein kinases are well known to exert cell cycle delay in the response to genotoxic stress by inducing phosphorylation of a various kinase checkpoint kinase 1 (Chk1) and Chk2 [Mazouzi et al., 2014]. For instance, Chk1 is phosphorylated at Ser<sup>317</sup> and Ser<sup>345</sup> by ATM, followed by autophosphorylation of Ser<sup>296</sup> in response to various types of DNA damage which can be induced by ionizing radiation, and prevents damaged cells from entering into mitosis by inactivating Cdc25 phosphatases or directly abrogate mitotic spindle formation by activating aurora B and BubR1 [Lossaint et al., 2011]. Chk2 is also activated by ATM in response to single or double-strand DNA breaks through dimerization and autophosphorylation, and consequently targets Cdc25C phosphatase by stabilizing p53 responsible for regulating activation of cyclin-dependent kinase 2 (Cdk2) and cyclin B1 to facilitate the G<sub>2</sub>/M phase cell cycle arrest under DNA damage [Stolz et al., 2011; Ito et al., 2007]. Therefore, ATM-mediated Chk1/2 is a main axis by generating reactive oxygen species (ROS) whether the damaged cells will be repaired or undergo G<sub>2</sub>/M phase arrest/apoptosis, suggesting that the pathway is a good therapeutic strategy as a drug target for cancer [Garber et al., 2005].

Nrf2 is a transcription factor that plays a pivotal role in activating an antioxidant response that decreases generation of reactive oxygen species (ROS) and induction of Nrf2-related genes are imperative for defected cells to counteract ROS-mediated oxidative damage [de Vries et al., 2008]. Additionally, disruption of Nrf2 causes the oxidant-mediated acute

lung injury and inflammation in mice and Nrf2 knockout mice are greatly predisposed to chemical-induced DNA damage [Reddy et al., 2009]. Previous study also reported that inhibition of Nrf2 by excessive ROS generation caused DNA damage, specifically DNA single or double strand breaks, leading to activating ATM [Chen et al., 2015]. Upon the ROS production, the activation of cell-cycle checkpoints in response to oxidative damage-mediated ATM phosphorylation is also essential for maintenance of genomic integrity and tumor suppression [Kim et al., 2012; Swift et al., 2014]. In particular, several kinds of cyclin and cyclin-dependent kinase (Cdk) complexes are well known to be implicated in DNA single or double strand breaks-induced the checkpoint responsible for cell cycle progression. Cyclin D and Cdk4/6 complex is active in early G<sub>1</sub> phase, whereas cyclin E-Cdk2 is required for entry into S phase [Asghar et al., 2015]. At oxidative stress involving DNA damage, p21-mediated cell cycle arrest would be also activated to interval for DNA repair and indeed p21 is an inhibitor of Cdk that regulates many cellular processes in a p53-dependent and independent manner [Piccolo et al., 2012]. Recent publication also showed that p21 protected the cells against oxidative stress through upregulation of Nrf2 by competing interacts with the motifs in Nrf2 and thus competes Keap1-Nrf2 binding, compromising ubiquitination of Nrf2 (Asghar et al., 2015). Therefore, ROS-mediated Nrf2 could be an important response to regulate cell cycle and apoptosis as a cell cycle checkpoint.

Camptothecin (CPT) specifically inhibits eukaryotic DNA topoisomerase I (topo I) by trapping a covalent enzyme-DNA intermediate [Chen et al., 2009]. Zeng *et al.*, showed that CPT induced apoptosis in cancer cells through targeting to the 3' untranslated (UTR) region of Bak1, p53, and Mcl1 by miR-125b mediated mitochondrial pathways [Pommier et al., 2006]. Park *et al.*, reported that CPT induced Cdc2 and cyclin E-associated kinase activities in response to DNA damage [Pommier et al., 2006]. Huang *et al.*, suggested that CPT-

induced DNA single-strand breaks are differentially involved in homologous recombination repair by Chk1 and Chk2 [Huang et al., 2008; Zuco et al., 2010]. Nevertheless, no detail reports emphasize whether CPT induces G<sub>2</sub>/M phase cell cycle arrest corresponding to the ROS/Nrf2-mediated cell cycle arrest and autophagy-mediated cytoprotection. In this study, we investigated that CPT induced an irreversible G<sub>2</sub>/M phase cell cycle arrest in LNCaP cells through the ROS-dependent Chk2/Cdc25C and the ATM-dependent Chk2/Cdc25C pathway by activating extracellular-signal regulated kinase (ERK) and c-jun-N-terminal kinase (JNK). Furthermore, CPT-induced autophagy protects cells from apoptosis and directs to the G<sub>2</sub>/M phase cell cycle arrest.

## 2.2 Materials and methods

### *Reagents and antibodies*

CPT, 3-(4,5-dimethylthiazol-2-yl)-2,5-diphenyltetrazolium bromide (MTT), propidium iodide, glutathione (GSH), *N*-acetyl-L-cysteine (NAC), MG132, 3-methyladenine (3MA), and bafilomycin A1 (BAF) were purchased from sigma (St. Louis, MO) and an enhanced chemiluminescence (ECL) kit was purchased from Amersham (Arlington Heights, IL). RPMI 1640 medium, fetal bovine serum (FBS), and antibiotics mixture was purchased from WelGENE (Daegu, Republic of Korea). PD98059, SP600125, and SB239063 were purchased from Calbiochem (San Diego, CA). Antibodies against Cdk2, cyclin B1, p21,  $\beta$ -actin, Nrf2, nucleolin, phospho (p)-ATM (Ser<sup>1981</sup>), ATM, Chk1, Chk2, p-Chk2 (Thr<sup>68</sup>), Cdc25c, p-Cdc25C (Ser<sup>216</sup>), ubiquitin, procaspase-3, procaspase-9, Cdk2, Bad, Beclin-1, LC3-II, and Atg-7 were purchased from Santa Cruz Biotechnology (Santa Cruz, CA). Antibodies against p-histone (H)-3, p-ERK, ERK, p-p38, p38, p-JNK, and JNK were purchased from Cell Signal (Beverly, MA). Peroxidase-labeled donkey anti-rabbit and sheep anti-mouse immunoglobulin

were purchased from Koma Biotechnology (Seoul, South Korea).

#### *Cell culture and viability assay*

Human prostate cancer cell lines LNCaP and DU145, human hepatoma carcinoma cell line Hep3B, and human leukemia cancer cell line U937 were obtained from the American Type Culture Collection. Cells were cultured at 37°C in a 5% CO<sub>2</sub>-humidified incubator and maintained in RPMI 1640 medium containing 10% heat-inactivated FBS and 1% antibiotics mixture. The cells were seeded ( $4 \times 10^4$  cells/ml) and then incubated with CPT for 24 h. MTT assays were performed to determine relative cell viability.

#### *DNA fragmentation assay*

After treatment with CPT for 24 h, LNCaP cells were lysed in DNA fragmentation lysis buffer containing 10 mM Tris (pH 7.4), 150 mM NaCl, 5 mM EDTA, and 0.5% Triton X-100 for 1 h on ice. Lysates samples were vortexed and separated centrifugation at 13,000 g for 15 min. Fragmented DNA in the supernatant was extracted with equal volume of phenol:chloroform:isoamyl alcohol (25:24:1) mixture and analyzed electrophoretically on 1.5 % agarose gels.

#### *Flow cytometric analysis*

Cells were fixed in 1 U/ml of RNase A (DNase free) and 10 µg/ml of propidium iodide overnight in the dark at room temperature. To assess whether apoptosis had occurred, the cells were incubated with annexin-V (R&D Systems). A FACSCalibur flow cytometer (Becton Dickinson, San Jose, CA) was used to determine the number of apoptotic cells, i.e., cells with sub-G<sub>1</sub> DNA that were annexin-V<sup>+</sup>.

### *Measurement of ROS*

Cells were plated at a density of  $5 \times 10^4$  cells/ml, allowed to attach for 24 h, and exposed to 5 mM NAC alone, 5 mM GSH alone, 4  $\mu$ M CPT alone, or NAC or GSH plus CPT for 1 h. The cells were stained with 10  $\mu$ M H<sub>2</sub>DCFDA for 10 min at 37°C and flow cytometry was used to determine the fluorescence intensity.

### *Western blot analysis*

Whole-cell lysates were prepared by PRO-PREP protein extraction solution (iNtRON Biotechnology, Sungnam, Republic of Korea). Cytoplasmic and nuclear protein extracts were prepared using NE-PER nuclear and cytosolic extraction reagents (Pierce, Rockford, IL). The cell lysates were harvested from the supernatant after centrifugation at 13,000 g for 20 min. Total cell proteins were separated on polyacrylamide gels and standard procedures were used to transfer them to the nitrocellulose membranes. The membranes were developed using an ECL reagent.

### *Electrophoretic mobility shift assay (EMSA)*

Transcription factor-DNA binding activity assays were carried out with nuclear protein extract. Synthetic complementary anti-oxidant response element (5'-TMANNRTGAYNNGCRWWW-3') binding oligonucleotides was 3'-biotinylated utilizing the biotin 3'-end DNA labeling kit (Pierce) according to the manufacturer's instructions, and annealed for 30 min at 37°C. Samples were loaded onto native 4% polyacrylamide gels pre-electrophoresed for 60 min in 0.5X Tris borate/EDTA (TBE) buffer on ice, in the presence of transferred onto a positively charged nylon membrane (Hybond<sup>TM</sup>-N+) in 0.5X TBE buffer at 100 V for 1 h on ice. The transferred DNA-protein complex was cross-linked to the

membrane at 120 mJ/cm<sup>2</sup>. Horseradish peroxidase-conjugated streptavidin was utilized according to the manufacturer's instructions to monitor the transferred DNA-protein complex.

#### *Small interfering RNA (siRNA)*

Cells were seeded on a 24-well plate at a density of  $1 \times 10^5$  cells/ml and transfected *Nrf2*-, *Chk1*-, and *Chk2*-specific silencing RNA (siRNA, Santa Cruz Biotechnology) for 24 h. For each transfection, 450  $\mu$ l growth medium was added to 20 nM siRNA duplex with the transfection reagent G-Fectin (Genolution Pharmaceuticals Inc., Seoul, Republic of Korea) and the entire mixture was added gently to the cells.

#### *Statistical analysis*

The images were visualized with Chemi-Smart 2000 (VilberLourmat, Marine, Cedex, France). Images were captured using Chemi-Capt (VilberLourmat) and transported into Photoshop. All bands were shown a representative obtained in three independent experiments and quantified by Scion Imaging software (<http://www.scioncorp.com>). Statistical analyses were conducted using SigmaPlot software (version 12.0). Values were presented as mean  $\pm$  standard error (S.E.). Significant differences between the groups were determined using the unpaired one-way and two-way ANOVA test. Statistical significance was regarded at <sup>a</sup> and <sup>b</sup>,  $p < 0.05$ .

## 2.3 Results

### 2.3.1 CPT irreversibly induces G<sub>2</sub>/M phase arrest in various cancer cell lines

CPT was known to inhibit tumor cell growth through the induction of apoptosis via p53 dependent and mitochondrial dependent pathways [Pommier et al., 2006]; however, mechanism by which CPT contributes to cell cycle progression is not known in detail. Therefore, we first investigated the effect of CPT on cell cycle distribution using propidium iodide. Treatment with CPT resulted in a significant increase in G<sub>2</sub>/M phase cells at 24 h which was accompanied by decreased in G<sub>0</sub>/G<sub>1</sub> phase cells in all cell lines studied such as LNCaP, DU145, HCT116, and Hep3B cells (Fig. 1A). Treatment of 4 μM CPT strongly induced over 55% G<sub>2</sub>/M phase arrest in all the cell lines. Additionally, the sub-G<sub>1</sub> population which indicates apoptotic cell death slightly increased in DU145 and HCT116 cell lines. In order to more clearly evaluate the G<sub>2</sub>/M phase arrest, the expressional changes of proteins that control the cell cycle transition were observed in LNCaP and Hep3B cells. As shown in Fig. 1B, gradual decrease of Cdk2 expression suggested that treatment with CPT moves the cells from G<sub>1</sub>/S phase to G<sub>2</sub>/M phase because Cdk2 is most active in the S phase and decreases in G<sub>2</sub>/M phase. Our data also confirmed that CPT induced G<sub>2</sub>/M phase arrest by inducing p21 and cyclin B1 expression, which functions as tumor suppressor and initiates cell cycle arrest by inhibiting Cdk activity in G<sub>2</sub>/M phase in response to DNA damage [Abbas et al., 2009]. Additionally, treatment with CPT resulted in a significant increase of p-H3 expression which is considered to be a crucial event in onset of mitosis [Hartwell et al., 1989]. Finally, in order to elucidate whether CPT-induced G<sub>2</sub>/M phase arrest was irreversible, the cells were treated with CPT for 24 h and then either checked out cell cycle distribution after exposure to CPT-free fresh media for the indicated times. Treatment with CPT increased the G<sub>2</sub>/M phase after 24 h compare to that of the untreated control and CPT-induced G<sub>2</sub>/M

phase arrest was sustained by 48 h (Fig. 1C), indicating that CPT irreversibly induces G<sub>2</sub>/M phase arrest. Taken together, these results indicate that CPT-induced G<sub>2</sub>/M arrest was irreversible.

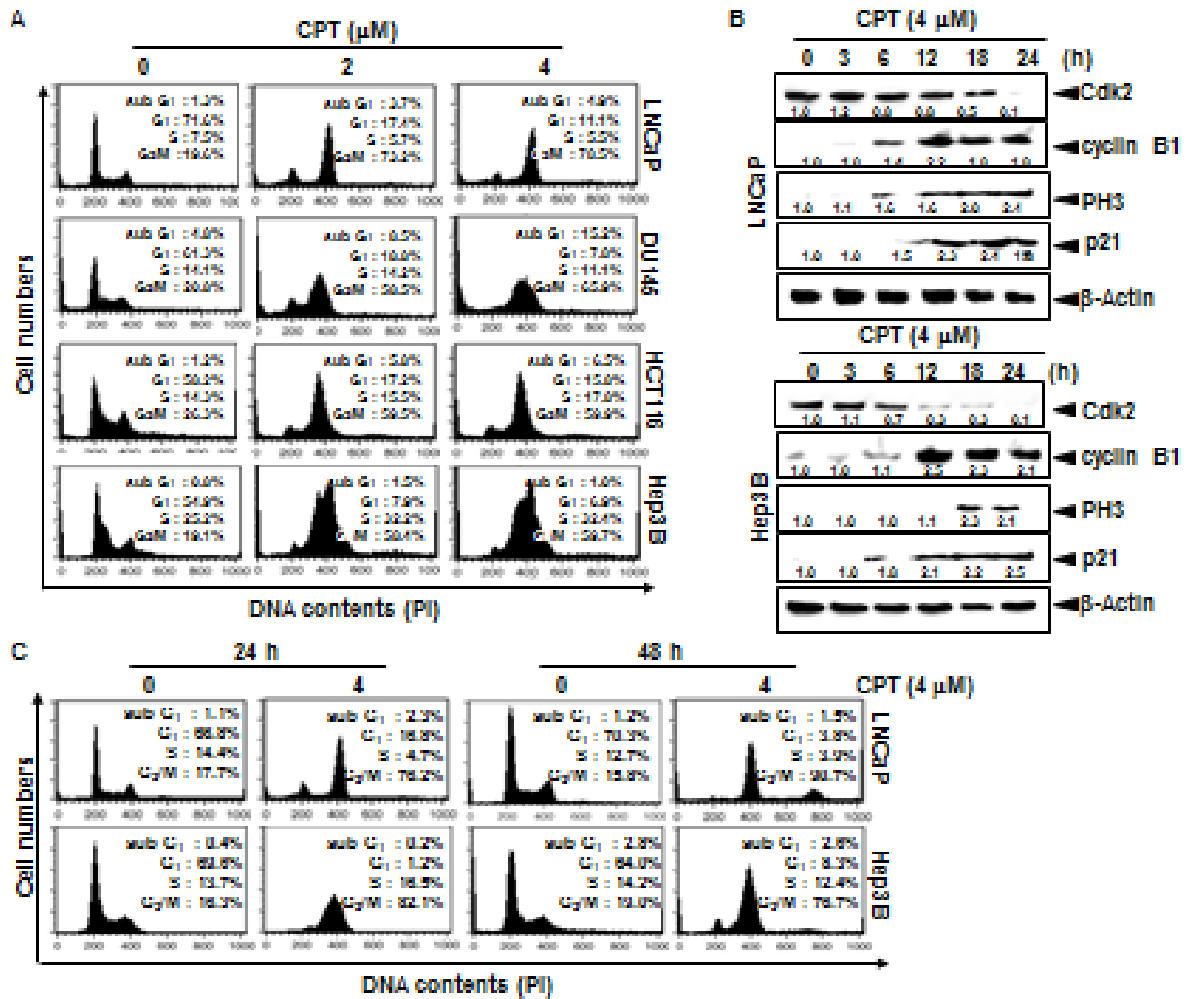


**Fig. 2.** Camptothecin (CPT)-induced G<sub>2</sub>/M phase arrest. Cells were seeded at  $1 \times 10^5$  cells/ml and were treated with 4 μM CPT for the indicated times. (A) Cells were harvested, stained with propidium iodide and analyzed for the cell cycle. (B) LNCaP cells and Hep3B cells were treated with 4 μM CPT for the indicated time points. Cell extracts were prepared for western blot analysis for anti-cyclin B1, anti-p-H3, anti-p21, anti-Cdk2, and anti-Cdc2. Cells were treated with 4 μM CPT for 24 h and subsequently the cells were processed for analysis for

cell cycle distribution or rest of the cells cultured in drug free culture media for another 24 h and cell cycle distribution was checked. Data from three independent experiments are presented.

### **2.3.2 ROS are potential initiators of CPT-induced G<sub>2</sub>/M phase arrest**

Recent publication shows that some chemical oxidant-mediated intracellular accumulation of ROS leads to DNA damage and checkpoint activation consequently induces cell cycle arrest [Guo et al., 2014]. Therefore, we monitored ROS generation in CPT-treated LNCaP cells using H<sub>2</sub>DCFDA which oxidized with the presence of ROS. CPT significantly induced the ROS formation in a time-dependent manner (Fig. 2A). Next, we measured the level of ROS generation and the cell cycle progression with the presence of ROS inhibitor GSH. Treatment with CPT significantly increased the G<sub>2</sub>/M phase by approximately 80% of cell population with high ROS generation, whereas pretreatment with GSH reversed CPT-induced G<sub>2</sub>/M phase arrest to approximately 55% while increasing the S phase cell portion with low ROS level, which indicated that GSH could not completely inhibit CPT-induced G<sub>2</sub>/M phase arrest, but delayed cell cycle or stop in the S phase (Fig. 2B). These data indicate that ROS are important regulators in CPT-induced G<sub>2</sub>/M phase arrest.

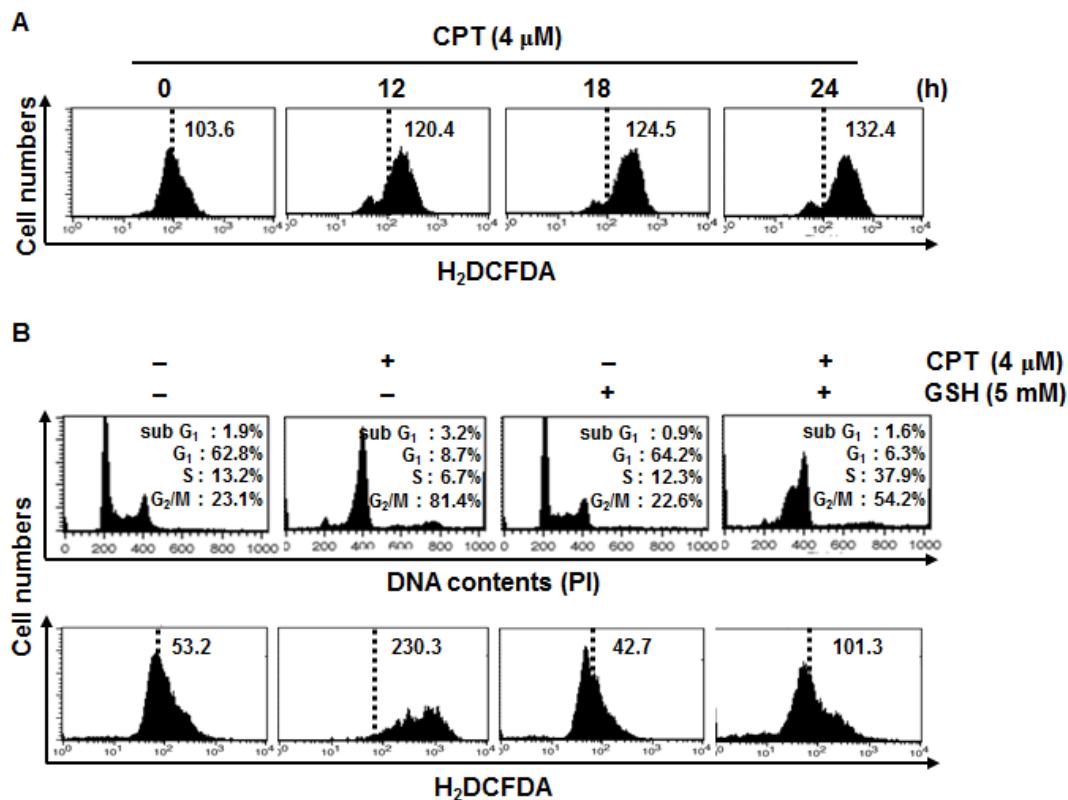


**Fig. 3.** Camptothecin (CPT)-induced reactive oxygen species (ROS) mediates G<sub>2</sub>/M phase cell cycle arrest. (A) Effect of CPT on ROS production. LNCaP cells were treated with 4  $\mu$ M CPT for the indicated time points. H<sub>2</sub>DCFDA-based fluorescence detection was done through flow cytometry. (B) LNCaP cells were treated with 5  $\mu$ M glutathione for 30 min and then incubated with 4  $\mu$ M CPT for 24 h. Cell cycle distribution was analyzed through flow cytometry after cells stained with propidium iodide. (C) Similar treatment was done and cells were stained with H<sub>2</sub>DCFDA-based fluorescence and detected through flow cytometry.

### 2.3.3 CPT-induced Nrf2 in the early stage delays cell cycle at the S phase

Nrf2 plays a pivotal role in activating an anti-oxidant response that counteracts the ROS to protect against cellular damage [de Vries et al., 2008]. Therefore, we investigated whether Nrf2 regulates CPT-induced G<sub>2</sub>/M phase arrest by inhibiting ROS generation. Western blot analysis revealed that treatment with CPT gradually increased Nrf2 expression in the

cytosolic compartment from at 18 h; however, nuclear translocation of Nrf2 significantly increased in the early stages before at 12 h and was suppressed from at 18 h (Fig. 3A). EMSA data also confirmed that CPT gradually induced the specific DNA-binding activity of Nrf2 at the early stage (at 6 h and 12 h) after CPT treatment and then the Nrf2 activity was completely decreased at 18 h (Fig. 3B), which indicated that Nrf2 at the early stages naturally occurred to alleviate ROS-mediated damage; however, Nrf2 at the late stages was completely downregulated by CPT-induced ROS. Similar to CPT-induced Nrf2 downregulation, GSH significantly inhibited the Nrf2-binding activity at the early stage. Next, we investigated whether CPT-induced Nrf2 at the early stage (at 12 h) influences ROS-mediated G<sub>2</sub>/M phase arrest. *Nrf2*-specific silencing siRNA (siNrf2) significantly reduced the Nrf2 protein level, compared to that of the control siRNA (Fig. 3C). In a parallel experiment, siNrf2 significantly increased CPT-induced G<sub>2</sub>/M phase arrest (approximately 53% to 70%) with high levels of ROS compared to those of CPT treatment alone; however, control siRNA (siCON) at 12 h delayed cell cycle at the S phase, suggesting that Nrf2 delays cell cycle at the S phase to slowly move into G<sub>2</sub>/M phase (Fig. 3D). As presumed, western blot analysis showed that siNrf2 sustained CPT-induced cyclin B1 and p21 expression because siNrf2 accelerates into G<sub>2</sub>/M phase arrest; however, Cdk2 surprisingly sustained at the early stage (at 12 h) under the same condition, resulting from that S phase cell population also increased in CPT-induced G<sub>2</sub>/M phase arrest in the presence of siNrf2 (Fig. 3E). In order to in detail confirm whether CPT/siNrf2-induced G<sub>2</sub>/M phase arrest directly involved in the ROS generation, we analyzed the cell cycle in the presence of ROS inhibitors, NAC and GSH. As shown in Fig. 3F, CPT/siNrf2 significantly increased G<sub>2</sub>/M phase cell cycle arrest by approximately 80%; however, NAC and GSH markedly downregulated the G<sub>2</sub>/M phase arrest by approximately 40% and 50%, and increased to sustain the cells in the S phase (Fig. 3F).

Taken together these results indicate that CPT induces ROS-mediated G<sub>2</sub>/M phase arrest regulated by the presence of Nrf2.

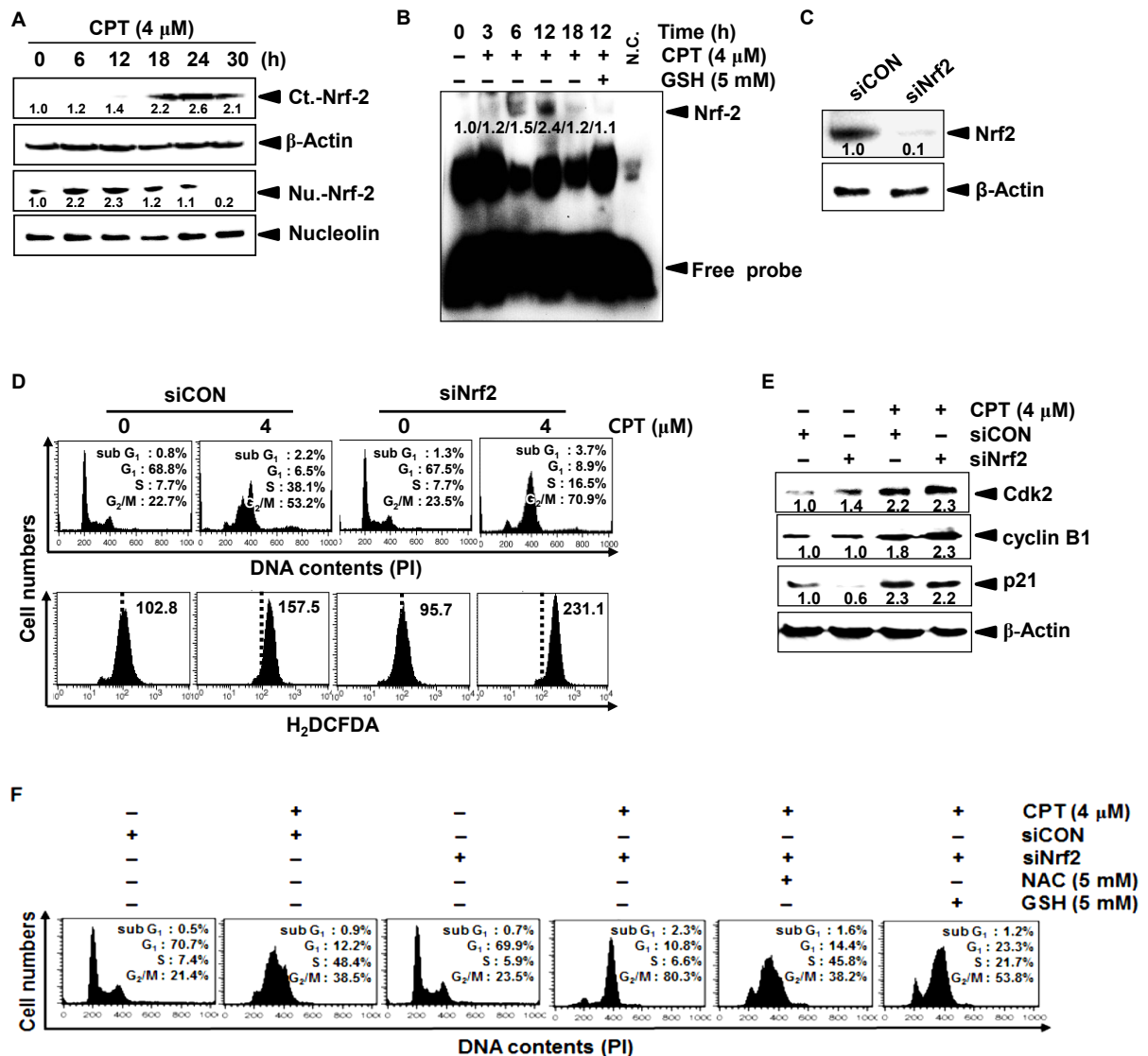


**Fig. 4.** Camptothecin (CPT)-induced the expression of Nrf2 level. (A) LNCaP cells were incubated with 4  $\mu$ M CPT for the indicated time, cytosol and nuclear lysates were resolved on SDS-polyacrylamide gels, transferred to nitrocellulose membranes, and probed with antibodies against Nrf2. (B) In a parallel experiment, nuclear extracts were prepared to analyze ARE-binding of Nrf2 by EMSA. (C) Cells were transiently transfected with siNrf2

and then check the expression level of Nrf2 by western blot analysis. (D) (at 12 h) Representative histograms for effect of CPT treatment on cell cycle distribution in LNCaP transfected with Nrf2 specific siRNA and control transfections. Parallel experiment was used to check out the level of ROS production by staining cells with H<sub>2</sub>DCFDA-based fluorescence under similar condition. (E) Effect of siRNA-based Nrf2 protein depletion on cell cycle protein. LNCaP cells were incubated with 4  $\mu$ M CPT for indicated time, cytosol and nuclear lysates were resolved on SDS-polyacrylamide gels, transferred to nitrocellulose membranes, and probed with antibodies against p21, Cdk2, and cyclin B1.  $\beta$ -Actin was used as the internal controls for western blot analysis. (F) Effect of siNrf2 on cell cycle distribution with the presence of ROS inhibitor. LNCaP cells were transiently transfected with siNrf2 for 24 h and then treated with 5 mM ROS inhibitors NAC and GSH for 1 h prior to incubate with 4  $\mu$ M CPT for 12 h. Representative histograms for effect of CPT treatment on cell cycle distribution were determined by flow cytometry.

#### **2.3.4 ATM-mediated Chk2 is a key checkpoint in CPT-induced G<sub>2</sub>/M phase arrest**

ATM is an upstream kinase implicated in phosphorylation and activation of Chk1 and Chk2, and is known to be activated in response to genotoxic stress-induced cellular senescence through the DNA damage response pathway in eukaryotic cells [Tyagi et al., 2005]. Western blot analysis revealed that phosphorylation of ATM increased in CPT-treated cells in a time-dependent manner, accompanied with significant expression of downstream molecules of ATM such as Chk1 and Chk2 which are important cell cycle checkpoint in G<sub>2</sub>/M phase (Fig. 4A). In order to further confirm whether ATM phosphorylation directly regulates Chk1 and Chk2-mediated G<sub>2</sub>/M phase arrest, LNCaP cells were pretreated with an ATM inhibitor. Western blot analysis showed that both CPT-induced expression of Chk1 and

Chk2 was significantly inhibited in response to an ATM inhibitor (Fig. 4B); an ATM inhibitor also abolished CPT-induced G<sub>2</sub>/M phase arrest (from approximately 72% to 47%) and increased G<sub>0</sub>/G<sub>1</sub> phase cell populations (Fig. 4C), which suggest that ATM is a key regulator of CPT-induced G<sub>2</sub>/M phase arrest. To in detail verify the role of Chk1 and Chk2 in CPT-induced G<sub>2</sub>/M phase arrest, we used knockdown of Chk1 and Chk2 using siRNA and analysis cell cycle distribution. Western blot analysis indicated that transient transfection of siChk1 and siChk2 significantly reduced the Chk1 and Chk2 protein level, compared with those of siCON (Fig. 4D). In further study, siChk1 and siChk2-transfected cells were treated with CPT and then cell cycle distribution were assessed after 24 h. siChk1 with CPT was not shown in any changes of G<sub>2</sub>/M phase cell population, comparted to that of siCON; however, siChk2 significantly attenuated CPT-induced G<sub>2</sub>/M phase arrest, suggesting that Chk2 functions a cell cycle checkpoint in G<sub>2</sub>/M phase arrest (Fig. 4E). These data indicate that CPT-mediated G<sub>2</sub>/M phase arrest is influenced by ATM-Chk2 axis.

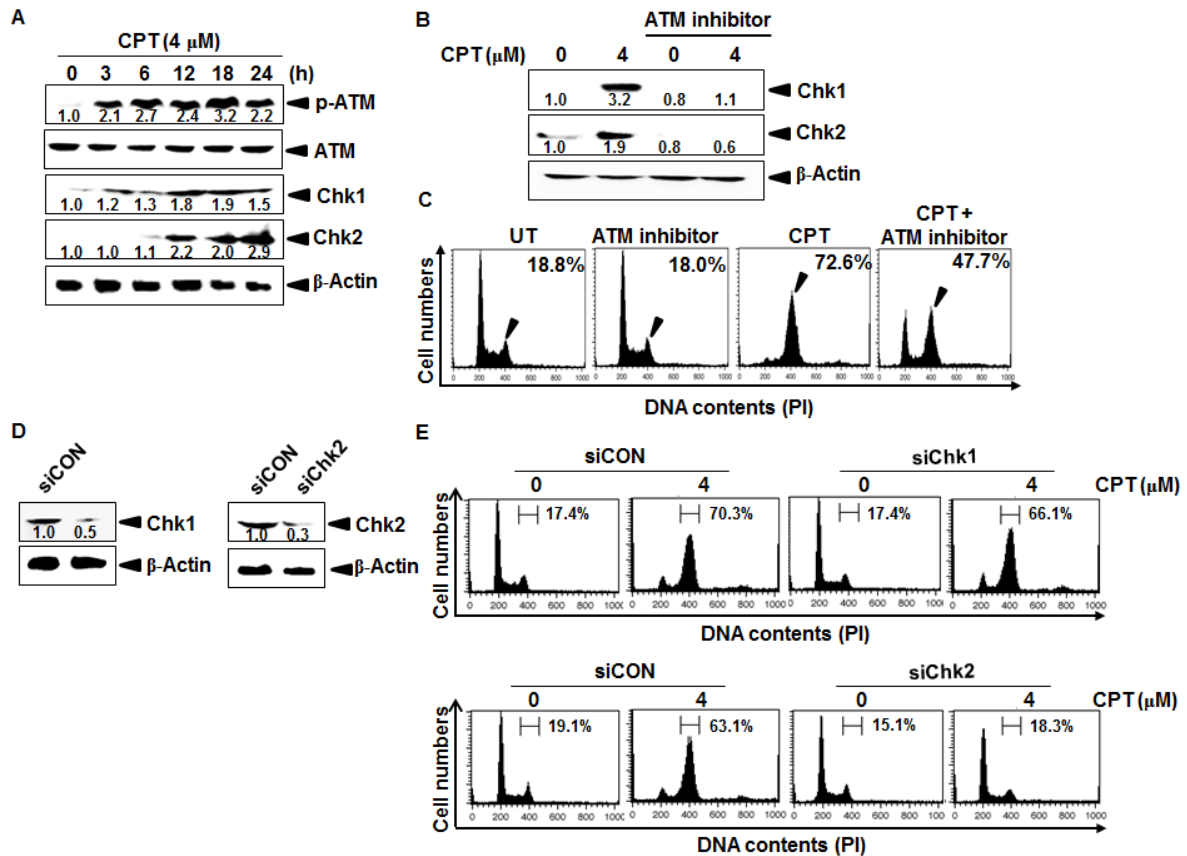


**Fig. 5.** Effect of camptothecin (CPT) on ATM and Chks activation in LNCaP cells. LNCaP cells were cultured in the presence of 4 μM CPT for 24 h. (A) Western blot analysis for the effects of CPT on protein level of phosphorylation of ATM and Chks. β-actin were used as the internal controls for western blot analysis. (B) Effect of ROS inhibitors on CPT induced ATM and Chk activation. LNCaP cells were pretreated with ROS inhibitors NAC and GSH prior to incubate with 4 μM CPT for 24 h. Total protein was subjected to 10% SDS-PAGE followed by western blot analysis with antibodies specific for phosphorylated forms of ATM and Chk1/2. (C) Effect of ATM inhibitors on CPT-induced Chks activation. LNCaP cells were pretreated with an ATM inhibitor prior to incubate with 4 μM CPT for 24 h. Western blot analysis was done with antibodies specific for Chk1 and Chk2. (D) In a parallel experiment, cells were harvested, stained with propidium iodine and analyzed for the cell cycle distribution. (E) Effect of Chks on CPT induces cell cycle arrest. LNCaP cells were

transiently transfected with siChk1/2 and then check the expression level of Chk1/2 by western blot analysis. (F) After LNCaP cells were transfected with Chk-targeted siRNA (siChk), the cells were treated with 4  $\mu$ M CPT and DNA content was analyzed using a flow cytometer.

### **2.3.5 CPT-induced Cdc25C degradation requires the proteasome pathway in G<sub>2</sub>/M phase arrest**

Two checkpoint kinases, Chk1 and Chk2, are known to phosphorylate Cdc25C on Ser<sup>216</sup> and consequently induced ubiquitination-mediated degradation of Cdc25C, which are required for entry into G<sub>2</sub>/M by activating the mitotic kinases Cdc2/cyclin B1 [Tyagi et al., 2005]. As shown in Fig. 5A, the level of Ser<sup>216</sup>-phosphorylated Cdc25C was significantly upregulated by treatment with CPT; however, total Cdc25C gradually decreased in response to CPT, which indicates that CPT induces phosphorylated-dependent Cdc25C degradation. Thus, we in detail investigated the increases of p-Cdc25C expression by CPT using anti-p-Cdc25C antibody conjugated-FITC staining. Our results showed that CPT significantly increased the intracellular phosphorylation of Cdc25C after 24 h treatment, accompanied with becoming bigger cells (toward high FSC) (Fig. 5B), suggesting that CPT suppresses cytokinesis. Next, we analyzed whether Cdc25C is regulated by CPT-induced Chk2 as a downstream molecule in LNCaP cells. CPT-induced Ser<sup>216</sup> phosphorylation of Cdc25C was more pronounced in siCON-transfected cells than the cells transfected with siChk2 and siChk2 recovered Cdc25C expression compared to that of siCON-transfected cells (Fig. 5C). Additionally, siChk2 downregulated CPT-induced cyclin B1 and p21, which indicate that siChk2 reduces the G<sub>2</sub>/M phase check point proteins such as cyclin B1 and p21 by restoring Cdc25C expression (Fig. 5C). In order to address whether the expression and phosphorylation of Cdc25C are regulated by its ubiquitination, we investigated the functional effect of

MG132, a specific proteasome inhibitor, in CPT-induced G<sub>2</sub>/M phase arrest. Upon treatment with CPT, the decline of CPT-induced Cdc25C protein level was blocked in the presence of MG132 (Fig. 5D); pretreatment with MG132 reversed CPT-induced G<sub>2</sub>/M phase arrest in LNCaP cells (approximately 20%) and Hep3B cells (approximately 10%) (Fig. 5E), suggesting that CPT regulates ubiquitination of Cdc25C in G<sub>2</sub>/M phase arrest. In a parallel experiment, we found that no apoptotic sub-G<sub>1</sub> phase was seen in CPT which induced G<sub>2</sub>/M phase arrest; however, combine treatment with CPT and MG132 significantly sensitized to induce DNA fragmentation as an apoptotic marker in LNCaP cells (Fig. 5F). Thus, we assumed whether combine treatment with CPT and MG132 could synergistically induce apoptosis in LNCaP cells. As shown in Fig 5G, treatment of LNCaP cells with a combination with CPT and MG132 for 24 h significantly increased the accumulation of sub-G<sub>1</sub> phase cells accompanied with a substantial decrease of G<sub>2</sub>/M phase cell population. Additionally, treatment with CPT and MG132 decreased the level of procaspase-3 and procaspase-9 indicated that CPT activates caspase dependent apoptosis (Fig. 5H). These data confirm that LNCaP cells sensitize the apoptosis in combine effect of CPT and MG132.

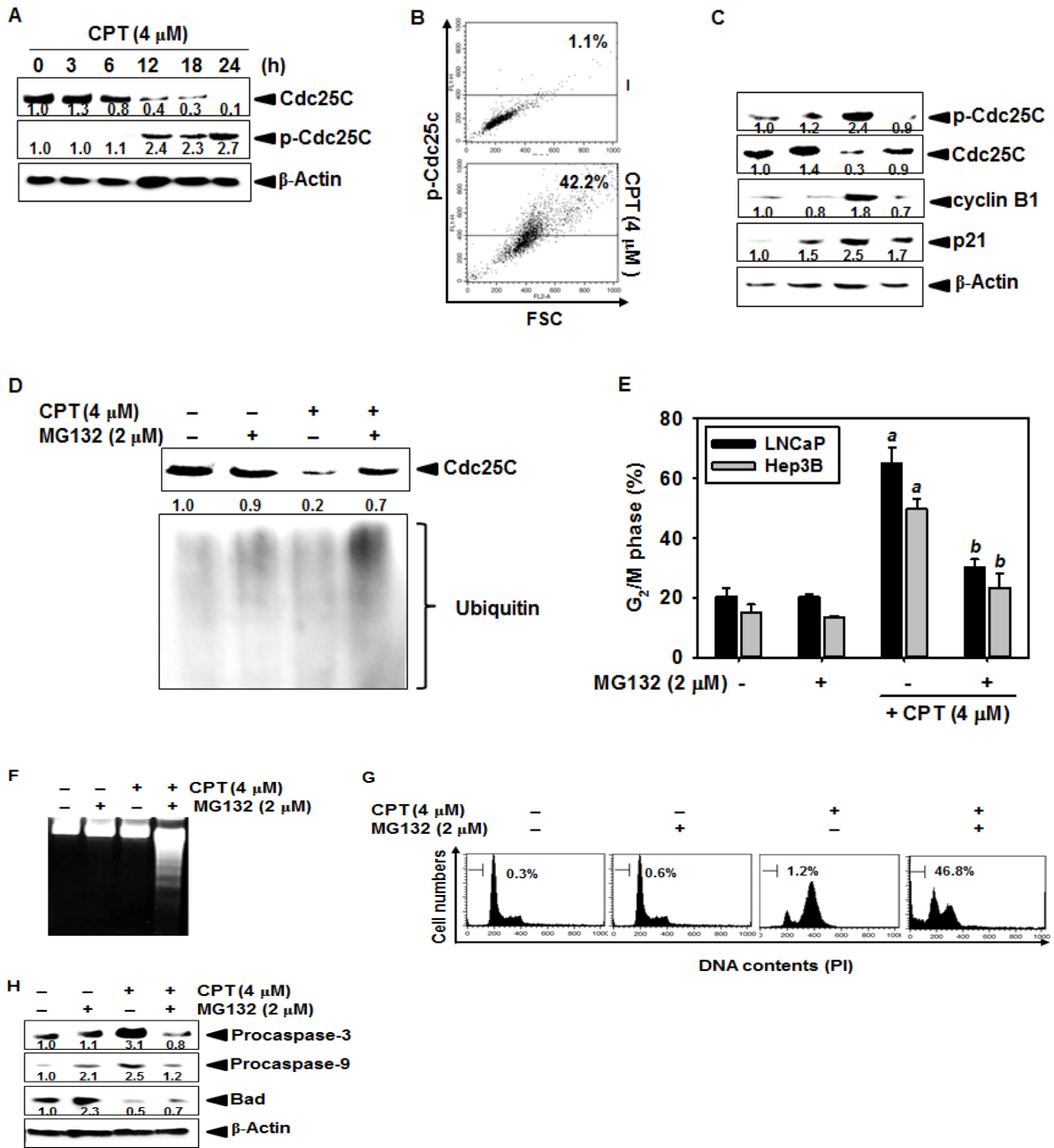


**Fig. 6.** Camptothecin (CPT)-induced Cdc25C degradation is mediated by a ubiquitin-proteasome pathway. (A) Western blot analysis for Cdc25C using lysates from control and CPT-treated LNCaP cells. LNCaP cells were cultured in the presence of 4  $\mu$ M CPT for 24 h. Total protein was subjected to 10% SDS-PAGE followed by western blotting with antibodies specific for phosphorylated forms of Cdc25C. (B) LNCaP cells were cultured in the presence of 4  $\mu$ M CPT for 24 h. Cells were measured by dual analysis of p-Cdc25C and DNA content

in control and CPT-treated cells. (C) Effect of Chk2 depletion on CPT-induced phosphorylation of Cdc25C and cell cycle protein. siChk2-transfected cells were treated with 4  $\mu$ M CPT for 24 h, harvested and process for western blot analysis using antibodies against Cdc25C, p-Cdc25C, cyclin B, and p21.  $\beta$ -Actin was used as the internal controls for western blot analysis. (D) Effect of proteasome inhibitor MG132 on CPT-induced decline in Cdc25C protein level. LNCaP cells were treated with 4  $\mu$ M CPT in the presence or absence of MG132 for 24 h. Cell lysates prepared for western blot analysis using antibodies against anti-ubiquitin antibody to determine the high molecular weight polyubiquitin conjugates. (E) Effect of MG132 on CPT-induced cell cycle arrest. LNCaP and Hep3B cells were treated with 4  $\mu$ M CPT in the presence or absence of MG132 prior to processing analysis for cell cycle distribution. (F) Effect of treatment with combination of CPT and MG132 on DNA fragmentation. After treatment of LNCaP cells as indicated for 24 h, fragmented DNAs were extracted from the treated cells and analyzed on 1.5% agarose gel. (G) Cells with sub-G<sub>1</sub> phase DNA content was detected by flow cytometry. The percentages of cells with sub-G<sub>1</sub> DNA content are represented in each panel. (H) Effect of treatment with a combination of CPT and MG132 on levels of pro-apoptotic and anti-apoptotic protein. LNCaP cells were treated with 2  $\mu$ M MG132 alone, 4  $\mu$ M CPT alone, or a combination of both for 24h. Cell extracts were prepared for Western blotting for caspase-8, caspase-3 and Bad.  $\beta$ -Actin was used as the internal controls for western blot analysis. Data from three independent experiments are expressed as the overall mean  $\pm$  S.E. Statistical significance was determined by one-way ANOVA (<sup>a</sup> and <sup>b</sup>,  $p < 0.05$  vs. control and CPT-treated group).

### **2.3.6 ERK and JNK regulate Cdc25C-mediated cyclin B and p21 expression in CPT-induced G<sub>2</sub>/M phase arrest**

In order to investigate whether mitogen-activated protein kinases (MAPKs) lead to regulate cell cycle progression, we exposed LNCaP cells with CPT for different times and determined the phosphorylation and activation of MAPKs. Our results showed that CPT increased the phosphorylation of JNK, ERK, and p38 at different time point (Fig. 6A). Thus, we investigated the protein expression of cell cycle upon the treatment of MAPK inhibitors. Pretreatment with a JNK inhibitor SP600125, an ERK inhibitor PD98059, and a p38 inhibitor SB203580 resulted in decreasing CPT-induced expression of p21 and cyclin B1 levels (Fig. 6B). Finally, we investigated the functional effects of MAPKs in CPT-induced G<sub>2</sub>/M phase arrest at 12 h and 24 h. Treatment with CPT alone showed S phase arrest at 12 h and moved into G<sub>2</sub>/M phase arrest at 24 h. However, pretreatment with SP600125 and PD98059 resulted in a greater decrease of S phase and G<sub>2</sub>/M phase cell population at both time points; in particular, SP600125 significantly induced apoptotic sub-G<sub>1</sub> phase population (Fig. 6C). However, a p38 inhibitor, SB203580, slightly affects the CPT-induced S phase arrest and G<sub>2</sub>/M phase arrest. These data indicate that the ERK and JNK signaling pathway in an important regulator in CPT-induced S phase arrest at 12 h and G<sub>2</sub>/M phase arrest at 24 h.

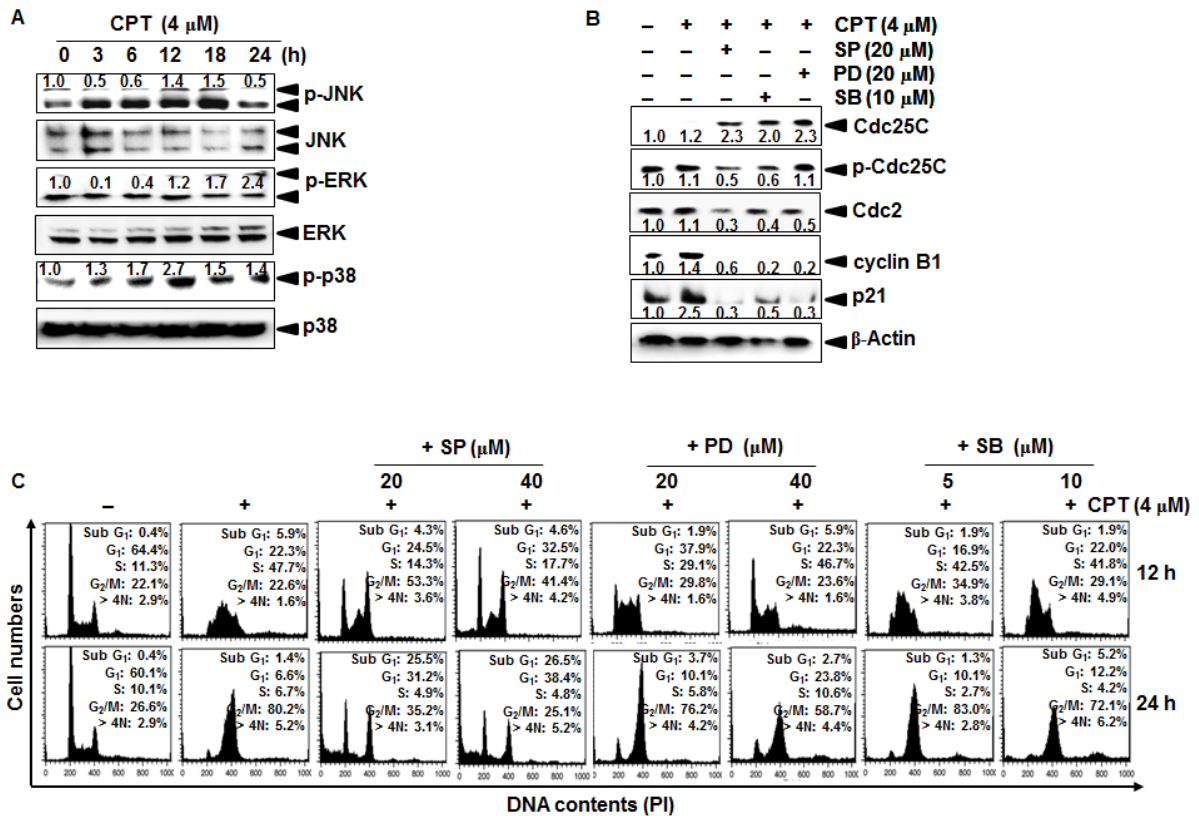


**Fig. 7.** Camptothecin (CPT)-induced G<sub>2</sub>/M phase arrest through JNK and ERK activity. (A) LNCaP cells were treated with 4 μM CPT for the indicated time. Cell lysates were resolved on SDS-polyacrylamide gels, transferred to nitrocellulose membranes and probed with antibodies against p-ERK, ERK, p-p38, p38, p-JNK, and JNK. (B) The LNCaP cells were stimulated with 4 μM CPT for indicated time after pretreatment with 20 μM SP600125, 20 μM PD98059, and 10 μM SB203580 for 1 h. Cell lysates were resolved on SDS-polyacrylamide gels, transferred to nitrocellulose membranes, and probed with antibodies against Cdc25C, p-Cdc25C, Cdk2, cyclin B, and p21. β-Actin was used as the internal controls for western blot analysis. LNCaP cells were stimulated with CPT 4μM for indicated time after pretreatment with SP600125 (10 and 20 μM), PD98059 (10 and 20 μM), and SB203580 (5 and 10 μM) for 1h. The cells were stained with propidium iodide and analyzed by flow cytometry at 12 h (top panel) and 24 h (bottom panel).

### **2.3.7 CPT decreases cell viability, but not induces cell death**

To determine the effect of CPT on cell viability and proliferation, human prostate cancer LNCaP and DU145 cells were treated with different concentrations of CPT and incubated for 24 h. Cell viability and growth were determined by MTT and trypan blue exclusion assays. As shown in Fig. 7A and 7B, CPT treatment resulted in a decreasing of cell viability percentage and proliferation, respectively. However, no apoptotic annexin V<sup>+</sup> populations were seen while LNCaP cells were treated with CPT until 24 h compared to the positive H<sub>2</sub>O<sub>2</sub>-treated group (Fig. 7C). Similarly, light microscopy results further proved that LNCaP cells showed apoptotic shrinkage in H<sub>2</sub>O<sub>2</sub>-treated group, but CPT-treated cells were intact (Fig. 7D). These data indicate that CPT inhibits proliferation of LNCaP cells, but not induces apoptosis.

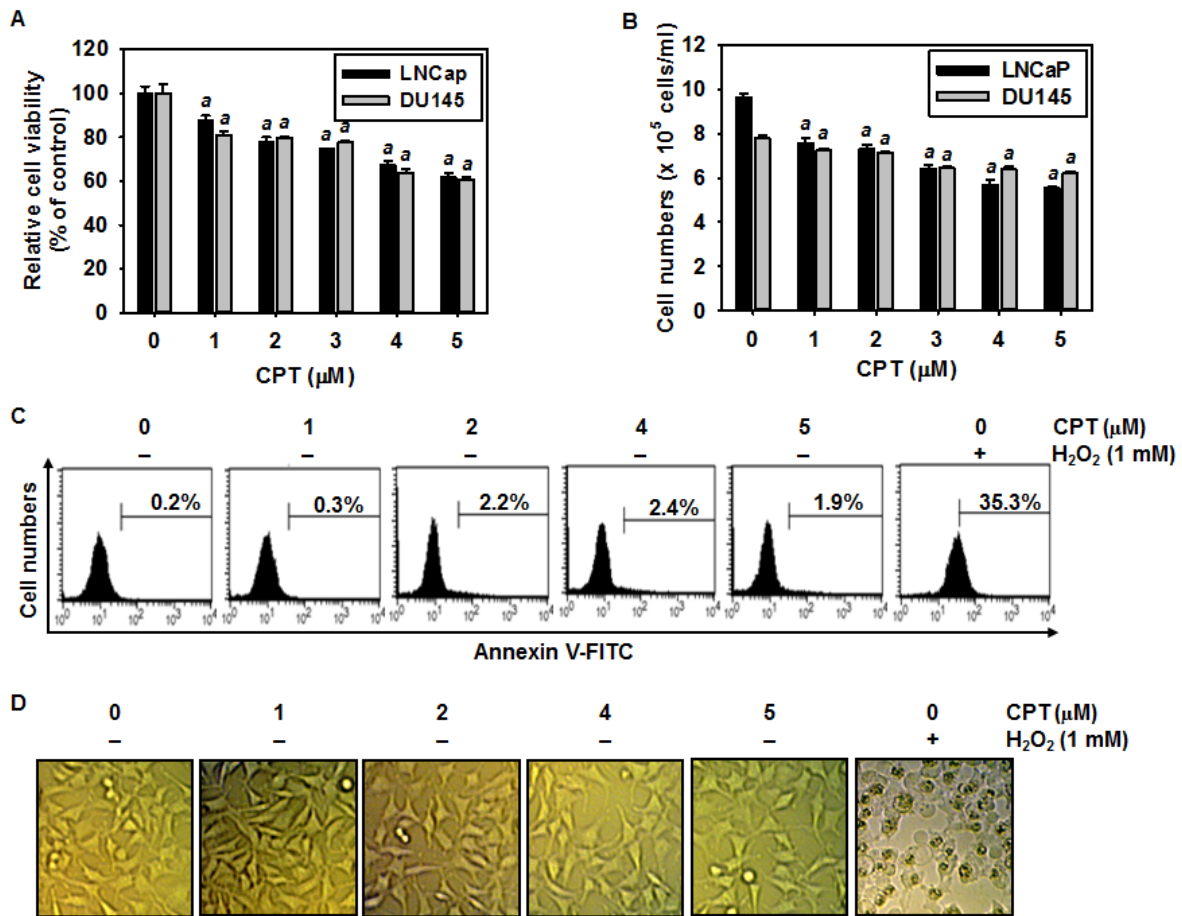


**Fig. 8.** Camptothecin (CPT)-decreased the cell proliferation in prostate cancer cells. Effect of treatment with CPT on cell viability. Human prostate cancer LNCaP and DU145 cells were treated with CPT at the indicated concentrations for 24 h. (A) MTT assay assessed cellular viability. (B) In a parallel, experiment cell number was counted using hemocytometer counts of trypan blue-excluding cells. (C) The cells are stained with annexin V<sup>+</sup> and analyzed by flow cytometry (D) The cellular morphology was examined under light microscopy. Data from three independent experiments are expressed as the overall mean  $\pm$  S.E. Statistical significance was determined by one-way ANOVA (<sup>a</sup>,  $p < 0.05$  vs. untreated control).

### 2.3.8 CPT-induced autophagy blocks cell death and leads to G<sub>2</sub>/M phase arrest

Since CPT had no apparent apoptotic death on LNCaP cells, we investigated the effect of CPT on induction of autophagy. Western blot analysis showed that CPT significantly induced the expression of autophagy-related proteins, Beclin-1, active LC3-II, and Atg-7 in a dose- (Fig. 8A) at 24 h and a time-dependent manner (Fig. 8B), respectively, indicating that CPT induces autophagy in LNCaP cells. Further, we investigated whether autophagy regulates CPT-induced inhibition of cell viability. For the functional study of autophagy, we pretreated with 3MA which inhibits LC3-I to LC3-II and BAF which blocks the fusion of autophagosomes and lysosomes in the presence of CPT. 3MA and BAF slightly decreased CPT-induced inhibition of cell viability (Fig. 8C). Next, we analyzed whether 3MA and BAF increased CPT-induced inhibition of cell viability without any apoptosis or changed the viability inhibition to apoptosis. Additionally, our data revealed that combine treatment with CPT and 3MA significantly increased the annexin-V<sup>+</sup> cell populations, indicating that CPT-induced autophagy blocks to move into apoptotic death (Fig. 8D). Western blot analysis confirmed that CPT has ability to decrease procaspases-3 and increased proapoptotic Bid which are apoptotic inducers (Fig. 8E). Finally, 3MA-induced inhibition of autophagy gradually increased DNA fragmentation in response to concentration-dependent CPT (Fig. 8F). Taken together, these results indicate that CPT-induced autophagy blocks cell death and increases G<sub>2</sub>/M phase arrest.

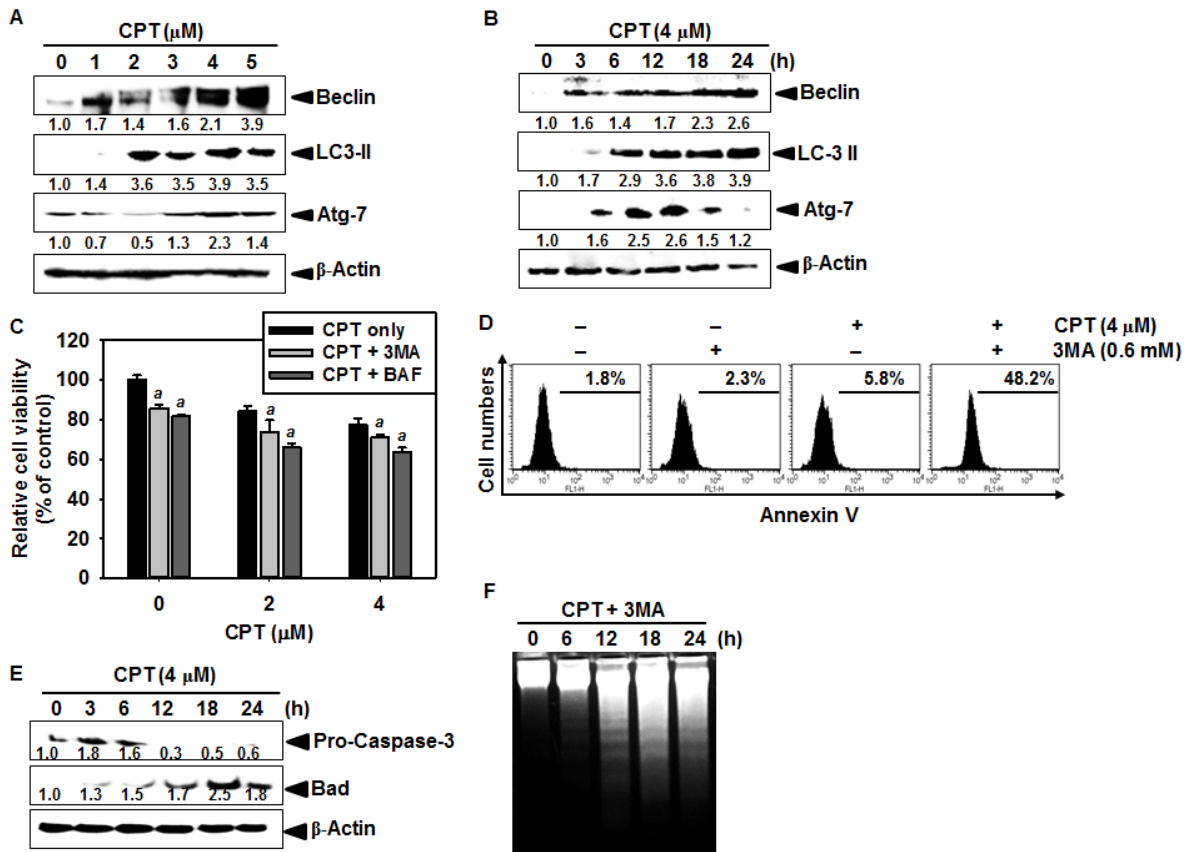


**Fig. 9.** Camptothecin (CPT)-induced autophagy as cytoprotection mechanism in LNCaP cells. LNCaP cells were treated with CPT at the indicated concentrations for 24 h (A) and 4  $\mu$ M CPT at the indicated time points (B). Cell lysates were resolved on SDS-polyacrylamide gels, transferred to nitrocellulose membranes and probed with antibodies against beclin 1, LC3II and Atg7.  $\beta$ -Actin was used as the internal controls for immunoblot. (C) LNCaP cells were pretreated with autophagy inhibitors 3-methyladenine (3MA) and bafilomycin (BAF) prior to incubate with 4  $\mu$ M CPT for 24 h. (C) Cellular viability was assessed by MTT treatment. (D) LNCaP cells were pretreated with autophagy inhibitors 3-methyladenine (3MA) and cells are stained with annexin V<sup>+</sup> and analyzed by flow cytometry. CPT induces apoptosis in U937 leukemia cancer cells. (E) U937 cells were treated with 4  $\mu$ M CPT at the indicated time points. Cell lysates were resolved on SDS-polyacrylamide gels, transferred to nitrocellulose membranes and probed with antibodies against caspases-3 and bid. (F) In a

parallel, experiment fragmented DNAs were isolated from the U937 cells and analyzed on 1.5% agarose gel. Data from three independent experiments are expressed as the overall mean  $\pm$  S.E. Statistical significance was determined by one-way ANOVA ( $a, p < 0.05$  vs. each CPT-treated control).

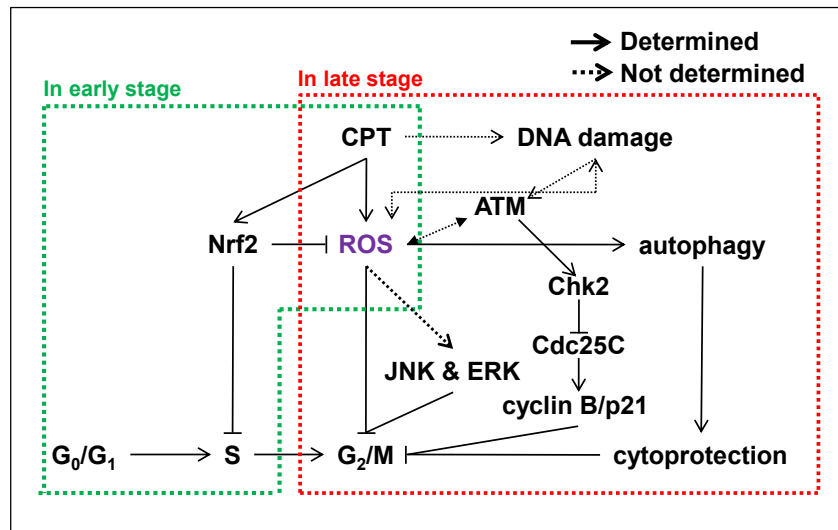


**Fig. 10.** Scheme of Camptothecin (CPT)-induced G<sub>2</sub>/M phase cell cycle arrest. Model for the proposed CPT-induced cell cycle regulation. CPT-caused the G<sub>2</sub>/M cell cycle arrest through activation of the ATM/Chk2/Cdc25C and ERK/JNK/cyclin B1 pathways. CPT-increased the ROS generation thus induce the phosphorylation of ATM, which turn phosphorylate Chks. Activated Chk2 caused phosphorylation of Cdc25C. CPT also increased the phosphorylation of ERK and JNK lead to increase the level of cyclin B and p21 expression which induced the G<sub>2</sub>/M phase arrest. Induction of ROS increased the autophagy mechanism which prevents cells from apoptosis, direct to cell cycle arrest. Induction of ROS also enhanced the Nrf2 translocation to activate the antioxidant genes and regulated the cell cycle.

## 2.4 Discussion

Previous data confirmed that CPT forms a ternary complex with DNA and topo I which unwinds DNA while replication and transcription, and blocks to rewind of cleaved DNA [Chen et al., 2009]. Consequently, the ternary complex, topo I-CPT-DNA, derives S and G<sub>2</sub> phase arrest-mediated cytotoxicity by inducing DNA-strand breaks [Cliby et al., 2002]. Therefore, CPT became a promising candidate for treating various malignant cancers; however, clinical use of CPT was limited because of poor solubility along with some side effects such as myelosuppression, diarrhea, and hemorrhagic cystitis [Muggia et al., 1972]. Nevertheless, CPT derivatives and analogues have been studied and designed for clinical practice because unique characteristics of CPT targeting topo I is attractive for the treatment of a broad spectrum of cancers [Jameson et al., 2013; Perez-Soler et al., 1996]. Therefore, we suggest that detail studies should be continued to elicit the molecular action of CPT, which will help to design new types of topo I-targeting drugs with lesser cytotoxicity. In this sense, we previously reported that CPT effectively inhibited phorbol myristate acetate (PMA)-induced prostate cancer invasion by inhibiting matrix metalloprotease-9 (MMP-9) and vascular endothelial growth factor (VEGF) expression, which are regulated by upregulating Nrf2-mediated heme oxygenase-1 (HO-1), indicating that CPT suppresses cancer cell invasion without direct cytotoxicity [Jayasooriya et al., 2015]. Moreover, combined treatment with CPT and TNF-related apoptosis-inducing ligand (TRAIL) sensitized apoptotic cell death in human hepatocarcinoma Hep3B cells by upregulating death receptor 5 (DR5) expression through the generation of ROS and the activation of ERK and of p38 MAPK, which suggests that sub toxic dosage of CPT can be used to kill cancer cells as a TRAIL sensitizer [28]. Above two our previous studies showed the new possibility of CPT for treatment of cancer cells with low concentrations which do not have direct cytotoxicity. Addition, we, in this

current, found that CPT induced S- and G<sub>2</sub>/M phase arrest by regulating cell cycle check point proteins.

Cell cycle checkpoints are central mechanisms in eukaryotic cells which control DNA replication, mitosis, and cytokinesis; however, harmful stresses potentially halt cell cycle and switch on checkpoint proteins to cure, if not, cells consequently reach to die [Mazouzi et al., 2014]. Therefore, cell cycle-targeting topo I inhibitors are fascinating pharmaceuticals to treat cancers, resulting from turning on the checkpoint proteins. In particular, the topo I-targeting drugs reveals specific to the S phase which is the stage of DNA replication [Wang et al., 2002]. In the current study, we first found that CPT sustained the S phase arrest along with induction of Nrf2 at early stage (at 12 h) and transient knockdown of Nrf2 swiftly moved cell cycle distribution into G<sub>2</sub>/M phase arrest, suggesting that CPT-mediated Nrf2 compromises the S phase arrest at early stage. Even though CPT potentially stops S phase in the cell cycle because CPT targets topo I which induces double-strand DNA breaks, CPT-induced S phase arrest transits into G<sub>2</sub>/M phase arrest at late stage (at 24 h). This result indicates that other factors activated by DBS are involved in moving into CPT-induced G<sub>2</sub>/M phase arrest. Surprisingly, inhibition of ROS generation restored CPT-induced G<sub>2</sub>/M phase arrest into S phase arrest, not into normal cell cycle distribution, indicating that CPT induces the S phase arrest by inducing topo I inhibition-mediated DBS, leading to ROS generation, which influences on G<sub>2</sub>/M phase arrest. However, still question exists how ROS are generated and when ROS are working for G<sub>2</sub>/M phase arrest. Kurz *et al.*, reported that ROS could induce topo I-mediated oxidative DNA damage in a ATM-dependent manner, leading to cell death [Kurz et al., 2004]. Recently, Ito *et al.*, reported that ATM-deficient patients or ATM<sup>-/-</sup> mice displayed a significant increase of ROS generation, suggesting that that impaired ATM function leads to defects in controls of ROS regardless of DNA damage [Ito et al., 2007]. In

the current study, we showed that ROS and ATM are key check point regulators of S and G<sub>2</sub>/M phase arrest; further studies will be necessary to analyze whether DBS-mediated ATM or DBS itself regulate ROS generation and vice versa. Macip *et al.*, previously reported that p21 caused to increase ROS levels in both normal and tumor cells [Macip et al., 2002] and Inoue *et al.*, showed that transfection of p21 in LoVo and HCT 116 cells triggered the level of ROS in the senescence or apoptotic cells [Inoue et al., 32]. In contrary, p21 stabilizes for diminishing oxidative stress, resulting from directly binding to Nrf2 and blocking its ubiquitination-dependent degradation [Chen et al., 16]. In the light of current study, p21-mediated Nrf2 at early stage (at 12 h) exerts to attenuate oxidative damage through S phase arrest; however, accumulated ROS overcomes Nrf2-mediated antioxidant effect at the late stage (at 24 h). In this sense, we cannot rule out the possibility that ROS play a different role in the different time points by regulating cell cycle checkpoint proteins.

S or G<sub>2</sub>/M phases are severely regulated by two checkpoint proteins, Chk1 and Chk2, which are activated by DNA damage-mediated phosphorylation of ATM and ATR [Inoue et al., 2009]. Chk1 is phosphorylated at Ser<sup>345</sup> or Ser<sup>317</sup> by ATM and/or ATR, which phosphorylates Cdc25A/C, leading to S or G<sub>2</sub>/M phase arrest [Mailand et al., 2000]. Chk2 is activated by phosphorylation of Thr<sup>68</sup> in an ATM-dependent manner [Ahn et al., 2000]. Previous data also showed that Chk1 and Chk2 are differentially regulated in cell cycle arrest in response to DNA-double-strand breaks induced by CPT, suggesting that Chk1 inhibition is attractive therapeutic strategy in CPT-driven DNA damage response [Huang et al., 2008]. Our data showed that CPT increased the expression of Chk1 and Chk2 in an ATM-dependent manner; however, transient knockdown of Chk2, but not Chk1, completely restored cell cycle distribution from G<sub>2</sub>/M phase arrest. Additionally, no S phase arrest was seen by Chk2 knockdown in response to CPT, suggesting that CPT-induced Nrf2 which stop cell cycle

distribution at S phase, is a upstream regulator of Chk2 because Chk2 broadly resides in S and G<sub>2</sub>/M phase. Under genomic stress, the activation of Chks renders inactive Cdc25C via phosphorylation at Ser<sup>216</sup> and ubiquitination-dependent degradation, leading to block the downstream signal pathway related to p21 and cyclin B1 activation which is required for entry into G<sub>2</sub>/M phase [Lee et al., 2010]. Our data also revealed that Chk2 induced phosphorylation at Ser<sup>216</sup> and ubiquitination-mediated degradation of Cdc25C, which led to downregulation of p21 and cyclin B1, leading to CPT-induced G<sub>2</sub>/M phase arrest.

MAPKs are a highly conserved serine/threonine protein kinases involved in a variety of fundamental cellular processes such as environmental stress response, proliferation, differentiation, survival, and apoptosis. In particular, activation of JNK and p38 pathways is responsible for the apoptotic response induced by some DNA-damaging agents whereas activation of ERK pathway associated with proliferation and differentiation [Lee et al., 2006]. Under UV irradiation, JNK activation causes phosphorylation of Cdc25C at Ser<sup>168</sup> during DNA damage-mediated G<sub>2</sub>/M phase arrest [Gutierrez et al., 2010]. Furthermore, ERK is required to regulate G<sub>2</sub>/M progression by disrupting cyclin B1-Cdc2 complex [Dumesic et al., 2009] and p38 MAPK also regulates mitotic stage by activating Cdc25C toward cyclin B1-Cdc2 interaction [Cha et al., 2007]. These above results indicated that MAPKs are essential to regulate cell cycle distribution; however, each number elicits against different stresses and drugs in a dissimilar manner. In the current study, we found that inhibition of JNK and ERK activity arrested CPT-induced G<sub>2</sub>/M phase arrest along with a significant decrease of Cdc25C phosphorylation at Ser<sup>216</sup>; p38 inhibition sustained CPT-induced phosphorylation of Cdc25C and has no influenced cell cycle distribution. Nevertheless, downstream molecules of Cdc25C such as Cdk1, cyclin B1, and p21 decreased in response to all MAPK inhibitors, suggesting that unknown mechanisms are involved in MAPK-mediated cell cycle

distribution. Additionally, recent study revealed that autophagy is a key player between apoptosis and cell cycle regulation and, in DNA damage, checkpoint proteins enhances autophagy in mitosis stage by inducing MAPK activation, suggesting that autophagy delays cell cycles to determine cell fate [Filippi-Chiela et al., 2011; Dotiwala et al., 2013]. Given the specific role of autophagy, MAPKs could regulate cell cycle distribution via autophagy. In this study, CPT inhibits cell proliferation, but not cell death; however, autophagy inhibition moved CPT-mediated G<sub>2</sub>/M phase arrest to apoptosis, which suggest that CPT-induced autophagy triggers cytoprotective effect, leading to residing G<sub>2</sub>/M phase arrest. Nevertheless, we did not show direct interaction between MAPKs and autophagy; therefore, we need to further study how MAPKs, especially JNK and ERK, interplay between G<sub>2</sub>/M phase arrest and autophagy in response to CPT.

## **2.5 Conclusion**

CPT promotes G<sub>2</sub>/M phase arrest along with Chk2 and Cdc25C, resulting from coordinative DNA damage-mediated ATP and ROS generation. The JNK and ERK signal pathway also involved CPT-induced G<sub>2</sub>/M phase arrest accompanied by autophagy. These converging views may offer great opportunities for pharmacological intervention of CPT in cell cycle regulation and apoptosis.

## **Chapter 3**

**Camptothecin induces mitotic arrest in LNCaP cells,  
resulting from Mad2-mediated cyclin B1 and Cdk1  
expression: Implication of tubulin polymerization**

## Abstract

Camptothecin (CPT) was first discovered as a topoisomerase I inhibitor, thus expanding to use clinical trial; however, its use has been limited because of adverse effect. Nevertheless, CPT is a prominent therapeutic model because CPT accurately targets topoisomerase I which is consistently active in cancer cells. Therefore, we investigated how CPT regulates cell cycle progression in human prostate cancer LNCaP cells. Our finding showed that treatment with CPT induced microtubule polymerization, not actin polymerization, resulting in remarkable upregulation of histone H3 phosphorylation which is a mitotic-specific marker and complex between Mad2 and Cdc20 known as mitotic checkpoint proteins, and thereby may increase mitotic prometaphase arrest. CPT also enhanced expression and activity of cyclin B1 and cyclin-dependent kinase 1 (Cdk1); thus, depletion of Mad2 completely restored cell cycle progression from CPT-induced mitotic arrest, accompanied by loss of cyclin B1 and Cdk1, suggesting that Mad-mediated cyclin B1 and Cdk1 complex is an important axis in CPT-induced mitotic arrest. Moreover, we found that c-Jun N-terminal kinase (JNK) is an upstream molecule for transcription factor Sp1 in response to CPT, which regulates p21-mediated mitotic arrest; however, knockdown of p21 slightly restored cell cycle progression from CPT-induced mitotic arrest. Nevertheless, inhibition of Cdks which are downstream targets of p21 completely restored from CPT-induced mitotic arrest. During mitotic arrest in response to CPT, we made a hypothesis that some cell survival signals block apoptosis, leading to enhance mitotic arrest. As presumed, a caspase-9 inhibitor, z-LEHD-FMK, and an autophagy inhibitor, 3-methyladenine (3MA), significantly diminished CPT-induced mitotic arrest with no apoptosis, suggesting that caspase-9 and autophagy are associated to with CPT-induced mitotic arrest. On the other hand, in depletion of Mad2, z-LEHD-FMK and 3MA remarkably increased apoptosis, accompanied by restoration from CPT-mediated cell cycle

progression. Taken together, these results indicate that CPT may be promising for decoding the molecular modes of topoisomerase I-mediated tubulin targeting drugs.

### 3.1 Introduction

The spindle assembly checkpoints (SACs) ensure cell cycle to delay until all duplicated chromosomes align and attach to the spindle, which guarantee genomic stability during mitosis (M) [Lara-Gonzalez et al., 2012]. Once mitotic spindles tightly bind to kinetochores through tubulin polymerization from prometaphase to metaphase, the spindle assembly checkpoints are inactivated, which allows tubulin depolymerization at anaphase [Wang et al., 2014]; when microtubule polymerization and depolymerization are incorrectly regulated, kinetochores trigger the spindle assembly checkpoint signal pathway, which halt cell cycle distribution in M phase. Therefore, microtubule-targeting strategy which disrupts or hyperstabilizes spindle microtubules, has been anti-mitotic therapeutics to treat various cancers. In particular, microtubule polymerization inhibitors such as colchicines and vinblastine, and microtubule depolymerization inhibitor such as paclitaxel are intensively used for binding to tubulins, which disrupt microtubule dynamics and induce M phase arrest [Jordan et al., 2004]. Additionally, recent studies showed that microtubule-targeting drugs has been successfully used in clinical trial with much interest because their action is totally different from other DNA-targeting drugs [Tsimberidou et al., 2011; Field et al., 2014]. In fact, SACs arrest cell cycle distribution in M phase in response to signal from kinetochores as a results of impaired binding to spindle microtubules due to lack of microtubule-kinetochore attachment or improper tension imposed on sister kinetochores [Musacchio et al., 2015]. In particular, improper tension of microtubules on kinetochores renders catalytic site for Mad2, which inhibits anaphase onset by suppressing the anaphase promoting complex APC with Cdc20

[Zhou et al., 2002]. Interaction among mitotic checkpoint complex such as Mad2 and Cdc20 inhibits the APC-mediated ubiquitination of securin and cyclin B1 [Tian et al., 2012].

Cyclin-dependent kinases (Cdks) are associated with different stages where cyclins regulate cell cycle distribution by inducing nuclear localization, phosphorylation, and dephosphorylation of the Cdks and degradation of the regulatory cyclin subunits [Dash et al., 2005]. Cyclins and Cdks bind p21 through the CRRL consensus site at N-terminal end required for inhibition of cell cycle progression [Rousseau et al., 1999]. In particular, p21<sup>-/-</sup> mice have markedly decreased the number of mitotic embryonic fibroblasts cells with cyclin B1, suggesting which value of p21 promotes late G<sub>2</sub>/M phase arrest by regulating cyclin B1-Cdk1 activity [Dash et al., 2005]. Induction of chromosomal instability by depletion of Mad2 reduces the time available to proper oriented chromosome in metaphase leading to activate JNK signaling to tolerate chromosomal instability induced by spindle checkpoint defects [Wong et al., 2014]. This activation and phosphorylation of JNK regulates of the stability of transcription factor Sp1 during mitosis [Chuang et al., 2008]. Phosphorylated p21 binds to cyclin B1 and Cdc2 phosphorylation on Y15 and phosphorylation on T161 promotes Cdc2 binding to the p21/cyclin B1 complex activated as a kinase which required Sp1 transcription [Dash et al., 2005; Kim et al., 2014]. Additionally, transient knockdown of cyclin B or Cdk1 inhibit or decreased the cells in M phase. Similarly, treatment with tubulin polymerization inhibitors nocodazole or tubulin depolymerization inhibitor paclitaxel also regulate the G<sub>2</sub>/M phase with marked induction of cyclin B1 and Cdk1 [Dash et al., 2005; Chadebech et al., 2000]. Choi *et al.* reported that selective knockdown of Mad2 resulted in degradation of cyclin B in nocodazole-treated G<sub>2</sub>/M stage; whereas the accumulation of cyclin B1 and Cdc2 is trigger the development of chromosomal condensation and segregation in prometaphase arrested cells [Choi et al., 2011].

Xiao *et al.*, reported that camptothecin (CPT)-induced S phase arrest which activate Chk1 and cause the rapid proteolysis of Cdc25A, whereas elimination of Chk1 expression through knockdown abrogate S phase and protect Cdc25A degradation [Choi et al., 2011]. CPT also induced apoptosis in cancer cells by miR-125b mediated mitochondrial pathways via targeting to the 3'UTR regions of p53, Bak1, and Mcl1 [Zeng et al., 2012]. Nevertheless, a little has been known on the molecular action of CPT in G<sub>2</sub>/M phase. In the present study, we investigated the molecular mechanisms underline activities of CPT in M phase of LNCaP cells. Additionally, we found that CPT-induced M phase arrest is regulated by Mad2-Cdc20 complex through JNK-dependent Sp1 pathway.

### 3.2 Materials and method

#### *Reagents and antibodies*

CPT, 3-(4,5-dimethylthiazol-2-yl)-2,5-diphenyltetrazolium bromide (MTT), propidium iodine, MG132, Cdk inhibitor (CdkI), 3-methyladenine (3MA), z-LEHD-FMK, and z-IETD-FMK were purchased from sigma (St. Louis, MO) and an enhanced chemiluminescence (ECL) kit was purchased from Amersham (Arlington Heights, IL). RPMI 1640 medium, fetal bovine serum (FBS), and antibiotics mixture were purchased from WelGENE (Daegu, Republic of Korea). Antibodies against Cdc20, Mad2,  $\beta$ -actin, cyclin B, Cdk1, Sp1, nucleolin, p21, phosphor (p)-21, Cdk1,  $\alpha$ -tubulin (polymeric), caspase-8, caspase-9, and Bax were purchased from Santa Cruz Biotechnology (Santa Cruz, CA). Antibodies against p-histone 3 (p-H3), p-JNK, JNK, p-c-Jun, p-PTEN, and PTEN were purchased from Cell Signal (Beverly, MA). Peroxidase-labeled donkey anti-rabbit and sheep anti-mouse immunoglobulin were purchased from Koma Biotechnology (Seoul, South Korea).

### *Flow cytometric analysis*

DNA was stained with propidium iodine and mitotic cells were quantified by measuring the expression of a mitotic-specific marker p-H3 or Mad2. In brief, the cells were trypsinized, washed once with PBS, fixed with ice-cold 70% ethanol for overnight and immune stained with a rabbit anti-p-H3 or anti-Mad2 antibody followed by a FITC-conjugated goat anti-rabbit antibody. The cells were then stained with 3 µg/ml propidium iodine in PBS containing 1% Triton X-100 and 0.1 mg/ml RNase A. p-H3 or Mad2 levels and the DNA content of individual cells were analyzed using a fluorescence-activated cell sorting cater-plus flow cytometry.

### *Western blot analysis*

Whole-cell lysates were prepared by PRO-PREP protein extraction solution (iNtRON Biotechnology, Sungnam, Republic of Korea). Cytoplasmic and nuclear protein extracts were prepared using NE-PER nuclear and cytosolic extraction reagents (Pierce, Rockford, IL). The cell lysates were harvested from the supernatant after centrifugation at 13,000 g for 20 min. Total cell proteins were separated on polyacrylamide gels and standard procedures were used the transfer them the nitrocellulose membranes. The membranes were developed using an ECL reagent.

### *Isolation of total RNA and reverse transcriptase-polymerase chain reaction (RT-PCR)*

Total RNA was isolated from LNCaP cells using Easy-Blue (iNtRON Biotechnology, Sungnam, Republic of Korea.) according to the manufacturer's instruction. RNA extracts was reverse-transcribed by M-MLV reverse transcriptase kit (BioNEER, Daejeon, Republic of Korea). In brief, cDNA synthetic was amplified via PCR using specific primer *GAPDH*

(forward 5'-TAC TAG CGG TTT TAC GGG CG-3' and reverse 5'-TCG AAC AGG AGG AGC AGA GAG CGA-3'), *p21* (forward 5'-GTA AAT CCT TGC CTG CCA GA -3' and reverse 5'-GGC TCC ACA AGG AAC TGA CT-3') and *Mad2* (forward 5'-CAT CCA CGC TGT TTT GAC CTC ACG-3' and reverse 5'-GGC TTT CTG GGA CTT TTC TCT-3'). The following PCR conditions were used: *GAPDH*, 27 cycles of denaturation at 94°C for 30 s, annealing at 60°C for 30 s, and extended at 72°C for 30 s; *p21*, 28 cycles of denaturation at 94°C for 30 s, annealing at 59°C for 30 s, and extended at 72°C for 30 s.

#### *Immunoprecipitation (IP)*

Cells were lysed in RIPA buffer containing 1 mM phenylmethylsulfonyl fluoride and protein inhibitor cocktail by sonication. After preclearing, 3 µl of antibodies was added for overnight and 20 µl of pierce protein A/G agarose was also added for 1 h. After centrifugation wash resin with 200 µl IP lysis/wash buffer (Thermo Scientific) in each wash. Bound proteins were separated by 10% SDS-PAGE gel electrophoresis and then analyzed by western blot analysis.

#### *Small interfering RNA (siRNA)*

Cells were seeded on a 24-well plate at a density of  $1 \times 10^5$  cells/ml and transfected *Mad2*-, *JNK*-, and *p21*-specific silencing RNA (siRNA, Santa Cruz Biotechnology) for 24 h. For each transfection, 450 µl growth medium was added to 20 nM siRNA duplex with the transfection reagent G-Fectin (Genolution Pharmaceuticals Inc., Seoul, Republic of Korea) and the entire mixture was added gently to the cells.

### *Cdk1 kinase activity*

Cdk1 kinase activity was measured by instructor protocol (MESACUP Cdk1 kinase assay kit, MBL International Corporation, Woburn MA). After the cells treated with CPT for 24 h sample were mixture with reaction mixture for 30 min. The absorbance of each well was taken at 492 nm using ELISA plate reader.

### *Immunofluorescence staining and confocal microscopy*

Cells were seeded on glass coverslips and incubated for 24h at 37°C with or without CPT washed twice with PBS and fixed with 90% methanol at 37°C for 30 min. The cells were again washed with PBS and blocked in 10% normal goat serum for 1 h and incubated with anti- $\alpha$ -tubulin antibody (1:200, Santa Cruz Biotechnology) overnight at 4°C. Primary antibody was removed by washing the membranes in PBS containing Triton-X (0.3%) and incubated for 1 h with Alexa 488-conjugated anti-mouse secondary antibody (1:200, Molecular Probes, Eugene, OR). Fluorescent signals were imaged using a confocal laser scanning microscope.

### *Electrophoretic mobility shift assay (EMSA)*

Transcription factor-DNA binding activity assays were carried out with nuclear protein extract. Synthetic complementary Sp1 (5'-ATT CGA TCG GGG CGG GCC GAG C-3', Santa Cruz Biotechnology) binding oligonucleotides was 3'-biotinylated utilizing the biotin 3'-end DNA labeling kit (Pierce) according to the manufacturer's instructions, and annealed for 30 min at 37°C. Samples were loaded onto native 4% polyacrylamide gels pre-electrophoresed for 60 min in 0.5X Tris borate/EDTA (TBE) buffer on ice, in the presence of transferred onto a positively charged nylon membrane (Hybond<sup>TM</sup>-N+) in 0.5X TBE buffer at

100 V for 1 h on ice. The transferred DNA-protein complex was cross-linked to the membrane at 120 mJ/cm<sup>2</sup>. Horseradish peroxidase-conjugated streptavidin was utilized according to the manufacturer's instructions to monitor the transferred DNA-protein complex.

#### *Tubulin polymerization in vitro assay*

Five mg/ml pure tubulin (cytoskeleton; Denver, CO) were brought to a steady state G-PEM buffer (100 mM PIPES (pH 6.9), 1 mM EGTA, 1 mM MgCl<sub>2</sub>, and 1 mM GTP) plus 10% glycerol in a 96-well plate by incubation at 37°C for 1 h. The effects on polymerization/depolymerization were quantified by measuring the absorbance at 340 nm (A<sub>340</sub>) with time.

#### *Biding of FITC-phalloidin to actin polymer*

Cells were stained with phalloidin-FITC at a concentration of 0.05 mg/ml to determine the amount of F-actin. Next cells were analyzed using a FACSCalibur flow cytometer.

#### *Cell culture and MTT assays*

Human prostate cancer cells were obtained from the American Type Culture Collection. Cells were cultured in RPMI 1640 medium supplemented with 10% FBS and antibiotics mixture. Cells were cultured at 37°C in a 5% CO<sub>2</sub>-humidified incubator in the presence or absence of CPT. The cytotoxicity was assessed by an MTT assay. Briefly, the cells were seeded in each well containing 500 µl of the RPMI medium supplemented with 10% FBS in a 24-well plate. After overnight, various concentrations of the indicated chemicals were added. After 24-h incubation, 70 µl MTT (5 mg/ml stock solution) were added and the plates were incubated for an additional 4 h. The medium was discarded and the formazan blue, which

was formed in the cells, was dissolved with 600  $\mu$ l dimethyl sulfoxide. The optical density was measured at 540 nm.

### *Statistical analysis*

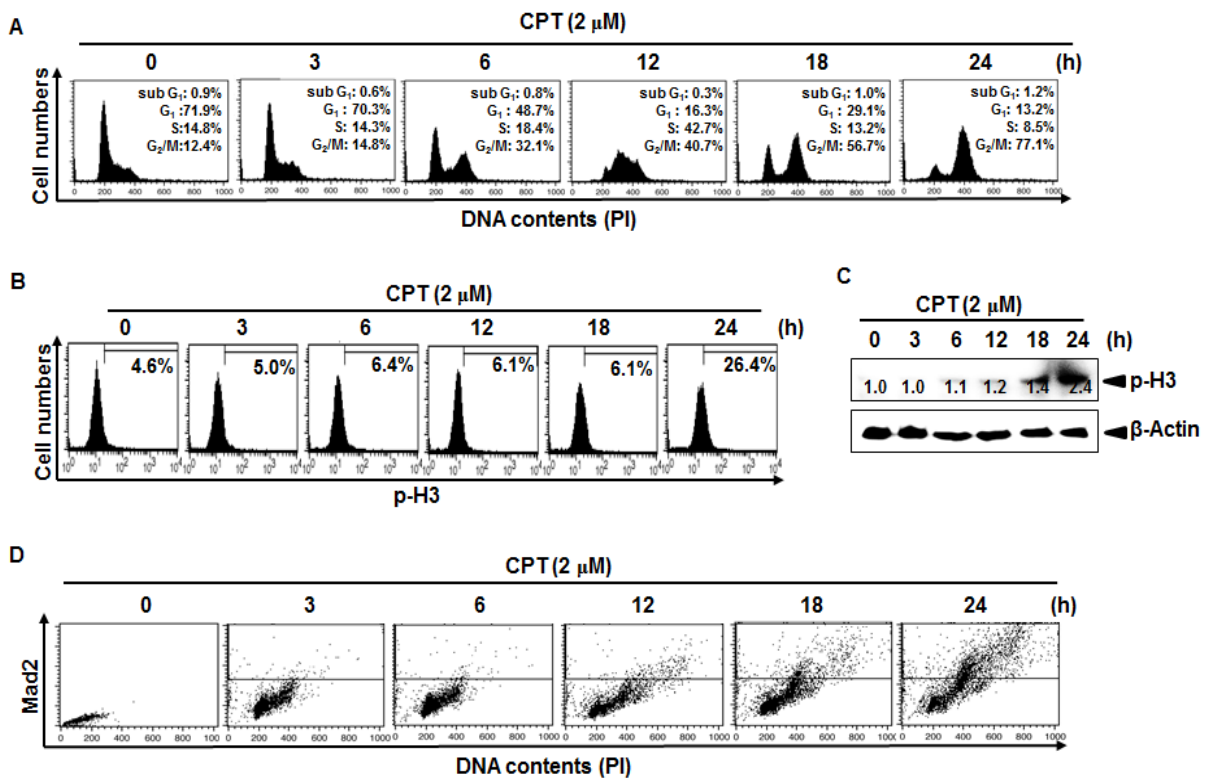
The images were visualized with Chemi-Smart 2000 (VilberLourmat, Marine, Cedex, France). Images were captured using Chemi-Capt (VilberLourmat) and transported into Photoshop. All bands were shown a representative obtained in three independent experiments and quantified by Scion Imaging software (<http://www.scioncorp.com>). Statistical analyses were conducted using SigmaPlot software (version 12.0) Values were presented as mean  $\pm$  standard error (S.E.). Significant differences between the groups were determined using the unpaired one-way and two-way ANOVA with Bonferroni post test. Statistical significance was regarded at <sup>a</sup> and <sup>b</sup>,  $p < 0.05$ .

### 3.3 Results

#### 3.3.1 Mad2 is a key M phase check point in CPT-induced cell cycle arrest

In order to assess if CPT regulates cell cycle arrest as shown in previous study [Zeng et al., 2012], we analyzed cell cycle progression of LNCaP cells. Florescence integration of G<sub>2</sub>/M phase significantly increased in a time-dependent manner in response to CPT, whereas G<sub>1</sub> phase markedly decreased (Fig. 1A). In peculiar, the cells stop S phase at 12 h after treatment with 2 μM of CPT and reached maximum G<sub>2</sub>/M phase arrest at 24 h. Nevertheless, apoptotic sub-G<sub>1</sub> phase was little seen in the presence, suggesting that CPT induces G<sub>2</sub>/M phase arrest with short stop at S phase, but not apoptosis. To identify in detail whether which stages, G<sub>2</sub> phase or M phase, are regulated, we examined phosphorylation of H3 because H3 is phosphorylated on Ser<sup>10</sup> during early mitosis which is relevant to chromatin condensation and a hall marker of M phase [Hirota et al., 2005]. We found that intracellular H3 phosphorylation significantly occurred at 24 h, which means that CPT-induced G<sub>2</sub> phase arrest appears at 18 h followed by M phase arrest at 24 h (Fig. 1B). Western blot analysis also confirmed that H3 undertook phosphorylation at Ser<sup>10</sup> at 18 h and significantly increased at 24 h (Fig. 1C). We next investigated the possibility that CPT regulates Mad2 expression because Mad2 monitors the kinetochore attachment to the spindle at M phase whereas the level of Mad2 increases with the unattached kinetochore [Saitoh et al., 2005]. Similar to the data of CPT-induced M phase arrest and H3 phosphorylation (Fig. 1A and 1B), CPT started in accumulation of intracellular Mad2 from at 12 h and maximum at 24 h, which may indicate that increase of Mad2 is consequence of cell cycle arrest or regulates M phase arrest (Fig. 1D). We also found that CPT gradually increased Mad2 expression in transcriptional and translational levels (Fig. 1E and 1F). Because, in addition to Mad2, Cdc20 is also known as a key component of spindle checkpoint machinery, which ensure proper attachment of

sister chromosome to kinetochores at the metaphase [Tian et al., 2012], we investigated binding activity Cdc20 to Mad2. CPT substantially enhanced Mad2 and Cdc20 binding complex at 12 h (Fig. 1G), which indicates that CPT enhances the formation of mitotic inhibitory checkpoint complex of Mad2/Cdc20 in LNCaP cells. In order to further understand the functional role of Mad2 in M phase arrest, endogenous level of Mad2 was transiently knock down by siMad2. Transient knockdown of Mad2 completely reversed CPT-induced M phase arrest to untreated-cell cycle distribution (Fig. 1H). These results indicate that CPT-induced Mad2 is a key player in M phase arrest.



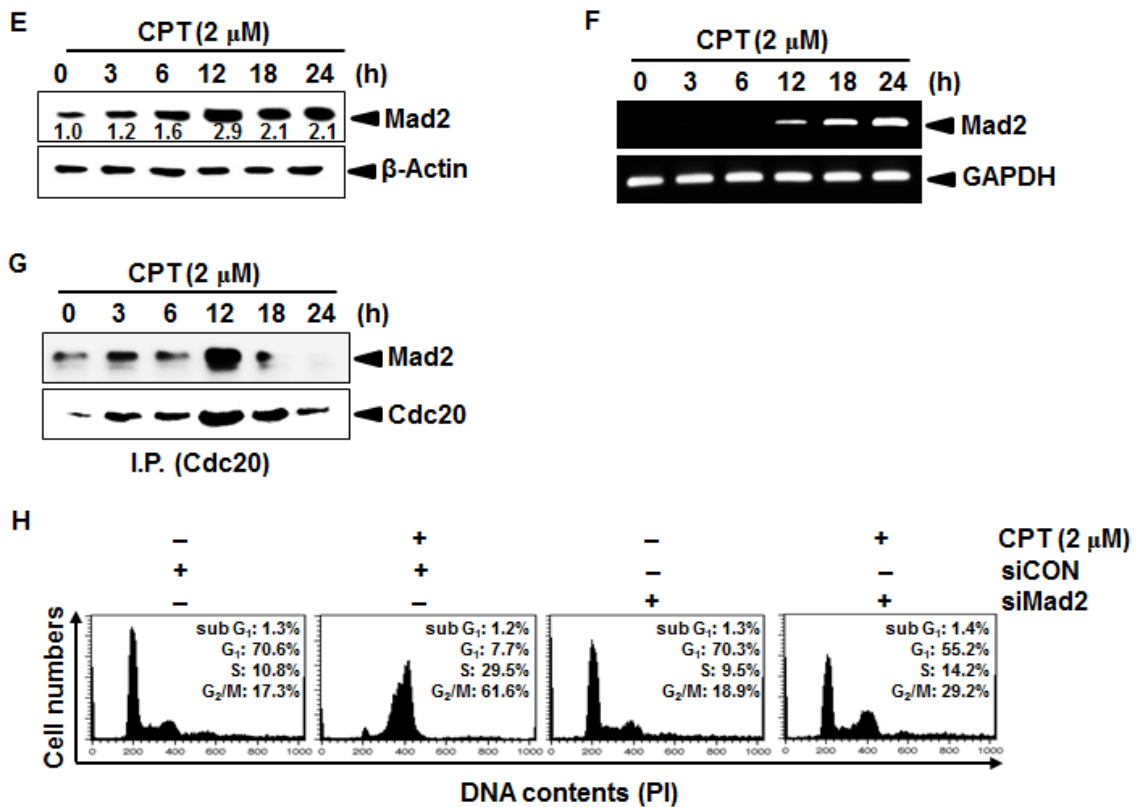


**Fig. 11.** Camptothecin (CPT)-induced Mad2 expression in LNCaP cells. LNCaP cells were seeded at  $1 \times 10^5$  cells/ml and were treated with 2  $\mu$ M CPT for the indicated times. (A) Cells were harvested, stained with PI, and analyzed for the cell cycle progression. (B) Cells stained with FITC-conjugated p-H3 antibody and analyzed by flow cytometer. (C) Total protein of p-H3 was subjected to 10% SDS-PAGE followed by western blotting with antibodies specific for p-H3. (D) LNCaP cells were cultured with 2  $\mu$ M CPT for 24 h. Cells were measured by dual analysis of Mad2 and DNA content (PI staining). (E) Western blot analysis for Mad2 using total protein lysates from control and CPT-treated LNCaP cells. LNCaP cells were cultured with 2  $\mu$ M CPT for 24 h. Total protein was subjected to 10% SDS-PAGE followed by western blotting with antibodies specific for Mad2. (F) In a parallel experiment, RNA was harvested and RT-PCR was performed for Mad2. (G) Cells were lysed and the cell lysates were immunoprecipitated with anti-Cdc20 antibody and precipitated with protein-G agarose. Bound protein were separated by gel electrophoresis and analyzed by western blot analysis.

(H) Effect of Mad2 on CPT-induced mitotic arrest. After cells were transfected with Mad2-targeted siRNA, the cells were treated with 2  $\mu$ M CPT, and DNA content was analyzed using a flow cytometer.  $\beta$ -Actin and GAPDH were used as the internal controls for western blot analysis and RT-PCR, respectively.

### 3.3.2 CPT-induced Mad2 regulates cyclin B1 and Cdk1

Mad2 delays metaphase progression by associating with Cdc20, thereby inhibiting APC/C activity resulting in an inability to degrade securin/cyclin B1 which is evidenced that accumulation of cyclin B1 in M phase arrest [Zeng et al., 2010]. Western blot analysis showed that treatment with CPT significantly increased in Cdk1 and cyclin B1 levels from at 6 h (Fig. 2A). Then, we studied that transient depletion of Mad2 expression by siMad2 inhibits CPT-induced Cdk1 and cyclin B1 levels. siMad2-transfected cells markedly decreased CPT-induced Cdk1 and cyclin B1 levels (Fig. 2B). Next, we were interested in measuring Cdk1 activity in response to CPT. Cdk1 activity upregulated 6 h after treatment with CPT and maximally reached at 24 (Fig. 2C). We also examined the subcellular localization of cyclin B1 using the immunofluorescence staining to identify the upregulation of cyclin B1 level in the absence of Mad2. Cyclin B1-GFP drastically increased by treatment with CPT compared to the untreated control (Fig. 2D). However, transient knockdown of Mad2 completely decreased the intensity of cyclin B1-GFP. These results indicate that CPT-induced Mad2 regulates cyclin B1 expression and Cdk1 activity.

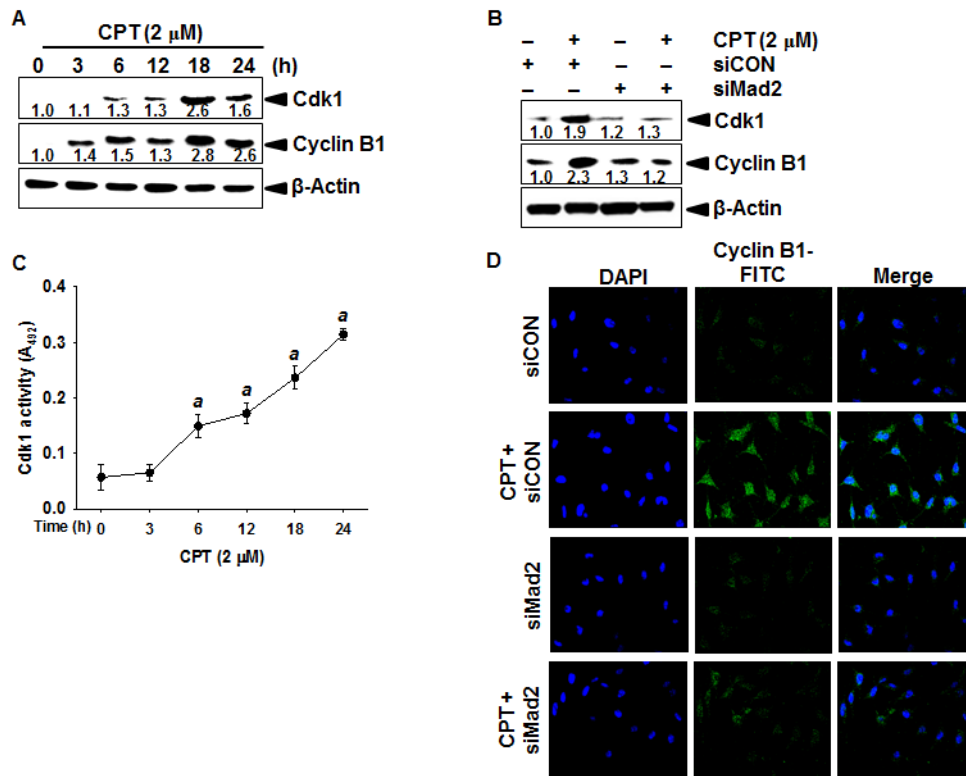


**Fig. 12.** Effect of camptothecin (CPT) on cyclin B1 and Cdk1. (A) LNCaP cells were seeded at  $1 \times 10^5$  cells/ml and were treated with 2  $\mu$ M CPT for the indicated times. Cell extracts were prepared for western blot analysis for cyclin B and Cdk1. (B) After LNCaP cells were transfected with Mad2-targeted siRNA, cells were treated with 2  $\mu$ M CPT, and then western blot analysis was performed with anti-cyclin B and anti-Cdk1. (C) LNCaP cells were seeded at  $1 \times 10^5$  cells/ml and were treated with 2  $\mu$ M CPT for the indicated times. Cdk1 activity was measured using an MESACUP Cdk1 kinase assay kit. (D) In a parallel experiment, cyclin B1 level was analyzed by immunofluorescence staining. LNCaP cells were fixed, permeabilized, and stained with anti-cyclin B monoclonal antibody. Monoclonal antibody was detected using an anti-rabbit secondary antibody conjugated with FITC under confocal microscopy.  $\beta$ -Actin was used as the internal controls for western blot analysis. Statistical significance was determined by one-way ANOVA (<sup>a</sup>,  $p < 0.05$  vs. 0 h).

### 3.3.3 CPT increases Mad2 expression by inducing JNK-mediated Sp1 activation

Recent data suggest that the JNK signaling pathways may be involved in controlling mitotic phase to tolerate chromosomal instability induced by spindle checkpoint defects [Hirota et al., 2005]. Therefore, we sought to evaluate the role of JNK in CPT-induced mitotic arrest in LNCaP cells. Treatment with 2  $\mu$ M CPT induced phosphorylation of JNK in a time-dependent manner. It clearly appeared after 12 h and peaked at 18 h in CPT-treated cells and the total JNK level was not altered. Another study showed that JNK led to phosphorylation and activation of several transcription factors including Sp1 during M phase [Chuang et al., 2008]. On the basis of above evidence, to evaluate activation of Sp1, we analyzed the nuclear translocation of Sp1 using CPT-treated nuclear extracts. The result showed that CPT induced translocation of Sp1 to the nucleus (Fig. 3B) and CPT also enhanced DNA-binding activity of Sp1 (Fig. 3C). To clarify the role of JNK in CPT-induced M phase arrest, we used siRNA approach to suppress JNK expression in LNCaP cells. siJNK significantly decreased CPT-induced DNA-binding activity of Sp1, which confirms that CPT-induced JNK activates Sp1 (Fig. 3D). Furthermore, transient knockdown of JNK (siJNK) abrogated CPT-induced increase of c-Jun phosphorylation compared to cells transfected with control siRNA (siCON) (Fig. 3E). Similarly, knockdown of JNK abrogated the CPT-induced upregulation of cyclin B1, Mad2, and p21, suggesting that JNK phosphorylation contributes to CPT-induced mitotic arrest by inducing Mad2-mediated cyclin B1/Cdk1. In order to verify whether CPT-induced JNK influence M phase arrest, we analyzed cell cycle progression. siJNK completely reversed CPT-induced M phase arrest with no apoptotic sub-G<sub>1</sub> phase. These data suggest that CPT-induced JNK is an important regulator resulting to Sp1 activation, which upregulates p21, Mad2, and cyclin B1.



### 3.3.4 CPT-induced phosphorylation of p21 promotes Mad2 expression

In order to determine relationship between increased p21 and CPT-induced M phase arrest, we analyzed expression and phosphorylation level of p21. CPT significantly induced the expression and phosphorylation level of p21 in transcription and translation stages (Fig. 4A and 4B). Treatment with CPT promoted the significant accumulation of p21 at 24 h after exposed. p21 is directly phosphorylated on Thr<sup>145</sup> and Ser<sup>146</sup> sites by inducing survival kinase PI3K and Akt, which are target molecules of PTEN. We also found that CPT increased the phosphorylation of PI3K and Akt in a time-dependent manner (unpublished data). Lin *et al.*, showed that attenuation of PTEN increased p21 stability by knockdown of PTEN; in contrary, inhibition of PTEN increased resistance to cisplatin-induced apoptosis associated with increased level of p21 [Lin et al., 2007]. Therefore, we demonstrated that CPT regulates expression and phosphorylation of PTEN. As presumed, treatment with CPT time-dependently resulted in downregulation of phosphorylated PTEN with total expression of PTEN (Fig. 4C). Next, we attempted to determine the precise role of p21 on M phase arrest. Transient transfection of sip21 slightly decreased the CPT-induced M phase cell population, but induced no sub-G<sub>1</sub> population (Fig. 4D); however, no normal cell cycle progression was recovered in response to sip21 transfection, suggesting that p21 is partially associated to CPT-induced M phase arrest. Nevertheless, transient knockdown of p21 (sip21) decreased CPT-induced Mad2 and cyclin B1 (Fig. 4E) as well as Cdk1 activity (Fig. 4F), which means that p21 is an upstream regulator in Mad2-mediated cyclin B1 and Cdk1. Finally, a CdkI completely restored CPT-induced M phase arrest to normal untreated cell cycle progression (Fig. 4G). These data indicate that p21 is partially associated to CPT-induced M phase arrest via Mad2-mediated cyclin B1 and Cdk1.

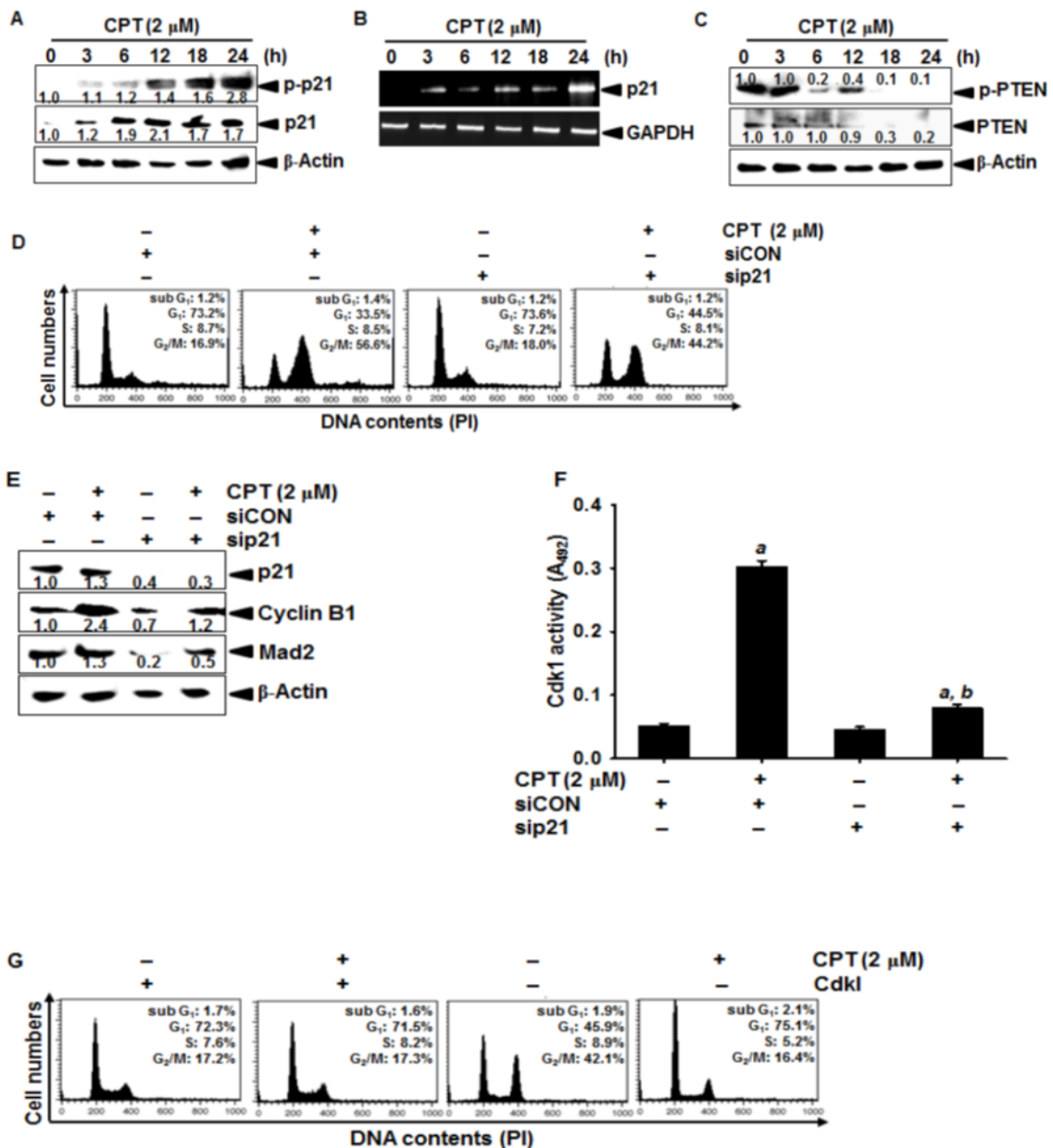


**Fig. 14.** Effect of camptothecin (CPT) on phosphorylation of p21 in LNCaP cells. (A and C) LNCaP cells were treated with 2  $\mu$ M CPT for the indicated times. Total protein was subjected to 10% SDS-PAGE followed by western blotting with antibodies specific for phosphorylated forms of p21(A) and PTEN (C). (B) Total RNA was isolated and RT-PCR analysis for p21 was performed. GAPDH was used as a loading control. (D) LNCaP cells were transiently transfected with sip21, the cells were treated with 2  $\mu$ M CPT, and DNA content was analyzed using a flow cytometer. (E) LNCaP cells were harvested at 24 h and whole-cell protein

lysates were prepared for detection of the indicated proteins by western blot analysis. (F) In a parallel experiment, Cdk1 kinase activity was measured using an MESACUP Cdk1 kinase assay kit. (G) LNCaP cells were pretreated with Cdk inhibitors (CdkI) and DNA content was analyzed using a flow cytometer 24 h after treatment with 2  $\mu$ M CPT.  $\beta$ -Actin and GAPDH were used as the internal controls for western blot analysis and RT-PCR, respectively. Statistical significance was determined by two-way ANOVA (a,  $p < 0.05$  vs. untreated control and b,  $p < 0.05$  vs. CPT-treated group).

### 3.3.5 CPT stimulates Mad2 expression resulting from tubulin polymerization

In order to investigate whether CPT activates Mad2 via actin or tubulin dysfunction in human LNCaP cells, we treated the cells with 2  $\mu$ M of CPT for 48 h. Treatment with CPT increased the nuclear structure size and enhanced an intensity of  $\alpha$ -tubulin staining measured by laser scan confocal microscopy (Fig. 5A, top); and treatment with CPT also increased cell size (Fig. 5A, bottom) compared to that of the untreated controls. Flow cytometric data also showed that treatment with CPT resulted in a significant increase of forward scatter (FSC) which means cell size and side scatter (SSC) which means granularity of cells (Fig. 5B), which indicates that CPT-induced M phase arrest results in cell division followed by bigger cell size and large granularity. Additionally, we found that long-term treatment with CPT increased M phase arrest resulting in endoreduplicated cell population which blocks cell division (Fig. 5C). Therefore, in order to attempt to find targets to induce M phase arrest and endoreduplication, we investigated whether CPT regulates tubulin or actin polymerization and/or depolymerization which are main target cytoskeletal dynamics for cell division. Addition of CPT induced significant tubulin polymerization from at 3 min compared to untreated control, similar to that of paclitaxel-treated positive control, suggesting that CPT

enhances tubulin polymerization (Fig. 5D). However, nocodazol caused to decrease tubulin polymerization. As shown in western blot analysis, CPT results in an increase of polymeric  $\alpha$ -tubulin to the level of paclitaxel. In a parallel experiment, treatment with CPT induced Mad2 expression was observed, which means that CPT-induced tubulin polymerization is a hall marker to block cell division with M checkpoint protein, Mad 2. Palloidin-FITC staining data showed that actin polymerization and/or depolymerization is not a target of CPT. Taken together these data indicate that CPT-induced tubulin polymerization block cell division, resulting in endoreduplication.

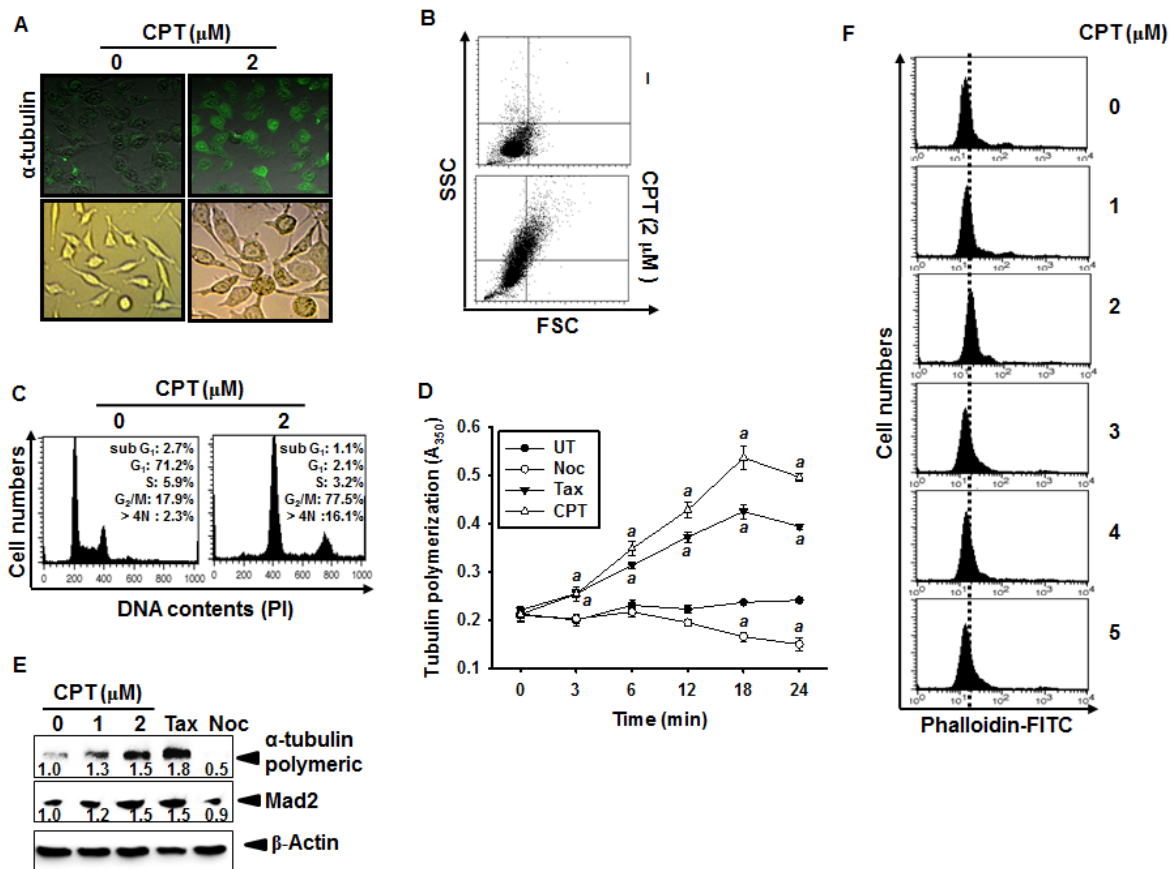


**Fig. 15.** Effect of camptothecin (CPT) on tubulin polymerization. LNCaP cells were seeded at  $1 \times 10^5$  cells/ml and were treated with 2  $\mu$ M CPT for the indicated times. (A) LNCaP cells were stained with  $\alpha$ -tubulin monoclonal antibody and analyzed by fluorescence microscopy. The morphology of cells was examined under a light microscopy. (B) Cell size (FSC) and intracellular granules (SSC) were detected by flow cytometric analysis 48 h after treatment with CPT. (C) LNCaP cells were treated with 2  $\mu$ M CPT for 48 h. The cells were stained with microtubulin polymerization. Microtubule associated protein-rich tubulin (1 mg/ml) was incubated at 37°C for 0–30 min and treated with 2  $\mu$ M CPT, 3  $\mu$ M nocodazole (Noc), and 3  $\mu$ M paclitaxel (Tax). (E) LNCaP cells were harvested and whole-cell protein lysates were prepared for detection of the Mad2 and  $\alpha$ -tubulin by western blot analysis. (F) LNCaP cells

were treated with CPT for the indicated concentrations. Cells stained with phalloidin-FITC and then analyzed using flow cytometer. Statistical significance was determined by one-way ANOVA ( $a$ ,  $p < 0.05$  vs. untreated group at each time point).  $\beta$ -Actin was used as the internal controls for western blot analysis.

### **3.3.6 Accumulation of procaspase-9 and autophagy regulates CPT-induced M phase arrest**

Recent studies showed that accumulation of several procaspases in M phase blocks the apoptosis [Matthess et al., 2010; Allan et al., 2007]. Therefore, we confirmed a hypothesis that CPT enhances M phase arrest by blocking apoptosis through accumulation of procaspases in the LNCaP cells. Western blot analysis confirmed that CPT time-dependently increased the expression of procaspase-9 and procaspase-8 (Fig. 6A). Next, we investigated cell viability in the presence of z-LEHD-FMK (a caspase-9 inhibitor), z-LETD-FMK (a caspase-8 inhibitor), and 3MA (an autophagy inhibitor). z-LEHD-FMK only but not z-LETD-FMK decreased relative cell viability in the presence of CPT (Fig. 6B); 3MA also showed similar action to z-LEHD-FMK, which suggest that accumulation of procaspase-9 and autophagy increases cell viability. Transfection of siMad2 did not significantly decrease z-LEHD-FMK and 3MA-induced cell viability in response to CPT. In order to verify in detail whether caspase-9 and autophagy regulate apoptosis in CPT-induced M phase arrest, we investigated cell cycle progression. CPT-induced M phase arrest decreased in the presence of z-LEHD-FMK and 3MA, which did not induce apoptosis, suggesting that accumulation of procaspase-9 and autophagy retain CPT-induced cell cycle progression in M phase. However, transfection of siMad2 replaced z-LEHD-FMK- and 3MA-induced restoration of cell cycle progression induced by CPT to apoptosis (Fig. 6C). Western blot analysis finally showed that transfection of siMad2 downregulated procaspase-9 and upregulated Bax in response to z-

LEHD-FMK and 3MA with CPT (Fig. 6D). Intriguingly, these data indicated that inhibition of caspase-9 and autophagy decreased CPT-induced M phase arrest in the presence of Mad2; however, the depletion of Mad2 increased CPT-mediated apoptosis in the presence of z-LEHD-FMK and 3MA.

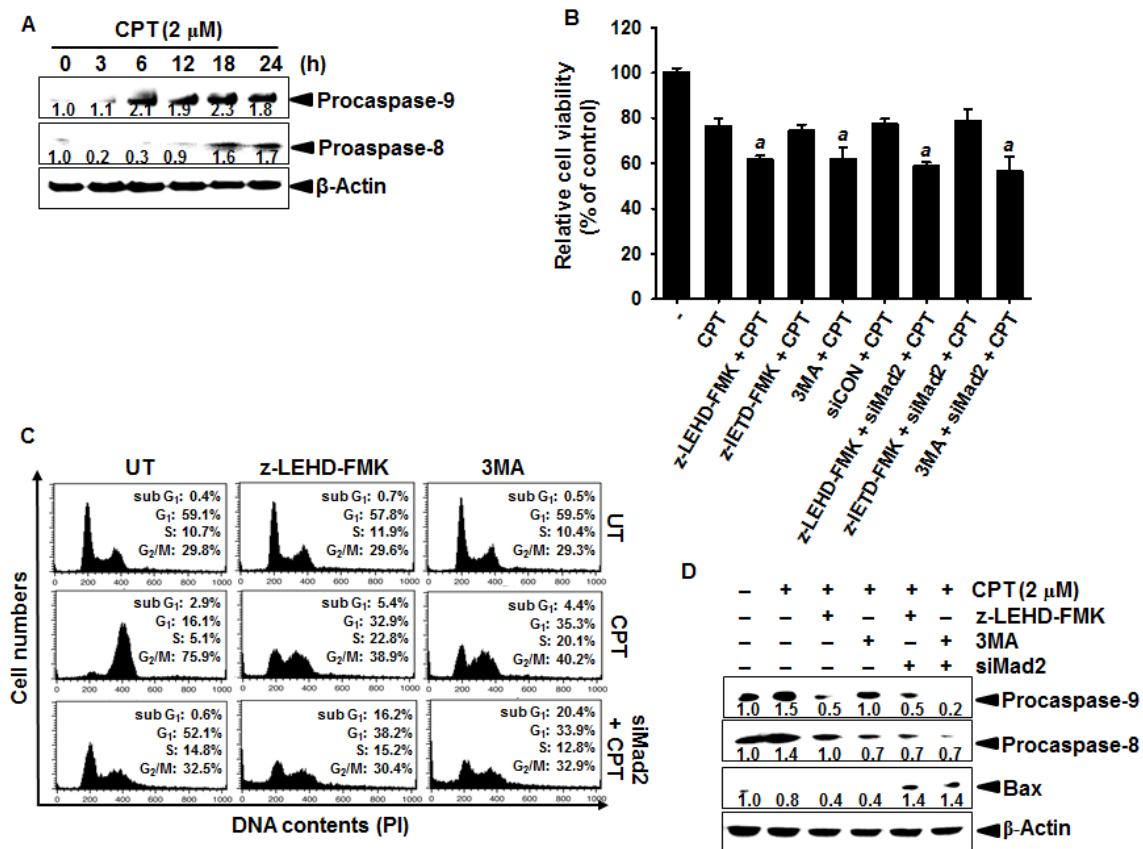


**Fig. 16.** Effect of camptothecin (CPT) on accumulation of caspase-9 and autophagy. LNCaP cells were seeded at  $1 \times 10^5$  cells/ml and were treated with 2 μM CPT for the indicated times. (A) LNCaP cells extracts were prepared for western blot analysis for caspase-8 and caspase-9. (B) Cells were pretreated with z-LEHD-FMK or z-IETD-FMK, 3-methyladenine (3MA) and siMad2, according to the indicated proportion, and cell viability was measured using an MTT assay. (C) LNCaP cells were transiently transfected with siMad2. The cells were treated with incubate with z-LEHD-FMK and 3-methyladenine (3MA) 2 μM before treatment with CPT and DNA content was analyzed using a flow cytometer. (D) In a parallel experiment,

LNCaP cells extracts were prepared for western blot analysis for Bax, caspase-8, and caspase-9. Statistical significance was determined by one-way ANOVA ( $^a$ ,  $p < 0.05$  vs. CPT-treated group).  $\beta$ -Actin was used as the internal controls for western blot analysis.

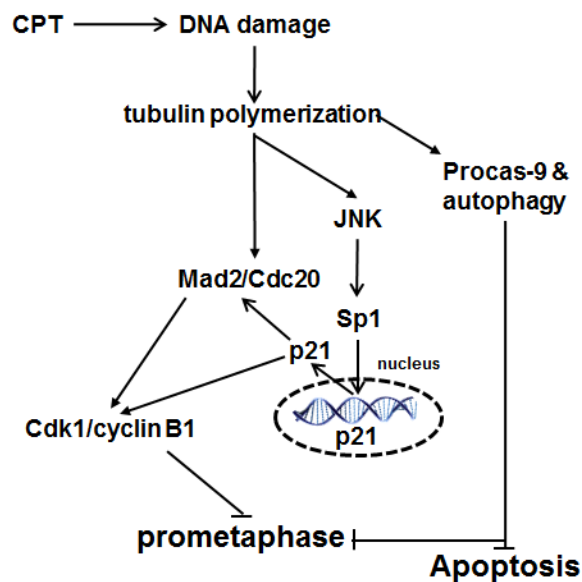


**Fig. 17.** Schematic explanation of camptothecin (CPT)-induced mitotic arrest. CPT directly binds to the topoisomerase I and DNA complex, resulting in a ternary complex and irreversibly stabilizing it, suggesting that unlike other direct tubulin-targeting drugs such as nocodazole and paclitaxel, CPT indirectly targets tubulin polymerization by chromosome instability. During CPT-induced chromosome instability, kinetochores lose equal tension of microtubule by tubulin polymerization, leading to engagement of Mad2, which prevents the cell cycle progression from prometaphase to metaphase and anaphase by inducing cyclin B1 and Cdk1 complex. Moreover, c-Jun-N-terminal kinase (JNK) partially stimulates Sp1-mediated p21 in Mad2-induced mitotic arrest in response to CPT. Additionally, accumulation of procaspase-9 and autophagy is required for the rapid increase of CPT-induced mitotic arrest. Following a prolonged prometaphase arrest, the CPT-treated cells are expected to undergo endoreduplication before apoptosis.

### 3.4 Discussion

Previous study showed that CPT is a novel anticancer drug as a strong inhibitor of the DNA-replicating enzyme topoisomerase I [Kim et al., 2015] which possesses immunomodulatory, anti-cancerous, and anti-proliferative effects [Mirakabadi et al., 2012]. We also published that CPT inhibited the invasion of cancer cells by inhibiting matrix metalloprotease-9 (MMP-9) and vascular endothelial growth factor (VEGF) expression via nuclear factor erythroid-derived 2-like 2 (Nrf2)-mediated hemoxygenase-1 (HO-1), and sensitized TNF- $\alpha$ -related apoptosis inducing ligand (TRAIL)-induced apoptosis [Jayasooriya et al., 2014; Jayasooriya et al., 2015]. Additionally, much evidence determined that CPT-induced cell cycle arrest was occurred in the different stages of various cell types [Shao et al., 1997; Park et al., 1997]. Recently, Kim *et al.*, reported that a synthetic water-soluble CPT derivative, CKD-602, induced G<sub>2</sub>/M phase arrest in oral squamous cancer cells [Kim et al., 2015]. Nevertheless, basic mechanism of CPT-induced cell cycle arrest has not been elucidated so far. CPT is a prominent therapeutic to treat cancers because CPT targets topoisomerase I which highly activated in cancer cells; however, CPT has not been used in clinical trial because of its low solubility and severe side effect such as diarrhea and hemorrhagic cystitis. Notwithstanding adverse effect of CPT, because of a promising capacity and specific-targeting ability of CPT in cancer cells, many scientists have been attempting to find CPT derivatives so far. In above respect, continuous studies on molecular mechanism of CPT might render basic information on molecular action of CPT derivatives because they aim a same molecular target, topoisomerase I, which shows similar pattern in anti-cancer effect. In the present study, we first investigated that the molecular mechanism responsible for CPT-induced M phase arrest by inducing Mad2, resulting in upregulation of Cdk1 and cyclin B1. Furthermore, CPT-induced Mad2 expression required JNK activation

which switches on the transcription factor Sp-1 (Fig. 7). Additionally, we found that CPT-induced accumulation of caspase-9 and autophagy render M phase arrest with Mad2 by blocking apoptosis.

SACs consistently monitors the integrity of spindle kinetochore attachment at prometaphase and/or metaphase for attain bipolar attachments [Gregan et al., 2011]. Mad2, BubR1, and other checkpoint components form an inhibitory ternary complex with E3 ligase, APC/C, and Cdc20. Once sister kinetochores correctly attach to bipolar region at metaphase, SACs are disabled and APC/Cdc20-mediated ubiquitination of securin and cyclin B required for the onset of anaphase [Foster et al., 2012]; however, after sister chromosome are inaccurately attached to kinetochores by microtubules at metaphase, SACs such as Mad2 is turned on, which delays cell cycle progression to enter from metaphase to anaphase [Allan et al., 2007]. The present study showed that Mad2 is upregulated in transcription and translation level in response to CPT, which indicates that CPT deregulated kinetochore attachment by inducing Mad2. We also found that CPT increased phosphorylation of H3 as an M phase maker, suggesting that CPT induces M phase arrest. Additionally, transient knockdown of Mad2 completely unraveled CPT-induced M phase arrest. Taken together, we concluded that CPT caused misconnection of microtubule to kinetochores of sister chromosomes, resulting in switching on SACs and consequently delayed or halted prometaphase or metaphase. In this study, we also found that depletion of Mad2 abrogated CPT-induced enhancing of cyclin B1 and Cdk1, suggesting that Mad2 mediates the upregulation of cyclin B1 and Cdk1. Transition from G<sub>2</sub> to M phase is triggered by the activation of the cyclin B1/Cdk1 complex which are sustained from prometaphase to metaphase and are totally destroyed in anaphase; in contrary, low cyclin B1/Cdk1 activity arrests cell cycle progression in S phase [Castedo et al., 2002]. Additionally, we showed that silencing of Mad2 significantly reduced CPT-induced M phase

accumulation without apoptotic sub G<sub>1</sub> phase. Taken together, our data indicate that CPT results in prometaphase or metaphase arrest without apoptosis by inducing the Mad2-mediated cyclin B1/Cdk1 pathway, resulting from instability of microtubules to kinetochores of sister chromosomes.

Recent study reported that JNK induced prometaphase and metaphase arrest by inducing JNK-mediated cyclin B1 and Cdk1 expression through phosphorylation and inhibition of Cdc25C, accompanied by chromatin abnormalities [Ribas et al., 2012]. Additionally, Gartel *et al.*, determined that JNK stabilized Sp1 via phosphorylation at Thr<sup>278</sup> and 739, leading to activate p21 which has six Sp1 binding sites at the core promoter region [Gartel et al., 2000]. Our earlier study showed that JNK inhibitor SP600125 inhibited the increase in the cellular content of p21 imply that important of JNK in p21 expression [Moon et al., 2011]. In the present study, CPT-induced Mad2 requires JNK activation, which in turn phosphorylates the transcription factor Sp1, thereby increasing Sp1 DNA-binding activity. Nevertheless, further experiment will be needed to identify other Mad2-regulating transcription factors because many transcription factors such as AP1, ATF-2, c-Jun, NF-κB directly bind to Mad2 promoter region and it is partly regulated by p53, Braca1 and Tax [Idikio et al., 2006]. We also found that knockdown of p21 slightly restored CPT-induced M phase arrest, but not completely; these data indicate that the JNK/Sp1/p21 pathway is partially involved in CPT-induced M phase arrest. p21 is well-known as a Cdk inhibitor 1 which directly binds and inhibits cyclin B1-Cdk1 complex in the transition from G<sub>2</sub> to M phase, and functions G<sub>2</sub>/M phase arrest [Abbas et al., 2009]; however, we found, in the present study, that p21 and cyclin B1-Cdk1 complex are simultaneously upregulated in response to CPT, suggesting that CPT regulates M phase arrest, not transition from G<sub>2</sub> to M phase. As the same of our data, previous studies confirmed that the treatment of cancer cells with microtubule inhibitors such as vinblastine,

paclitaxel, and nocodazole causes upregulation of cyclin B1 and Cdk1 complex, and Mad2 [Choi et al., 2012; Dumontet et al., 2010] however, there was no mention why p21 simultaneously upregulated. Charrier-Savournin *et al.*, clearly determined that p21 strictly sequestered cyclin B1 and Cdk1 complex, resulting in inactivation of the complex and consequently maintained G<sub>2</sub> phase arrest [Charrier-Savournin et al., 2004; Dulić et al., 1998]. Interestingly, Lindqvist *et al.*, proposed that mitotic cyclin B1-Cdk1 activity gradually increased after M phase entry and sustained by metaphase, allowing to efficient mitotic progression and beginning of mitotic exit [Lindqvist et al., 2007]. Moreover, microtubule inhibitors dramatically stabilized p21 in M phase, mainly sustaining in the cytosol, not in the nucleus, thus assisting cell survival signal [Kreis et al., 2015]. Though we need additional experiment whether p21 is in the cytosol and the nucleus of M phase arrest, CPT-induced p21 might be in the cytosol to trigger cell survival signal and CPT-induced free cyclin B1-Cdk1 complex monitors M phase progression.

Alenzi previously reviewed that cell cycle progression and apoptosis may be closely linked and thus cell cycle checkpoint molecules are requisite for apoptosis; in peculiar, during mitotic phase arrest, apoptosis seems to be restrained [Alenzi et al., 2004]. We also found that apoptosis appeared not to be seen in response to CPT; however, CPT remarkably increased mitotic phase arrest, thus promoting endoreduplication. Surprisingly, the new function of cyclin B1-Cdk1 complex during mitosis showed that key regulators which induce apoptosis such as caspases (caspase-8 and -9) are phosphorylated, leading to their inactivation by inhibiting active cleavage of caspases [Parrish et al., 2013]. Procaspase-8 is phosphorylated by Cdk1/cyclin B1 on Ser<sup>387</sup> in mitotic cells, which protect mitotic cells against extrinsic death stimuli [Matthess et al., 2010]. Caspase-9 is also phosphorylated at Thr<sup>125</sup> in mitosis by a Cdk1/cyclin B1, thus inducing mitotic arrest by microtubule dysfunction and a

nonphosphorylatable mutant of caspase-9 became sensitive to apoptosis [Allan et al., 2007]. In the present study, CPT treatment induced accumulation of procaspases-8 and -9 in mitotic arrest; unlike what we had thought, a caspase-9 inhibitor only decreased CPT-induced mitotic arrest through an unclear mechanism. An autophagy inhibitor, 3MA, also showed the same molecular pattern with a caspase-9 inhibitor, z-LEHD-FMK, which suggesting that accumulation of procaspase-9 and autophagy protects apoptosis, leading to CPT-induced mitotic arrest. Moreover, under transient knockdown of Mad2, z-LEHD-FMK and 3MA enhanced apoptosis with restoration of cell cycle progression from CPT-induced mitotic arrest, indicating that depletion of Mad2 induced apoptosis in the inhibition of caspase-9 and autophagy in response to CPT. Taken together, our data indicate that CPT induces Mad2-mediated cyclin B1 and Cdk1, leading to accumulation of procaspase-9 and autophagy, and thus induced mitotic phase arrest against apoptosis.

### **3.5 Conclusion**

In summary, our findings indicate that microtubule dynamic instability in response to CPT leads to prometaphase arrest by inducing Mad2-mediated cyclin B1 and Cdk1 via the JNK/Sp1/p21 pathway. Moreover, CPT-induced delay apoptosis was related to accumulation of procaspase-9 and autophagy. These novel biological properties of CPT may be attractive for understanding the molecular action of topoisomerase I-mediated tubulin targeting drugs.

## **Chapter 4**

### **Camptothecin enhances c-Myc-mediated endoplasmic reticulum stress, leading to autophagy**

## Abstract

Camptothecin (CPT) is known to selectively inhibit the nuclear enzyme DNA topoisomerase I which catalyzes the relaxation of negatively supercoiled DNA, leading to cell cycle arrest and apoptosis through DNA damages. However, whether CPT induces endoplasmic reticulum (ER) stress and autophagy has not been clearly understood. Therefore, the present study first reported that CPT enhanced expression and DNA-binding activity of c-Myc in LNCaP cells and transient knockdown of c-Myc completely abrogated reactive oxygen species (ROS) generation, resulting ER stress-regulating proteins such as PERK, eIF2 $\alpha$ , ATF4, and CHOP, which suggests that CPT-induced c-Myc triggered ER stress along with the PERK-eIF2 $\alpha$ -ATF4-CHOP pathway by increasing ROS generation. Moreover, CPT promoted autophagy formation accompanied by increase of autophagic proteins such as beclin-1 and Atg7, and decrease of p62 which is degraded in autophagosomes. Transfection of eIF2 $\alpha$ -targeted siRNA attenuated CPT-induced beclin-1 and Atg7 expression, and restored the level of p62. Treatment with autophagy inhibitors such as 3-methyladenine and bafilomycin A1 downregulated relative cell viability in response to CPT, indicating that CPT induces ER stress-mediated cytoprotective autophagy. Additionally, CPT significantly released intracellular Ca<sup>2+</sup> and upregulated Ca<sup>2+</sup>-mediated AMPK phosphorylation. is involved in CPT-mediated autophagy. A Ca<sup>2+</sup> chelator, ethylene glycol tetra acetic acid (EGTA) and a CaMKII inhibitor, K252a remarkably decreased CPT-induced beclin-1 and Atg7, accompanied by downregulation of AMPK phosphorylation, which suggests that CPT-induced Ca<sup>2+</sup> release leads to activate autophagy through CaMK-mediated AMPK phosphorylation. Moreover, CPT significantly phosphorylated JNK and activated DNA-binding activity of AP-1; knockdown of JNK abolished the expression level of beclin-1 and Atg7, implying that the JNK-AP-1 pathway is a potent mediator on CPT-induced autophagy.

Our findings indicate that CPT promotes ROS-mediated ER stress through the PERK-eIF2 $\alpha$ -ATF-4-CHOP pathway, which enhances cytoprotective autophagy, resulting from the Ca<sup>2+</sup>-AMPK pathway and the JNK-AP-1 pathway.

## 4.1 Introduction

The endoplasmic reticulum (ER) is a major site of protein synthesis in the eukaryotic organisms, which belongs to diverse machinery to ensure correct folding and assembly [Ellgaard et al., 2013]. Accumulation of unfolded or misfolded proteins due to redox environment alterations triggers the unfolded protein response (UPR), which causes evolutionally conserved stress in the lumen of ER (ER stress) [Teske et al., 2011]. In the basal ER state, ER chaperones such as BiP are sequester the UPR sensor proteins (PERK, IRE1, and ATF6), which represses the ER stress signal pathway, whereas the accumulation of misfolded proteins in the lumen of ER causes the saturation of ER chaperones, leading to ER stress [Hetz et al., 2014]. Under ER stress condition, three major the UPR sensor proteins fulfill three different signal pathways. First, PERK (PEK/EIF2AK3) mediates the translational control arm of the UPR by enhancing phosphorylation of eIF2 $\alpha$  inhibiting cap-mediated eukaryotic translation initiation [Joyce et al., 2013; Han et al., 2013]. Stress inducible transcription factor ATF4 is preferentially upregulated upon EIF2S1/eIF2 $\alpha$  phosphorylation, leading to activate CHOP [Masuda et al., 2013]. Second, IRE1 activates c-Jun-NH<sub>2</sub>-terminal kinase (JNK), accompanied by scaffold proteins and induces splicing of XBP1, which enhances ER chaperones [Chen et al., 2014]. Third, activated ATF6 moves into Golgi complex where is the machinery to cleave the cytoplasmic domain of ATF6 by site-1 protease and site-2 protease [Walter et al., 2011]. The ER stress basically prevents cells against UPR stress by increasing much ER chaperones; however, excessive ER stress

enhances apoptosis by interplaying between ER and mitochondria [Xu et al., 2005]. Therefore, ER stress is an important interplayer between cell survival and cell death.

Accumulation evidence suggested that reactive oxygen species (ROS) generation is integral component between ER stress and mitochondria, which effectively induces apoptosis by activating the intrinsic apoptotic pathway [Bhandary et al., 2013; Tabas et al., 2011]. In peculiar, the PERK/eIF2/ATF4/CHOP pathway transports well-tuned cell death signal by inducing apoptotic genes such as Puma and Noxa; CHOP which is also a downstream molecule of ATF6, inhibits expression of anti-apoptotic genes such as Bcl-2 and Bcl-XL; and IRE1 prevent the expression of anti-apoptotic genes by activating JNK [Iurlaro et al., 2015]. Moreover, it is suggested that, during ER stress,  $Ca^{2+}$  transits apoptotic signal from ER to mitochondria via the various signal pathways such as GRP78 and p53 [Hammadi et al., 2013; Giorgi et al., 2015]. In contrary, ER stress activates autophagy to overcome the stress compensatory pathway for ER-associated degradation, resulting in cell survival [Ishida et al., 2009]. Moreover, Shen *et al.*, reported that ROS-mediated JNK switches from ER stress-mediated apoptosis to autophagy by activating the PERK-dependent ATF4 pathway [Shen et al., 2015]. eIF2 $\alpha$  and ATF4 are also essential for ER stress-mediated autophagy by upregulating expression of autophagic gene such as beclin-1, Atg7, Atg12, and p62 [B'chir et al., 2013]. Additionally, activation of IRE1 connects autophagy to ER stress by activating JNK, which is known to control the key autophagy regulator beclin-1 expression [Cheng et al., 2014]. However, excessive ER stress fails to trigger apoptosis, the stress massively increases, leading to cell damage and necrotic death [Cheng et al., 2011]. Therefore, accumulation of much evidence suggests that survival and death are regulated by modulating the implication between autophagy and ER stress.

c-Myc is a transcription factor that activates expression of many genes involved in

multiple physiological functions, including control of cell cycle progression, apoptosis, nucleotide biosynthesis, and basal metabolism [Dang et al., 1999]. A previous study showed that c-Myc promotes mitochondrial gene expression and biogenesis, leading to ROS generation from mitochondria, which results in oxidative damage-mediated genomic instability [Dang et al., 2005]. On the other hand, during ER stress, hyperactive c-Myc-mediated eIF2 $\alpha$  phosphorylation enhances total protein synthesis and simultaneously accumulates unfolded or misfolded proteins in the lumen of ER and the active eIF2 $\alpha$  also induces autophagy by joining ATF4, which also transcribes CHOP by means of c-Myc [Dey et al., 2013]. Taken together, these discrepancy shows that c-Myc is a messenger between ER stress-mediated autophagy and apoptosis. Recently, camptothecin (CPT) derivatives, hydroxycamptothecin, stimulates expression of the UPR sensor proteins such as PERK, ATF6, and IRE1, leading to increase apoptosis via the mitochondrial apoptotic pathway, accompanied by S phase arrest [Yin et al., 2013]. Accordingly, c-Myc enhances CPT-induced apoptosis by inducing protein kinase C delta (PKC $\delta$ ) [Albihn et al., 2007]. However, there is no evidence whether CPT-induced c-Myc is a mediator in the ER stress response, resulting in induction of autophagy. Here, we found that c-Myc is an important factor to downregulate expression of the UPR sensor proteins in LNCaP cells accompanied by ROS generation; which induces autophagy formation via the Ca<sup>2+</sup> and the JNK signal pathway.

## 4.2 Materials and methods

### *Reagents and antibodies*

CPT, 3-(4,5-dimethylthiazol-2-yl)-2,5-diphenyltetrazolium bromide (MTT), glutathione (GSH), 3-methyladenine (3MA), bafilomycin A1 (BAF), ethylene glycol tetraacetic acid (EGTA), and K252a were purchased from Sigma (St. Louis, MO) and an enhanced chemiluminescence (ECL) kit was purchased from Amersham (Arlington Heights, IL). RPMI 1640 medium, fetal bovine serum (FBS), and antibiotics mixture was purchased from WelGENE (Daegu, Republic of Korea). Antibodies against CHOP, PERK, phospho (p)-PERK, eIF2 $\alpha$ , p-e-IF2 $\alpha$ , ATF4, AMPK, p-AMPK, beclin 1, and  $\beta$ -actin were purchased from Santa Cruz Biotechnology (Santa Cruz Biotechnology, San Diego, CA). Antibodies against c-Myc, Atg7, p62, p-JNK, JNK, and p-c-Jun were purchased from Cell Signaling (Beverly, MA). 2',7'-Dichlorodihydrofluorescein diacetate (H2DCFDA), Fluo3-AM, ER-tracker, and acridine orange were purchased from Molecular Probes (Eugene, OR). SP600125 was purchased from Calbiochem (San Diego, CA). Peroxidase-labeled donkey anti-rabbit and sheep anti-mouse immunoglobulin was purchased from Koma Biotechnology (Seoul, South Korea).

### *Cell culture and viability assay*

Human prostate cancer LNCaP cells were obtained from the American Type Culture Collection. The cells were cultured at 37°C in a 5% CO<sub>2</sub>-humidified incubator and maintained in RPMI 1640 culture medium containing 10% FBS and antibiotics mixtures. The cells were seeded ( $4 \times 10^4$  cells/ml) and then incubated for 24 h with CPT. MTT assays were done to assess cell viability.

### *Isolation of total RNA and RT-PCR*

Total RNA was isolated from LNCaP cells using Easy-Blue (iNtRON Biotechnology, Sungnam, Republic of Korea.) according to the manufacturer's instruction. RNA extracts was reverse-transcribed by M-MLV reverse transcriptase kit (BioNEER, Daejeon, Republic of Korea). In brief, cDNA synthetic was amplified via PCR using specific primer c-Myc (Forward: 5'-AAT GAA AAG GCC CCC AAG GTA GTT ATC C-3', Reverse: 5'-GTC GTT TCC GCA ACA AGT CCT CTT C-3') and GAPDH (forward 5'-TAC TAG CGG TTT TAC GGG CG-3' and reverse 5'-TCG AAC AGG AGG AGC AGA GAG CGA-3'). The following PCR conditions were used: GAPDH, 27 cycles of denaturation at 94°C for 30 s, annealing at 60°C for 30 s, and extended at 72°C for 30 s; c-Myc, 28 cycles of denaturation at 94°C for 30 s, annealing at 59°C for 30 s, and extended at 72°C for 30 s.

### *Western blot analysis*

Total cell extracts were prepared using the PRO-PREP protein extraction solution (iNtRON Biotechnology; Sungnam, Republic of Korea). Cell lysates were centrifuged at  $16,000 \times g$  at 4°C for 20 min to gain supernatants. Cytoplasmic and nuclear protein extracts were prepared using NE-PER nuclear and cytosolic extraction reagents (Pierce, Rockford, IL). Total cell extracts were separated on polyacrylamide gels and standard procedures were used to transfer them to the nitrocellulose membranes. The membranes were developed using an ECL reagent.

### *Electrophoretic mobility shift assay (EMSA)*

DNA binding activity assays were carried out with nuclear protein extract. Synthetic complementary c-Myc -binding oligonucleotides (5'-GGA AGC AGA CCA CGT GGT CTG

CTT CC-3', Santa Cruz Biotechnology) was 3'-biotinylated using a biotin 3'-end DNA labeling kit (Pierce) according to the manufacturer's instructions, and annealed for 30 min at 37°C. Samples were loaded onto native 4% polyacrylamide gels pre-electrophoresed for 60 min in 0.5× Tris borate/EDTA (TBE) buffer on ice and transferred onto a positively charged nylon membrane (Hybond<sup>TM</sup>-N<sup>+</sup>) in 0.5× TBE buffer at 100 V for 1 h on ice. The transferred DNA-protein complex was cross-linked and horseradish peroxidase-conjugated streptavidin was utilized according to the manufacturer's instructions to monitor the transferred DNA-protein complex.

#### *Transfection of small interfering RNA (siRNA)*

Cells were seeded on a 24-well plate at a density of  $1 \times 10^5$  cells/ml and transfected *c-Myc*-, *JNK*-, and *eIF2 $\alpha$* -specific silencing RNA (siRNA, Santa Cruz Biotechnology) for 24 h. For each transfection, 450  $\mu$ l growth medium was added to 20 nM siRNA duplex with the transfection reagent G-Fectin and the entire mixture was added gently to the cells. Transfected cells were maintained in culture for 24 h before harvesting for further analysis. The efficiency of the siRNA knockdown for each gene was determined by western blot analysis.

#### *Immunofluorescence staining and confocal microscopy*

LNCaP cells were seeded on glass coverslips and incubated for 24 h at 37°C with or without CPT, washed twice with PBS, and fixed with 90% methanol at 37°C for 30 min. The cells were again washed with PBS, blocked in 10% normal goat serum for 1 h, and incubated with p-PERK and beclin overnight at 4°C. Primary antibody was removed by washing the membranes in PBS containing Triton-X (0.3%) and incubated for 1 h with Alexa 488-

conjugated anti-mouse secondary antibody (Molecular Probes, Eugene, OR, 1:200). Fluorescent signals were imaged using a confocal laser scanning microscope.

#### *Measurement of reactive oxygen species*

LNCaP cells were seeded on 24-well plate at a density of  $2 \times 10^5$  cells/ml and sic-Myc transfected for 24 h. Then cells were preincubated with cell-permeable H<sub>2</sub>DCFDA fluorescence dye for 1 h and then treated the indicated concentrations of CPT for 24 h. The cells were lysed with Triton X-100 and supernatant was analyzed for ROS production using a GLOMAX luminometer (Promega, Madison, WI). In a parallel experiment, DCFDA fluorescence intensity was also analyzed by a FACSCalibur flow cytometry (Becton Dickinson, San Jose, CA).

#### *Measurement of autophagy*

Cells were plated at a density of  $2 \times 10^5$  cells/ml and exposed for the 2  $\mu$ M CPT for indicated time points. The cells were stained with acridine orange for 30 min at 37°C and flow cytometry was used to determine the fluorescence intensity.

#### *Ca<sup>2+</sup> influx assay*

The intracellular free Ca<sup>2+</sup> was measured with Flu3-AM dye. The cells were stained with Flu3-AM for 30 min at room temperature, cells were treated with the indicated concentration of CPT and fluorescence intensity was obtained using flow cytometry.

#### *Statistical analysis*

The images were visualized with Chemi-Smart 2000 (VilberLourmat, Marine, Cedex,

France). Images were captured using Chemi-Capt (VilberLourmat) and transported into Photoshop. All bands were shown a representative obtained in three independent experiments and quantified by Scion Imaging software (<http://www.scioncorp.com>). Statistical analyses were conducted using SigmaPlot software (version 12.0) Values were presented as mean  $\pm$  standard error (S.E.). Significant differences between the groups were determined using the unpaired one-way and two-way ANOVA with Bonferroni post test. Statistical significance was regarded at <sup>a</sup> and <sup>b</sup>,  $p < 0.05$ .

## 4.3 Results

### 4.3.1 CPT induces c-Myc-mediated ROS generation, accompanied by CHOP expression

Because CPT induces apoptosis by inducing DNA damage [Shen et al., 2015; B'chir et al., 2013], we first investigated whether CPT regulates c-Myc-mediated ROS generation in response to the damage. RT-PCR and western blot analysis showed that CPT enhanced expression of c-Myc at the transcription (Fig. 1A) and the translation (Fig. 1B) levels in a time-dependent manner. An EMSA also confirmed that CPT induced c-Myc translocation to the nucleus and enhanced DNA-binding activity of c-Myc when cells exposed to the c-Myc response element containing oligonucleotide (Fig. 1C). Because recent study also showed that transfection of c-Myc elevated the ROS levels [Shen et al., 2015], we, therefore, analyzed that CPT-induced c-Myc is involved in ROS generation in LNCaP cells. As presumed, CPT significantly increased ROS generation compared to that of untreated control; however, transient knockdown of c-Myc completely downregulated CPT-induced ROS generation (Fig. 1D). In order to verify interrelationship between c-Myc and ROS in response to CPT, we also examined CPT-mediated ROS generation in c-Myc-transfected LNCaP cells. As same to the result of Fig. 1D, depletion of c-Myc alleviated the intensity of DCFDA

fluorescence in response to CPT (Fig. 1E). Next, we investigated whether CPT regulates expression of CHOP in LNCaP cells, because c-Myc-mediated ROS increases CHOP expression accompanied with ATF4, which induces ER stress [B'chir et al., 2013]. Western blot analysis showed that CPT gradually increased CHOP expression in a time-dependent manner (Fig. 1F). Moreover, knockdown of c-Myc downregulated the CPT-induced CHOP expression, which suggests that CPT multiplies c-Myc-mediated ROS generation, leading to increase CHOP expression which may increase ER stress.

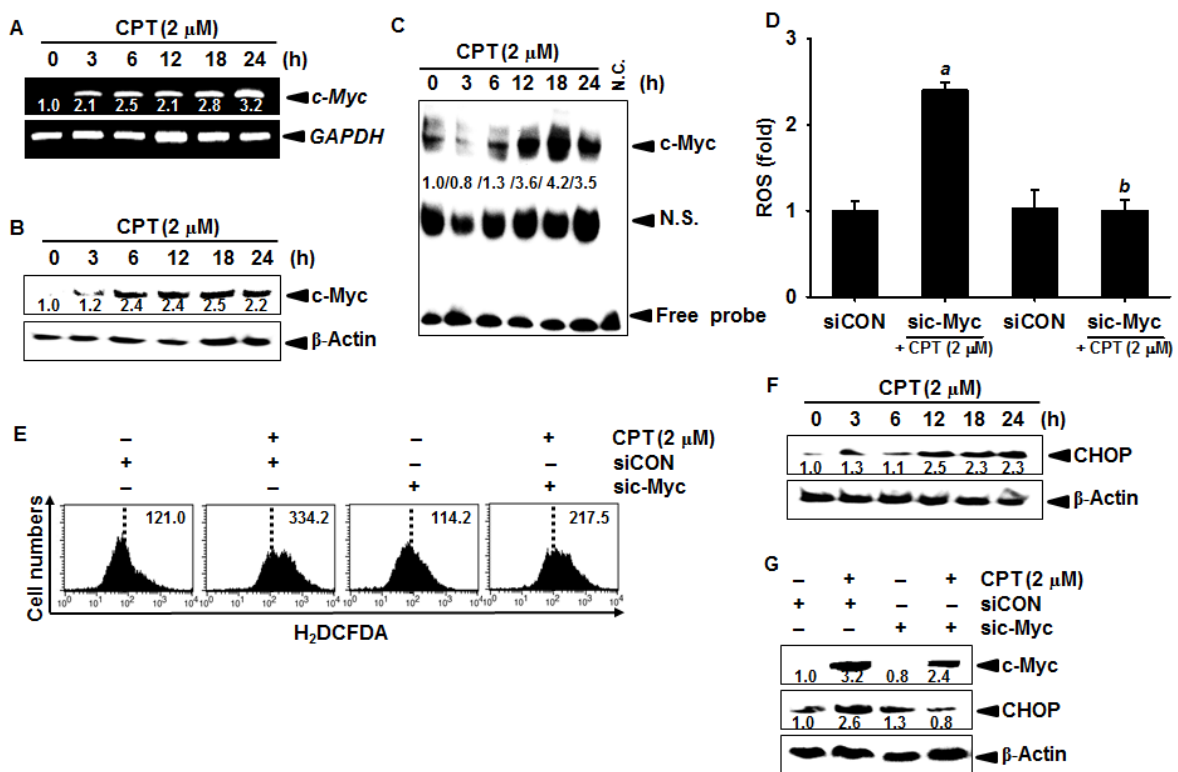


**Fig. 18.** Effect of camptothecin (CPT) on c-Myc dependent reactive oxygen species (ROS) production. (A) LNCaP cells were treated with 2  $\mu$ M CPT for the indicated time point. Total (B) Equal amount of cell lysates were resolved on SDS-polyacrylamide gels, transferred to nitrocellulose membranes and probed with antibodies against c-Myc. (C) In a parallel experiment, nuclear extracts were prepared to analyze DNA-binding activity of c-Myc by EMSA. (D) LNCaP cells were transiently transfected with c-Myc siRNA (sic-Myc) and then

ROS production was measured at 24 h using a fluorometer. (E) Cells were stained with H<sub>2</sub>DCFDA and ROS level was analyzed for flow cytometer. (F) Equal amount of cell lysates were resolved on SDS-polyacrylamide gels, transferred to nitrocellulose membranes and probed with antibodies against CHOP. (G) In a parallel experiment equal amount of cell lysates were resolved on SDS-polyacrylamide gels, transferred to nitrocellulose membranes and probed with antibodies against c-Myc and CHOP.  $\beta$ -Actin and GAPDH were used as the internal controls for western blot analysis and RT-PCR, respectively. Statistical significance was determined by two-way ANOVA (<sup>a</sup>,  $p < 0.05$  vs. untreated control and <sup>b</sup>,  $p < 0.05$  vs. siCON-treated group). N.S.; nonspecific.

#### 4.3.2 c-Myc regulates CPT-induced ER stress by inducing ROS generation

In order to assess in detail whether CPT induces ER stress because CPT stimulates c-Myc-mediated ROS generation, resulting in CHOP expression which is a key transcription factor of ER stress, we verify expression of PERK, eIF2 $\alpha$ , and ATF4. Treatment with CPT increased phosphorylation of PERK and eIF2 $\alpha$ , and expression of ATF4 in a time-dependent manner, which means that CPT activates the PERK-eIF2 $\alpha$ -ATF4 pathway (Fig. 2B). Next, live cells were stained with ER-tracker-FITC dye, which increased the intensity according to the concentrations of CPT, leading to ER stress (Fig. 2B). Immunofluorescent staining results showed that CPT-treated cells exhibited significant increase of p-eIF2 $\alpha$ -FITC intensity compared that of untreated control, suggesting that CPT increased ER stress (Fig. 2C). However, transfection of sic-Myc completely reduced the intensity of p-eIF2 $\alpha$ -FITC, which may imply that CPT-induced phosphorylation of eIF2 $\alpha$  are regulated by c-Myc (Fig. 2D). Moreover, as presumed, depletion of c-Myc abrogated CPT-induced phosphorylation of PERK and eIF2 $\alpha$ , and expression of ATF-4. Then, we examined the effect of inhibition of

ROS with the presence of antioxidant on ER marker protein. Treatment with GSH significantly downregulated the level of eIF2 $\alpha$  phosphorylation and ATF4 expression in LNCaP cells. Taken together, these results indicate that CPT stimulates the PERK-eIF2 $\alpha$ -ATF4 pathway, resulting from c-Myc-induced ROS generation, which lead to ER stress.

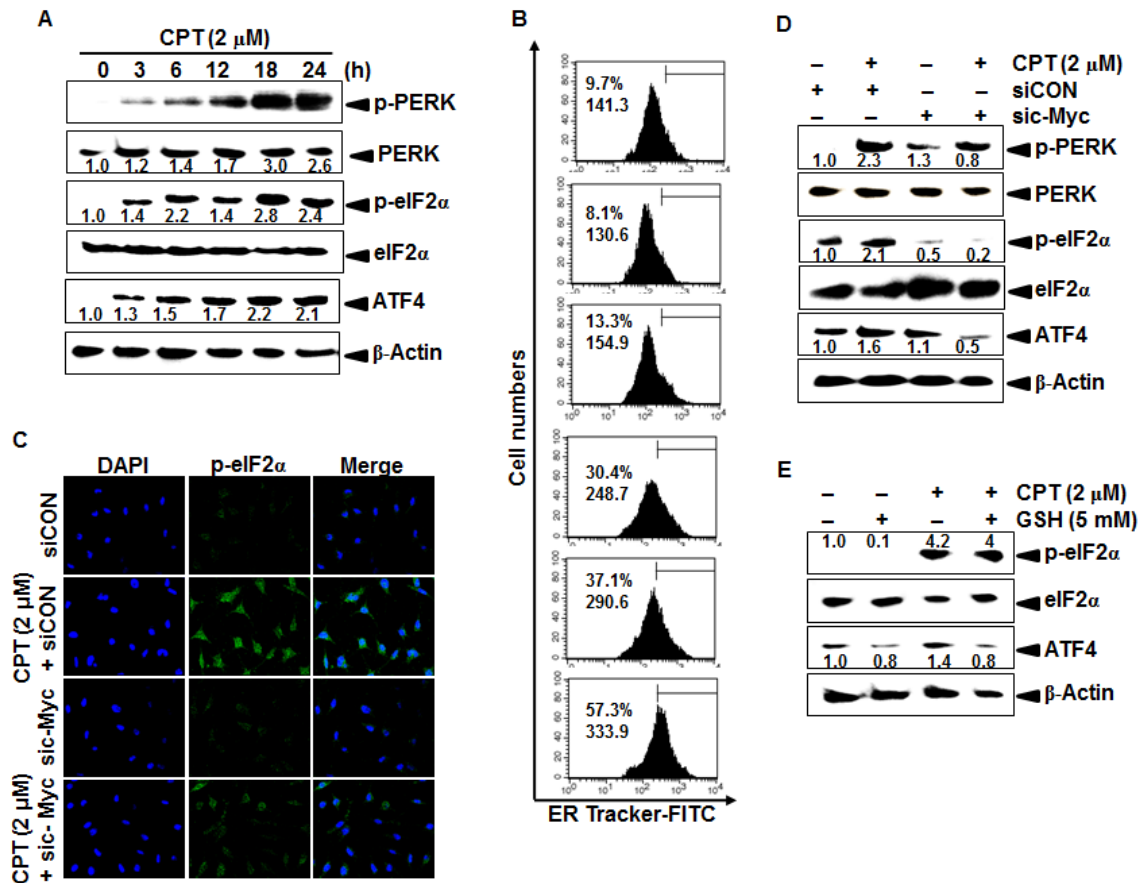


**Fig. 19.** Effect of camptothecin (CPT) on endoplasmic reticulum (ER) stress. LNCaP cells were treated with 2  $\mu$ M CPT for the indicated time point. (A) Equal amount of cell lysates were resolved on SDS-polyacrylamide gels, transferred to nitrocellulose membranes and probed with antibodies against indicated protein. (B) LNCaP cells were treated with 2  $\mu$ M CPT at the indicated times and then stained with FITC-conjugated ER-Tracker. The fluorescence intensity of the ER Tracker was analyzed by a flow cytometer. (C) After LNCaP cells were transfected with c-Myc-targeted siRNA (sic-Myc), the cells were treated with 2  $\mu$ M CPT and then p-eIF2 $\alpha$  level was analyzed by immunofluorescence staining. The cells were fixed, permeabilized, and stained with anti-p-eIF2 $\alpha$  monoclonal antibody. Monoclonal antibody was detected using an anti-rabbit secondary antibody conjugated with FITC under confocal microscopy. (D) LNCaP cells were preincubated with GSH prior to treatment with 2

$\mu\text{M}$  CPT for 24 h. Equal amount of cell lysates were resolved on SDS-polyacrylamide gels, transferred to nitrocellulose membranes, and probed with antibodies against indicated protein. (E) After cells transfected with sic-Myc, cells were treated with 2  $\mu\text{M}$  CPT and the indicated proteins were analyzed using western blot analysis.  $\beta$ -Actin was used as the internal control for western blot analysis.

#### **4.3.3 CPT promotes autophagy formation, resulting from ER stress**

Since CPT had no morphologically apparent apoptotic effect on LNCaP cells (data not shown), we investigated the effect of CPT on induction of autophagy. Flow cytometry data confirmed that LNCaP cells stained with acridine orange time-dependently increased the fluorescent intensity, which indicates that CPT increases autophagy in LNCaP cells (Fig. 3A). Fig. 3B showed that the expression levels of autophagy related proteins beclin-1 and Atg7 markedly increased in response to CPT in a time-dependent manner. Western blot analysis also revealed that CPT concomitantly abrogated the autophagy initiating p62 expression. Additionally, intensity of FITC-conjugated beclin-1 was observed under laser scan confocal microscopy. Fluorescent intensity of beclin-1 dose-dependently increased in LNCaP cells in response to CPT. Recent study showed that UPR activation results in ER expansion and the formation of autophagosomes, leading to cell survival [Dang et al., 2005]. Therefore, we investigated whether inhibition of ER stress using siEIF2 $\alpha$  has effect on autophagy-regulating proteins. As shown in Fig. 3D, knockdown of eIF2 $\alpha$  downregulated the level of beclin-1 and atg7, whereas upregulated the level of p62. These data indicate that CPT induces autophagy formation in LNCaP cells, resulting from ER stress. Because dual function of autophagy interplays between cell survival and cell death, we needed to elucidate the role of CPT-induced autophagy. To address the function of autophagy in response to CPT, we measured

the cell viability in the presence of autophagy inhibitors, 3MA and BAF. Pretreatment with autophagy inhibitors diminished the cell viability, but the effect was slight than our expectation. Taken together, these results suggest that CPT promotes autophagy as partial cytoprotection by stimulating ER stress.

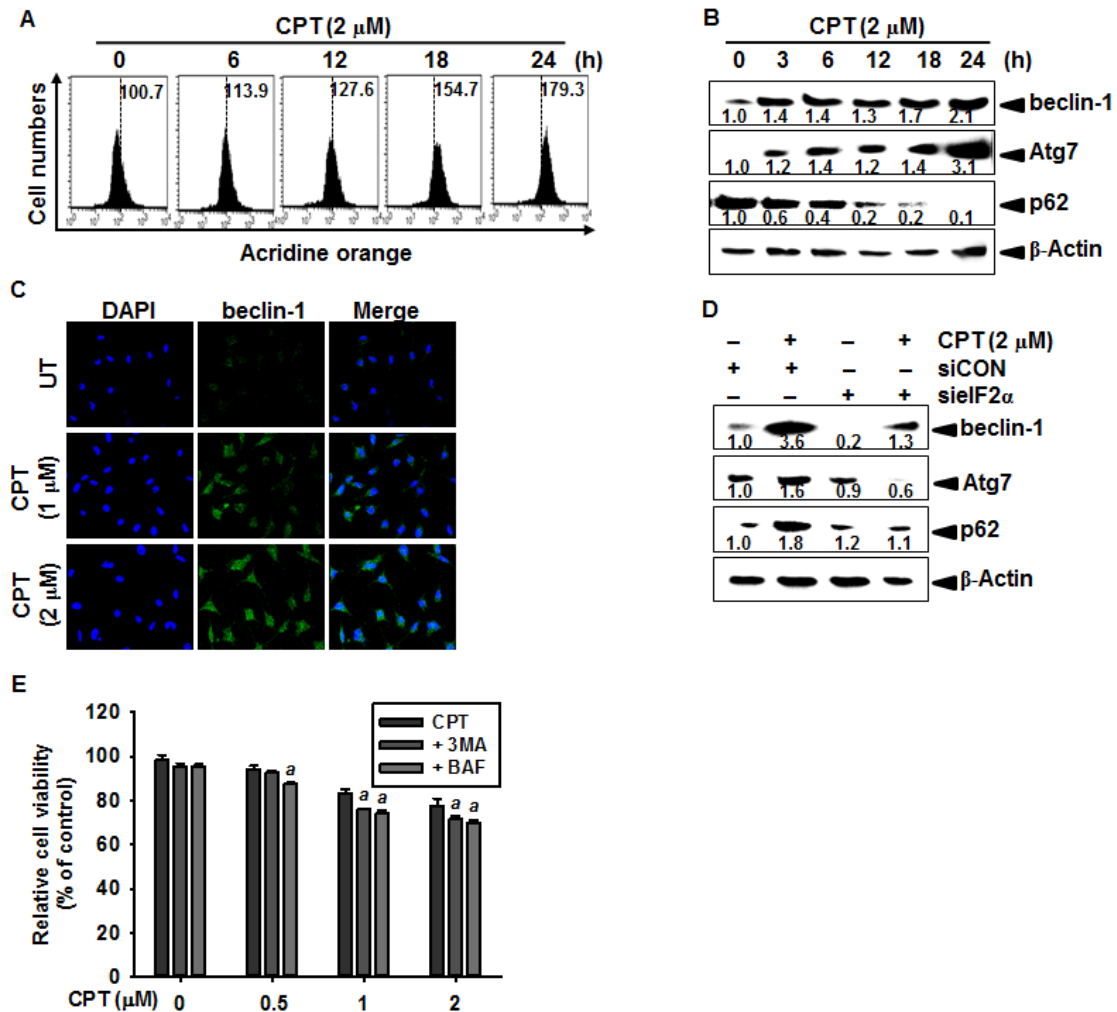


**Fig. 20.** Effect of camptothecin (CPT) on autophagy formation. LNCaP cells were treated with 2  $\mu$ M CPT for the indicated time point. (A) Equal amount of cell lysates were resolved on SDS-polyacrylamide gels, transferred to nitrocellulose membranes, and probed with antibodies against the indicated protein. (B) LNCaP cells were treated with 2  $\mu$ M CPT and cells were treated with beclin 1 as primary antibody. Monoclonal antibody was detected using

an anti-rabbit secondary antibody conjugated with FITC under confocal microscopy. (C) Cells were stained with acridine orange and analyzed for flow cytometer. (D) After cells transfected with eIF2 $\alpha$ -targeted siRNA (sieIF2 $\alpha$ ), cells were treated with 2  $\mu$ M CPT, equal amount of cell lysates were resolved on SDS-polyacrylamide gels, transferred to nitrocellulose membranes, and probed with antibodies against indicated protein. (E) Cells were pretreated with 3-methyladenine (3MA) and bafilomycin A1 (BAF) before treatment with 2  $\mu$ M CPT and cellular viability was determined by an MTT assay.  $\beta$ -Actin was used as the internal control for western blot analysis. Statistical significance was determined by one-way ANOVA (<sup>a</sup>,  $p < 0.05$  vs. each CPT-treated control).

#### **4.3.4 CPT promotes autophagy by increasing intracellular Ca<sup>2+</sup> release**

It previously demonstrated that CPT activates the calcium channel and induces the influx of calcium to intracellular cytosol (23). However, the CPT-induced Ca<sup>2+</sup> signal pathway has not to be fully understood. As shown in Fig. 4A, CPT gradually increased the intensity of Ca<sup>2+</sup> fluorescence dye, Fluo 3-AM. Moreover, confocal microscopy images clearly demonstrated that intracellular Ca<sup>2+</sup> concentration increased in response to CPT; however, the level of intracellular Ca<sup>2+</sup> was further decreased when pretreatment with a Ca<sup>2+</sup> chelator, EGTA (Fig. 4B). The phosphorylation of AMPK, a metabolic master switch that regulates several intracellular systems, is controlled by two Ca<sup>2+</sup>-dependent kinases, LKB1 and CaMKK. Since CPT regulated intracellular Ca<sup>2+</sup> release, we next examined that the phosphorylation level of AMPK is regulated in response to CPT. As presumed, CPT increased the AMPK phosphorylation in a time-dependent manner (Fig. 4C). Furthermore, in order to investigate Ca<sup>2+</sup>-dependent AMPK phosphorylation, LNCaP cells were pretreated with a calcium chelator, EGTA and an ROS inhibitor, GSH and then we analyzed AMPK

phosphorylation. Our data showed that CPT-induced AMPK phosphorylation remarkably downregulated in the presence of EGTA and GSH (Fig. 4D), indicating that  $\text{Ca}^{2+}$  and ROS regulates AMPK phosphorylation. Because  $\text{Ca}^{2+}$  accumulation in the cytosol is required for phosphorylation of AMPK, leading to induction of autophagy, we analyzed expression of autophagy proteins in the presence of EGTA and CaMKII inhibitor, K252a. EGTA and K252a completely abrogated CPT-induced beclin 1 and Atg7 (Fig. 4E), suggesting that CPT-induced  $\text{Ca}^{2+}$  release promotes autophagy via the CAMKII-AMPK pathway. Taken together, these results suggest that CPT activates CaMKII-mediated AMPK phosphorylation by accumulating intracellular  $\text{Ca}^{2+}$ , leading to autophagy formation.

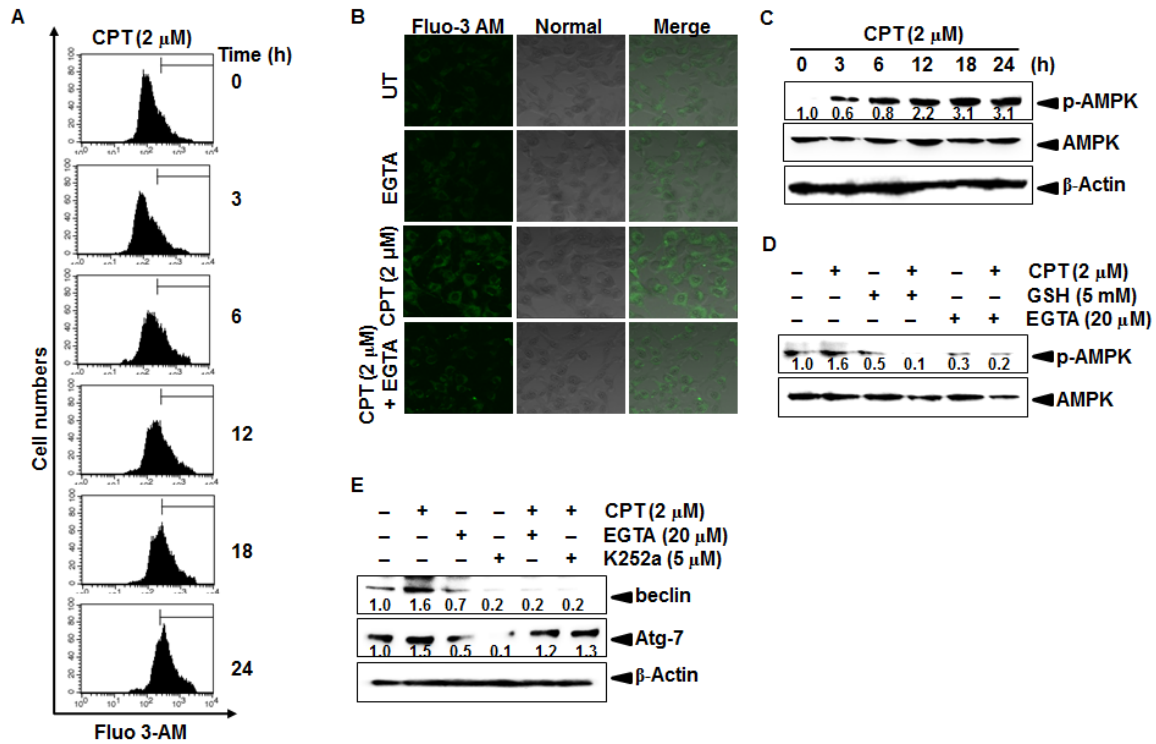


**Fig. 21.** Effect of camptothecin (CPT) for intracellular  $\text{Ca}^{2+}$  release. (A and B) LNCaP cells were treated with 2  $\mu\text{M}$  CPT at the indicated times and then stained with Fluo 3-AM. The fluorescence intensity of the Fluo 3-AM and was analyzed by a flow cytometer and a confocal microscopy. (C) LNCaP cells were treated with 2  $\mu\text{M}$  CPT for the indicated time point and equal amount of cell lysates were resolved on SDS-polyacrylamide gels, transferred to nitrocellulose membranes and probed with antibodies against p-AMPK and AMPK. (D) To examine the effect of EGTA and K252a on autophagy protein, cells were pretreated with 2  $\mu\text{M}$  EGTA or K252a for 1 h, further treated with 2  $\mu\text{M}$  CPT for 24 h, and western blot analysis was performed to detect indicated protein. (E) To examine the effect of EGTA and ROS inhibitor GSH on phosphorylation of AMPK, cells were pretreated with indicated concentration of EGTA or GSH for 1 h and further treated with 2  $\mu\text{M}$  CPT for 24 h and western blot analysis was performed to detect indicated protein.  $\beta$ -Actin was used as the internal control for western blot analysis.

#### 4.3.5 CPT induces JNK-dependent autophagy by enhancing AP-1 activity

Recently published work provided new insights on the JNK pathway to control the balance of autophagy and apoptosis in response to genotoxic stress. Here, we sought to evaluate the role of JNK in CPT-induced autophagy in LNCaP cells. As we can see in Fig. 5A, treatment with CPT gradually increased phosphorylation of JNK in a time-dependent manner. The phosphorylation of JNK clearly appeared at 12 h and maximally reached at 24 h after exposure of CPT; however, no total JNK level was altered. The JNK pathway is a potential mediator of ROS response by activating AP-1, resulting in autophagy formation [Cheng et al., 2011]. Therefore, we attempted to analyze CPT-induced JNK expression through AP-1 activity. CPT treatment resulted in a significant increase of DNA-binding activity of AP-1 in LNCaP cells; however, pretreatment of JNK inhibitor, SP600125, and siJNK transfection abolished CPT-induced AP-1 activity (Fig. 5B), suggesting that the JNK-AP-1 pathway is generated in response to CPT. Pretreatment with antioxidant GSH also abolished phosphorylation of CPT-induced c-Jun, which implies that CPT-induced ROS activates the JNK-AP-1 signaling pathways in LNCaP cells (Fig. 5C). Moreover, knockdown of JNK significantly abolished the expression level of beclin-1 and Atg7, accompanied by dephosphorylation of c-Jun (Fig. 5D). Taken together, these data indicate that CPT-induced ROS generation is a potential mediator of the JNK-AP-1 pathway, resulting in autophagy.

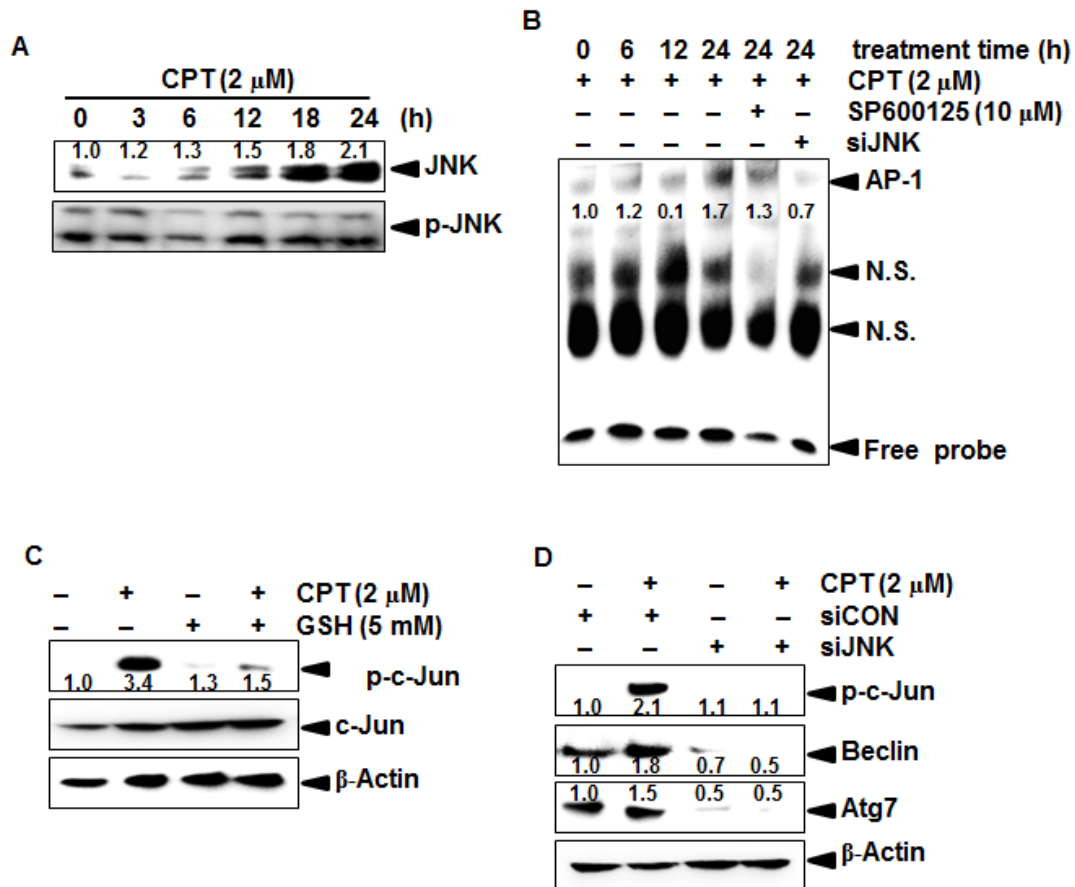


**Fig. 22.** Effect of camptothecin (CPT) on JNK-dependent AP1 activity. LNCaP cells were treated with 2  $\mu$ M CPT for the indicated time point. (A) Equal amount of cell lysates were resolved on SDS-polyacrylamide gels, transferred to nitrocellulose membranes, and probed with antibodies against JNK and p-JNK. (B) In a parallel experiment, nuclear extracts were prepared to analyze DNA-binding activity of AP-1 by EMSA. (C) LNCaP cells were pretreated with GSH for 1 h prior to treatment 2  $\mu$ M CPT and western blot analysis was performed for indicated protein. (D) After LNCaP cells transfected with JNK-targeted siRNA (siJNK), the cells were treated with 2  $\mu$ M CPT for 24 h. Equal amount of cell lysates were resolved on SDS-polyacrylamide gels, transferred to nitrocellulose membranes, and probed with antibodies against indicated protein.  $\beta$ -Actin was used as the internal control for western blot analysis. N.S.; nonspecific.

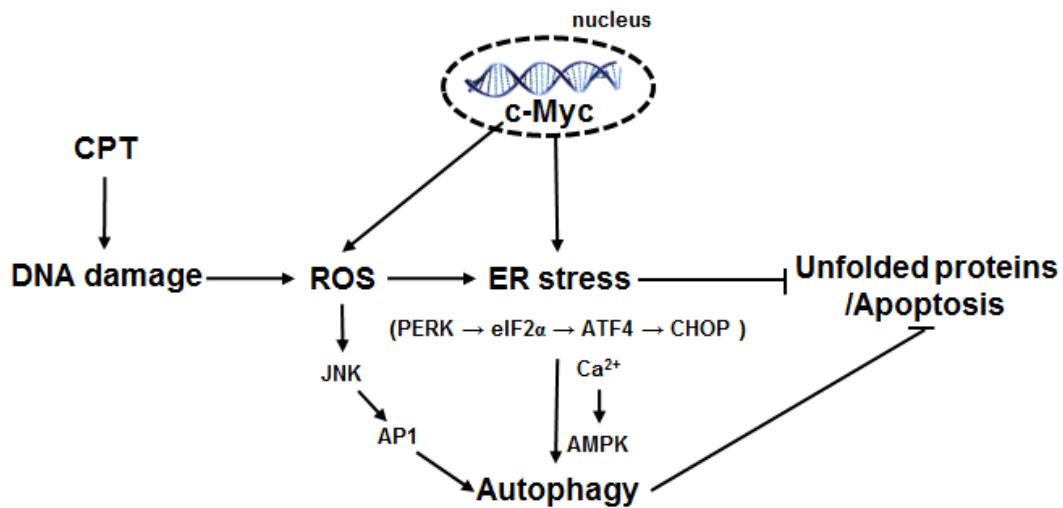


**Fig. 23.** CPT-induced unfolded protein response (UPR) signal pathways. CPT regulates c-Myc-mediated ROS generation in response to the DNA damage. CPT enhances c-Myc-mediated ROS generation, leading to increase CHOP expression which increases ER stress. Treatment of CPT increased phosphorylation of PERK and eIF2 $\alpha$ , and expression of ATF4, which indicated that CPT activates the PERK-eIF2 $\alpha$ -ATF4 pathway. CPT also induces autophagy as cytoprotection mechanism in LNCaP cells, resulting from ER stress. CPT also increased the intracellular Ca<sup>2+</sup> concentration which target phosphorylation AMPK dependent autophagy. Additionally, JNK signaling is a potential mediator of ROS response via AP-1 transcription activation, resulting in autophagy induction.

## 4.4 Discussion

In the present study, we demonstrated that CPT enhanced c-Myc-mediated ROS generation in LNCaP cells, which stimulates the PERK-eIF2 $\alpha$ -ATF-4 route during ER stress-induced autophagy. In previous, the PERK-eIF2 $\alpha$ -ATF-4 pathway is well-tuned responsible not only for translational attenuation, but also for activation of their target genes such as CHOP during ER stress [Teske et al., 2011]. We found that CPT activates the PERK-eIF2 $\alpha$ -ATF-4 pathway, resulting from ROS generation, whereas the presence of antioxidant abolished CPT-induced ER stress. Nevertheless, detail study on ROS production may be performed in CPT-induced ER stress, because the molecular mechanism of ROS generation remains unclear and may involve multiple pathways. JNK is an important member of the MAPK superfamily, the members of which are readily activated by many environmental stimuli. Recently, Shen et al., reported that ROS-mediated JNK switches from apoptosis to autophagy via ER stress, accompanied by AP-1 activation [West et al., 2012]. Zhou et al., intensively supported that autophagy was attributed to induction of ROS, whereas inhibition of JNK or expression of dominant negative c-Jun and a ROS scavenger prevented autophagy, indicating that ROS-mediated activation of the JNK signaling pathway contributed to autophagy [Zhou et al., 2014]. In the present study, we also verified that CPT regulates JNK-dependent autophagy by inducing AP-1 activation. Nevertheless, another study showed that other MAPKs such as ERK and p38 MAPK play a pivotal role in ER stress and autophagy [Zhou et al., 2015]. Therefore, further studies will be needed to find out the possibility of other MAPKs to regulate CPT-induced ER stress-mediated autophagy. Additionally, no another potential could be ignored, because ER stress transit cellular signal to IRE1, which leads to phosphorylation of JNK [Teske et al., 2011]. During ER stress, intracellular Ca<sup>2+</sup> remarkably involves the onset of autophagy via CaMKII-AMPK pathway [Pfisterer et al.,

2011]. Zhang *et al.*, reported that CPT induced autophagy through the AMPK pathway, leading to cell survival [Hart *et al.*, 2012]. Nevertheless, no study has been shown on relation between ER stress and autophagy. In the current study, we found that CPT-induced ER stress plays an indispensable role in promoting  $\text{Ca}^{2+}$ -mediated autophagy formation by establishing c-Myc-mediated ROS generation (Fig. 6).

c-Myc is a target of chromosomal translocation and central oncogenic switch for oncogenes during cell growth, apoptosis, and metabolism [Dang *et al.*, 20]. Recent study also showed that c-Myc activation is associated with robust upregulation of protein synthesis related to ER stress, leading to a significant increase of cell survival through cytoprotective autophagy [Hart *et al.*, 2012]. On the other hand, Kagaya *et al.*, reported that c-Myc induced cell death associated with activation of JNK and caspase-3 through nucleosomal DNA degradation [Kagaya *et al.*, 1997]. Additionally, excessive loading of unfolded or misfolded proteins transit into apoptosis by upregulation of c-Myc-mediated CHOP [Benbrook *et al.*, 2012]. Interestingly, our data revealed that CPT increased c-Myc-dependent ER stress, which activates beclin-1 and Atg7, leading to autophagy. The discrepancy on the role of c-Myc between cell survival and cell death might be further studying; nevertheless, we found that CPT-induced c-Myc is an important upstream molecule for ER stress-mediated cytoprotective autophagy through ROS generation. Wang *et al.*, also reported that rapid elevation of intracellular  $\text{Ca}^{2+}$  resulted in the cell death, suggesting that the release of  $\text{Ca}^{2+}$  from ER plays a crucial role in apoptosis [Wang *et al.*, 2008]. In peculiar, intracellular free  $\text{Ca}^{2+}$  irritates mitochondrial membrane potential and permeability transition, which increases the release of cytochrome C into the cytosol, resulting in activation of the caspase cascade and consequent apoptosis [Gogvadze *et al.*, 2006]. Resveratrol-induced apoptosis was also mediated by the process of autophagy via  $\text{Ca}^{2+}$ /AMPK-mTOR signaling pathway [Zhang *et*

al., 2013]. However, our data showed that CPT-induced autophagy through the  $\text{Ca}^{2+}$ /AMPK pathway promoted cytoprotective function; the phenomenon is attributable to CPT-induced  $\text{G}_2/\text{M}$  phase arrest (data not shown), suggesting that CPT boosted  $\text{G}_2/\text{M}$  phase arrest by blocking cell death through autophagy-mediated cell survival.

#### **4.5 Conclusion**

The present study demonstrated that activation of c-Myc increased ER stress through the ROS-mediated PERK-eIF2 $\alpha$ -ATF-4 pathway, leading to autophagy accompanied by the JNK and  $\text{Ca}^{2+}$  routes. These data are the first established on the relationship between ER stress and autophagy in response to CPT and would be potentially beneficial in cancer therapy.

## **Chapter 5**

# **CPT induces c-Myc- and Sp1-mediated hTERT expression in LNCaP cells: involvement of reactive oxygen species and PI3K/Akt**

## Abstract

Camptothecin (CPT) is a potentially interesting candidate for use in cancer chemotherapy because its specific molecular target is topoisomerase I which constitutively increases in cancer cells, not normal cells. However, the molecular mechanisms responsible for CPT-induced telomerase inhibition remain to be poorly known. In this study, we examined the effects of CPT on human telomerase reverse transcriptase (hTERT) expression and telomerase activity in LNCaP cells. In this study, we found that CPT caused upregulation of hTERT expression and a concomitant increased of telomerase activity. Transfection of hTERT-targeting siRNA has no effect on CPT-induced G<sub>2</sub>/M phase arrest, suggesting that increased hTERT expression prevents the cells against apoptosis, leading to promote survival rate and consequently delay cell cycle progression. CPT enhanced hTERT expression by inducing c-Myc and Sp1. As we presumed, treatment with CPT increased the level of intracellular reactive oxygen species (ROS), whereas pretreatment with antioxidants, *N*-acetyl-cysteine (NAC) or glutathione (GSH), completely attenuated ROS generation accompanied by downregulation of hTERT. Moreover, c-Myc stimulated ROS generation in response to CPT, leading to Sp1 activation, which promotes hTERT expression. Treatment with CPT also enhances phosphorylation of PI3K and Akt which are upstream regulator in controlling hTERT phosphorylation for translocation into the nucleus. These findings demonstrate the effectiveness of CPT in controlling telomerase activity by upregulating hTERT expression.

## 5.1 Introduction

Telomerase is a specialized ribonucleoprotein that functions reverse transcription in maintaining telomeric repeats at the ends of eukaryotic chromosomes [Romaniuk et al., 2014]. Activation of telomerase is important for the continued growth of several human tumors, resulting in a critical role in cell cycle and tumorigenesis [Ferguson et al., 2015]. Cancer cells and spontaneously immortalized cells elevates telomerase activity to preserve the telomeric ends of chromosomes; however, most normal human somatic cells progressively lose their telomeres with each cell division because of functional inactivation of telomerase, which suggests that the enzyme offers potentially valuable target for chemotherapy [Shay et al., 2013]. The telomerase complex is composed of a catalytic subunit, including human telomerase reverse transcriptase (hTERT), telomerase RNA (TR), chaperone proteins (p23 and Hsp90), and telomerase-associated proteins (TEP1) [Shay et al., 2013]. TR, TEP1, p23, and Hsp90 are ubiquitously expressed in a wide variety of cells irrespective of telomerase activity, which indicates that those catalytic proteins are not promising target; however, there have been numerous studies focused on hTERT regulation in controlling apoptosis of cancer cells because cancer cells specifically express hTERT, but not normal cells. Previous studies revealed that knockdown of hTERT completely suppressed cancer cell growth by inactivating telomerase capability, whereas overexpression of hTERT results in a significant decrease of anti-cancer drug sensitivity [Li et al., 2015, Xue et al., 2015]. Therefore, many scientists have been attempting to find specific hTERT-targeting drugs for cancer chemotherapy.

The hTERT promoter region is located within the 1375 bp upstream of the transcription-starting site and is rich in variety of transcription factor binding sites [Zhang et al., 2006]. The region includes two typical E-boxes and several GC-boxes for binding with transcription

factors such as c-Myc and Sp1, respectively [8]. c-Myc directly binds with E-box and remarkably induces hTERT transcription, leading to subsequent cell proliferation [Kyo et al., 2008]. In addition, activation of c-Myc potentiates hTERT expression accompanied by FOXO3a, which recruits c-Myc to the hTERT promoter through c-Myc-mediated histone acetylation [10]. Moreover, mutations of two E-boxes in the hTERT promoter blocked DNA-binding activity of c-Myc, leading to decrease hTERT promoter activity, and inhibited its activity induced by overexpressing c-Myc; however, hTERT promoter activity still maintained in direct knockdown of c-Myc [Zhao et al., 2014], which suggests that c-Myc prevents accessibility of repressive transcription factor for hTERT promoter, not regulating direct increase of hTERT. The core promoter of hTERT also contains Sp1/Sp3 binding sites, which are necessary for hTERT expression [Liu et al., 2012]. In peculiar, Zhao *et al.*, reported Sp1 silencing completely inhibited telomerase activity by suppressing hTERT expression, leading promotes apoptosis. Taken together, c-Myc and Sp1 cooperatively regulates hTERT promoter; nevertheless, direct targeting c-Myc and Sp1 would be bad strategy in modulating hTERT expression for cancer therapy because the transcription factors are ubiquitously expressed in not only cancer cells, but also normal cells. Posttranslational modification of hTERT is also required for telomerase activity for nuclear translocation by phosphorylating hTERT at Ser<sup>227</sup> via the Akt pathway, which increases binding affinity of hTERT to importin- $\alpha$  [Bisson et al., 2015]. Accordingly, hTERT overexpression reduces the basal level of intracellular reactive oxygen species (ROS) and suppresses ROS-mediated apoptosis [Indran et al., 2011]. Nuclear factor erythroid 2-related factor 2 (Nrf2) binds to antioxidant response elements (AREs) and stimulates transcription of antioxidant proteins, leading to decrease ROS generation [Kovac et al., 2015]. However, little is known the mechanism behind the Nrf2 regulates hTERT expression.

Camptothecin (CPT) is a potent topoisomerase I inhibitor by binding with topoisomerase I-DNA complex responsible for apoptosis of cancer cells [Zeng et al., 2012]. Our previous data also showed that CPT triggered tumor necrosis factor-related apoptosis-inducing ligand (TRAIL) and inhibited cancer cell invasion by suppressing matrix metalloproteinase-9 [Jayasooriya et al., 2014]. CPT also regulated G<sub>2</sub>/M arrest, resulting from cell cycle checkpoint modulation [Huang et al., 2008]. Murofushi *et al.*, found that the highest levels of hTERT expression and telomerase activity were observed from G<sub>1</sub> to S phase, which were 2-3-fold higher than the lowest levels in G<sub>0</sub> phase [Murofushi et al., 2006]. Kalpper *et al.*, reported that treatment with topoisomerase II inhibitor increased the telomerase activity after DNA damage [Kalpper et al., 2003]. Even though no report has been whether CPT regulates G<sub>2</sub>/M arrest, resulting from alleviating of hTERT, above studies verified that most DNA-targeting topoisomerase including CPT regulates cell cycle progression and telomerase activity.

In the present study, we found that CPT promoted c-Myc- and Sp1-mediated hTERT activity, which did not regulate G<sub>2</sub>/M phase arrest. Moreover, CPT induced posttranslational phosphorylation of hTERT through the PI3K and Akt pathway.

## 5.2 Materials and method

### *Reagent and antibodies*

CPT, *N*-acetylcysteine (NAC), glutathione (GSH), 3-(4,5-dimethylthiazol-2-yl)-2,5-diphenyltetrazolium bromide (MTT), propidium iodide, and 2',7'-Dichlorodihydrofluorescein diacetate (H<sub>2</sub>DCFDA) were purchased from Sigma (St. Louis, MO) and an enhanced chemiluminescence (ECL) kit was purchased from Amersham (Arlington Heights, IL). RPMI 1640 medium, fetal bovine serum (FBS), and antibiotics mixture was purchased from WelGENE (Daegu, Republic of Korea). SP600125 and Watmannin were purchased from Calbiochem (San Diego, CA). Antibodies against hTERT, cyclin E, cyclin B1, Cdk1, Sp1, nucleolin, p21, Nrf2, and  $\beta$ -actin were purchased from Santa Cruz Biotechnology (Santa Cruz, CA). Antibodies against c-Myc, PI3K, p-PI3K, JNK, and p-JNK were purchased from Cell Signal (Beverly, MA). Peroxidase-labeled donkey anti-rabbit and sheep anti-mouse immunoglobulin were purchased from KOMA Biotechnology (Seoul, South Korea).

### *Cell culture and viability assay*

Human prostate cancer LNCaP cells and human leukemia U937 cells were purchased from American Type Culture Collection (Rockville, MD). Cells were cultured at 37°C in a 5% CO<sub>2</sub>-humidified incubator and maintained in RPMI 1640 medium containing 10% heat-inactivated FBS and 1% antibiotics mixture. The cells were seeded ( $1 \times 10^5$  cells/ml) and then incubated with CPT for 24 h. MTT assays were performed to determine relative cell viability.

### *RNA extraction and RT-PCR*

Total RNA was isolated using Trizol reagent (GIBCO-BRL; Gaithersburg, MD)

according to the manufacturer's recommendations. Genes of interest were amplified from cDNA that was reverse-transcribed from 1 µg total RNA using the One-Step RT-PCR Premix (iNtRON Biotechnology; Sungnam, Republic of Korea). Primers for *hTERT* sense (5'-CCG AAG AGT GTC TGG AGC AA-3'); *hTERT* antisense (5'-GGA TGA AGC CGA GTC TGG A-3'); and *glyceraldehydes-3-phosphate dehydrogenase (GAPDH)* sense (5'-CCA CCC ATG GCA AAT TCC ATG GCA-3'); *GAPDH* antisense (5'-TCT AGA CGG CAG GTC AGG TCC ACC-3') have been described previously. PCR reaction was initiated at 94°C for 2 min followed by 28 cycles of 94°C for 1 min, 1-min annealing temperature, 72°C for 1 min followed by final extension at 72°C for 5 min. Annealing temperatures for *hTERT* and *GAPDH* were 58°C and 60°C, respectively. After amplification, PCR products were separated on 1.5% agarose gels and visualized by ethidium bromide fluorescence using Chemi-Smart 2000 (VilberLourmat; Marine, Cedex, France).

#### *Western blot analysis*

Whole-cell lysates were prepared by PRO-PREP protein extraction solution (iNtRON Biotechnology, Sungnam, Republic of Korea). Cytoplasmic and nuclear protein extracts were prepared using NE-PER nuclear and cytosolic extraction reagents (Pierce, Rockford, IL). The cell lysates were harvested from the supernatant after centrifugation at 13,000 g for 20 min. Total cell proteins were separated on polyacrylamide gels and standard procedures were used the transfer them the nitrocellulose membranes. The membranes were developed using an ECL reagent.

### *Electrophoretic mobility shift assay*

Transcription factor-DNA binding activity assays were carried out with nuclear protein extract. Synthetic complementary c-Myc (5'-GGA AGC AGA CCA CGT GGT CTG CTT CC-3') and Sp1 (5'-ATT CGA TCG GGG CGG GGC GAG C-3') binding oligonucleotides was 3'-biotinylated utilizing the biotin 3'-end DNA labeling kit (Pierce) according to the manufacturer's instructions, and annealed for 30 min at 37°C. Samples were loaded onto native 4% polyacrylamide gels pre-electrophoresed for 60 min in 0.5X Tris borate/EDTA (TBE) buffer on ice, in the presence of transferred onto a positively charged nylon membrane (Hybond<sup>TM</sup>-N<sup>+</sup>) in 0.5X TBE buffer at 100 V for 1 h on ice. The transferred DNA-protein complex was cross-linked to the membrane at 120 mJ/cm<sup>2</sup>. Horseradish peroxidase-conjugated streptavidin was utilized according to the manufacturer's instructions to monitor the transferred DNA-protein complex.

### *Flow cytometric analysis*

Cell cycle progression, ROS production, and intracellular PI3K and Akt were analyzed by flow cytometry. Cells were analyzed by using a FACSCalibur flow cytometer (Becton Dickenson, San Jose, CA), after each staining.

### *Telomerase activity assay*

Telomerase activity was measured using a PCR-based telomeric repeat amplification protocol (TRAP) enzyme-linked immunosorbent assay (ELISA) kit (Boehringer Mannheim, Mannheim, Germany) according to the manufacturer's description. In brief, cells were treated with CPT, harvested, and approximately  $1 \times 10^6$  cells were lysed in 200  $\mu$ l lysis reagent and incubated on ice for 30 min. For the TRAP reaction, 2  $\mu$ l cell extract (containing 2  $\mu$ g protein)

was added to 25  $\mu$ l reaction mixture with the appropriate amount of sterile water to make a final volume of 50  $\mu$ l. PCR was performed as follows: primer elongation (25°C for 30 min), telomerase inactivation (94°C for 5 min), product amplification by the repeat of 30 cycles (94°C for 30 s, 50°C for 30 s, and 72°C for 90 s). Hybridization and the ELISA reaction were carried out following the manufacturer's instructions.

#### *Luciferase assays*

LNCaP cells were seeded at a density of  $2 \times 10^5$  cells/ml and grown overnight and the cells were cotransfected with 1  $\mu$ g hTERT promoter and 0.2  $\mu$ g pCMV- $\beta$ -galactosidase plasmid using Lipofectamin Plus reagent (Life Technologies) following the manufacturer's instructions. After 24 h-incubation, the cells were incubated with or without CPT for another 24 h. Luciferase and  $\beta$ -galactosidase activities were assayed according to the manufacturer's protocol (Promega, Madison, WI).

#### *Small interfering RNA (siRNA)*

Cells were seeded on a 24-well plate at a density of  $1 \times 10^5$  cells/ml and transfected hTERT-, c-Myc-, and Sp1-specific silencing RNA (siRNA, Santa Cruz Biotechnology) for 24 h. For each transfection, 450  $\mu$ l growth medium was added to 20 nM siRNA duplex with the transfection reagent G-Fectin (Genolution Pharmaceuticals Inc., Seoul, Republic of Korea) and the entire mixture was added gently to the cells

### *Immunofluorescence staining and confocal microscopy*

Cells were seeded on glass coverslips and incubated for 24 h at 37°C with or without CPT washed twice with PBS and fixed with 90% methanol at 37°C for 30 min. The cells were again washed with PBS and blocked in 10% normal goat serum for 1 h and incubated with anti-p-PI3K and p-Akt antibody (1:200, Santa Cruz Biotechnology) overnight at 4°C. Primary antibody was removed by washing the membranes in PBS containing Triton-X (0.3%) and incubated for 1 h with Alexa 488-conjugated anti-mouse secondary antibody (1:200, Molecular Probes, Eugene, OR). Fluorescent signals were imaged using a confocal laser scanning microscope.

### *DNA fragmentation assay*

After treatment of CPT for 24 h in LNCaP cells were lysed in DNA fragmentation lysis buffer containing 10 mM Tris (pH 7.4), 150 mM NaCl, 5 mM EDTA and 0.5% Triton X-100 for 1 h on ice. Lysates samples were vortexed and separated centrifugation at 15,000 RPM for 15 min. Fragmented DNA in the supernatant was isolated with equal volume of phenol:chloroform:isoamyl alcohol mixture and analyzed electrophoretically on 1.5% agarose gel.

### *Statistical analysis*

The images were visualized with Chemi-Smart 2000 (VilberLourmat, Marine, Cedex, France). Images were captured using Chemi-Capt (VilberLourmat) and transported into Photoshop. All bands were shown a representative obtained in three independent experiments and quantified by Scion Imaging software (<http://www.scioncorp.com>). Statistical analyses were conducted using SigmaPlot software (version 12.0). Values were presented as mean  $\pm$  standard error (S.E.). Significant differences between the groups were determined using the

unpaired one-way and two-way ANOVA test. Statistical significance was regarded at <sup>a</sup> and <sup>b</sup>,  $p < 0.05$ .

## 5.3 Results

### 5.3.1 CPT increases hTERT expression and activity, which is not associated with G<sub>2</sub>/M phase arrest

In order to determine the effect of CPT on cell viability, LNCaP cells were treated with the indicated concentrations of CPT for 24 and the cell viability was determined by an MTT assay. CPT decreased cell viability in a dose-dependent manner and significant anti-proliferative effect in response to CPT was observed from at 2  $\mu$ M CPT (Fig 1A). However, no apoptotic morphological changes were seen in response to CPT (data not shown). We next examined whether CPT regulates hTERT expression and telomerase activity in LNCaP cells. Treatment with CPT dose-dependently increased hTERT expression at both the transcriptional and translational levels in LNCaP cells (Fig. 1B). In addition, we revealed the underlying mechanisms involved in CPT-induced transcriptional control of hTERT using the luciferase system containing hTERT gene promoter region. CPT significantly stimulated hTERT promoter activity (Fig. 1C). In order to elucidate the regulatory effect on telomerase activity by treatment with CPT, telomerase activity measured using a TRAP assay kit. The assay data also showed that CPT augments telomerase activity (Fig. 1D), suggesting that CPT enhances hTERT expression, leading to telomerase activity.

Recent study showed that hTERT regulated the cell cycle through specific localization of telomerase, peaking at mid-S phase. Because our previous data also showed that CPT-induced G<sub>2</sub>/M phase arrest without apoptosis, we hypothesized that CPT-induced G<sub>2</sub>/M phase arrest might be induced by increasing hTERT expression in LNCaP cells. In order to

investigate hTERT function in G<sub>2</sub>/M phase arrest, LNCaP cells were transfected with hTERT siRNA (sihTERT) to analyze the role of hTERT. sihTERT significantly reduced the hTERT protein level, compared to that transfected control siRNA (siCON). As shown in Fig. 1F, CPT significantly induced G<sub>2</sub>/M phase arrest; however, dissimilar to our hypothesis, sihTERT had no effect on the CPT-mediated G<sub>2</sub>/M cell cycle arrest. Furthermore, no protein level of cyclin E1, cyclin B, and p21 were significantly altered upon the depletion of hTERT. These results indicate that telomerase activity and G<sub>2</sub>/M phase arrest were not correlated to molecular function of CPT.

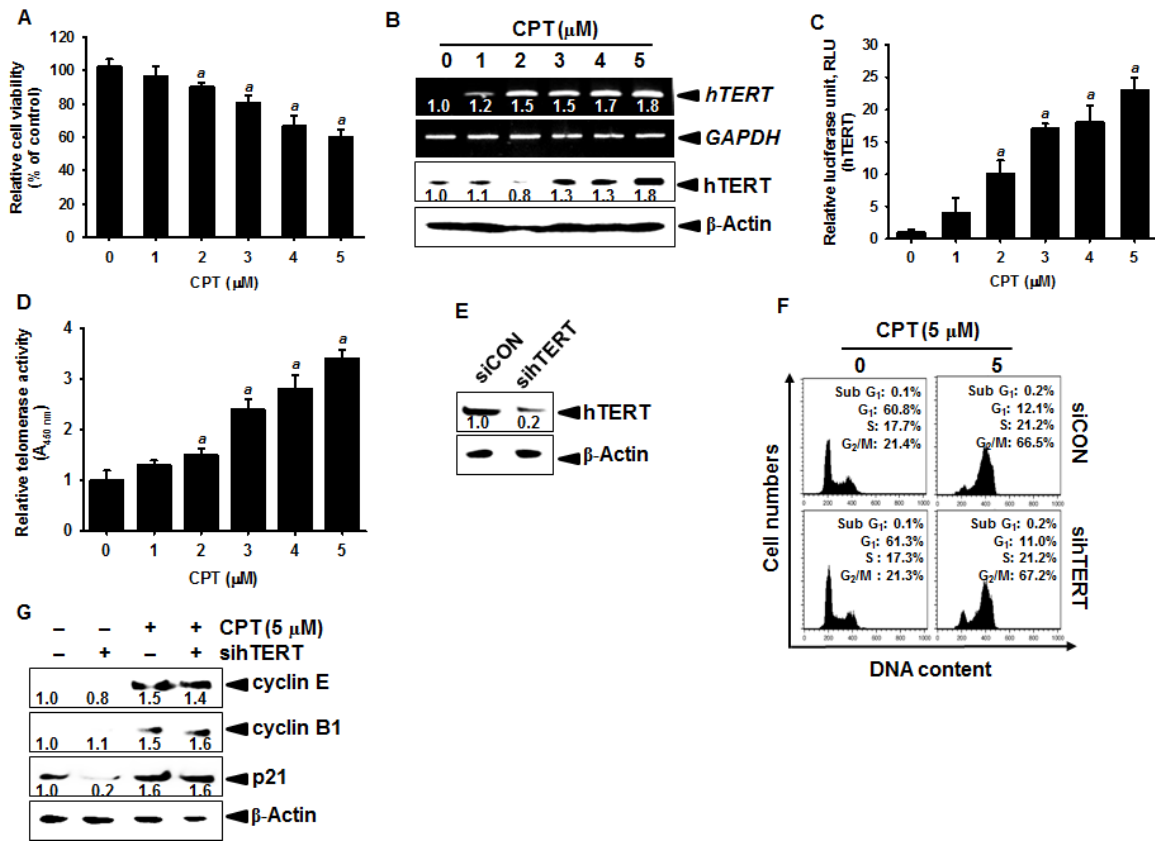


**Fig. 24.** Camptothecin (CPT)-induced telomerase activity and hTERT expression. (A) After 24 h incubation with CPT, cell viability was determined by MTT assay. (B) Total RNA was extracted in Trizol reagent. One microgram of RNA was reverse-transcribed, the resulting cDNA was subjected to PCR with hTERT primers, and visualized by EtBr staining. GAPDH was used as an internal control. Equal amounts of cell lysate were subjected to Western blot analysis with specific antibodies.  $\beta$ -Actin was used as an internal loading control. (C) Telomerase activity of LNCaP cells was measured using a luciferase assay. (D) Telomerase activity of LNCaP cells was measured using a TRAP-ELISA. (E) Cells were transiently transfected with *hTERT* siRNA and then check the expression level of hTERT by western blot analysis. (F) Representative histograms for effect of CPT treatment on cell cycle distribution in LNCaP transfected with hTERT specific siRNA and control transfections. (G) In a parallel experiment western blot was done for indicated proteins. Data from three independent

experiments are expressed as the overall mean  $\pm$  S.E. Statistical significance was determined by one-way ANOVA (<sup>a</sup>,  $p < 0.05$  vs. untreated control).

### 5.3.2 ROS regulate CPT-induced hTERT expression

Nrf2 is essential for camptothecin (CPT)-induced hTERT expression. LNCaP cells were treated with the indicated concentration of CPT, NAC, or GSH, or treated with combined CPT with NAC or GSH. (A) Intracellular ROS generation was determined by flow cytometry using the peroxide-sensitive dye DCFDA. The number means total mean fluorescent intensity. Apoptotic annexin-V<sup>+</sup> population was analyzed by flow cytometry. (B) Telomerase activity of LNCaP cells was measured using a TRAP-ELISA. (C) Cells were seeded at  $1 \times 10^5$  cells/ml and treated with the indicated concentrations of NAC and GSH for 24 h. Equal amounts of cell lysate were subjected to Western blot analysis with hTERT antibodies.  $\beta$ -Actin was used as an internal loading control. (D) Nuclear extracts were prepared to analyze DNA-binding of Nrf2 by EMSA. (E) In a parallel experiment western blot analysis was done for indicated proteins. (F) Cells were transiently transfected with Nrf2 siRNA and then check the production of ROS using fluorometer. (G) Expression level of hTERT by western blot analysis and RTPCR. (H) In a parallel experiment telomerase activity of LNCaP cells was measured using a luciferase assay. Data from three independent experiments are expressed as the overall mean  $\pm$  S.E. Statistical significance was determined by two-way ANOVA (<sup>a</sup> and <sup>b</sup>,  $p < 0.05$  vs. untreated control and CPT-treated group).

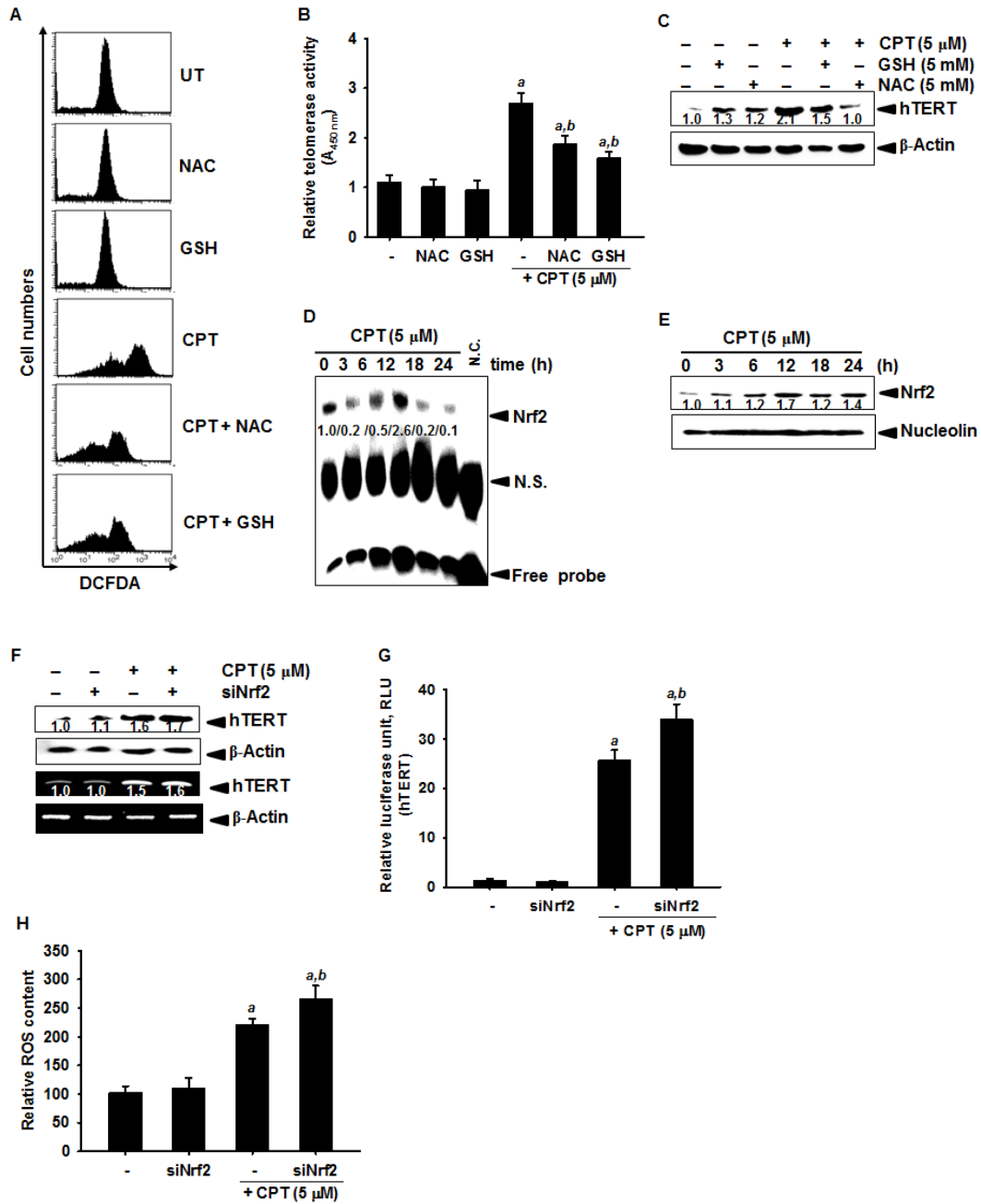


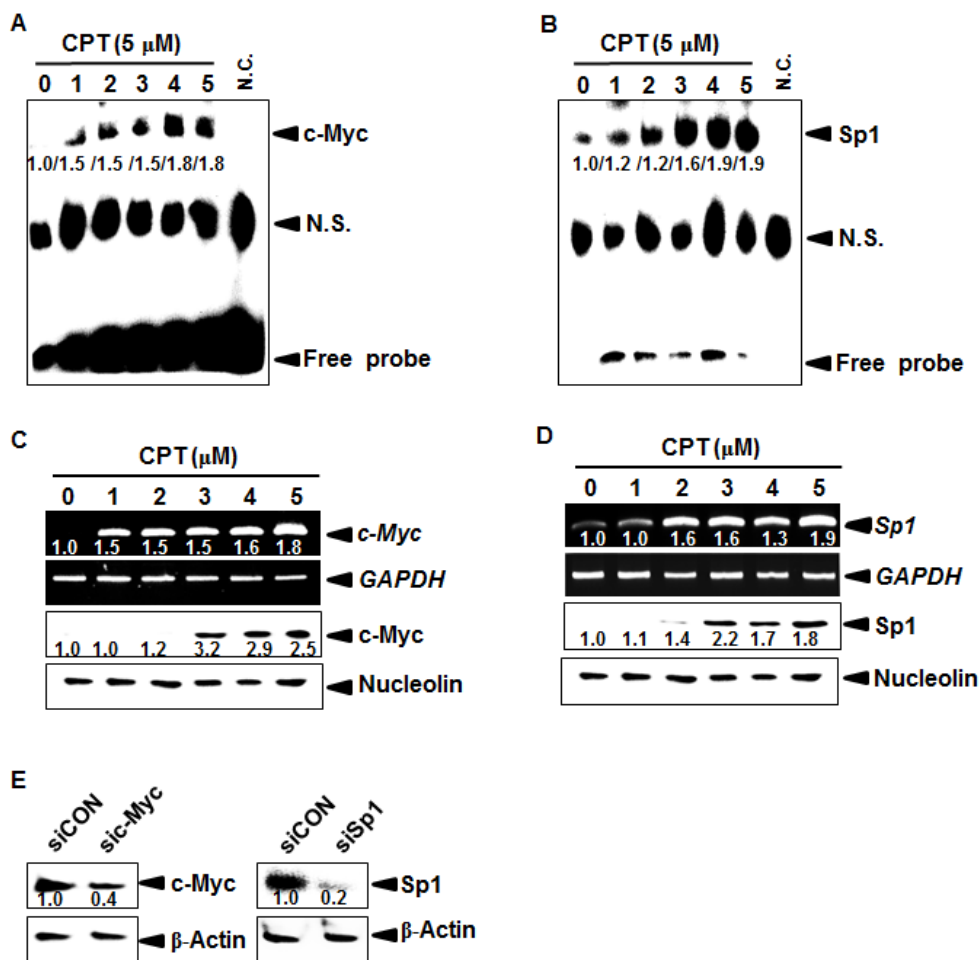
**Fig. 25.** Nrf2 is essential for camptothecin-induced hTERT expression. LNCaP cells were treated with the indicated concentration of CPT, NAC, or GSH, or treated with combined CPT with NAC or GSH. (A) Intracellular ROS generation was determined by flow cytometry using the peroxide-sensitive dye DCFDA. The number means total mean fluorescent intensity. Apoptotic annexin-V<sup>+</sup> population was analyzed by flow cytometry. (B) Telomerase activity of LNCaP cells was measured using a TRAP-ELISA. (C) Cells were seeded at

$1 \times 10^5$  cells/ml and treated with the indicated concentrations of NAC and GSH for 24 h. Equal amounts of cell lysate were subjected to Western blot analysis with hTERT antibodies.  $\beta$ -Actin was used as an internal loading control. (D) Nuclear extracts were prepared to analyze DNA-binding of Nrf2 by EMSA. (E) In a parallel experiment western blot was done for indicated proteins. (F) Cells were transiently transfected with *Nrf2* siRNA and then check the production of ROS using flourometer. (G) Expression level of hTERT by western blot analysis and RT-PCR. (H) In a parallel experiment telomerase activity of LNCaP cells was measured using a luciferase assay. Data from three independent experiments are expressed as the overall mean  $\pm$  S.E. Statistical significance was determined by two-way ANOVA (<sup>a</sup> and <sup>b</sup>,  $p < 0.05$  vs. untreated control and CPT-treated group).

### 5.3.3 CPT regulates c-Myc- and Sp1-dependent hTERT expression

The *hTERT* gene has an important promoter site (-181 bp) containing two c-Myc and Sp1 binding regions, and c-Myc and Sp1 have previously shown to directly regulate telomerase activity through hTERT expression. Since c-Myc and Sp1 are directly involved in hTERT expression and regulation, we attempted to determine whether CPT alters c-Myc and Sp1 activity and expression in LNCaP cells. CPT resulted in a significant increase of c-Myc- and Sp1-DNA binding activity in a dose-dependent manner. Additionally, the levels of c-Myc mRNA (*top*) and protein (*bottom*) were markedly enhanced in CPT-treated cells. Sp1 was also upregulated in mRNA and protein levels, at the same conditions (Fig. 3D). Next, we evaluated the role of c-Myc and Sp1 in CPT-induce hTERT expression via transient knockdown of c-Myc and Sp1. As shown in Fig. 3E, siRNA transfection was efficient in the cells. Depletion of c-Myc inhibited CPT-induced hTERT luciferase activity (Fig. 3F) and transfection of siSp1 resulted in reduction of CPT-induced telomerase activity in LNCaP cells

(Fig. 3G). Both of sic-Myc and siSp1 abrogated CPT-induced hTERT expression (Fig. 3H and 3I). Finally, we performed that CPT regulates the activity of c-Myc and Sp1 in the presence of NAC. RT-PCR data showed that *c-Myc* and *Sp1* were significantly upregulated by CPT alone, but NAC abolished CPT-induced *Sp1* expression, but not *c-Myc*. These results indicate that CPT increases *hTERT* gene expression through enhancement of c-Myc-mediated ROS generation, resulting in Sp1 expression, which increases telomerase activity.



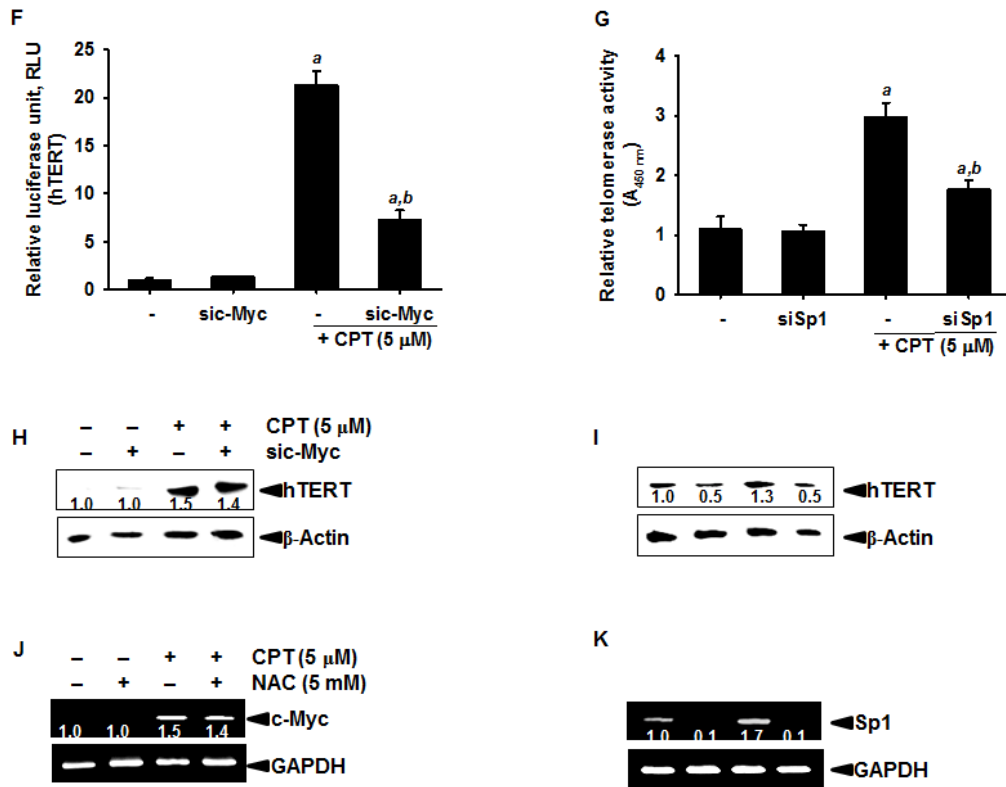


**Fig. 26.** Upregulation of c-Myc and Sp1 by camptothecin (CPT). 2 μM of CPT for indicated time point. (A and B) c-Myc and Sp1 DNA binding activity was analyzed by a LightShift™ chemiluminescent EMSA kit. (C and D) Total RNA was isolated using a Trizol reagent and RT-PCR was performed. Western blot was performed by standard procedure. (E) Cells were transiently transfected with c-Myc and Sp1 siRNA and then check the expression level of hTERT by western blot analysis. (F) Cells were transiently transfected with c-Myc siRNA and telomerase activity of LNCaP cells was measured using a luciferase assay. (G) Cells were transiently transfected with Sp1 siRNA and telomerase activity of LNCaP cells was measured using TRAP-ELISA. (H and I) In a parallel experiment western blot was done to check the expression level of hTERT. (J and K) LNCaP cells were preincubated with NAC and then treated with 2 μM of CPT for 6 h. Total RNA was isolated using a Trizol reagent and RT-PCR was performed. Data from three independent experiments are expressed as the overall mean ± S.E. Statistical significance was determined by two-way ANOVA.

#### 5.3.4 CPT induces PI3K/Akt signaling involved in hTERT expression

PI3K/Akt is well known to enhance human telomerase activity through phosphorylation of hTERT, which stimulates nuclear translocation of phosphorylated hTERT. Therefore, we analyzed whether CPT-induced telomerase activity was associated with activation of PI3K/Akt. To address the mechanism of hTERT at the posttranslational level, we analyzed phosphorylation of PI3K and Akt. Flow cytometry data showed that CPT increased intracellular phosphorylation of PI3K and Akt in a time-dependent manner (Fig. 4A). Western blot analysis also confirmed that CPT increased the phosphorylation levels of Akt and PI3K, although no total Akt and PI3K levels were altered in response to CPT (Fig. 4B). Accordingly, immunohistochemistry data revealed that treatment with CPT enhanced the intensity of green colors, p-Akt and p-PI3K, compared to the untreated control group (fig. 4C). To further confirm the functional role of Akt and PI3K, we investigated CPT-mediated hTERT expression telomerase activity in the presence of PI3K/Akt inhibitors, LY294002 and Wortmannin. Our data showed that pretreatment with LY294002 and Wortmannin decreased the CPT-induced hTERT level (Fig. 4D). Furthermore, a parallel experimental condition was applied to measure telomerase activity using a TRAP-ELISA. Treatment with PI3K/Akt inhibitors significantly abolished CPT-induced telomerase activity (Fig. 4E). These results suggest that CPT may increase phosphorylation of hTERT and thereby possibly inhibit its translocation to the nucleus by inducing phosphorylation of Akt.

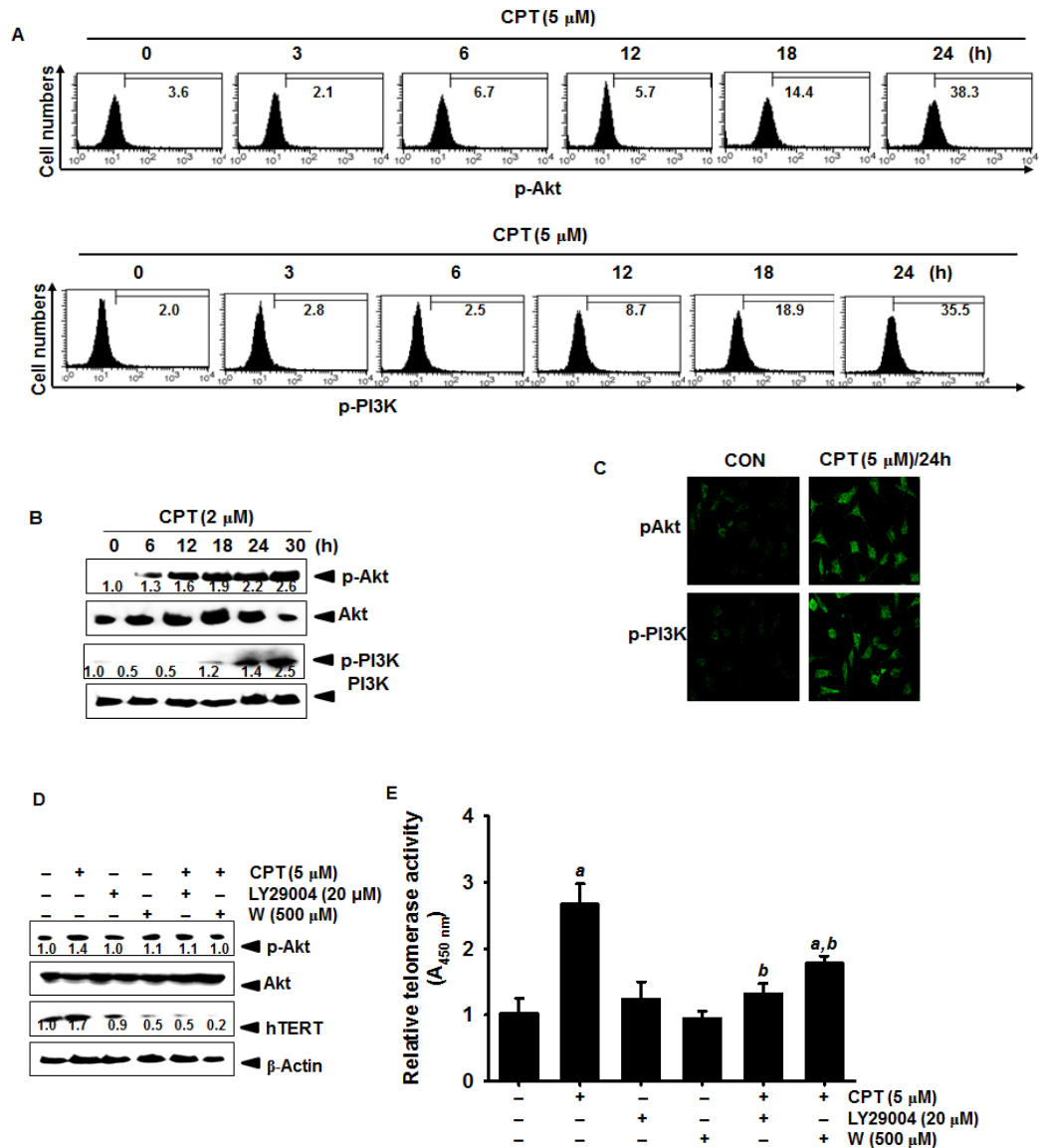


**Fig. 27.** Camptothecin (CPT)-induced phosphorylation of Akt in LNCaP cell. (A) Cells were incubated with the indicated time of 2  $\mu$ M CPT. Cells were treated with p-Akt and pPI3K as primary antibody. Monoclonal antibody was detected using an anti-rabbit secondary antibody conjugated with FITC under flow cytometer and (C) confocal microscopy. (B) Total protein was subjected to 10% SDS-PAGE, transferred to nitrocellulose membranes, and protein levels were analyzed by Western blot analysis using anti-p-PI3K, anti-PI3K, anti-p-Akt, and anti-Akt antibodies. (D) LNCaP cells were preincubated with LY294002 and Wortmannin

then treated with 2  $\mu$ M CPT for 24 h. Equal amounts of cell lysate were subjected to Western blot analysis with specific antibodies. (E) In a parallel experiment LNCaP cells was measured using TRAP-ELISA. Data from three independent experiments are expressed as the overall mean  $\pm$  S.E. Statistical significance was determined by two-way ANOVA (<sup>a</sup> and <sup>b</sup>,  $p < 0.05$  vs. untreated control and CPT-treated group).

### **5.3.5 CPT induces apoptosis in human leukemia cells**

Camptothecin (CPT) decreases cell viability and proliferation in leukemia cell lines. Cells were seeded at  $1 \times 10^5$  cells/ml and treated with the indicated concentrations of CPT for 24 h. (A) Cell viability were determined by MTT assay. (B) In a parallel experiment DNA fragment was analyzed by DNA fragmentation assay. (C) Representative histograms for effect of CPT treatment on cell cycle distribution in Leukemia cells were analyzed. Data from three independent experiments are expressed as the overall mean  $\pm$  S.E. Statistical significance was determined by one-way ANOVA (<sup>a</sup>,  $p < 0.05$  vs. untreated control).

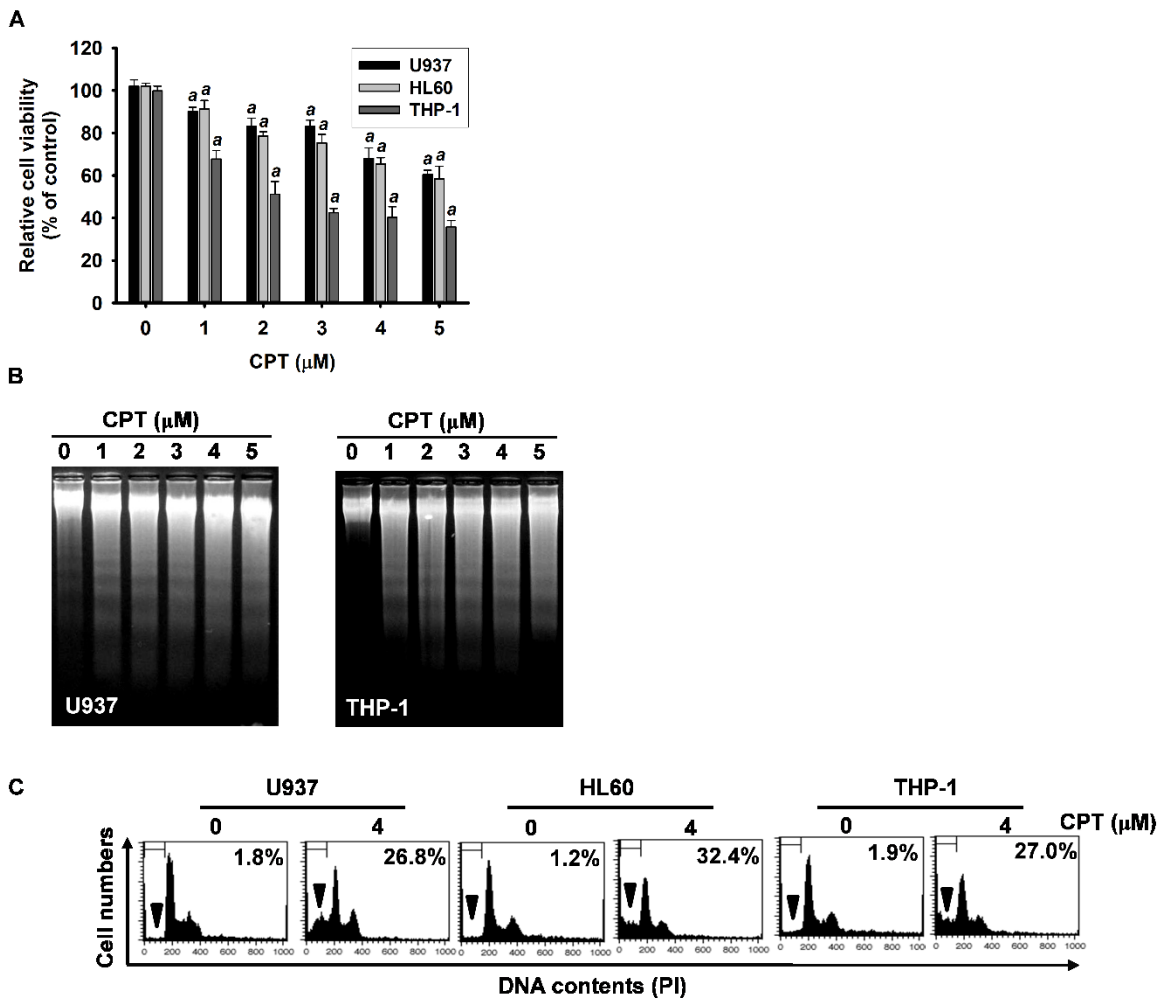


**Fig. 28.** Camptothecin (CPT) decreases cell viability and proliferation in leukemia cell lines. Cells were seeded at  $1 \times 10^5$  cells/ml and treated with the indicated concentrations of CPT for 24 h. (A) Cell viability were determined by MTT assay. (B) In a parallel experiment DNA fragment was analyzed by DNA fragmentation assay. (C) Representative histograms for effect of CPT treatment on cell cycle distribution in Leukemia cells were analyzed. Data from three independent experiments are expressed as the overall mean  $\pm$  S.E. Statistical significance was determined by one-way ANOVA (<sup>a</sup>,  $p < 0.05$  vs. untreated each group).

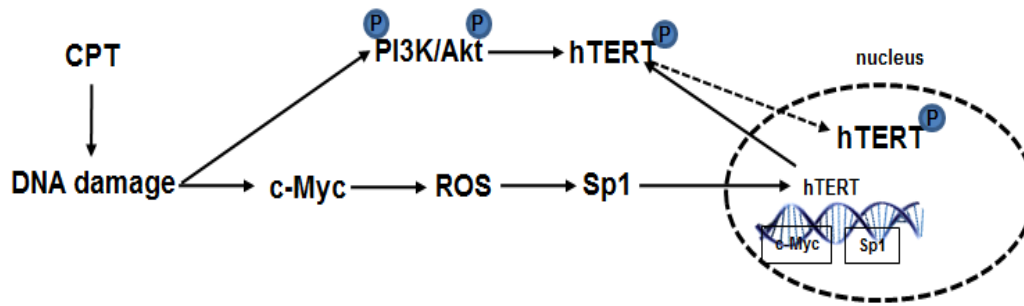


**Fig. 29.** Schematic explanation of camptothecin (CPT) in controlling hTERT. CPT regulates hTERT expression and telomerase activity through the phosphorylation of PI3K/Akt LNCaP cells. In addition, CPT-enhanced the c-Myc dependent ROS production which increase the Sp1 transcription activity. Both c-Myc and Sp1 are directly involved in hTERT expression and regulation in LNCaP cells.

## 5.4 Discussion

Telomerase activation is strongly suppressed in normal human somatic cells, but reactivated in immortal cells, suggesting that upregulation of telomerase activity is crucial to the process of oncogenesis. Therefore, many studies reported that hTERT expression, in combination with oncogenes, are sufficient to induce normal human epithelial and fibroblast cells to become tumor cells, with the majority of cancer cells exhibiting high telomerase activity which enable their uncontrolled growth [Zhang et al., 2006]. Therefore, scientists have suggested that the expression of hTERT is closely correlated with the telomerase activity [Takakura et al., 2008] It is also concern that telomerase has been identified as a promising target for human cancer gene therapy, and its inhibition allows telomere shortening to occur in cancer cells which in turn is thought to trigger apoptosis [Kyo et al., 2000]. Despite, Murofushi *et al.*, reported that endogenous telomerase activity and hTERT expression could also be detected in an S phase-specific manner in normal somatic fibroblasts

[Saretzki et al., 2003]. Liang *et al.*, reported that immortalized human NP cells are protected against serum starvation-induced G<sub>1</sub> arrest via overexpression of hTERT [Liang et al., 2012]. Nevertheless, in the present study, knockdown of hTERT didn't alter CPT-induced G<sub>2</sub>/M phase arrest, which indicates that CPT increases hTERT expression and telomerase activity, which is not involved in CPT has no effect on CPT-mediated G<sub>2</sub>/M phase arrest. Even though another report showed that upregulation of hTERT protected the cells from apoptosis, depletion of hTERT didn't induced apoptosis in LNCaP cells. One possibility is that CPT-induced G<sub>2</sub>/M phase arrest could be impact on hTERT upregulation. Therefore, further studies are needed to elucidate the mechanism of hTERT regulation in response to CPT. The hTERT core promoter contains numerous transcription factor binding sites, including two for c-Myc, five for Sp1, one for Ets, and two for Inr [Kalpper et al., 2003]. Out of all these transcription factors, c-Myc has been studied most extensively for its role in the regulation of hTERT transcription [Kyo et al., 2008]. In addition to the c-Myc recognition sequence (E-box), Sp1 is involved in the regulation of hTERT promoter activity in various human cells [Kalpper et al., 2003]. In this study, we found that expression of c-Myc and Sp1 mRNA and protein was enhanced by CPT, depletion of c-Myc and Sp1 abolished CPT-induced hTERT expression. Nevertheless, we could not rule out the possibility that other transcriptional factors might also be involved in the suppression of hTERT gene expression by CPT, because Ets and NF- $\kappa$ B are implicated in the repression of telomerase activity [Bu et al., 2010].

According to recent research, activation of telomerase by hTERT overexpression inhibits ROS-mediated apoptosis by repressing intracellular ROS production, suggesting that ROS alleviates telomerase activity [Indran et al., 2010]. Additionally, Shay and Wright showed that hTERT overexpression not only reduces the basal cellular ROS levels but also inhibits endogenous ROS production in response to stimuli that induce intracellular ROS generation;

conversely, siRNA-mediated gene silencing of hTERT potentiated the increase in cellular ROS levels following exposure to oxidative stress [Shay et al., 2006]. Our previous study also found that apigenin treatment decreases telomerase activity via an ROS-independent pathway in leukemia cells [Shay et al., 2006]. However, in this study, we found that inhibition of ROS decreased hTERT expression, which indicates that ROS might indirectly play a role in CPT-induced hTERT expression. Normally, ROS levels are tightly controlled and predominantly regulated by the transcription factor Nrf2 and its repressor protein Keap1 [DeNicola et al., 2011]. As shown in our data, depletion of Nrf2 triggers CPT-induced hTERT expression accompanied by increase of ROS generation, suggesting that Nrf2 directly controls the hTERT level or enhances ROS production. However, further experiments are needed to find out hidden mechanism of Nrf2/ROS in regulating hTERT expression.

PI3K/Akt is a potent inhibitor of apoptosis, acting by blocking caspase activation and inhibiting chromatin condensation [Yu et al., 2008]. Akt phosphorylation could be a potent inducer for telomerase activation via hTERT phosphorylation linked to its nuclear localization [Wojtyla et al., 2011]. Nuclear translocation of hTERT from a presumably nonfunctional cytosolic location may be one important mechanism involved in telomerase activity in the nucleus [Kyo et al., 2002]. The increased of PTEN, which acts as a counterpart of Akt, may allow malignant cells to induce telomerase activity through increasing hTERT mRNA levels [Zhu et al., 2009]. This discrepancy implies that various kinases could possess different functions in the various signal pathways. In the present study, we observed that CPT treatment upregulates phosphorylation of PI3K and Akt, leading to increase of hTERT. These results clearly suggest that CPT regulates hTERT at the posttranslational level by inducing its phosphorylation by the Akt pathway. Recently, mitogen-activated protein kinases (MAPKs) and serine/threonine kinases are also shown to

phosphorylate hTERT and regulate telomerase activity [Naka et al., 2004]. Since we previously published CPT increased the MAPK activity, further studies will be necessary to determine whether MAPK or serine/threonine kinases are related to CPT-induced upregulation of hTERT.

## **5.5 Conclusion**

CPT enhanced c-Myc- and Sp1-mediated hTERT expression, leading to upregulate telomerase activity. In addition, phosphorylation of Akt increased by CPT may affect phosphorylation and translocation of hTERT. These evidences suggest that CPT could be used to effectively regulate telomerase activity through the transcriptional and posttranslational modification of hTERT.

## **Chapter 6**

# **Camptothecin suppresses matrix metalloproteinase-9 and vascular endothelial growth factor in DU145 cells through Nrf2-dependent HO-1 induction**

## Abstract

Camptothecin (CPT) possesses potent anti-inflammatory, immunomodulatory, anti-cancerous, and antiproliferative effects. However, little is known about the mechanism by which CPT regulates metastasis and invasion of cancer cells. Therefore, the current study aimed to investigate the effects of CPT on the expression of matrix metalloproteinase (MMP-9) and vascular endothelial growth factor (VEGF) which are important factors for invasion and metastasis, in prostate cancer cells. CPT *in vitro* resulted in a modulate inhibition of cell proliferation and in a significant reduction of matrigel invasion of human prostate DU145 and LNCaP cells without direct cytotoxicity. Treatment with CPT also reversed phorbol-12-myristate-13-acetate (PMA)- and tumor necrosis factor- $\alpha$  (TNF- $\alpha$ )-induced MMP-9 and VEGF activity. We also found that CPT down-regulates the expression of *MMP-9* and *VEGF* genes by inhibiting NF- $\kappa$ B activity *via* sustainment of NF- $\kappa$ B subunits, p65 and p50, in cytosolic compartment. Downregulation of PI3K/Akt phosphorylation in response to CPT was also revealed as an upstream pathway responsible for the expression of *MMP-9* and *VEGF* accompanying with inhibition of NF- $\kappa$ B activity. We further showed that CPT inhibits PMA-induced MMP9 and VEGF expression and production by upregulating nuclear erythroid 2-related factor-2 (Nrf2)-mediated heme oxygenase-1 (HO-1). Taken together, these data indicate that CPT inhibits invasion of prostate cancer cells accompanying with suppression of MMP-9 and VEGF production, mainly via the PI3K/Akt-mediated NF- $\kappa$ B pathway and the Nrf2-dependent HO-1 pathway, suggesting that CPT may be a good candidate eligible to downregulate cancer invasion by inhibiting MMP-9 and VEGF.

## 6.1 Introduction

Prostate cancers are often difficult to cure, because of broad spread known as invasion and metastasis, to distinct location in the body such as pelvic lymph nodes, ureters, bone, rectum, or bladder [Dasgupta et al., 2012]. Due to severe invasion and metastasis, targeting matrix metalloproteinase-9 (MMP-9) and vascular endothelial growth factor (VEGF) has been thought as good strategies to treat prostate cancers [Jang and Kim, 2012]. MMP-9, a group of zinc-dependent endopeptidases, is implicated in the degradation of extracellular matrix (ECM) during pathological conditions, such as inflammatory, vascular and autoimmune disorders, and carcinogenesis in tumor invasion and metastasis [Curran and Murray, 2000; Kessenbrock et al., 2010; Koutroulis et al., 2008]. It has been previously reported that some polyphenols and flavonoids are chemo preventive candidates to suppress tumor invasion and metastasis *via* inhibition of MMP-9 activity [Jayasooriya et al., 2013; Lü et al., 2012]. Therefore, MMP-9 has been considered as potential diagnostic and prognostic biomarkers in many types and stages of cancers [Zucker and Vacirca, 2004]. Additionally, VEGF upregulated by various oncogenes and growth factors, is a key mediator of angiogenesis in cancer patients and consequently forms new vasculature around the tumor, allowing it to exponentially grow [Appelmann et al., 2010; Risau, 1997]. Recently, Corrie et al. reported that inhibitors of angiogenesis primarily target the VEGF ligand/receptor pathway in clinical application [Corrie et al., 2010]. Notably, VEGF receptor tyrosine kinase inhibitors, monoclonal antibodies to VEGF, have also been directed against the extracellular domain of VEGFRs, thereby preventing the binding interaction with VEGF ligand and subsequent inhibition of tumor invasion and metastasis [Chen et al., 2012]. Therefore, inhibition of the MMP-9 and VEGF production and signaling pathway may be a good strategy for treatment and regulation of invasion and metastasis of prostate cancers.

Nuclear factor- $\kappa$ B (NF- $\kappa$ B) is a proinflammatory transcription factor that has emerged as an important effector responsible for *VEGF* and *MMP-9* expression in several types of cancer cells [Pahl, 1999]. Previous studies showed that the inhibition of NF- $\kappa$ B activity in human prostate cancer cells decreases their tumorigenic and metastatic abilities by suppressing angiogenesis and invasion through downregulation of MMP-9 and VEGF activity [Fujioka et al., 2003; Rafiee et al., 2004]. Additionally, some researches demonstrated that heme oxygenase-1 (HO-1) which is an inducible cyto-protective enzyme that catalyzes the initial rate-limiting reaction in heme catabolism, plays a key modulator in the adaptation of cells to stressful conditions such as hypertension, acute pancreatitis, asthma, and cancers [Cho et al., 2010; Vicente et al., 2003]. Recently, Yin et al. directly determined that downregulation of HO-1 leads to a significant increase of MMP-9 and VEGF expression in gastric cancer cells [Yin et al., 2012]. Martin et al. also reported that HO-1 expression may be regulated by nuclear erythroid 2-related factor-2 (Nrf2) in response to antioxidant chemical [Martin et al., 2004]. Additionally, an *in vivo* study showed that *Nrf2*-knockout results in a significant increase of NF- $\kappa$ B activity and consequent upregulation of MMP-9 and VEGF expression in mice [Mao et al., 2010], implying that MMP-9 and VEGF are regulated by correlation between NF- $\kappa$ B and Nrf2-mediated HO-1. Nevertheless, precise mechanism whether Nrf2<sup>-/-</sup> regulates invasion and metastasis by suppressing MMP-9 and VEGF expression has not been elucidated, to date.

Camptothecin (CPT), a naturally occurring cytotoxic alkaloid and novel effective anticancer drug, was originally isolated from *Camptotheca acuminata* [Zhou et al., 2010] as a strong inhibitor of the DNA-replicating enzyme topoisomerase I [Stewart and Schütz, 1987]. Nevertheless, because anti-invasive and anti-metastatic ability of CPT is little understood, we, in the present study, evaluated the effects of CPT on MMP-9 and VEGF

expression and activity in human prostate cancer DU145 cells. In conclusion, we found that CPT downregulates phorbol-12-myristate-13-acetate (PMA)- and tumor necrosis factor- $\alpha$  (TNF- $\alpha$ )-induced MMP-9 and VEGF expression by suppressing NF- $\kappa$ B activation. Furthermore, CPT-induced inhibition of MMP-9 and VEGF is associated with Nrf2-mediated HO-1 induction in prostate cancer DU145 cells.

## 6.2 Materials and methods

### *Reagent and antibodies*

CPT was purchased from Sigma (St. Louis, MO) and dissolved in DMSO (vehicle). Antibodies against MMP-9, VEGF,  $\beta$ -actin, p65, p50, PI3K, phospho (p)-PI3K, Akt, p-Akt, HO-1, and Nrf2 were purchased from Santa Cruz Biotechnology (Santa Cruz, CA). Peroxidase-labeled goat anti-rabbit immunoglobulin and TNF- $\alpha$  were purchased from KOMA Biotechnology (Seoul, Republic of Korea). A specific Akt inhibitor LY294002 was purchased from Calbiochem (San Diego, CA). PMA, 3-(4,5-dimethyl-2-thiazolyl)-2,5-diphenyl-2H-tetrazolium bromide (MTT), and propidium iodine (PI) were obtained from Sigma (St. Louis, MO). Cobalt protoporphyrin (CoPP) and zinc protoporphyrin (ZnPP) were purchased from Tocris Bioscience (Bristol, UK).

### *Cell culture and viability*

Human prostate cancer DU145 and LNCaP cells, breast carcinoma MDA-MB-231 cells, and bladder carcinoma T24 cells were obtained from the American Type Culture Collection (Manassas, VA). Cells were maintained in RPMI medium (WelGENE Inc., Daegu, Republic of Korea) supplemented with 10% heat-inactivated FBS (WelGENE Inc.) and 1% penicillin-streptomycin (WelGENE Inc.) in 5% CO<sub>2</sub> at 37°C. Cells were seeded at  $1 \times 10^5$  cells/ml and

then treated with various concentrations of CPT. After 24-h incubation, the viability was determined by an MTT assay. Morphology of the cells was examined by a phase contrast microscope (Ceti N.V., Antwerpen, Belgium). In a parallel experiment, annexin-V<sup>+</sup> apoptotic cells were analyzed using a FACSCalibur flow cytometer (Becton Dickinson, San Jose, CA).

#### *DNA fragmentation assay*

Cells were treated with the indicated chemicals for 24 h and then lysed on ice in a buffer containing 10 mM Tris-HCl (pH 7.4), 150 mM NaCl, 5 mM EDTA, and 0.5% Triton X-100 for 30 min. Lysates were vortexed and cleared by centrifugation at 16,000 g for 20 min. Fragmented DNA in the supernatant was extracted with an equal volume of neutral phenol:chloroform:isoamylalcohol (25:24:1, v/v/v) and electrophoretically analyzed on 1.5% agarose gel containing ethidium bromide.

#### *Invasion assay*

Invasion assays were performed using modified Boyden chambers with polycarbonate nucleopore membrane (Corning, Corning, NY). Precoated filters (6.5 mm in diameter, 8 μm pore-size, Matrigel 100 μg/cm<sup>2</sup>) were rehydrated and 5 × 10<sup>4</sup> cells in medium with or without CPT were seeded into the upper part of each chamber. After incubating for 24 h, non-migratory cells on the upper surface of the filter were wiped with a cotton swab and migrated cells on the lower surface of the filter were fixed and stained with 0.125% coomassie Blue in a methanol:acetic acid:water mixture (45:10:45, v/v/v). Random fields were counted under a light microscope.

### *Gelatin zymography*

Cells were treated with the indicated concentrations of CPT in serum-free RPMI medium for 24 h and MMP-9 activity was determined by gelatin zymography using 0.1% gelatin as a substrate. Culture media were mixed with SDS-PAGE sample buffer in the absence of reducing agent and electrophoresed in 8% polyacrylamide gel. After electrophoresis, the gels were washed three times with 2.5% Triton X-100 in water and then incubated overnight in a closed container at 37°C in 0.2% Brij, 35.5 mM CaCl<sub>2</sub>, 1 mM NaCl, and 50 mM Tris (pH 7.4). The gels were stained for 30 min with 0.25% coomassie blue R-250 in 10% acetic acid and 45% methanol and then destained for 30 min using an aqueous mix of 20% acetic acid, 20% methanol, and 17% ethanol. Areas of protease activity appeared as clear bands.

### *RNA extraction and RT-PCR*

Total RNA was isolated using Easy-blue reagent (iNtRON Biotechnology, Sungnam, Republic of Korea) according to the manufacturer's recommendations. Genes of interest were amplified from cDNA that was reverse-transcribed from 1µg of total RNA using the One-Step RT-PCR Premix (iNtRON Biotechnology). Primers for MMP-9 sense (5'-CCT GGA GAC CTG AGA ACC AAT CT-3'); MMP-9 antisense (5'-CCA CCC GAG TGT AAC CAT AGC -3'); VEGF sense (5'-AGG AGG GCA GAA TCA TCA CG-3'); VEGF antisense (5'-TAT GTG CTG GCC TTG GTG AG-3'); HO-1 sense (5'-TCG CCA CCA GAA AGC TGA GTA TAA-3'); HO-1 antisense (5'-ATT GCC AGT GCC ACC ACC AAG TTC AAG-3'); and glyceraldehydes-3-phosphate dehydrogenase (GAPDH) sense (5'-CCA CCC ATG GCA AAT TCC ATG GCA-3'); and GAPDH antisense (5'-TCT AGA CGG CAG GTC AGG TCC ACC-3') were used. PCR reaction was initiated at 94°C for 2 min followed by 31 cycles of 94°C for 30 min, 30-min annealing temperature, 72°C for 30 min followed by final extension at 72°C

for 5 min. Annealing temperatures for MMP-9, VEGF, HO-1, and GAPDH were 63°C, 61°C, 62°C and 62°C, respectively. After amplification, PCR products were separated on 1.5% agarose gels and visualized by ethidium bromide fluorescence.

#### *Western blot analysis*

Total cell extracts were prepared using PRO-PREP protein extraction solution (iNtRON Biotechnology). Proteins were separated by SDS-PAGE and electro transferred to nitrocellulose membranes (Amersham, Arlington Heights, IL). The detection of specific proteins was carried out with an ECL Western blotting kit (Amersham) according to the recommended procedure.

#### *Enzyme-linked immunosorbent assay (ELISA) for VEGF*

Cells were incubated in medium supplemented with CPT for 24 h. The cell culture supernatant was harvested, and cell debris was removed. The supernatant was assayed immediately using commercially available VEGF ELISA Kits (R&D Systems).

#### *Electrophoretic mobility shift assay (EMSA)*

The preparation of cytoplasmic and nuclear extracts was conducted using the NE-PER nuclear and cytoplasmic extraction reagents (Pierce, Rockford, IL). DNA-protein binding assays were carried out with nuclear extract. Synthetic complementary NF- $\kappa$ B-binding oligonucleotides (5'-AGT TGA GGG GAC TTT CCC AGG C-30') binding oligonucleotides (Santa Cruz Biotechnology) were biotinylated using the biotin 30-end DNA labeling kit (Pierce) according to the manufacturer's instructions and annealed for 1h at room temperature. Binding reactions were carried out for 20 min at room temperature in the

presence of 50 ng/ml poly(dI-dC), 0.05% nonidet P-40, 5 mM MgCl<sub>2</sub>, 10 mM EDTA, and 2.5% glycerol in 1×binding buffer (LightShift™ chemiluminescent EMSA kit) with 20 fmol of biotin-end-labeled target DNA and 10 µg of nuclear extract. Assays were loaded onto native 4% polyacrylamide gels pre-electrophoresed for 60 min in 0.5×Tris borate/EDTA and before being transferred onto a positively charged nylon membrane (Hybond™-N<sup>+</sup>) in 0.5×Tris borate/EDTA at 100 V for 30 min. Transferred DNAs were cross-linked to the membrane at 120 mJ/cm<sup>2</sup> and detected using horseradish peroxidase-conjugated streptavidin according to the manufacturer's instructions.

#### *Luciferase assay*

NF-κB reporter construct was purchased from Clontech (Palo Alto, CA) and MMP-9 promoter was obtained from Prof. T.K. Kwon (School of Medicine, Keimyung University, Daegu, Republic of Korea). Briefly, DU145 cells were plated onto six-well plates at a density of  $5 \times 10^5$  cells/well and grown overnight. Cells were transfected with 2 µg of each plasmid construct by the Lipofectamine method for 6 h. After transfection, the cells were cultured in 10% FBS containing RPMI medium with the indicated concentrations of CPT for 24 h. Cells were lysed with lysis buffer (20 mM Tris-HCl, pH 7.8, 1% Triton X-100, 150 mM NaCl, and 2 mM DTT). Five µl cell lysates were mixed with 25 µl luciferase activity assay reagent and luminescence produced for 5 s was measured using a GLOMAX luminometer (Promega, Madison, WI).

#### *Transfection assay (Nrf2)*

DU145 cells were seeded on a 24-well plate at a density of  $1 \times 10^5$  cells/ml and transfected *Nrf2*-specific silencing RNA (siRNA, Santa Cruz Biotechnology) for 24 h. For

each transfection, 450  $\mu$ l of growth medium was added to 20 nM siRNA duplex with the transfection reagent G-Fectin (Genolution Pharmaceuticals Inc., Seoul, Republic of Korea) and the entire mixture was added gently to the cells.

### *Statistical analysis*

Images were visualized with Chemi-Smart 2000 (Vilber Lourmat, Cedex, France). Images were captured using Chemi-Capt (Vilber Lourmat) and transported into Adobe Photoshop (version 11.0). All data are presented as mean  $\pm$  S.E. Significant differences between the groups were determined using one-way ANOVA test. A value of \*,  $p < 0.05$  was accepted as an indication of statistical significance.

## **6.3 Results**

### **6.3.1 CPT has no influence on cell viability**

To determine the cytotoxic potential of CPT on cell viability in DU145 and LNCaP cells, an MTT assay was performed at 24 h after treatment with various concentrations of CPT. Treatment with CPT slightly decreased cell proliferation in a dose-dependent manner (Fig. 1A). To assess whether treatment with CPT resulted in a decrease of apoptosis-dependent cell proliferation, we next analyzed in detail the effect of CPT on DU145 cell viability and cytotoxicity. Significant amounts of DNA fragmentation were observed in the positive H<sub>2</sub>O<sub>2</sub>-treated group; however, no fragmented DNA was seen in CPT-treated DU145 cells (Fig. 1B). According to data of the annexin-V staining, the H<sub>2</sub>O<sub>2</sub>-treated DU145 cells were composed of approximately 80% annexin-V<sup>+</sup> apoptotic cell populations; however, a little annexin-V<sup>+</sup> population was observed in the CPT-treated DU145 cells, thereby suggesting that CPT has no influence on apoptotic cell death in prostate cancer DU145 cells (Fig. 1C). When phase

contrast microscopy was used to examine the change of cell morphology, only H<sub>2</sub>O<sub>2</sub>-treated group displays decreased cell number with some apoptotic cell shrinkage compared to that of the untreated group (Fig. 1D). Treatment with CPT significantly enlarged cell size implied that CPT induces G<sub>2</sub>/M phase arrest as previously published [Wu et al., 2010]. Taken together, these data suggested that a little decrease of cell proliferation shown in Fig. 1A may be due to cell cycle arrest, not apoptotic cell death. Additionally, treatment with CPT resulted in a significant reduction of DU145 penetration through a matrigel-coated membrane compared to that in the untreated group. These results indicate that CPT inhibits invasion of prostate cancer DU145 cells without direct cytotoxicity.

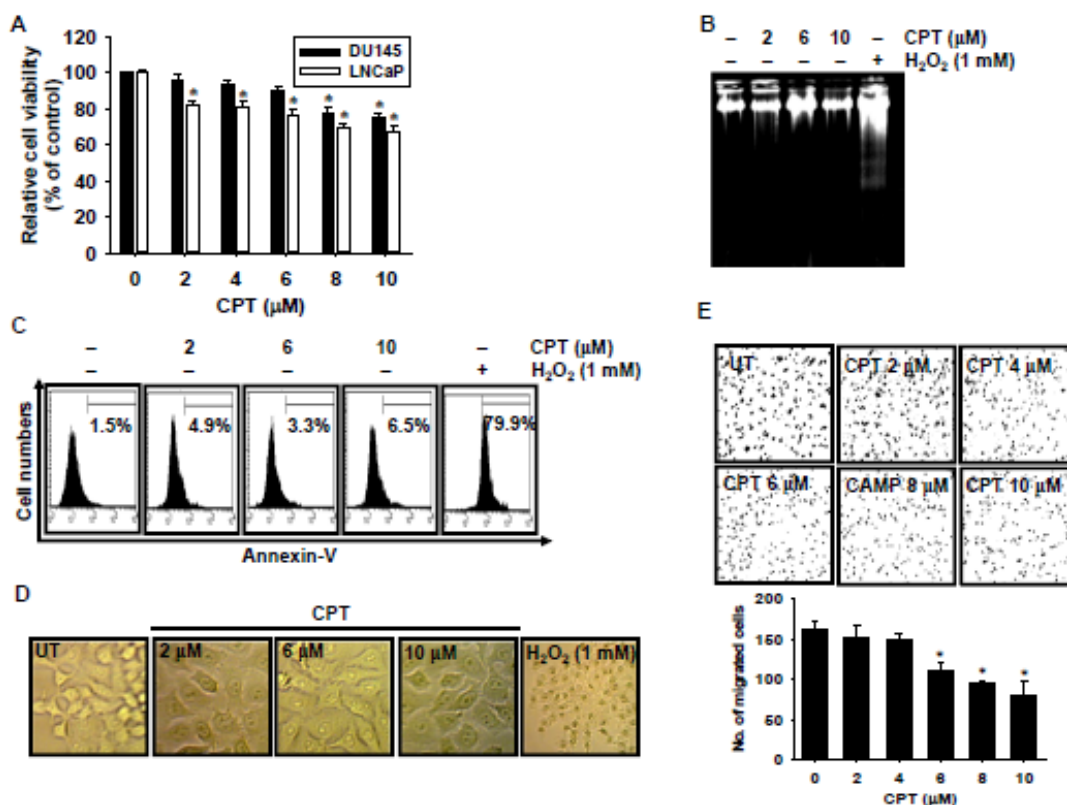


**Fig. 30** Effect of CPT on the viability of prostate cancer DU145 and LNCaP cells. DU145 and LNCaP cells ( $2 \times 10^5$  cells/ml) were incubated with the indicated concentrations of CPT

for 24 h. (A) Cell viability was determined by an MTT assay. (B) Total DNAs were extracted at 24 h and DNA fragmentation assay was analyzed on 1.5% agarose gel. (C) In a parallel experiment, percentages of apoptotic cells were measured by flow cytometric analysis. Percentages of gates (apoptosis) were represented in each panel. (D) Cell morphology was examined by phase contrast microscopy. (E) The upper parts of the transwells were coated with matrigel for the invasion assay. Then, the cells were cultured in serum-free media for 3h before treatment with the indicated concentrations of CPT. After 24-h incubation, the numbers of cells passing through the matrigel to the membrane were dyed using 0.125% Coomassie blue in ethanol. Statistical significance was determined by one-way ANOVA test (\*,  $p < 0.05$  vs. untreated control).

### 6.3.2 CPT suppresses MMP-9 expression and activity

Since MMP-9 has been thought to be critically involved in the processes of tumor invasion, metastasis, and angiogenesis, zymography, RT-PCR, and western blot analysis were conducted to assess whether CPT regulates MMP-9 expression in prostate cancer DU145 and LNCaP cells. Zymography data showed that gelatinase activity of MMP-9 is significantly decreased in response to CPT in a dose-dependent manner at 24 h (Fig. 2A) and RT-PCR analysis also confirmed that treatment with CPT inhibits the expression of *MMP-9* gene in both the prostate cancer cell lines (Fig. 2B). We also found that CPT significantly downregulates PMA- and TNF- $\alpha$ -induced MMP-9 mRNA and protein expression (Fig. 2C). Additionally, CPT substantially downregulated the expression of PMA-stimulated *MMP-9* mRNA in human breast carcinoma MDA-MB-231 cells and bladder carcinoma T24 cells (Fig. 2D), indicating that CPT suppresses MMP-9 expression in many different types of cancer cells. These results indicate that CPT inhibits MMP-9 expression and activity.

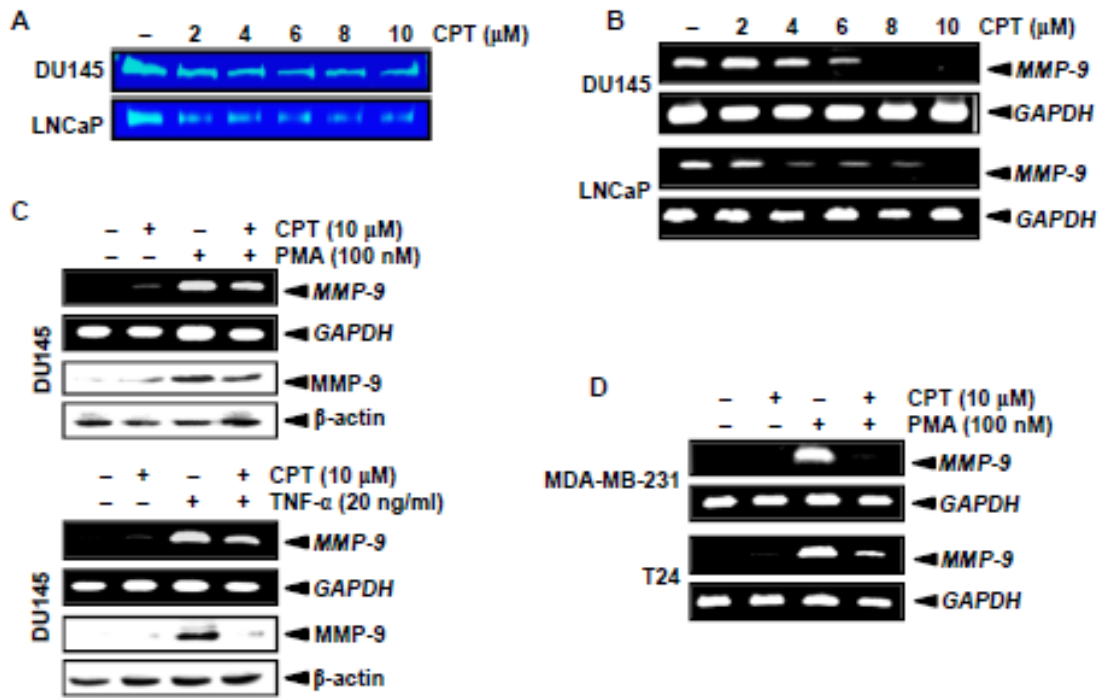


**Fig. 31.** Effect of CPT on MMP-9 activity and expression. (A) DU145 and LNCaP cells ( $2 \times 10^5$  cells/ml) were treated with the indicated concentrations of CPT. Conditioned medium was collected at 24h, followed by gelatin zymography. (B) Total RNA was isolated at 6 h, and RT-PCR analysis of *MMP-9* was performed. (C) DU145 cells were treated with 10  $\mu$ M CPT 2 h before treatment with 100 nM PMA and 20 ng/ml TNF- $\alpha$ . Total RNA was isolated at 6 h and RT-PCR analysis of *MMP-9* was performed. Protein lysates were prepared at 24 h, subjected to SDS-PAGE, and immunoblotted using specific antibodies against MMP-9. (D) Breast carcinoma MDA-MB-231 cells and bladder carcinoma T24 cells were treated with 10  $\mu$ M CPT 2h before treatment with 100nM PMA for 6 h. Total RNA was isolated and RT-PCR analysis of *MMP-9* was performed. GAPDH and  $\beta$ -actin were used as an internal control for RT-PCR and western blot analysis, respectively.

### 6.3.3 CPT inhibits VEGF expression and production

To further investigate that CPT exerts inhibitory effects on VEGF induction, ELISA, RT-PCR, and western blot analyses were conducted in DU145 and LNCaP cells. Treatment with CPT dose-dependently decreased the level of VEGF secreted into the culture medium in the both prostate cancer DU145 and LNCaP cells compared to the untreated control group (Fig. 3A). A parallel experiment showed that treatment with CPT significantly suppresses the level of *VEGF* mRNA in DU145 and LNCaP cells in a dose-dependent manner (Fig. 3B). Next, we also evaluated whether stimulant-induced VEGF mRNA and protein levels were regulated in response to CPT. RT-PCR analysis confirmed that stimulation of cells with PMA and TNF- $\alpha$  results in a significant increase of VEGF expression in DU145 cells compared to that in the untreated control; however, treatment with CPT suppresses PMA- and TNF- $\alpha$ -induced VEGF upregulation at the protein and mRNA levels (Fig. 3C). Moreover, pretreatment with CPT significantly inhibited PMA- and TNF- $\alpha$ -induced *VEGF* upregulation at the mRNA level in breast carcinoma MDA-MB-231 cells and bladder carcinoma T24 cells (Fig. 3D). Taken together, these results suggest that CPT down regulates carcinogen or stimulant-induced expression and production of VEGF in various cancer cells.

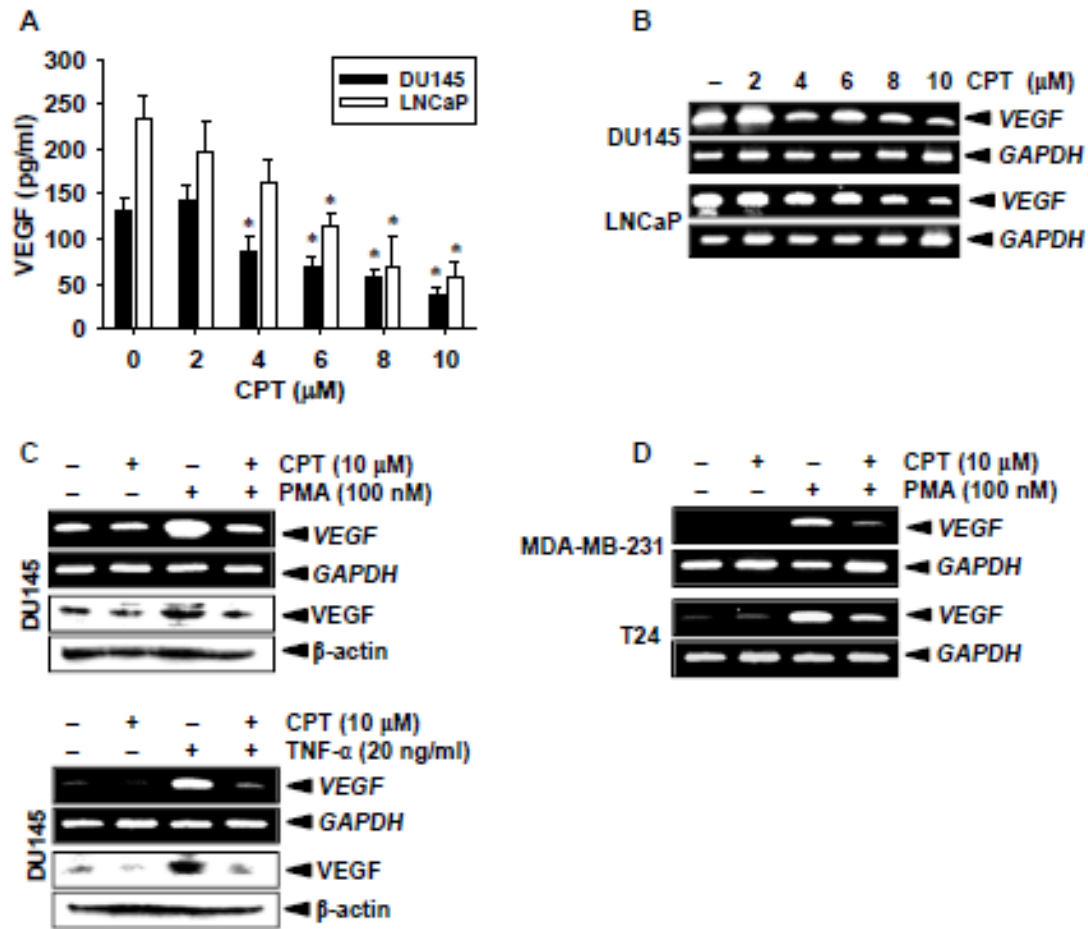


**Fig. 32.** Effects of CPT on VEGF expression. (A) DU145 and LNCaP cells ( $2 \times 10^5$  cells/ml) were treated with the indicated concentrations of CPT for 24 h. The VEGF level in the culture medium was measured by ELISA. (B) DU145 and LNCaP cells were treated with the indicated concentration of CPT for 6h. Total RNA was isolated and RT-PCR analysis of *VEGF* was performed. (C) DU145 cells ( $2 \times 10^5$  cells/ml) were treated with 10  $\mu$ M CPT 2h before treatment with 100nM PMA and 20 ng/ml TNF- $\alpha$ . Total RNA was isolated at 6 h and RT-PCR analysis of *VEGF* was performed. Protein lysates were prepared at 24 h, subjected to SDS-PAGE, and immunoblotted using specific antibodies against VEGF. (D) Breast carcinoma MDA-MB-231 cells and bladder carcinoma T24cells were pretreated with 10  $\mu$ M CPT 2h before treatment with 100nM PMA for 6 h. Total RNA was isolated, and RT-PCR

analysis of *VEGF* was performed. GAPDH and  $\beta$ -actin were used as an internal control for RT-PCR and western blot analysis, respectively. Statistical significance was determined by one-way ANOVA test (\*,  $p < 0.05$  vs. untreated control).

#### 6.3.4 CPT downregulates NF- $\kappa$ B activity

NF- $\kappa$ B is a key transcription factor for expression of *MMP-9* and *VEGF*, and consequently promotes tumor invasion, metastasis, and angiogenesis [Pahl, 1999]. Therefore, we assessed whether CPT regulates the specific DNA-binding activity of NF- $\kappa$ B. Treatment with CPT reduced the DNA-binding activity of NF- $\kappa$ B in a dose-dependent manner at 24 h (Fig. 4A) and a time-dependent manner (Fig. 4B). We also conducted a promoter assay in DU145 cells transiently transfected with a luciferase reporter vector that included the NF- $\kappa$ B binding sites. Luciferase activity in the cells was also reduced by treatment with CPT in a dose-dependent manner (Fig. 4C). In a parallel experiment, to determine whether nuclear translocation of NF- $\kappa$ B subunit is regulated by CPT, p65 and p50 expression was determined in the cytosolic compartment. Treatment with CPT sustained the expression of NF- $\kappa$ B subunits, p65 and p50, in the cytosolic fraction, compared to the untreated control (Fig. 4D). Then, we investigated whether CPT regulates PMA- and TNF- $\alpha$ -induced NF- $\kappa$ B activity. Stimulation with PMA and TNF- $\alpha$  caused a remarkable increase in the binding complexes between NF- $\kappa$ B and specific-binding DNA; however, pretreatment with CPT significantly reduced PMA- and TNF- $\alpha$ -induced NF- $\kappa$ B activity at 24 h (Fig. 4E). These results indicate that CPT inhibits NF- $\kappa$ B activity.

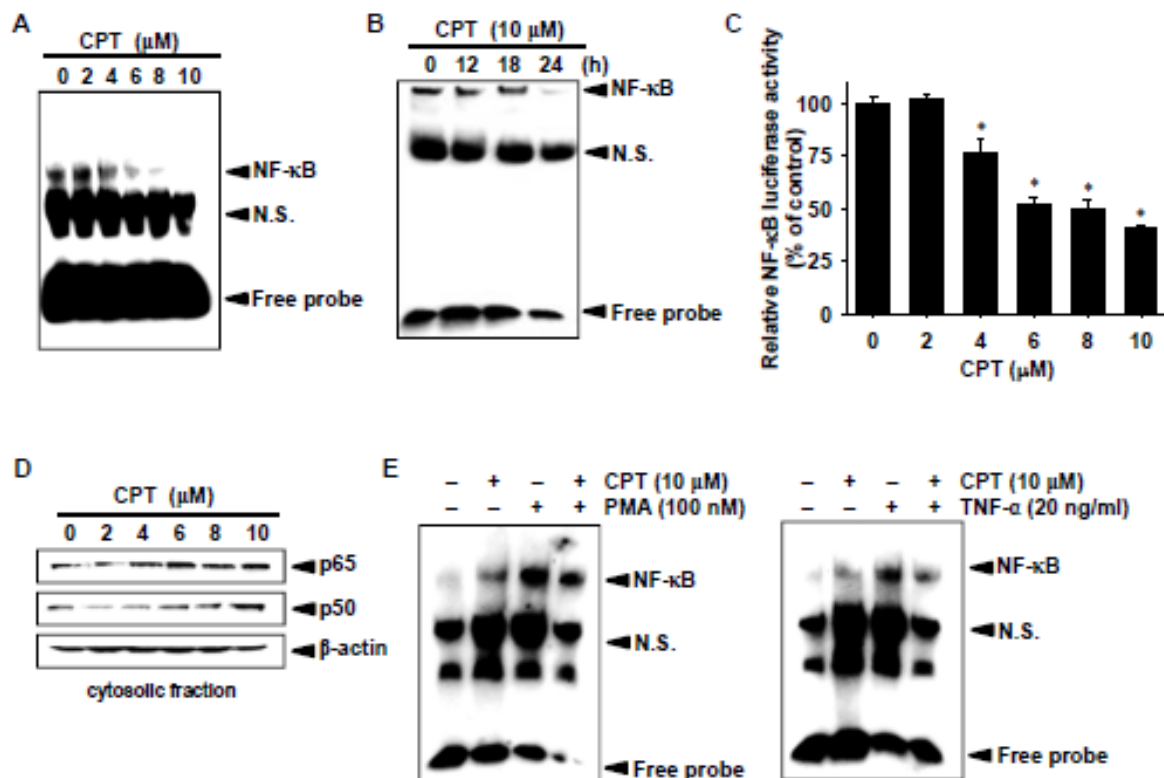


**Fig. 33.** Effect of CPT on NF- $\kappa$ B DNA binding activity. DU145 cells were treated with the indicated concentrations of CPT for 24h (A) and with 10  $\mu\text{M}$  CPT at various time points (B). Nuclear extracts were assayed for DNA-binding activity of NF- $\kappa$ B by EMSA. (C) The cells were transfected with WT-NF- $\kappa$ B promoter-containing reporter vector and luciferase activity was measured 24 h after transfection. (D) In a parallel experiment, protein lysates were prepared at 24 h, subjected to SDS-PAGE, and immunoblotted using specific antibodies against p50 and p65.  $\beta$ -Actin was used as an internal control for western blotting analysis. (E) The cells were pre-incubated with 10  $\mu\text{M}$  CPT 2 h before treatment with 100nM PMA (left panel) and 20 ng/ml TNF- $\alpha$  (right panel) for 30 min. Nuclear extracts were assayed for DNA-binding activity of NF- $\kappa$ B by EMSA. Statistical significance was determined by one-way ANOVA test (\*,  $p < 0.05$  vs. untreated control). N.S., non-specific.

### 6.3.5 HO-1 induces CPT-induced MMP9 and VEGF inhibition

Because increased endogenous HO-1 provides low levels of MMP-9 and VEGF [Bussolati et al., 2004; Chao et al., 2013], we performed RT-PCR and western blot analysis to evaluate whether CPT regulates HO-1 expression. Treatment of DU145 cells with CPT resulted in a significant increase of *HO-1* expression at 6 h (Fig. 6A, upper panel) and in a dose-dependent manner at 12 h (Fig. 6A, lower panel). Western blot analysis also showed that CPT increases HO-1 expression in a dose-dependent manner at 24 h (Fig. 6B). Next, we analyzed whether an HO-1 inducer, CoPP, affects to the regulation of PMA-induced *MMP9* and *VEGF* expression. Pretreatment with CoPP significantly decreased the PMA-induced *MMP9* and *VEGF* expression (Fig. 6C); in contrary, HO-1 inhibitor, ZnPP, reversed CPT-induced *MMP9* and *VEGF* inhibition in PMA-stimulated DU145 cells (Fig. 6D), which indicates that HO-1 tightly regulates the expression of *MMP9* and *VEGF* genes. In addition, MMP-9 luciferase activity was increased approximate 4-fold in PMA-stimulated DU145 cells, compared to the untreated control group; however, the PMA-induced MMP-9 luciferase activity was significantly reduced by treatment with CoPP (Fig. 6E, upper panel). On the other hand, HO-1 inhibitor ZnPP reversed CPT-induced inhibition of MMP-9 luciferase activity in PMA-stimulated DU145 cells (Fig. 6E, lower panel). We also found that the level of PMA-induced VEGF secreted into the culture medium significantly reduces by treatment with CoPP (Fig. 6F, left panel) and ZnPP reverses CPT-induced VEGF inhibition in PMA-stimulated DU145 cells (Fig. 6F, right panel). Taken together, these results indicate that CPT inhibits PMA-induced MMP9 and VEGF production by inducing HO-1.

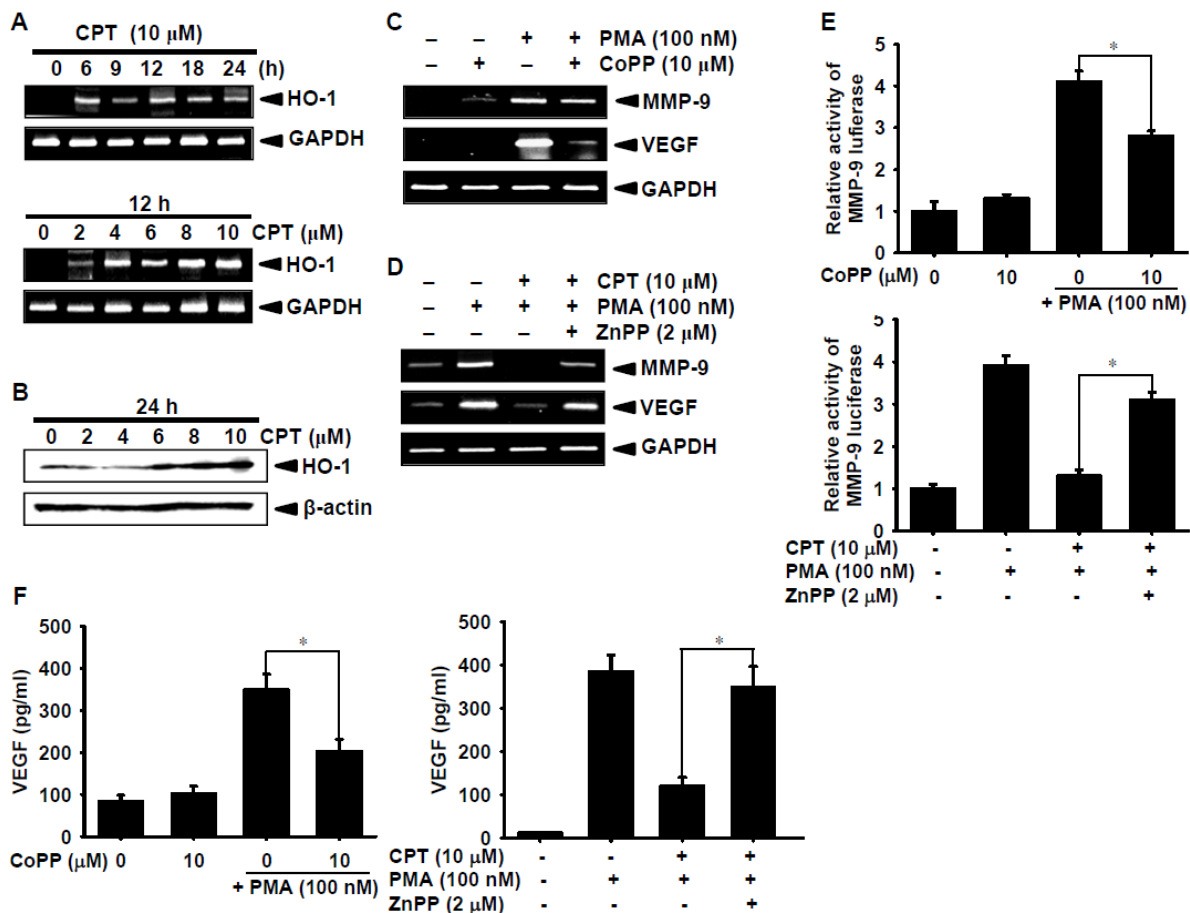


**Fig. 34.** Effect of CPT on the expression of HO-1 in DU145 cells. (A) DU145 cells were pretreated with 10  $\mu$ M CPT for the indicated times (0-24 h, upper panel) and the indicated concentrations of CPT for 12 h (lower panel). Total RNA was isolated and an RT-PCR analysis of *HO-1* was performed. (B) In a parallel experiment, equal amounts of cell lysates were resolved on SDS-polyacrylamide gels at 24 h, transferred to nitrocellulose membranes, and probed with specific antibodies against HO-1. (C) The cells were pretreated with 10  $\mu$ M CoPP for 2 h and then incubated with 100 nM PMA for 6 h. (D) The cells were pretreated with 10  $\mu$ M CPT in the presence or absence of 2  $\mu$ M ZnPP for 2 h and then incubated with 100 nM PMA for 6 h. The expression of *MMP9* and *VEGF* was determined by RT-PCR. GAPDH and  $\beta$ -actin were used as an internal control for RT-PCR and western blot analysis, respectively. (E) The cells were transfected with WT-MMP-9 promoter-containing reporter

vector, pretreated with 10  $\mu$ M CoPP (top) or 2  $\mu$ M ZnPP (bottom) for 2 h, and then incubated with 100nM PMA for 24 h in the presence or absence of 10  $\mu$ M CPT. Luciferase activity was measured 24 h after transfection. (F) In a parallel experiment, VEGF level in the culture medium was measured by ELISA. Statistical significance was determined by one-way ANOVA test (\*,  $p < 0.05$  vs. CoPP-treated or CPT/PMA-treated group).

### **6.3.6 Nrf2 regulates CPT-induced MMP-9 and VEGF expression by inducing HO-1 expression**

Since Nrf2 is a main transcription factor responsible for HO-1 expression, we determined whether Nrf2 is involved in CPT-induced inhibition of MMP-9 and VEGF expression by inducing HO-1 expression. EMSA data showed that CPT upregulates specific DNA-binding activity of Nrf2 in DU145 cells in a dose-dependent manner (Fig. 7A). To investigate whether CPT inhibits MMP-9 and VEGF expression via Nrf2-mediated HO-1 induction, a specific siNrf2 was transfected into DU145 cells. Transient knockdown of siNrf2 alone induced the expression of *MMP9* and *VEGF* genes, and significantly reduced the level of CPT-induced HO-1; however, treatment with CPT downregulated siNrf2-mediated expression of *MMP-9* and *VEGF* genes accompanying with recover of HO-1 induction (Fig. 7B), which indicates that Nrf2-mediated HO-1 axis is a main flow in CTP-induced reduction of *MMP-9* and *VEGF* expression. Additionally, siNrf2 significantly reversed CPT-mediated inhibition of MMP-9 luciferase activity (Fig. 7C) and VEGF production (Fig. 7D) in PMA-treated DU145 cells. These results indicate that CPT inhibits MMP-9 and VEGF expression via Nrf2-dependent HO-1 induction.

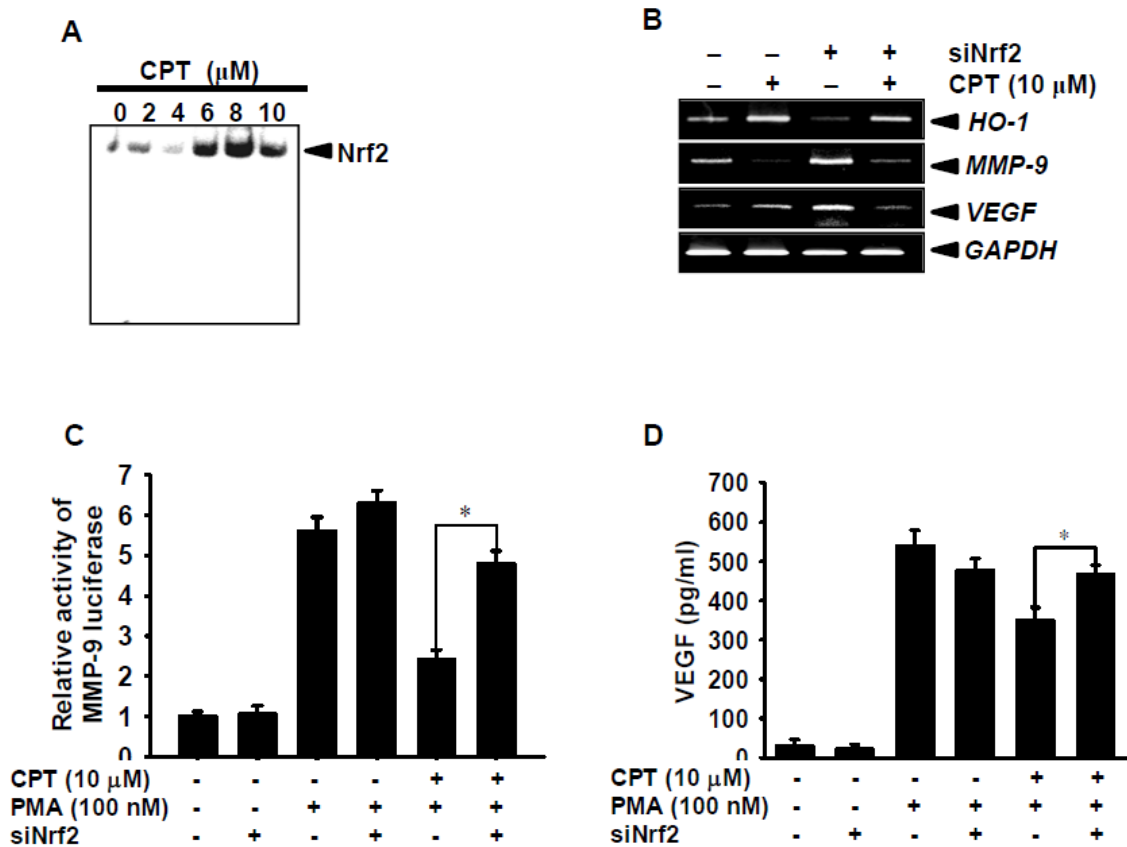


**Fig. 35.** Effect of CPT on the expression of Nrf-2 in DU145 cells. (A) DU145 cells were incubated with the indicated concentrations of CPT for 24 h. Nuclear extracts were prepared and analyzed for ARE-binding of Nrf-2 by EMSA. (B) The cells were transiently transfected with Nrf2 siRNA for 24 h and then treated with or without CPT for 2 h. Total RNA was isolated at 6 h, and an RT-PCR analysis of *HO-1*, *MMP-9*, and *VEGF* was performed. GAPDH was used as an internal control for RT-PCR. (C) The cells were transiently transfected with Nrf2 siRNA for 24 h and then cells were transfected with WT-MMP-9 promoter-containing reporter vector for 24h, treated the indicated concentration of CPT, and luciferase activity was measured 24 h after transfection. (D) In a parallel experiment, VEGF level in the culture medium was measured by ELISA. Statistical significance was determined by one-way ANOVA test (\*,  $p < 0.05$  vs. CPT/PMA-treated group).



## 6.4 Discussion

Because of cytotoxic mechanism of CPT, it has a plethora of biological features including antitumor activity and apoptosis-inducing capacity in a broad spectrum of cancer cell lines both *in vitro* and *in vivo*, especially in colon, lung, breast, ovarian, and melanoma cancers [Dunn et al., 1997; Goldwasser et al., 1996; Pommier, 2006]. Some researchers suggested that CPT is a promising antimetastatic candidate in a wide range of cancers, such as melanoma, ovarian, colon, and pancreatic cancers [De Cesare et al., 2004; Potmesil et al., 1995]. Nevertheless, it is not fully known how CPT regulates anticancer activity by the invasion and metastasis process. Therefore, we, in the present study, determined that CPT lead to decrease of invasion by regulating MMP-9 and VEGF expression by suppressing NF- $\kappa$ B activity and upregulating Nrf2-mediated HO-1 (Fig. 8).

NF- $\kappa$ B is involved in the promotion of angiogenesis, by which tumor cells promote neovascularization for invasion and metastasis. NF- $\kappa$ B is normally located in the cytoplasm as an inactivated dimer composed of p65 and p50 subunits (Pahl, 1999). In stimulating with carcinogens, I $\kappa$ B is phosphorylated, degraded, and then NF- $\kappa$ B is released and translocated to the nucleus. Ultimately, NF- $\kappa$ B activation is associated with invasive and metastatic phenotypes by inducing MMP-9 and VEGF, and inhibition of NF- $\kappa$ B activation has been shown to suppress MMP-9 and VEGF expression and thus decreased tumor invasion [Gupta et al., 2010]. Tumor cells metastasize by various proteolytic enzymes contributing to the degradation of extracellular membrane and basement membrane. Notably, MMP-9 is a key effector molecule that promotes tumor cell invasion and metastasis through type-IV collagen degradation-dependent extracellular matrix remodeling and thus is overexpressed in many human cancers with invasive and metastatic capabilities [Gialeli et al., 2011]. Additionally, VEGF is an interesting inducer of angiogenesis and lymphangiogenesis, because it is a highly

specific mitogen for endothelial cells responsible for proliferation, vascular permeability, and new blood vessel formation [Neufeld et al., 1999]. Numerous reports have demonstrated that the metastatic potential of tumor cells is directly correlated with the VEGF expression level, and tumor growth and invasion were significantly suppressed through inhibition of VEGF-induced angiogenesis both *in vitro* and *in vivo* [Chen et al., 2012; Wang et al., 2013]. In the present study, we also found that CPT reduces invasion of DU145 cells accompanying with downregulation of MMP-9 and VEGF via NF- $\kappa$ B inhibition, which indicates that CPT may be a good candidate to regulate cancer invasion. We also investigated whether CPT inhibits PI3K and Akt phosphorylation, because PI3K and Akt have been known as upstream regulators of NF- $\kappa$ B [Martin et al., 2004]. The present data indirectly supported that the PI3K/Akt-mediated NF- $\kappa$ B axis pathway regulates the expression of MMP-9 and VEGF in response to CPT. Additionally, many other transcription factors such as AP-1 and Sp1 for MMP-9 and AP-1, AP-2, E2F1, and GATA-6 for VEGF were found [Mittelstadt and Patel, 2012; Minchenko et al., 1994; Tischer et al., 1991]. In particular, AP-1 binding to the MMP-9 promoter region is also thought to be important for regulating MMP-9 expression in response to transforming growth factor- $\alpha$  (TGF $\alpha$ ) [Meissner et al., 2011] and TNF- $\alpha$ , in contrary, promotes MMP-9 expression by significantly inducing Sp1 activation accompanying with NF- $\kappa$ B activation [Li et al., 2007]. Beside of NF- $\kappa$ B, E2F1 as well as AP-1 and AP-2 around Sp1 site also promotes angiogenesis through VEGF-VEGFR axis [Engelmann et al., 2013; Tischer et al., 1991]. Therefore, further study is required to determine whether other transcriptional factors are regulated in CPT-induced MMP-9 and VEGF downregulation.

A substantial evidences point to an important functional role of HO-1 in providing cellular protection against carcinogens [Cho et al., 2010; Vicente et al., 2003]. Recently, Yu et al. reported that HO-1 suppresses reactive oxygen species-dependent MMP-9 expression and

VEGF-mediated angiogenesis by inhibiting reactive oxygen species and further strengthened that HO-1 is indeed an important molecule in the host's and cell's defense against oxidant stress [Yu et al., 2013]. In this study, we found that CPT increases the expression of HO-1 and CoPP, an HO-1 inducer inhibits PMA-induced MMP9 and VEGF expression, while the suppressive effect of those gene expression due to CPT is significantly reversed by potent HO-1 inhibitor ZnPP, which indicates that CPT-induced HO-1 expression is intimately associated with the downregulation of PMA-induced MMP-9 and VEGF. Nrf2 is a relatively well-known transcription factor essential for HO-1 expression [Farombi and Surh, 2006] and Nrf2, in response to diverse HO-1 inducers, translocates from the cytosol to the nucleus where it binds to the antioxidant response element in the promoter region of the *HO-1* gene [Scapagnini et al., 2011]. We demonstrated that CPT leads induction of Nrf2 by a mechanism dependent on HO-1 expression assuming that CPT reverses PMA-induced MMP-9 and VEGF expression via Nrf2-dependent HO-1 expression. It is confirmed by silencing of Nrf2 increases the *MMP9* and *VEGF* expression accompanying with induction of HO-1.

## 6.5 Conclusion

In summary, current results indicate that CPT inhibits *MMP-9* and *VEGF* expression via blockade of the PI3K/Akt-dependent NF- $\kappa$ B pathways as well as induction of Nrf2-mediated HO-1. Therefore, CPT maybe a potentially effective therapeutic agent for the inactivation of NF- $\kappa$ B and activation of Nrf2 to regulate the expression of MMP-9 and VEGF, resulting in an inhibition of cell growth and invasion of prostate cancer.

## **Chapter 7**

**Camptothecin sensitizes human hepatoma Hep3B cells to TRAIL-mediated apoptosis via ROS-dependent death receptor 5 upregulation with the involvement of MAPKs**

## **Abstract**

Tumor necrosis factor-related apoptosis-inducing ligand (TRAIL) induces apoptosis in various types of malignant cancer cells, but several cancers have acquired potent resistance to TRAIL-induced cell death by unknown mechanisms. Camptothecin (CPT) is a quinolone alkaloid that induces cytotoxicity in a variety of cancer cell lines. However, it is not known whether CPT triggers TRAIL-induced cell death. In this study, we found that combined treatment with subtoxic doses of CPT and TRAIL (CPT/TRAIL) potentially enhanced apoptosis in a caspase-dependent manner, suggesting that this combined treatment would be an attractive option for safely treating human cancers. CPT/TRAIL effectively induced the expression of death receptor (DR) 5, which is a specific receptor of TRAIL. In addition, CPT-mediated sensitization to TRAIL was efficiently reduced by treatment with a chimeric blocking antibody specific for DR5, suggesting that CPT functionally triggers DR5-mediated cell death in response to TRAIL. CPT-induced generation of reactive oxygen species (ROS) preceded the upregulation of DR5 in response to TRAIL. The involvement of ROS in DR5 upregulation confirmed that pretreatment with antioxidants, including *N*-acetyl-L-cysteine (NAC) and glutathione (GSH), significantly inhibits CPT/TRAIL-induced cell death by suppressing DR5 expression. The specific inhibitors of extracellular signal-regulated kinase (ERK) and p38 also decreased CPT/TRAIL-induced cell death by blocking DR5 expression. In conclusion, our results suggest that CPT sensitizes cells to TRAIL-induced apoptosis via ROS and ERK/p38-dependent DR5 upregulation.

## 7.1 Introduction

To date, the use of tumor necrosis factor (TNF) family members in anticancer therapy has been limited because they can cause severe cytotoxicity in normal cells. However, many scientists have still tried to develop anticancer drugs derived from TNF family members [Roberts et al., 2011]. TNF-related apoptosis-inducing ligand (TRAIL), a member of the TNF superfamily, is considered as a promising anticancer agent because the cytotoxic activity of TRAIL is selective in human tumor cells and does not appear to exert any adverse effects on normal cells [Walczak et al., 1999]. TRAIL binds to 2 death receptors, that is, death receptor (DR) 4 and DR5 that are highly expressed in cancer cells and contain a cytoplasmic functional death domain. Normal cells show high expression of decoy receptors, which have a higher-binding affinity with TRAIL DR4 and DR5 do, but do not have a signaling cytoplasmic death domain [Degli-Esposti et al., 1997]. The binding of TRAIL to DRs triggers cell death through at least 2 fundamental apoptotic pathways, referred to as the extrinsic pathway and the intrinsic pathway [Ganten et al., 2005]. The binding of TRAIL to DR4 or DR5 leads to the activation of Fas-associated death domain (FADD) and procaspase-8, which then form a death-inducing signaling complex to amplify death signaling. In essence, the extrinsic pathway involves DR engagement, formation of the death-inducing signaling complex, and proteolytic activation of caspase-8 [Johnstone et al., 2008]. Proteolytic caspase-8 further activates Bid, which in turn translocates to the mitochondria and activates the caspase-9-dependent intrinsic pathway [Ganten et al., 2006]. However, a recent study has demonstrated that many tumor cells acquire resistance to TRAIL-induced cell death through the downregulation of their DRs and other unknown mechanisms [Srivastava, 2001]. Therefore, it is important to develop an agent that can regulate DR expression and overcome TRAIL resistance.

Natural products have played a highly significant role as sources new drugs in recent decades. Therefore, natural products with strong synergistic activity with TRAIL, but minimal toxicity in normal cells are thought to be sources for new chemotherapeutic tools for TRAIL-based cancer therapy [Roberts et al., 2011]. Camptothecin (CPT) was isolated from the bark and stem of the *Camptotheca acuminata* tree, which is a traditional Asian medicine used to treat cancer [Wall et al., 1986]. Initially, it was discovered that CPT potentially targets topoisomerase I activity by inhibiting the rejoining step during the cleavage and relegation of DNA, resulting in topoisomerase I-induced DNA single-strand break repair pathways, ultimately leading to cell death [Pan et al., 2013; Strumberq et al., 2000]. Research also suggests that CPT possesses promising antitumor activities against a broad spectrum of cancer cell lines, such as those for melanoma, breast, colon, lung, and ovarian cancers, because many cancer cells are defective in the downregulation of topoisomerase I activity [Liu et al., 2010; Wang et al., 2008]. To date, most studies have been focused on topoisomerase I activity in CPT-induced cancer cell death. However, the anticancer mechanisms of CPT in TRAIL-mediated cell death remain unclear.

In this study, we examined whether combined treatment with a sub lethal dose of CPT and TRAIL (CPT/TRAIL) induces cell death in human hepatocarcinoma Hep3B cells. We found that CPT/TRAIL increases cell death via upregulation of DR5 expression through the generation of reactive oxygen species (ROS) and the activation of extracellular signal-regulated protein kinase (ERK) and of p38 mitogen-activated protein kinases (MAPKs). Taken together, these findings suggest that CPT is an ideal candidate for TRAIL-induced apoptosis.

## 7.2 Materials and methods

### *Reagents and antibodies*

Antibodies against caspase-3, caspase-8, caspase-9, poly(ADP-ribose) polymerase (PARP), DR5, IAP-1, IAP-2, Bcl-2, and Bax were purchased from Santa Cruz Biotechnology (Santa Cruz, CA). The antibody against  $\beta$ -actin was purchased from Sigma (St. Louis, MO). Peroxidase-labeled donkey anti-rabbit and sheep anti-mouse immunoglobulins, as well as recombinant human TRAIL/Apo2 ligand (the non-tagged 19-kDa protein, amino acids 114–281) were purchased from KOMA Biotechnology (Seoul, Republic of Korea). The blocking antibody against DR5 was obtained from R&D Systems (Minneapolis, MN). 6-Carboxy-2',7'-dichlorofluorescein diacetate (H<sub>2</sub>DCFDA) was purchased from Molecular Probes (Eugene, OR). Glutathione and *N*-acetyl-L-cysteine (NAC) were purchased from Sigma (St. Louis, MO). Camptothecin was also purchased from Sigma and dissolved in DMSO (vehicle). PD98059, SP600125, SB203580, and z-IETD-fmk were purchased from Calbiochem (San Diego, CA).

### *Cell culture and viability assay*

Human hepatocellular carcinoma cell lines Hep3B and HepG2, human breast cancer cell line MDA-MB-231, and human bladder cancer cell line T24 were obtained from the American Type Culture Collection (Manassas, VA). Cells were cultured at 37°C in a 5% CO<sub>2</sub>-humidified incubator and maintained in RPMI1640 culture medium containing 10% heat-inactivated fetal bovine serum and 1% antibiotics mixture. The cells were seeded ( $5 \times 10^4$  cells/ml), grown for 24 h, and then incubated for up to 24 h with CPT and/or TRAIL. An MTT assay was performed to assess cell viability.

### *Flow cytometric analysis*

Cells were fixed in 1 U/ml of RNase A (DNase free) and 10 µg/ml of propidium iodide (Sigma) overnight in the dark at room temperature. For annexin-V staining, live cells were washed in phosphate-buffered saline (PBS) and then incubated with annexin-V FITC (R&D Systems). Cells were analyzed by flow cytometry (Becton Dickinson, San Jose, CA).

### *DNA fragmentation*

Cells were treated under various conditions and then lysed on ice in a buffer containing 10 mM Tris-HCl (pH 7.4), 150 mM NaCl, 5 mM EDTA, and 0.5% Triton X-100 for 30 min. Lysates were vortexed and cleared by centrifugation at 10,000 g for 20 min. Fragmented DNA in the supernatant was extracted with an equal volume of neutral phenol/chloroform/isoamylalcohol (25:24:1, v/v/v) and was analyzed electrophoretically on a 1.5% agarose gel containing ethidium bromide.

### *Western blot analysis*

Total cell extracts were prepared using the PRO-PREP protein extraction solution (iNtRON Biotechnology, Sungnam, Republic of Korea). Total cell extracts were separated on polyacrylamide gels and standard procedures were used to transfer them to the nitrocellulose membranes. The membranes were developed using an ECL reagent (Amersham, Arlington Heights, IL).

### *RNA extraction and reverse transcription-PCR*

Total RNA was extracted from Hep3B cells using Easy-blue reagent (iNtRON Biotechnology, Sungnam, Republic of Korea). Genes of interest were amplified from cDNA that was reverse-transcribed from 1 µg of total RNA using RT-PCR Premix (KOMA Biotechnology). The sense primer 5'-GTC TGC TCT GAT CAC CCA AC-3' and the anti-sense primer 5'-CTG CAA CTG TGA CTC CTA TG-3' were used to amplify human *DR5* mRNA. For *glyceraldehyde-3-phosphate dehydrogenase (GAPDH)*, the sense primer 5'-CGT CTT CAC CAT GGA GA-3' and the anti-sense primer 5'-CGG CCA TCA CGC CCA CAG TTT-3' were used.

### *Statistical analysis*

All data were derived from at least three independent experiments. The images were visualized with Chemi-Smart 2000 (Vilber Lourmat, Cedex, France). Images were captured using Chemi-Capt (Vilber Lourmat) and transported into Adobe Photoshop (version 8.0). All data are presented as mean ± standard error (SE). Significant differences between the groups were determined with one-way analysis of variance (ANOVA). A value of \* and # $P < 0.05$  was accepted as an indication of statistical significance.

## 7.3 Results

### 7.3.1 CPT sensitizes various types of cancer cells to TRAIL-mediated cell death

The antiproliferative activity of a combined treatment was analyzed in 4 human cancer cell lines, that is, Hep3B, HepG2, MDA-MB231, and T24 cells. Treatment with TRAIL alone induced limited inhibition of cell proliferation (by <15%) at 24 h, suggesting that these cells are highly resistant to TRAIL-induced apoptosis (Fig. 1A). However, treatment with CPT alone decreased cell viability of HepG2 and T24 cells in a dose-dependent manner up to 20  $\mu\text{M}$ , indicating that these cells are sensitive to CPT-induced antiproliferation. The decrease of cell proliferation on combined treatment with sublethal doses of CPT and TRAIL was significantly higher than that obtained with CPT or TRAIL alone. MDA-MB-231 cells were highly resistant to CPT alone and TRAIL alone; however, sub lethal doses of CPT (10  $\mu\text{M}$  and 20  $\mu\text{M}$ ) significantly enhanced the antiproliferative activity in MDA-MB-231 cells in the presence of TRAIL. In addition, CPT/TRAIL-induced cell death was more drastic in HepG2 and T24 cells than in Hep3B cells. These results show that treatment with CPT/TRAIL effectively inhibits cell proliferation in TRAIL-resistant cells in a cell-type-nonspecific manner, although the combined treatment induces different antiproliferation rates. These results indicate that CPT stimulates TRAIL-induced cell death, but is not cell-type specific.

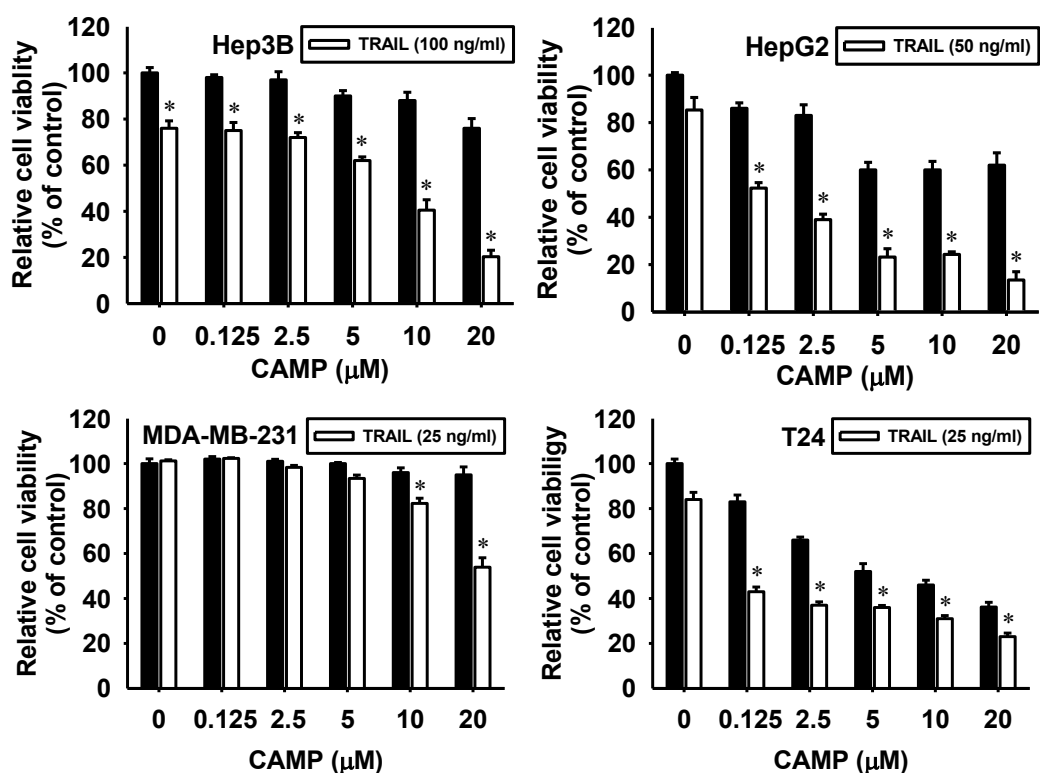


**Fig. 37.** CPT sensitizes TRAIL-induced cell death regardless of cell-type specificity. (A) Human hepatocarcinoma Hep3B and HepG2, human breast cancer MDA-MB-231, and human bladder T24 cells were treated with CPT for 1 h at the indicated concentrations and were further treated with or without TRAIL for 24 h. An MTT assay was used to assess cellular viability. Data are expressed as the overall mean  $\pm$  S.E. values for 3 independent experiments. Significance was determined by one-way ANOVA (# and \*,  $P < 0.05$  vs. untreated control group and TRAIL-treated group, respectively).

### 7.3.2 CPT/TRAIL activates apoptotic signals via the extrinsic and intrinsic pathways

Hepatocarcinoma cells are resistant to TRAIL, because of the blocked activation of the extrinsic pathway and death signaling at the mitochondrial level [Ganten et al., 2005]. Therefore, western blot analyses of proapoptotic and antiapoptotic factors were performed in

Hep3B cells to monitor changes in the activation of caspases and the expression of the Bcl-2 and IAP family proteins that contribute to increased mitochondrial permeability. Treatment with CPT alone or TRAIL alone minimally decreased the expression of procaspases at 24 h (Fig. 2A). However, CPT/TRAIL significantly downregulated the expression of procaspase-3, procaspase-8, and procaspase-9 by procaspases cleavage. Consequently, CPT/TRAIL caused significant truncation of PARP, which is a primary enzyme that induces DNA damage during apoptosis. CPT/TRAIL also decreased the expression of antiapoptotic proteins, such as Bcl-2, IAP-1, and IAP-2. In contrast, the level of Bax expression was significantly upregulated (Fig. 2B). In addition, the DNA fragmentation assay showed typical DNA fragmentation in Hep3B cells treated with CPT/TRAIL. However, DNA fragmentation was rarely seen in cells treated with CPT alone or TRAIL alone (Fig. 2C). Flow cytometric data also showed that CPT/TRAIL significantly increased annexin-V<sup>+</sup> staining (top) and the accumulation of sub-G<sub>1</sub> phase cells (bottom) at 24 h, whereas treatment with CPT alone or TRAIL alone caused only a slight increase (Fig. 2D). In addition, pretreatment with a caspase-8 inhibitor z-IETD-fmk significantly blocked apoptotic characteristics, such as DNA fragmentation, the presence of an annexin-V<sup>+</sup> population, and the sub-G<sub>1</sub> phase induced by CPT/TRAIL, indicating that CPT sensitizes Hep3B cells to TRAIL-induced apoptosis in a caspase-dependent manner. These results indicate that CPT/TRAIL treatment triggers the expression of multiple proteins associated with the extrinsic and intrinsic apoptotic signaling pathways.

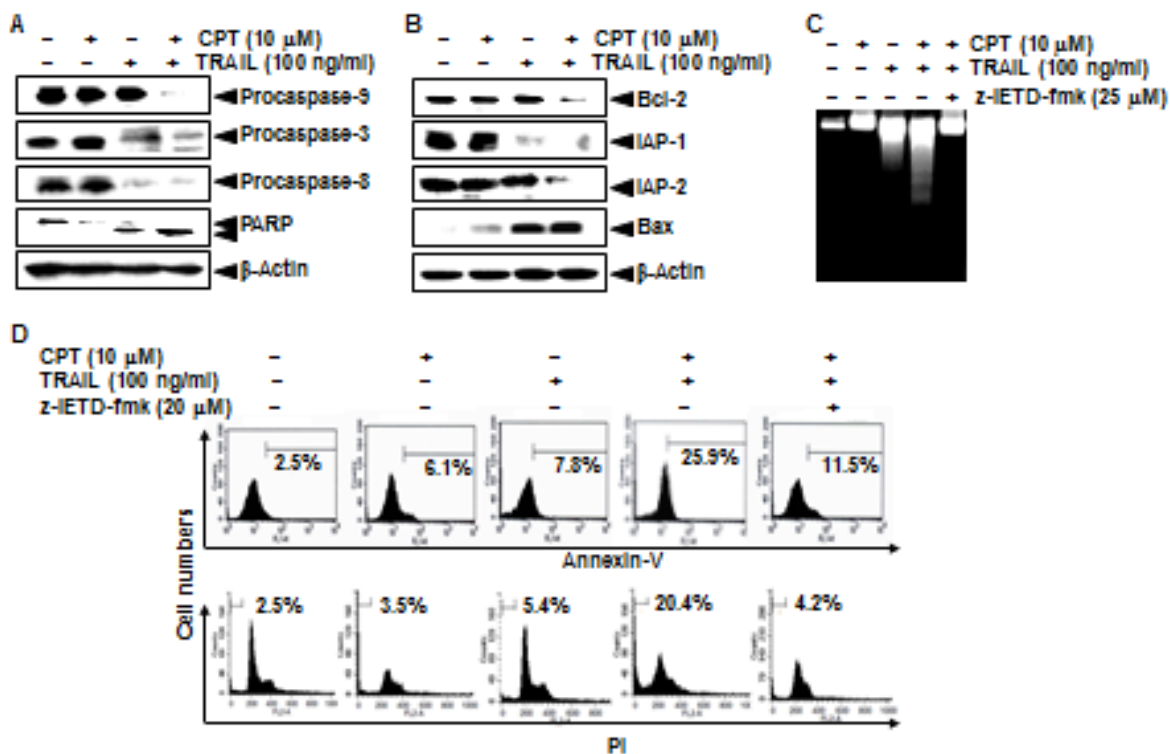


**Fig. 38.** Effect of CPT and/or TRAIL on the expression of caspases and various intracellular regulators of apoptosis. (A and B) Hep3B cells were treated with 100 ng/ml TRAIL alone, 10  $\mu$ M CPT alone, or a combination of both for the indicated time points. Cell extracts were prepared for western blot analysis of caspase-8, caspase-9, caspase-3, PARP, IAPs, Bcl-2, and Bax. (C) Effect of the combined treatment with CPT/TRAIL on DNA fragmentation. After treatment of Hep3B cells (as indicated in the figure) for 24 h, fragmented DNA was extracted from the treated cells and analyzed on 1.5% agarose gel. To examine the effect of the inhibition of pan-caspase, Hep3B cells were pretreated with 25  $\mu$ M z-IETD-fmk for 30 min and were further treated with CPT/TRAIL for 24 h. (D) Flow cytometric analysis of the annexin-V<sup>+</sup> (top) and DNA content (bottom) of the cells was shown.

### 7.3.3 DR5 upregulation is required for CPT/TRAIL-induced apoptosis

TRAIL is known to trigger apoptotic signals via DR5; therefore, to elucidate the molecular mechanism underlying the enhancement of TRAIL-induced apoptosis by CPT, we examined the expression of DR5 at the mRNA and protein levels. CPT/TRAIL significantly increased the DR5 level at the transcriptional and translational levels, although treatment with CPT alone or TRAIL alone only minimally increased DR5 expression (Fig. 3A). To confirm the functional role of DR5, we further examined the effect of the DR5-specific blocking chimera antibody on CPT/TRAIL-induced apoptosis. The administration of DR5-specific blocking antibody dose-dependently reversed CPT/TRAIL-induced cell death in Hep3B cells (Fig. 3B). In addition, the suppression of DR5 expression by pretreatment with the DR5-specific blocking antibody significantly decreased the percentage of the annexin-V<sup>+</sup> population induced by the CPT/TRAIL treatment. These results indicate that CPT enhances the molecular actions of TRAIL through interactions between TRAIL and DR5 via DR5 overexpression.

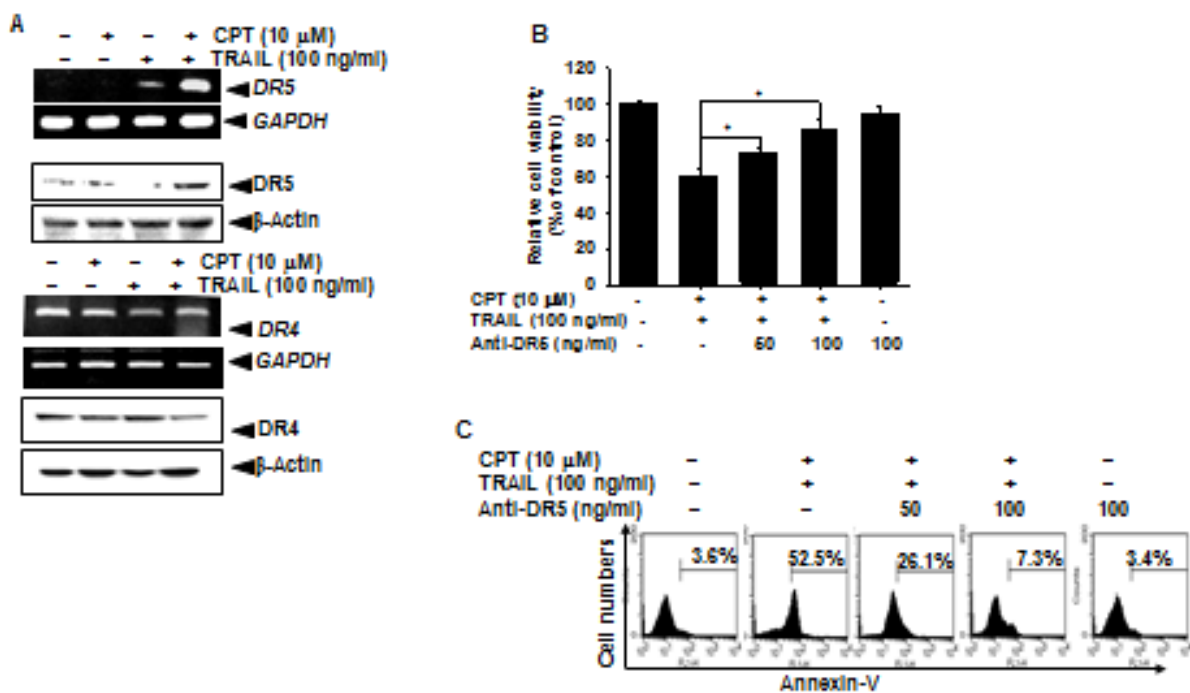


**Fig. 39.** Effect of CPT and/or TRAIL on DR5 expression. (A) Hep3B cells were treated with the indicated concentrations of CPT with or without 100 ng/ml TRAIL. Total RNA was isolated and reverse transcription-PCR analysis was conducted for DR5. Total protein extraction was performed, and western blot analysis was used for DR5.  $\beta$ -Actin was used as the internal control. (B) Effect of DR5-specific blocking chimera antibody on CPT/TRAIL-induced apoptosis. Hep3B cells were pretreated with or without 10  $\mu$ M CPT for 30 min, which was followed by treatment with or without 100 ng/ml TRAIL for 24 h in the presence of the indicated concentrations of the DR5-specific blocking chimera antibody. Cell viabilities were measured by an MTT assay. (C) In a parallel experiment, flow cytometric analysis was performed for annexin-V<sup>+</sup> cells. Data are expressed as the overall mean  $\pm$  S.E. values of 3 independent experiments. Significance was determined by one-way ANOVA (\*,  $p < 0.05$  vs. CPT/TRAIL-treated group).

#### 7.3.4 Reactive oxygen species (ROS) mediate CPT/TRAIL-induced upregulation of DR5

Recent research has shown that ROS-mediated DR5 upregulation is critical in chemotherapy-sensitized TRAIL-induced apoptosis [Jung et al., 2005]. Therefore, we examined the effect of ROS generation on CPT/TRAIL-induced DR5 upregulation. H<sub>2</sub>DCFDA-based fluorescence analysis showed that treatment of Hep3B cells with CPT alone or TRAIL alone slightly increased ROS generation. However, CPT/TRAIL substantially increased the level of ROS generation when compared to the level obtained with CPT alone or TRAIL alone (Fig. 4A). Next, we identified the effect of ROS generation on cell viability by the MTT assay. As previously shown, treatment with CPT/TRAIL decreased the viability of cells by 60%, whereas pretreatment with the ROS inhibitor NAC and GSH resulted in a significant increase in the cell viability (Fig. 4B). Furthermore, pretreatment with ROS inhibitors also decreased the percentage of sub-G<sub>1</sub> phase cells induced by CPT/TRAIL treatment (Fig. 4C). To examine the effects of ROS on DR5 expression, we performed RT-PCR analysis. Pretreatment with NAC or GSH significantly attenuated CPT/TRAIL-induced upregulation of DR5 at the mRNA level (Fig. 4D). These data indicate that CPT/TRAIL-induced apoptosis is mediated by the upregulation of DR5 expression *via* ROS generation.

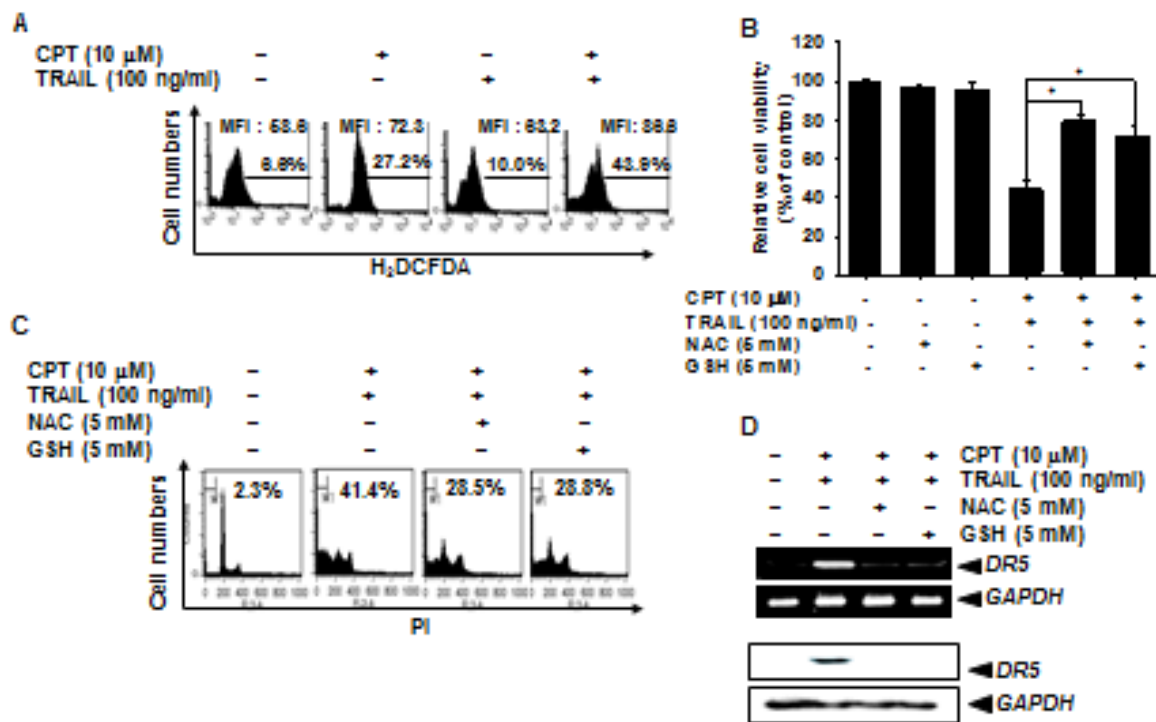


**Fig. 40.** CPT and/or TRAIL induce ROS-mediated DR5 expression. (A) Hep3B cells were treated with 100 ng/ml TRAIL alone, 10  $\mu$ M CPT alone, or a combination of both for the indicated time points. H<sub>2</sub>DCFDA-based fluorescence detection was measured by flow cytometry. (B) Hep3B cells were pretreated with 5 mM NAC and GSH for 30 min and were further treated with 100 ng/ml TRAIL alone, 10  $\mu$ M CPT alone, or a combination of both for 24 h. Cell viabilities were measured by MTT assay. (C) Sub-G<sub>1</sub> cell distribution was analyzed using a flow cytometer. (D) Hep3B cells were pretreated with 5 mM NAC and 5 mM GSH for 30 min and the indicated concentrations of CPT with or without 100 ng/ml TRAIL. Total RNA was isolated, and reverse transcription-PCR analysis was conducted for DR5.  $\beta$ -Actin was used as the internal control. Data are expressed as the overall mean  $\pm$  S.E. values from 3 independent experiments. Significance was determined by one-way ANOVA (\*,  $P < 0.05$  vs. CPT/TRAIL-treated group).

### 7.3.5 ERK and p38 potentiate CPT/TRAIL-mediated DR5 expression

A recent study showed that MAPKs are important regulators of DR5 expression via the non-canonical TRAIL-sensitizing signaling pathway [Azijli et al., 2013]. Therefore, to determine whether CPT/TRAIL-mediated DR5 upregulation is MAPK-dependent, an MTT assay was performed in the presence of specific inhibitors for ERK, p38, and JNK. Interestingly, only the inhibition of ERK and p38 MAPK by PD98059 and SB203580, respectively, significantly restored CPT/TRAIL-induced cell death. However, pretreatment with SP600125 increased only a small portion of the cell population under the same experimental conditions. Furthermore, flow cytometric analysis showed that the sub-G<sub>1</sub> population substantially decreased, when the cells were treated with ERK and p38 inhibitors (Fig. 5B). Pretreatment with SP600125 sustained the sub-G<sub>1</sub> population, as compared to the CPT/TRAIL-treated group. In addition, to examine the effects of MAPKs on the expression of DR5 mRNA, Hep3B cells were incubated with CPT/TRAIL in the presence of 3 MAPK inhibitors. As expected, the level of DR5 mRNA was downregulated only in the presence of ERK and p38 inhibitors (Fig. 5C). These data indicate that the ERK and p38 signaling pathways act as non-canonical regulators in CPT/TRAIL-induced apoptosis by regulating DR5 expression.

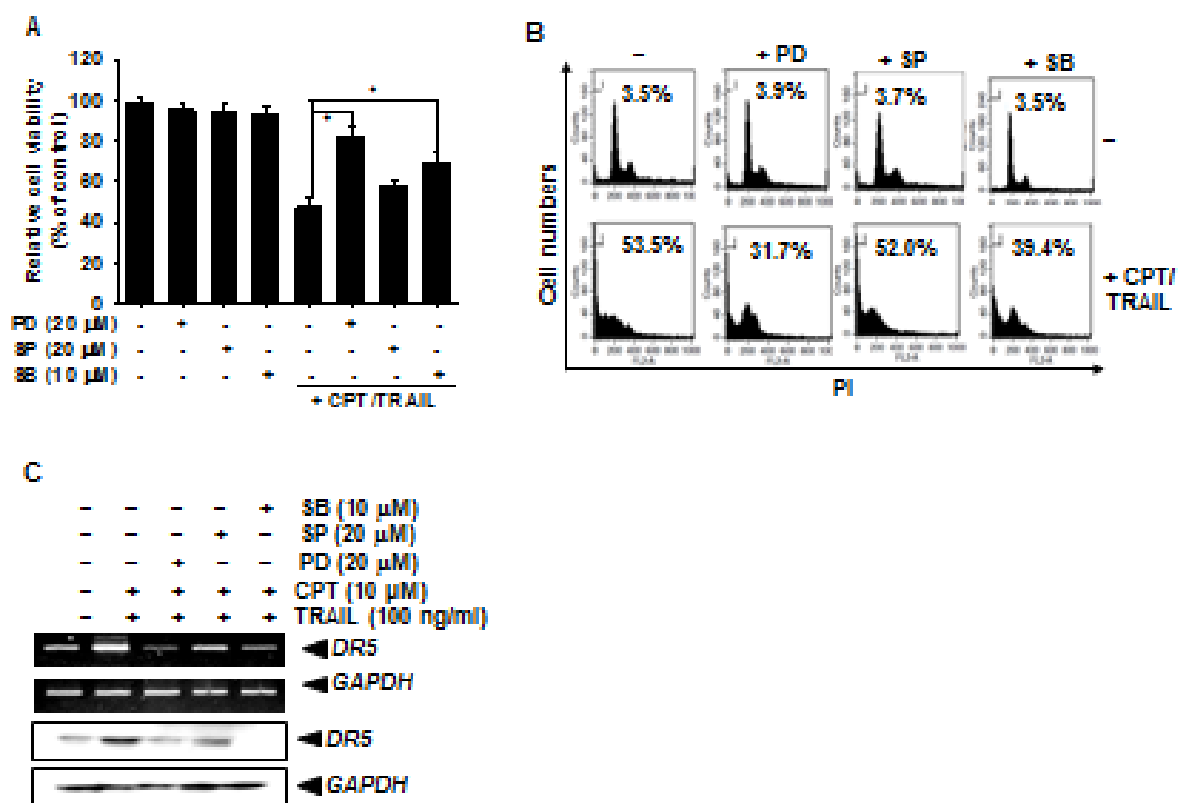


**Fig. 41.** Transcription of the DR5 promoter requires ERK and p38 activation. (A) Hep3B cells were treated with 100 ng/ml TRAIL alone, 10  $\mu$ M CPT alone, or a combination after pretreatment with 20  $\mu$ M PD98059, 20  $\mu$ M SP600125, and 10  $\mu$ M SB203580 for 1 h. Cell viabilities were measured by an MTT assay. (B) Sub-G<sub>1</sub> cell distribution was analyzed using a flow cytometer. (C) Hep3B cells were pretreated with the indicated concentrations of the MAPK inhibitors for 30 min and the indicated concentrations of CPT with and without 100 ng/ml TRAIL. Total RNA was isolated, and reverse transcription-PCR analysis was conducted for DR5.  $\beta$ -Actin was used as the internal control. Data are expressed as the overall mean  $\pm$  S.E. values from 3 independent experiments. Significance was determined by one-way ANOVA (\*,  $p < 0.05$  vs. CPT/TRAIL-treated group).

## 7.4 Discussion

Although TRAIL has been thought to be a highly promising candidate for cancer treatment based on growing evidence, its clinical applications are limited, because of the acquired resistance against TRAIL seen in a variety of cancer cells. Therefore, TRAIL-sensitizing agents are believed to be required in chemotherapeutics to treat TRAIL-resistant cancers. Many scientists have reported that different types of compounds such as histone deacetylase inhibitors, proteasome inhibitors, and cyclin-dependent kinase inhibitors, as well as irradiation, substantially sensitize TRAIL-resistant cancer cells to TRAIL-induced apoptosis [Inoue et al., 2004; Palacios et al., 2006]. Extremely advanced anticancer therapeutic designs have been suggested for identifying agents that activate DRs or block anti apoptotic effectors for amplifying TRAIL-induced apoptosis. In particular, a recent study emphasized that DR5 may play a more prominent role than DR4 in TRAIL-induced apoptosis [Huang and Sheikh et al., 2007]. In the current study, we found that CPT effectively sensitizes human hepatocarcinoma Hep3B cells to TRAIL-induced apoptosis through the upregulation of DR5, which is mediated by ROS and the MAPK signaling pathways.

DRs contain an amino-terminal leader cleavage site, which is followed by an extracellular region containing 2 cysteine-rich repeats (a central transmembrane domain). Guan et al. (2001) reported that some chemicals or proteins sensitize TRAIL-induced apoptosis through overexpression of DR4. However, a recent study showed that DR5 may play a significantly more prominent role than DR4 in TRAIL-induced apoptosis [Truneh et al., 2000]. In our study, combined treatment with CPT/TRAIL resulted in a significant increase in the mRNA and protein levels of DR5. However, the combined treatment did not change the expressional level of DR4 (data not shown). In addition, the DR5-specific blocking chimeric antibody effectively inhibited cell death induced by CPT/TRAIL

combination. Furthermore, a previous study has shown that DR5 is regulated by either a p53-dependent or a p53-independent mechanism [Sheikh et al., 1998]. In the current study, we found that CPT/TRAIL induced the expression of DR5 in the entire cancer cell lines tested, (i.e., p53-positive [HepG2 and T24] and p53-negative [Hep3B and MDA-MB-231 cell lines]), indicating that CPT upregulates DR5 expression in a p53-independent manner.

In recent years, it has been shown that Sp1 binding might lead to augmentation of DR5 transcriptional activity in several types of cancer cells and Sp1 is known to bind to G-rich elements, such as the GC-box (GGGGCGGGG) and GT-box (GGTGTGGGG) [Sun et al., 2008]. Moreover, we previously published data indicating that Sp1 is a primary transcriptional regulator for DR5 expression in TRAIL-induced apoptosis [Kim et al., 2010; Moon et al., 2010]. However, treatment with CPT/TRAIL decreased Sp1-DNA binding activity (data not shown), suggesting that induction of Sp1 is not related to CPT/TRAIL-induced DR5 expression. Nevertheless, we cannot rule out the possibility that other transcriptional factors are involved in CPT/TRAIL-induced apoptosis. In addition, ROS generation has been proposed to be involved in DR5 upregulation which is a major target for triggering and amplifying TRAIL-dependent apoptosis through DR5 [Jung et al., 2006; Kim et al., 2008]. Our data indicate a mechanism where by CPT/TRAIL induces DR5 upregulation through ROS-mediated transcriptional regulation and pretreatment with antioxidants (e.g., NAC and GSH), thus significantly preventing CPT/TRAIL-mediated DR5 upregulation and cell death. Further studies are required to clarify how ROS increases the transcriptional activity of the DR5 promoter. In addition, MAPKs directly stimulate DR5 expression by generating ROS [Higuchi, et al., 2004]. Therefore, we hypothesize that CPT/TRAIL sensitizes the ROS-MAPK signaling cascades to activate DR5 expression. Only the ERK inhibitor PD98059 and the p38 inhibitor SB203580 significantly blocked

CPT/TRAIL-mediated DR5 upregulation and cell death. These data indicate that the ERK and p38 signaling pathways may also be related to DR5 regulation in CPT/TRAIL-induced apoptosis, although we did not note direct regulation of ERK and p38 by ROS generation. In addition, the process involved in promoting resistance to cell death occurs as a result of abnormal activation of intracellular antiapoptotic pathways. Thus, NF- $\kappa$ B, which include p50/p65, seems to play a key role in the resistance of hepatoma cancer cells to TRAIL-induced apoptosis. NF- $\kappa$ B subunits move into the nucleus and bind to their specific promoter regions to regulate specific gene expression [Ravi et al., 2001]. Therefore, we performed an electrophoretic mobility assay for demonstrating the involvement of the NF- $\kappa$ B transcription factor in CPT/TRAIL-induced apoptosis. CPT treatment decreased TRAIL-mediated NF- $\kappa$ B DNA-binding activity, indicating that inhibition of NF- $\kappa$ B transcription by CPT induces apoptosis (data not shown). Therefore, further studies are required to determine whether ROS generation regulates NF- $\kappa$ B and MAPKs in CPT/TRAIL-induced apoptosis.

## 7.5 Conclusion

To our knowledge, this study provides the first evidence that CPT sensitizes TRAIL-induced apoptosis through the upregulation of DR5 expression and the suppression of TRAIL-mediated ROS generation and MAPK activation in hepatocellular carcinoma cells. However, p53 is not necessary for CPT/TRAIL-induced DR5 expression and triggers apoptosis. Further studies are required to elucidate the exact *in vivo* mechanisms by which CPT/TRAIL treatment increases the sensitivity of cancer cells to TRAIL-mediated apoptosis.

## Bibliography

- Abbas, T., Dutta, A., 2009. p21 in cancer: intricate networks and multiple activities. *Nat. Rev. Cancer* 9, 400–414.
- Ahn, J.Y., Schwarz, J.K., Piwnica-Worms, H., Canman, C.E., 2000. Threonine 68 phosphorylation by ataxia telangiectasia mutated is required for efficient activation of Chk2 in response to ionizing radiation. *Cancer Res.* 60, 21, 5934–5936.
- Albihn, A., Mo, H., Yang, Y., Henriksson, M., 2007. Camptothecin-induced apoptosis is enhanced by Myc and involves PKCdelta signaling. *Int. J. Cancer.* 121, 1821–1829.
- Alenzi, F.Q.B., 2004. Links between apoptosis, proliferation and the cell cycle. *Br. J. Biomed. Sci.* 612, 99–102.
- Allan, L.A., Clarke, P.R., 2007. Phosphorylation of Caspase-9 by CDK1/Cyclin B1 Protects Mitotic Cells against Apoptosis. *Mol. Cell* 26, 301–310.
- Amaravadi, R.K., Yu, D., Lum, J.J., Bui, T., Christophorou, M.A., Evan, G.I., Tikhonenko, A.T., Thompson, C.B., 2007. Autophagy inhibition enhances therapy-induced apoptosis in a Myc-induced model of lymphoma. *J. Clin. Invest.* 117, 326–336.
- Appelmann, I., Liersch, R., Kessler, T., Mesters, R.M., Berdel, W.E., 2010. Angiogenesis inhibition in cancer therapy: platelet-derived growth factor (PDGF) and vascular endothelial growth factor (VEGF) and their receptors: biological functions and role in malignancy. *Recent Results Cancer Res.* 180, 51–81.
- Asghar, U., Witkiewicz, A.K., Turner, N.C., Knudsen, E.S., 2015. The history and future of targeting cyclin-dependent kinases in cancer therapy. *Nat. Rev. Drug Discov.* 14, 130–146.
- Azijli, K., Weyhenmeyer, B., Peters, G.J., de Jong, S., Kruyt, F.A., 2013. Non-canonical kinase signaling by the death ligand TRAIL in cancer cells: discord in the death receptor family. *Cell Death Differ.* (doi:10.1038/cdd.2013.28).
- Babcock, J.T., Nguyen, H.B., He, Y., Hendricks, J.W., Wek, R.C., Quilliam, L.A., 2013. Mammalian target of rapamycin complex 1 (mTORC1) enhances bortezomib-induced death in tuberous sclerosis complex (TSC)-null cells by a c-MYC-dependent induction of the unfolded protein response. *J. Biol. Chem.* 288, 15687–15698.
- Banadyga, L., Veugelers, K., Campbell, S., Barry, M., 2009. The fowlpox virus BCL-2 homologue, FPV039, interacts with activated Bax and a discrete subset of BH3-only proteins to inhibit apoptosis. *J. Virol.* 83, 7085-7098.
- Bansal, H., Seifert, T., Bachier, C., Rao, M., Tomlinson, G., Lyer, S.P., Bansal, S., 2012. The transcription factor Wilms tumor 1 confers resistance in myeloid leukemia cells against the proapoptotic therapeutic agent TRAIL (tumor necrosis factor  $\alpha$ -related apoptosis-inducing ligand) by regulating the antiapoptotic protein Bcl-xL. *J. Biol. Chem.* 287, 32875-32880.
- B'chir, W., Maurin, A.C., Carraro, V., Averous, J., Jousse, C., Muranishi, Y., Parry, L., Stepien, G., Gafournoux, P., Bruhat, A., 2013. The eIF2 $\alpha$ /ATF4 pathway is essential for stress-induced autophagy gene expression. *Nucleic Acids Res.* 41, 7683–7699.

- Bertoli, C., de Bruin, R.A., 2014. Turning cell cycle entry on its head. *eLife* 3, e03475.
- Bhandary, B., Marahatta, A., Kim, H., Chae, H., 2013. An involvement of oxidative stress in endoplasmic reticulum stress and its associated diseases. *Int. J. Mol. Sci.* 14, 434–456.
- Bhandary, B., Marahatta, A., Kim, H., Chae, H., 2013. An involvement of oxidative stress in endoplasmic reticulum stress and its associated diseases. *Int. J. Mol. Sci.* 14, 434–456.
- Bharadwaj, U., Marin-Muller, C., Li, M., Chen, C., Yao, Q., 2011. Mesothelin confers pancreatic cancer cell resistance to TNF- $\alpha$ -induced apoptosis through Akt/PI3K/NF- $\kappa$ B activation and IL-6/Mcl-1 overexpression. *Mol. Cancer.* 10, 106.
- Bisson, F., Paquet, C., Bourget, J.M., Zaniolo, K., Rochette, P.J., Landreville, S., Damour, O., Boudreau, F., Auger, F.A., Guérin, S.L., Germain, L., 2015. Contribution of Sp1 to telomerase expression and activity in skin keratinocytes cultured with a feeder layer. *J. Cell. Physiol.* 230, 308-317.
- Bu, D., Johansson, M.E., Ren, J., Xu, D.W., Johnson, F.B., Edfeldt, K., Yan, Z.Q., 2010. NF- $\kappa$ B-mediated transactivation of telomerase prevents intimal smooth muscle cell from replicative senescence during vascular repair. *Arterioscler Thromb. Vasc. Biol.* 30, 2604–2610.
- Bussolati, B., Ahmed, A., Pemberton, H., Landis, R.C., Di, Carlo, F., Haskard, D.O., Mason, J.C., 2004. Bifunctional role for VEGF-induced hemeoxygenase-1 *in vivo*: induction of angiogenesis and inhibition of leukocytic infiltration. *Blood* 103, 761–766.
- Castedo, M., Perfettini, J.L., Roumier, T., Kroemer, G., 2002. Cyclin-dependent kinase-1: linking apoptosis to cell cycle and mitotic catastrophe. *Cell Death Differ.* 9, 1287–1293.
- Cha, H., Wang, X., Li, H., Fornace, A.J., Jr., 2007. A functional role for p38 MAPK in modulating mitotic transit in the absence of stress. *J. Biol. Chem.* 282, 22984–22992.
- Chadebech, P., Truchet, I., Bricchese, L., Valette, A., 2000. Up-regulation of cdc2 protein during paclitaxel-induced apoptosis. *Int. J. Cancer* 87, 779–786.
- Chao, C.Y., Lii, C.K., Hsu, Y.T., Lu, C.Y., Liu, K.L., Li, C.C., Chen, H.W., 2013. Induction of heme oxygenase-1 and inhibition of TPA-induced matrix metalloproteinase-9 expression by andrographolide in MCF-7 human breast cancer cells. *Carcinogenesis* 34, 1843–1851.
- Charrier-Savournin, F.B., Château, M.T., Gire, V., Sedivy, J., Piette, J., Dulic, V., 2004. p21-Mediated nuclear retention of cyclin B1-Cdk1 in response to genotoxic stress. *Mol. Biol. Cell.* 15, 3965–3976.
- Chen, B., Lu, Y., Chen, Y., Cheng, J., 2015. The role of Nrf2 in oxidative stress-induced endothelial injuries. *J. Endocrinol.* 225, 83–99.
- Chen, L., Xu, S., Liu, L., Wen, X., Xu, Y., Chen, J., Teng, J., 2014. Cab45S inhibits the ER stress-induced IRE1-JNK pathway and apoptosis via GRP78/BiP. *Cell Death Dis.* 5, e1219.
- Chen, J.C., Chang, Y.W., Hong, C.C., Yu, Y.H., Su, J.L., 2012. The role of the VEGF-C/VEGFRs axis in tumor progression and therapy. *Int. J. Mol. Sci.* 14, 88–107.

- Chen, W., Sun, Z., Wang, X., Jiang, T., Huang, Z., Fang, D., Zhang, D.D., 2009. Direct interaction between Nrf2 and p21<sup>Cip1/WAF1</sup> upregulates the Nrf2-mediated antioxidant response. *Mol. cell* 34, 663–673.
- Chen, X., Ding, W.X., Ni, H.M., Gao, W., Shi, Y.H., Gambotto, A.A., Fan, J., Beg, A.A., Yin, X.M., 2007. Bid-independent mitochondrial activation in tumor necrosis factor alpha-induced apoptosis and liver injury. *Mol. Cell Biol.* 27, 541-553.
- Cheng, X., Liu, H., Jang, C.C., Fang, L., Chen, C., Zhang, X.D., Jiang, Z.W., 2014. Connecting endoplasmic reticulum stress to autophagy through IRE1/JNK/beclin-1 in breast cancer cells. *Int. J. Mol. Med.* 34, 772–781.
- Cheng, Y., Yang, J.M., 2011. Survival and death of endoplasmic-reticulum-stressed cells: Role of autophagy. *World J. Biol. Chem.* 2, 226–231.
- Choi, H.J., Fukui, M., Zhu, B.T., 2011. Role of Cyclin B1/Cdc2 Up-Regulation in the Development of Mitotic Prometaphase Arrest in Human Breast Cancer Cells Treated with Nocodazole. *PLOS ONE*.
- Choi, H.J., Zhu, B.T., 2012. Critical role of cyclin B1/Cdc2 up-regulation in the induction of mitotic prometaphase arrest in human breast cancer cells treated with 2-methoxyestradiol. *Biochim. Biophys. Acta* 1823 (8), 1306–1315.
- Choi, J.H., Lee, S.K., Lee, J.W., Kim, E.C., 2010. The role of heme oxygenase-1 in mechanical stress- and lipopolysaccharide-induced osteogenic differentiation in human periodontal ligament cells. *Angle Orthod.* 80, 552–559.
- Chuang, J.Y., Wang, Y.T., Yeh, S.H., Liu, Y.W., Chang, W.C., Hung, J.J., 2008. Phosphorylation by c-Jun NH2-terminal kinase 1 regulates the stability of transcription factor Sp1 during mitosis. *Mol. Biol. Cell* 19, 1139–1151.
- Cliby, W.A., Lewis, K.A., Lilly, K.K., Kaufmann, S.H., 2002. S phase and G<sub>2</sub> arrests induced by topoisomerase I poisons are dependent on ATR kinase function. *J. Biol. Chem.* 277, 1599–1606.
- Chung, J., Khadka, P., Chung, I.K., 2012. Nuclear import of hTERT requires a bipartite nuclear localization signal and Akt-mediated phosphorylation. *J. Cell Sci.* 125, 2684-2697.
- Corrie, P.G., Basu, B., Zaki, K.A., 2010. Targeting angiogenesis in melanoma: prospects for the future. *Ther. Adv. Med. Oncol.* 2, 367–380.
- Cortes, F., Pastor, N., 2003. Induction of endoreduplication by topoisomerase II catalytic inhibitors. *Mutagenesis* 18, 105–112.
- Curran, S., Murray, G.I., 2000. Matrix metalloproteinases: molecular aspects of their roles in tumour invasion and metastasis. *Eur. J. Cancer* 36, 1621–1630.
- Dang, C.V., 1999. C-Myc target genes involved in cell growth, apoptosis, and metabolism. *Mol. Cell. Biol.* 19, 1–11.
- Dang, C.V., Li, F., Lee, L.A., 2005. Could MYC induction of mitochondrial biogenesis be linked to ROS production and genomic instability? *Cell Cycle* 4, 1465–1466.

- Dasgupta, S., Srinidhi, S., Vishwanatha, J.K., 2012. Oncogenic activation in prostate cancer progression and metastasis: Molecular insights and future challenges. *J. Carcinog.* 11, 4.
- Dash, B.C., El-Deiry, W.S., 2005. Phosphorylation of p21 in G<sub>2</sub>/M Promotes Cyclin B-Cdc2 Kinase Activity. *Mol. Cell Biol.* 25, 3364–3387.
- De Cesare, M., Pratesi, G., Veneroni, S., Bergottini, R., Zunino, F., 2004. Efficacy of the novel camptothecin gimatecan against orthotopic and metastatic human tumor xenograft models. *Clin. Cancer Res.*, 10, 7357–7364.
- de Vries, H.E., Witte, M., Hondius, D., Rozemuller, A.J., Drukarch, B., Hoozemans, J., van Horsen, J., 2008. Nrf2-induced antioxidant protection: a promising target to counteract ROS-mediated damage in neurodegenerative disease? *Free Radic. Biol. Med.* 45, 1375–1383.
- Degli-Esposti, M.A., Dougall, W.C., Smolak, P.J., Waugh, J.Y., Smith, C.A., Goodwin, R.G., 1997. The novel receptor TRAIL-R4 induces NF- $\kappa$ B and protects against TRAIL-mediated apoptosis, yet retains an incomplete death domain. *Immunity* 7, 813–8
- Dang, C.V., 2012. *MYC* on the Path to Cancer. *Cell* 149, 22–35.
- Dasgupta, S., Srinidhi, S., Vishwanatha, J.K., 2012. Oncogenic activation in prostate cancer progression and metastasis: molecular insights and future challenges. *J. Carcinogen.* 11, 39–49.
- DeNicola, G.M., Karreth, F.A., Humpton, T.J., Gopinathan, A., Wei, C., 2011. Oncogene-induced Nrf2 transcription promotes ROS detoxification and tumorigenesis. *Nature* 475, 106–109.
- Deryugina, E.I., Quigley, J.P., Matrix metalloproteinases and tumor metastasis. *Cancer Metastasis Rev.* 25, 9–34.
- Dey, S., Tameire, F., Koumenis, C., 2013. PERK-ing up autophagy during MYC-induced tumorigenesis. *Autophagy* 9, 612–614.
- DiDonato, J.A., Mercurio, F., Karin, M., NF- $\kappa$ B and the link between inflammation and cancer. *Immunol. Rev.* 246, 379–400.
- Dotiwala, F., Eapen, V.V., Harrison, J.C., Arbel-Eden, A., Ranade, V., Yoshida, S., Haber, J.E., 2013. DNA damage checkpoint triggers autophagy to regulate the initiation of anaphase. *Proc. Natl. Acad. Sci. USA* 110, E41–E49.
- Dulić, V., Stein, G.H., Far, D.F., Reed, S.I., 1998. Nuclear accumulation of p21<sup>Cip1</sup> at the onset of mitosis: a role at the G<sub>2</sub>/M-phase transition. *Mol. Cell Biol.* 18, 546–557.
- Dumesic, P.A., Scholl, F.A., Barragan, D.I., Khavari, P.A., 2009. Erk1/2 MAP kinases are required for epidermal G<sub>2</sub>/M progression. *J. Cell Biol.* 185, 409–422.
- Dumontet, C., Jordan, M.A., 2010. Microtubule-binding agents: a dynamic field of cancer therapeutics. *Nat. Rev. Drug Discov.* 9, 790–803.
- Dunn, S.E., Hardman, R.A., Kari, F.W., Barrett, J.C., 1997. Insulin-like growth like growth factor1 (IGF-1) alters drug sensitivity of HBL 100 human breast cancer cells. By inhibition of

apoptosis induced by diverse anticancer drugs. *Cancer Res.* 57, 2687–2693.

Engelmann, D., Mayoli-Nüssle, D., Mayrhofer, C., Fürst, K., Alla, V., Stoll, A., Spitschak, A., Abshagen, K., Vollmar, B., Ran, S., Pützer, B.M., 2013. E2F1 promotes angiogenesis through the VEGF-C/VEGFR-3 axis in a feedback loop for cooperative induction of PDGF-B. *J. Mol. Cell Biol.* 5, 391–403.

Ellgaard, L., Helenius, A., 2003. Quality control in the endoplasmic reticulum. *Nat. Rev. Mol. Cell Biol.* 4, 181–191.

Farombi, E.O., Surh, Y.J., 2006. Heme oxygenase-1 as a potential therapeutic target for hepatoprotection. *J. Biochem. Mol. Biol.* 39, 479–491.

Ferguson, L.R., Chen, H., Collins, A.R., Connell, M., Damia, G., Dasgupta, S., Malhotra, M., Meeker, A.K., 2015. Genomic instability in human cancer: Molecular insights and opportunities for therapeutic attack and prevention through diet and nutrition. *Semin. Cancer Biol.* 35, Suppl:S5-S24.

Filippi-Chiela, E.C., Villodre, E.S., Zamin, L.L., Lenz, G., 2011. Autophagy interplay with apoptosis and cell cycle regulation in the growth inhibiting effect of resveratrol in glioma cells. *PLoS One* 6, e20849.

Field, J.J., Kanakkanthara, A., Miller, J.H., 2014. Microtubule-targeting agents are clinically successful due to both mitotic and interphase impairment of microtubule function. *Bioorg. Med. Chem.* 22, 5050–5059.

Foster, S.A., Morgan, D.O., 2012. The APC/C subunit Mnd2/Apc15 promotes Cdc20 autoubiquitination and spindle assembly checkpoint inactivation. *Mol. Cell* 47, 921–932.

Frank, S.R., Parisi, T., Taubert, S., Fernandez, P., Fuchs, M., Chan, H.M., Livingston, D.M., Amati, B., 2003. MYC recruits the TIP60 histone acetyltransferase complex to chromatin. *EMBO Rep.* 4, 575–580.

Fujioka, S., Sclabas, G.M., Schmidt, C., Frederick, W.A., Dong, Q.G., Abbruzzese, J.L., Evans, D.B., Baker, C., Chiao, P.J., 2003. Function of nuclear factor kappaB in pancreatic cancer metastasis. *Clin. Cancer Res.* 9, 346–354.

Ganten, T.M., Koschny, R., Haas, T.L., Sykora, J., Li-Weber, M., Herzer, K., Walczak, H., 2005. Proteasome inhibition sensitizes hepatocellular carcinoma cells, but not human hepatocytes, to TRAIL. *Hepatology* 42, 588–597.

Ganten, T.M., Koschny, R., Sykora, J., Schulze-Bergkamen, H., Büchler, P., Hass, T.L., Schader, M.B., Untergasser, A., Stremmel, W., Walczak, H., 2006. Preclinical differentiation between apparently safe and potentially hepatotoxic applications of TRAIL either alone or in combination with chemotherapeutic drugs. *Clin. Cancer Res.* 12, 2640–2646.

Garber, K., 2005. New checkpoint blockers begin human trials. *J. Natl. Cancer Inst.* 97, 1026–1028.

Gartel, A.L., Goufman, E., Najmabadi, F., Tyner, A.L., 2000. Sp1 and Sp3 activate p21 (WAF1/CIP1) gene transcription in the Caco-2 colon adenocarcinoma cell line. *Oncogene* 19, 5182–5188.

- Giorgi, C., Bonora, M., Sorrentino, G., Missiroli, S., Poletti, F., Suski, J.M., Galindo Ramirez, F., Rizzuto, R., Di Virgilio, F., Zito, E., Pandolfi, P.P., Wieckowski, M.R., Mammano, F., Del Sal, G., Pinton, P., 2015. p53 at the endoplasmic reticulum regulates apoptosis in a Ca<sup>2+</sup>-dependent manner. *Proc. Natl. Acad. Sci. USA* 112, 1779–1784.
- Gialeli, C., Theocharis, A.D., Karamanos, N.K., 2011. Roles of matrix metalloproteinases in cancer progression and their pharmacological targeting. *FEBS J.* 278, 16–27.
- Goldwasser, F., Shimizu, T., Jackman, J., Hoki, Y., O'Connor, P.M., Kohn, K.W., Pommier, Y., 1996. Correlations between S and G<sub>2</sub> arrest and the cytotoxicity of camptothecin in human colon carcinoma cells. *Cancer Res.* 56, 4430–4437.
- Gogvadze, V., Orrenius, S., Zhivotovsky, B., 2006. Multiple pathways of cytochrome *c* release from mitochondria in apoptosis. *Biochim. Biophys. Acta* 1757, 639–647.
- Gómez, D.L., Farina, H.G., Gómez, D.E., 2013. Telomerase regulation: A key to inhibition? (Review). *Int. J. Oncol.* 43, 1351–1356.
- Gregan, J., Polakova, S., Zhang, L., Tolić-Nørrelykke, I.M., Cimini, D., 2011. Merotelic kinetochore attachment: causes and effects. *Trends Cell Biol.* 21, 374–381.
- Guan, B., Yue, P., Clayman, G.L., Sun, S.Y., 2001. Evidence that the death receptor DR4 is a DNA damage-inducible, p53-regulated gene. *J. Cell. Physiol.* 188, 98–105.
- Gupta, S.C., Kim, J.H., Prasad, S., Aggarwal, B.B., 2010. Regulation of survival, proliferation, invasion, angiogenesis, and metastasis of tumor cells through modulation of inflammatory pathways by nutraceuticals. *Cancer Metastasis Rev.* 29, 405–434.
- Gutierrez, G.J., Tsuji, T., Cross, J.V., Davis, R.J., Templeton, D.J., Jiang, W., Ronai, Z.A., 2010. JNK-mediated phosphorylation of Cdc25C regulates cell cycle entry and G<sub>2</sub>/M DNA damage checkpoint. *J. Biol. Chem.* 285, 14217–14228.
- Guo, J., Wu, G., Bao, J., Hao, W., Lu, J., Chen, X., 2014. Cucurbitacin B induced ATM-mediated DNA damage causes G<sub>2</sub>/M cell cycle arrest in a ROS-dependent manner. *PLoS One* 9, e88140.
- Hahn, W.C., Meyerson, M., 2001. Telomerase activation, cellular immortalization and cancer. *Ann. Med.* 33, 123–129.
- Hammadi, M., Oulidi, A., Gackière, F., Katsogiannou, M., Slomianny, C., Roudbaraki, M., Dewailly, E., Delcourt, P., Lepage, G., Lotteau, S., Ducreux, S., Prevarskaya, N., Van Coppenolle, F., 2013. Modulation of ER stress and apoptosis by endoplasmic reticulum calcium leak via translocon during unfolded protein response: involvement of GRP78. *FASEB J.* 27, 1600–1609.
- Han, J., Back, S.H., Hur, J., Lin, Y.H., Gildersleeve, R., Shan, J., Yuan, C.L., 2013. ER stress-induced transcriptional regulation increases protein synthesis leading to cell death. *Nat. Cell Biol.* 15, 481–490.
- Hartwell, L.H., Weinert, T.A., 1989. Checkpoints: controls that ensure the order of cell cycle events. *Science* 246, 629–634.

- Hellwig, C.T., Rehm, M., 2012. TRAIL signaling and synergy mechanisms used in TRAIL-based combination therapies. *Mol. Cancer Ther.* 3, 13.
- Hetz, C., Mollereau, B., 2014. Disturbance of endoplasmic reticulum proteostasis in neurodegenerative diseases. *Nat. Rev. Neurosci.* 15, 233–249.
- Higuchi, H., Grambihler, A., Canbay, A., Bronk, S.F., Gores, G.J., 2004. Bile acids up regulate death receptor 5/TRAIL-receptor 2 expression via a c-Jun N-terminal kinase-dependent pathway involving Sp1. *J. Biol. Chem.* 279, 51–60.
- Hirota, T., Lipp, J.J., Toh, B.H., Peters, J.M., 2005. Histone H3 serine 10 phosphorylation by Aurora B causes HP1 dissociation from heterochromatin. *Nature* 438, 1176–1180.
- Huang, M., Miao, Z.H., Zhu, H., Cai, Y.J., Lu, W., Ding, J., 2008. Chk1 and Chk2 are differentially involved in homologous recombination repair and cell cycle arrest in response to DNA double-strand breaks induced by camptothecins. *Mol. Cancer Ther.* 7, 1440–1449.
- Huang, Y., Sheikh, M.S., 2007. TRAIL death receptors and cancer therapeutics. *Toxicol. Appl. Pharmacol.* 224, 284–289.
- Huang, M., Miao, Z.H., Zhu, H., Cai, Y.J., Lu, W., Ding, J., 2008. Chk1 and Chk2 are differentially involved in homologous recombination repair and cell cycle arrest response to DNA double-strand breaks induced by camptothecins. *Mol. Cancer Ther.* 7, 1440-1449.
- Idikio, H.A., 2006. Spindle Checkpoint Protein hMad2 and Histone H3 Phosphoserine 10 Mitosis Marker in Pediatric Solid Tumors. *Anticancer Res.* 26, 4687–4694.
- Indran, I.R., Hande, M.P., Pervaiz, S., 2010. hTERT overexpression alleviates intracellular ROS production, improves mitochondrial function, and inhibits ROS-mediated apoptosis in cancer cells. *Cancer Res.* 71, 266-276.
- Indran, I.R., Hande, M.P., Pervaiz, S., 2011. hTERT overexpression alleviates intracellular ROS production, improves mitochondrial function, and inhibits ROS-mediated apoptosis in cancer cells. *Cancer Res.* 71, 266-276.
- Inoue, S., MacFarlane, M., Harper, N., Wheat, L.M., Dyer, M.J., Cohen, G.M., 2004. Histone deacetylase inhibitors potentiate TNF-related apoptosis-inducing ligand (TRAIL)-induced apoptosis in lymphoid malignancies. *Cell Death Differ.* 11, S193–S206.
- Inoue, T., Kato, K., Kato, H., 2009. Asanoma K, Kuboyama A, Ueoka Y, Yamaguchi S, Ohgami T, Wake N. Level of reactive oxygen species induced by p21<sup>Waf1/Cip1</sup> is critical for the determination of cell fate. *Cancer Sci.* 100, 1275–1283.
- Iseli, T.J., Turner, N., Zeng, X.Y., Cooney, G.J., Kraegen, E.W., Yao, S., Ye, Y., James, D.E., Ye, J.M., 2013. Activation of AMPK by bitter melon triterpenoids involves CaMKK $\beta$ . *PLoS One* 8, e62309.
- Ishida, Y., Nagata, K., 2009. Autophagy eliminates a specific species of misfolded procollagen and plays a protective role in cell survival against ER stress. *Autophagy* 5, 1217–1219.

Ito, K., Takubo, K., Arai, F., Satoh, H., Matsuoka, S., Ohmura, M., Naka, K., Azuma, M., 2007. Regulation of reactive oxygen species by Atm is essential for proper response to DNA double-strand breaks in lymphocytes. *J. Immunol.* 178, 103–110.

Jameson, G.S., Hamm, J.T., Weiss, G.J., Alemany, C., Anthony, S., Basche, M., Ramanathan, R.K., Borad, M.J., Tibes, R., Cohn, A., Hinshaw, I., Jotte, R., Rosen, L.S., Hoch, U., Eldon, M.A., Medve, R., Schroeder, K., White, E., Von Hoff, D.D., 2013. A multicenter, phase I, dose-escalation study to assess the safety, tolerability, and pharmacokinetics of etirinotecan pegol in patients with refractory solid tumors. *Clin. Cancer Res.* 19, 268–278.

Jang, J.H., Lee, T.J., Yang, E.S., Min, D.S., Kim, Y.H., Kim, S.H., Choi, Y.H., Park, J.W., Choi, K.S., Kwon, T.K., 2010. Compound C sensitizes Caki renal cancer cells to TRAIL-induced apoptosis through reactive oxygen species-mediated down-regulation of c-FLIPL and Mcl-1. *Exp. Cell Res.* 316, 2194–2203.

Jang, J.Y., Kim, Y.S., 2012. Is prostate biopsy essential to diagnose prostate cancer in the older patient with extremely high prostate-specific antigen? *Korean J. Urol.* 53, 82–86.

Janknecht, R., 2004. On the road to immortality: hTERT upregulation in cancer cells. *FEBS Lett.* 564, 9–13

Jayasooriya, R.G., Choi, Y.H., Hyun, J.W., Kim, G.Y., 2014. Camptothecin sensitizes human hepatoma Hep3B cells to TRAIL-mediated apoptosis via ROS-dependent death receptor 5 upregulation with the involvement of MAPKs. *Environ. Toxicol. Pharmacol.* 38, 959–967.

Jayasooriya, R.G.P.T., Lee, Y.G., Kang, C.H., Lee, K.T., Choi, Y.H., Park, S.Y., Hwang, J.K., Kim, G.Y., 2013. Piceatannol inhibits MMP-9-dependent invasion of tumor necrosis factor- $\alpha$ -stimulated DU145 cells by suppressing the Akt-mediated nuclear factor- $\kappa$ B pathway. *Oncol. Lett.* 5, 341–347.

Jayasooriya, R.G., Park, S.R., Choi, Y.H., Hyun, J.W., Chang, W.Y., Kim, G.Y., 2015. Camptothecin suppresses expression of matrix metalloproteinase-9 and vascular endothelial growth factor in DU145 cells through PI3K/Akt-mediated inhibition of NF- $\kappa$ B activity and Nrf2-dependent induction of HO-1 expression. *Environ. Toxicol. Pharmacol.* 39, 1189–1198.

Jayasooriya, R.G., Choi, Y.H., Hyun, J.W., Kim, G.Y., 2014. Camptothecin sensitizes human hepatoma Hep3B cells to TRAIL-mediated apoptosis via ROS-dependent death receptor 5 upregulation with the involvement of MAPKs. *Environ. Toxicol. Pharmacol.* 38, 959–967.

Jayasooriya, R.G., Park, S.R., Choi, Y.H., Hyun, J.W., Chang, W.Y., Kim, G.Y., 2015. Camptothecin suppresses expression of matrix metalloproteinase-9 and vascular endothelial growth factor in DU145 cells through PI3K/Akt-mediated inhibition of NF- $\kappa$ B activity and Nrf2-dependent induction of HO-1 expression. *Environ. Toxicol. Pharmacol.* 39, 1189–1198.

Jeong, S.A., Kim, K., Lee, J.H., Cha, J.S., Khadka, P., Cho, H.S., Chung, I.K., 2015. Akt-mediated phosphorylation increases the binding affinity of hTERT for importin  $\alpha$  to promote nuclear translocation. *J. Cell Sci.* 128, 2287–2301.

Johnstone, R.W., Frew, A.J., Smyth, M.J., 2008. The TRAIL apoptotic pathway in cancer onset, progression and therapy. *Nat. Rev. Cancer* 8, 782–798.

Jordan, M.A., Wilson, L., 2004. Microtubules as a target for anticancer drugs. *Nat. Rev. Cancer* 4, 253–265.

Joyce, B.J., Tampaki, Z., Kim, K., Wek, R.C., Sullivan, W.J., 2013. The unfolded protein response in the protozoan parasite *Toxoplasma gondii* features translational and transcriptional control. *Eukaryot. Cell* 12, 979–989.

Jung, E.M., Park, J.W., Choi, K.S., Park, J.W., Lee, H.I., Lee, K.S., Kwon, T.K., 2006. Curcumin sensitizes tumor necrosis factor-related apoptosis-inducing ligand (TRAIL)-induced apoptosis through reactive oxygen species mediated upregulation of death receptor 5 (DR5). *Carcinogenesis* 27, 2008–2017.

Kagaya, S., Kitanaka, C., Noguchi, K., Mochizuki, T., Sugiyama, A., Asai, A., Yasuhara, N., Eguchi Y., Tsujimoto, Y., Kuchino, Y., 1997. A functional role for death proteases in s-Myc- and c-Myc-mediated apoptosis. *Mol. Cell. Biol* 17, 6736–6745.

Kalpper, W., Qian, W., Schulte, C., Parwaresch, R., 2003. DNA damage transiently increases TRF2 mRNA expression and telomerase activity. *Leukemia* 10, 2007–2015.

Kale, A., Gawande, S., Kotwal, S., Cancer phytotherapeutics: role for flavonoids at the cellular level. *Phytother. Res.* 22, 567–577.

Kessenbrock, K., Plaks, V., Werb, Z., 2010. Matrix metalloproteinases: regulators of the tumor microenvironment. *Cell* 141, 52–67.

Kim, M.O., Moon, D.O., Choi, Y.H., Lee, J.D., Kim, N.D., Kim, G.Y., 2008. Platycodin D induces mitotic arrest in vitro, leading to endoreduplication, inhibition of proliferation and apoptosis in leukemia cells. *Int. J. Cancer* 122, 2674–2681.

Kim, M.O., Moon, D.O., Kang, C.H., Kwon, T.K., Choi, Y.H., Kim, G.Y., 2010.  $\beta$ -Ionone enhances TRAIL-induced apoptosis in hepatocellular carcinoma cells through Sp1-dependent upregulation of DR5 and downregulation of NF- $\kappa$ B activity. *Mol. Cancer Ther.* 9, 833–843.

Kim, D.S., Jeon, B.K., Lee, Y.E., Woo, W.H., Mun, Y.J., 2012. Diosgenin induces apoptosis in HepG2 cells through generation of reactive oxygen species and mitochondrial pathway. *Evid. Based Complement Alternat. Med.* 2012, 981675.

Kim, H.S., Heo, J.I., Park, S.H., Shin, J.Y., Kang, H.J., Kim, M.J., Kim, S.C., Kim, J., Park, J.B., Lee, J.Y., 2014. Transcriptional activation of p21(WAF<sup>1</sup>/CIP<sup>1</sup>) is mediated by increased DNA binding activity and increased interaction between p53 and Sp1 via phosphorylation during replicative senescence of human embryonic fibroblasts. *Mol. Biol. Rep.* 41, 2397–2408.

Kim, Y.H., Jung, E.M., Lee, T.J., Kim, S.H., Choi, Y.H., Park, J.W., Park, J.W., Choi, K.S., Kwon, T.K., 2008. Rosiglitazone promotes tumor necrosis factor-related apoptosis-inducing ligand-induced apoptosis by reactive oxygen species-mediated up-regulation of death receptor 5 and down-regulation of c-FLIP. *Free Radic. Biol. Med.* 44, 1055–1068.

Kim, Y.K., Koo, N.Y., Yun, P.Y., 2015. Anticancer effects of CKD-602 (Camtobell<sup>®</sup>) via G2/M phase arrest in oral squamous cell carcinoma cell lines. *Oncol. Lett.* 9, 136–142.

- Kimmelman, A.C., 2011. The dynamic nature of autophagy in cancer. *Genes Dev.* 25, 1999–2010.
- Koutroulis, L., Zarros, A., Theocharis, S., 2008. The role of matrix metalloproteinases in the pathophysiology and progression of human nervous system malignancies: a chance for the development of targeted therapeutic approaches? *Expert Opin. Ther. Targets* 12, 1577–1586.
- Kovac, S., Angelova, P.R., Holmström, K.M., Zhang, Y., Kostova, A.T.D., Abramov, A.Y., 2015. Nrf2 regulates ROS production by mitochondria and NADPH oxidase. *Biochim. Biophys Acta.* 1850, 794–801.
- Kreis, N.N., Louwen, F., Yuan, J., 2015. Less understood issues: p21Cip1 in mitosis and its therapeutic potential. *Oncogene* 34, 1758–1767.
- Kurz, E.U., Douglas, P., Lees-Miller, S.P., 2004. Doxorubicin activates ATM-dependent phosphorylation of multiple downstream targets in part through the generation of reactive oxygen species. *J. Biol. Chem.* 279, 53272–53281.
- Kyo, S., Takakura, M., Fujiwara, T., Inoue, M., 2008. Understanding and exploiting hTERT promoter regulation for diagnosis and treatment of human cancers. *Cancer Sci.* 99, 1528–1538.
- Kyo, S., Takakura, M., Taira, T., Kanaya, T., Itoh, H., Yutsudo, M., Ariga, H., Inoue, M., 2000. Sp1 cooperates with c-Myc to activate transcription of the human telomerase reverse transcriptase gene (*hTERT*). *Nucleic Acids Res.* 28, 669–677.
- Kyo, S., Inoue, M., 2002. Complex regulatory mechanisms of telomerase activity in normal and cancer cells: How can we apply them for cancer therapy? *Oncogene* 21, 688–697.
- Kyo, S., Takakura, M., Taira, T., Itoh, H., Yutsudo, M., Ariga, H., Inoue, M., 2000. Sp1 cooperates with c-Myc to activate transcription of the human telomerase reverse transcriptase gene (*hTERT*). *Nucleic Acids Res.* 28, 669–677.
- Laddha, S.V., Ganesan, S., Chan, C.S., White, E., 2014. Mutational Landscape of the Essential Autophagy Gene *BECN1* in Human Cancers. *Mol. Cancer Res.* 12, 485–490.
- Lara-Gonzalez, P., Westhorpe, F.G., Taylor, S.S., 2012. The spindle assembly checkpoint. *Curr. Biol.* 22, R966–R980.
- Lee, H.J., Hwang, H.I., Jang, Y.J., 2010. Mitotic DNA damage response: Polo-like kinase-1 is dephosphorylated through ATM-Chk1 pathway. *Cell Cycle* 9, 2389–2398.
- Leone, R.D., Amaravadi, R.K., 2013. Autophagy: a targetable linchpin of cancer cell metabolism. *Trends Endocrinol. Metab.* 24, 209–217.
- Lindqvist, A., van Zon, W., Karlsson Rosenthal, C., Wolthuis, R.M., 2007. Cyclin B1-Cdk1 activation continues after centrosome separation to control mitotic progression. *PLoS Biol.* 5, e123.
- Liou, G.Y., Storz, P., 2010. Reactive oxygen species in cancer. *Free Radic. Res.* 44.
- Liu, Y., Gao, X., Deeb, D., Arbab, A.S., Gautam, S.C., 2012. Telomerase reverse transcriptase

(TERT) is a therapeutic target of oleanane triterpenoid CDDO-Me in prostate cancer. *Molecules* 17, 14795–14809.

Li, H., Liang, J., Castrillon, D.H., DePinho, R.A., Olson, E.N., Liu, Z.P., 2007. FoxO4 regulates tumor necrosis factor alpha-directed smooth muscle cell migration by activating matrix metalloproteinase 9 gene transcription. *Mol. Cell. Biol.* 27, 2676–2686.

Li, H.Y., Zhang, J., Sun, L.L., Li, B.H., Gao, H.L., Xie, T., Zhang, N., Ye, Z.M., 2015. Celastrol induces apoptosis and autophagy via the ROS/JNK signaling pathway in human osteosarcoma cells: an *in vitro* and *in vivo* study. *Cell Death Dis.*, e1604.

Li, J., Lei, H., Xu, Y., Tao, Z.Z., 2015. miR-512-5p suppresses tumor growth by targeting hTERT in telomerase positive head and neck squamous cell carcinoma *in vitro* and *in vivo*. *PLoS One* 10, e0135265.

Liang, W., Ye, D., Dai, L., Shen, Y., Xu, J., 2012. Overexpression of hTERT extends replicative capacity of human nucleus pulposus cells, and protects against serum starvation-induced apoptosis and cell cycle arrest. *J. Cell Biochem.* 113, 2112–2121.

Lin, P.Y., Fosmire, S.P., Park, S.H., Park, J.Y., Baksh, S., Modiano, J.F., Weiss, R.H., 2007. Attenuation of PTEN increases p21 stability and cytosolic localization in kidney cancer cells: a potential mechanism of apoptosis resistance. *Mol. Cancer* 6, 16.

Liu, X.P., Zhou, S.T., Li, X.Y., Chen, X.C., Zhao, X., Qian, Z.Y., Zhou, L.N., Li, Z.Y., Wang, Y.M., Zhong, Q., Yi, T., Li, Z.Y., He, X., Wei, Y.Q., 2010. Anti-tumor activity of N-trimethyl chitosan-encapsulated camptothecin in a mouse melanoma model. *J. Exp. Clin. Cancer Res.* 29, 76.

Lori, S.H., Cunningham, J.T., Datta, T., Dey, S., Tameire, F., Lehman, S.L., Qiu, B., Zhang, H., Cerniglia, G., Bi, M., Li, Y., Gao, Y., Liu, H., Li, C., Maity, A., Thomas-Tikhonenko, A., Perl, A.E., Koong, A., Fuchs, S.Y., Diehl, J.A., Mills, I.G., Ruggero, D., Koumenis, C., 2012. ER stress-mediated autophagy promotes Myc-dependent transformation and tumor growth. *J. Clin. Invest.* 122, 4621–4634.

Lossaint, G., Besnard, E., Fisher, D., Piette, J., Dulic, V., 2011. Chk1 is dispensable for G2 arrest in response to sustained DNA damage when the ATM/p53/p21 pathway is functional. *Oncogene* 30, 4261–4274.

Lü, L., Tang, D., Wang, L., Huang, L.Q., Jiang, G.S., Xiao, X.Y., Zeng, F.Q., 2012. Gambogic acid inhibits TNF- $\alpha$ -induced invasion of human prostate cancer PC3 cells *in vitro* through PI3K/Akt and NF- $\kappa$ B signaling pathways. *Acta Pharmacol. Sin.* 33, 531–541.

Lurlaro, R., Muñoz Pinedo, C., 2015. Cell death induced by endoplasmic reticulum stress. *FEBS J.* 2015 (DOI: 10.1111/febs.13598)

Macip, S., Igarashi, M., Fang, L., Chen, A., Pan, Z., Lee, S.W., Aaronson, S.A., 2002. Inhibition of p21-mediated ROS accumulation can rescue p21-induced senescence. *EMBO J.* 21, 2180–2188.

Mailand, N., Falck, J., Lukas, C., Syljuåsen, R.G., Welcker, M., Bartek, J., Lukas, J., 2000. Rapid destruction of human Cdc25A in response to DNA damage. *Science* 288, 1425–1429.

- Magnani, M., Crinelli, R., Bianchi, M., Antonelli, A., 2000. The ubiquitin-dependent proteolytic system and other potential targets for the modulation of nuclear factor- $\kappa$ B (NF- $\kappa$ B). *Curr. Drug Targets* 1, 387–399
- Mao, L., Wang H., Qiao, L., Wang, X., 2010. Disruption of Nrf2 enhances the upregulation of nuclear factor-kappaB activity, tumor necrosis factor- $\alpha$ , and matrix metalloproteinase-9 after spinal cord injury in mice. *Mediators Inflamm.* 2010, 238321.
- Martin, D., Rojo, A.I., Salinas, M., Diaz, R., Gallardo, G., Alam, J., De Galarreta, C.M., Cuadrado, A., 2004. Regulation of hemoxygenase-1 expression through the phosphatidylinositol3-kinase/Akt pathway and the Nrf2 transcription factor in response to the antioxidant phytochemical carnosol. *J. Biol. Chem.* 279, 8919–8929.
- Matthess, Y., Raab, M., Sanhaji, M., Lavrik, I.N., Strebhardt, K., 2010. Cdk1/cyclin B1 controls Fas-mediated apoptosis by regulating caspase-8 activity. *Mol. Cell. Biol.* 30, 5726–5440.
- Mazouzi, A., Velimezi, G., Loizou, J.I., 2014. DNA replication stress: Causes, resolution and disease. *Exp. Cell Res.* 329, 85–93.
- Meissner, M., Berlinski, B., Doll, M., Hrgovic, I., Laubach, V., Reichenbach, G., Kippenberger, S., Gille, J., Kaufmann, R., 2011. AP1-dependent repression of TGF $\alpha$ -mediated MMP9 upregulation by PPAR $\delta$  agonist in keratinocytes. *Exp. Dermatol.* 20, 425–429.
- Minchenko, A., Salceda, S., Bauer, T., Caro, J., 1994. Hypoxia regulatory elements of the human vascular endothelial growth factor gene. *Cell. Mol. Biol. Res.* 40, 35–39.
- Mirakabadi, A.Z., Sarzaem, A., Moradhaseli, S., Sayad, A., Negahdary, M., 2012. Necrotic effect versus apoptotic nature of camptothecin in human cervical cancer cells. *Iran. J. Cancer Prev.* 5, 109–116.
- Mittelstadt, M.L., Patel, R.C., 2012. AP-1 mediated transcriptional repression of matrix metalloproteinase-9 by recruitment of histone deacetylase 1 in response to interferon  $\beta$ . *PLoS One* 7, e42152.
- Moon, D.O., Choi, Y.H., Kim, G.Y., 2011. Role of p21 in SP600125-induced cell cycle arrest, endoreduplication, and apoptosis. *Cell Mol. Life Sci.* 68, 3249.
- Moon, M.O., Kang, S.H., Kim, K.C., Kim, M.O., Choi, Y.H., Kim, G.Y., 2010. Sulforaphane decreases viability and telomerase activity in hepatocellular carcinoma Hep3B cells through the reactive oxygen species-dependent pathway. *Cancer Lett.* 295, 260–266
- Moon, D.O., Kim, M.O., Choi, Y.H., Kim, G.Y., 2010. Butein sensitizes human hepatoma cells to TRAIL-induced apoptosis via extracellular signal-regulated kinase/Sp1-dependent DR5 upregulation and NF- $\kappa$ B inactivation. *Mol. Cancer Ther.* 9, 1583–1595.
- Muggia, F.M., Creaven, P.J., Hansen, H.H., Cohen, M.H., Selawry, O.S., 1972. Phase I clinical trial of weekly and daily treatment with camptothecin (NSC-100880): correlation with preclinical studies. *Cancer Chemother. Rep.* 56, 515–521.
- Munoz-Pinedo, C., Guio-Carrion, A., Goldstein, J.C., Fitzgerald, P., Newmeyer, D.D., Green,

D.R., 2006. Different mitochondrial intermembrane space proteins are released during apoptosis in a manner that is coordinately initiated but can vary in duration. *Proc. Natl. Acad. Sci. USA* 103, 11573–11578.

Murofushi, Y., Nagano, S., Kamizono, J., Takahashi, T., Fujiwara, H., Komiya, S., Matsuishi, T., Kosai, K., 2006. Cell cycle-specific changes in hTERT promoter activity in normal and cancerous cells in adenoviral gene therapy: a promising implication of telomerase-dependent targeted cancer gene therapy. *Int. J. Oncol.* 29, 681–688.

Musacchio, A., 2015. The molecular biology of spindle assembly checkpoint signaling dynamics. *Curr. Biol.* 25, R1002–R1018.

An important role for CDK2 in G1 to S checkpoint activation and DNA damage response in human embryonic stem cells. *stem cells* 29, 651–659.

Naka, K., Tachibana, A., Ikeda, K., Motoyama, N., 2004. Stress-induced premature senescence in hTERT-expressing ataxia telangiectasia fibroblasts. *J. Biol. Chem.* 279, 2030–2037.

Neufeld, G., Cohen, T., Gengrinovitch, S., Poltorak, Z., 1999. Vascular endothelial growth factor (VEGF) and its receptors. *FASEB J.* 13, 9–22.

Newshean, S., Yang, E.S., 2012. The intersection between DNA damage response and cell death pathways. *Exp. Oncol.* 34, 243–254.

Oulton, R., Harrington, L., 2000. Telomeres, telomerase, and cancer: life on the edge of genomic stability. *Curr. Opin. Oncol.* 12, 74–81.

Palacios, C., Yerbes, R., López-Rivas, A., 2006. Flavopiridol induces cellular FLICE-inhibitory protein degradation by the proteasome and promotes TRAIL-induced early signaling and apoptosis in breast tumor cells. *Cancer Res.* 66, 8858–8869.

Pan, P., Li, Y., Yu, H., Sun, H., Hou, T., 2013. Molecular principle of topotecan resistance by topoisomerase I mutations through molecular modeling approaches. *J. Chem. Inf. Model.* 53, 997–1006.

Park, D.S., Morris, E.J., Greene, L.A., Geller, H.M., 1997. G<sub>1</sub>/S cell cycle blockers and inhibitors of cyclin-dependent kinases suppress camptothecin-induced neuronal apoptosis. *J. Neurosci.* 17, 1256–1270.

Parrish, A.B., Freel, C.D., Kornbluth, S., 2013. Cellular mechanisms controlling caspase activation and function. *Cold Spring Harb. Perspect. Biol.* 5, 1–24.

Perez-Soler, R., Fossella, F.V., Glisson, B.S., Lee, J.S., Murphy, W.K., Shin, D.W., Kemp, B.L., Lee, J.J., Kane, J., Robinson, R.A., Lippman, S.M., Kurie, J.M., Huber, M.H., Raber, M.N., Hong, W.K., 1996. Phase II study of topotecan in patients with advanced non-small-cell lung cancer previously untreated with chemotherapy. *J. Clin. Oncol.* 14, 503–513.

Pfisterer, S.G., Mauthe, M., Codogno, P., Proikas-Cezanne, T., 2011. Ca<sup>2+</sup>/calmodulin-dependent kinase (CaMK) signaling via CaMKI and AMP-activated protein kinase contributes to the regulation of WIPI-1 at the onset of autophagy. *Mol. Pharmacol.* 80, 1066–1075.

- Phan, L.M., Yeung, S.J., Lee, M., 2014. Cancer metabolic reprogramming: importance, main features, and potentials for precise targeted anti-cancer therapies. *Cancer Biol. Med.* 11, 1–19.
- Piccolo, M.T., Crispi, S., 2012. The dual role played by p21 may influence the apoptotic or anti-apoptotic fate in cancer. *J. Cancer Res.* 1, 189–202.
- Pommier, Y., 2006. Topoisomerase I inhibitors: camptothecins and beyond. *Nat. Rev. Cancer* 6, 789–802.
- Pommier, Y., Barcelo, J., Rao, V.A., Sordet, O., Jobson, A.G., Thibaut, L., Miao, Z., Seiler, J., 2006. Repair of Topoisomerase I-Mediated DNA Damage. *Prog. Nucleic Acid Res. Mol. Biol.* 81, 179–229.
- Potmesil, M., Vardeman, D., Kozielski, A.J., Mendoza, J., Stehlin, J.S., Giovanella, B.C., 1995. Growth inhibition of human cancer metastases by camptothecins in newly developed xenograft models. *Cancer Res.* 55, 5637–5641.
- Rafiee, P., Heidemann, J., Ogawa, H., Johnson, N.A., Fisher, P.J., Li, M.S., Otterson, M.F., Johnson, C.P., Binion, D.G., 2004. Cyclosporin A differentially inhibits multiple steps in VEGF induced angiogenesis in human microvascular endothelial cells through altered intracellular signaling. *Cell Commun. Signal.* 2, 3.
- Ramos, S., 2007. Effects of dietary flavonoids on apoptotic pathways related to cancer chemoprevention. *Nutr. Biochem.* 18, 427–442.
- Ravi, R., Bedi, G.C., Engstrom, L.W., Zeng, Q., Mookerjee, B., Gélinas, C., Fuchs, E.J., Bedi, A., 2001. Regulation of death receptor expression and TRAIL/Apo2L-induced apoptosis by NF- $\kappa$ B. *Nat. Cell Biol.* 3, 409–416.
- Reed, J.C., 2000. Mechanisms of apoptosis. *Am. J. Pathol.* 157, 1415–1430.
- Reddy, N.M., Kleeberger, S.R., Kensier, T.W., Yamamoto, M., Hassoun, P.M., Reddy, S.P., 2009. Disruption of Nrf2 impairs the resolution of hyperoxia-induced acute lung injury and inflammation in mice. *J. Immunol.* 182, 7264–7271.
- Ribas, V.T., Goncalves, B.S., Linden, R., Chiarini, 2012. Activation of c-Jun N-terminal kinase (JNK) during mitosis in retinal progenitor cells. *PLoS One* 7, e34483.
- Risau, W., 1997. Mechanisms of angiogenesis. *Nature* 386, 671–674.
- Roberts, N.J., Zhou, S., Diaz, L.A. Jr., Holdhoff, M., 2011. Systemic use of tumor necrosis factor alpha as an anticancer agent. *Oncotarget* 2, 739–751.
- Romaniuk, A., Kopczyński, P., Ksiazek, K., Rubis, B., 2014. Telomerase modulation in therapeutic approach. *Curr. Pharm. Des.* 20:6438–6451.
- Rousseau, D., Cannella, D., Boulaire, J., Fitzgerald, P., Fotedar, A., Fotedar, R., 1999. Growth inhibition by CDK-cyclin and PCNA binding domains of p21 occurs by distinct mechanisms and is regulated by ubiquitin-proteasome pathway. *Oncogene* 18, 3290–3302.

- Saitoh, S., Ishii, K., Kobayashi, Y., Takahashi, K., 2005. Spindle checkpoint signaling requires the mis6 kinetochore subcomplex, which interacts with mad2 and mitotic spindles. *Mol. Biol. Cell* 16, 3666–3677.
- Saretzki, G., von Zglinicki, T., 2003. Telomerase as a promising target for human cancer gene therapy. *Drugs Today (Brac)* 39, 265–276.
- Scapagnini, G., Vasto, S., Abraham, N.G., Caruso, C., Zella, D., Fabio, G., 2011. Modulation of Nrf2/ARE pathway by food polyphenols: a nutritional neuroprotective strategy for cognitive and neurodegenerative disorders. *Mol. Neurobiol.* 44, 192–201.
- Sen, N., Das, B.B., Ganguly, A., Mukherjee, T., Bandyopadhyay, S., Majumder, H.K., 2004. Camptothecin-induced imbalance in intracellular cation homeostasis regulates programmed cell death in unicellular hemoflagellate *Leishmania donovani*. *J. Biol. Chem.* 279, 52366–52375.
- Sharma, P.S., Sharma, R., Tyagi, T., VEGF/VEGFR pathway inhibitors as anti-angiogenic agents: present and future. *Curr. Cancer Drug Targets* 11, 624–653.
- Sheikh, M.S., Burns, T.F., Huang, Y., Wu, G.S., Amundson, S., Brooks, K.S., Formace, A.J. Jr., el-Deiry, W.S., 1998. p53-dependent and -independent regulation of the death receptor KILLER/DR5 gene expression in response to genotoxic stress and tumor necrosis factor. *Cancer Res.* 58, 1593–1598.
- Shen, Y., Yang, J., Zhao, J., Xiao, C., Xiang, Y., 2015. The switch from ER stress-induced apoptosis to autophagy via ROS-mediated JNK/p62 signals: A survival mechanism in methotrexate-resistant choriocarcinoma cells. *Exp. Cell Res.* 334, 207–218.
- Shay, J.W., Wright, W.E., 2006. Telomerase therapeutics for cancer: challenges and new directions. *Rev. Drug Discov.* 5, 577–584.
- Shay, J.W., Wright, W.E., 2010. Telomeres and telomerase in normal and cancer stem cells. *FEBS Lett.* 584, 3819–3825.
- Shiozaki, E.N., Chai, J., Shi, Y., 2002. Oligomerization and activation of caspase-9, induced by Apaf-1 CARD. *Proc. Natl. Acad. Sci. USA* 99, 4197–4202.
- Spano, D., Heck, C., De Antonellis, P., Christofori, G., Christofori, G., Zollo, M., 2012. Molecular networks that regulate cancer metastasis. *Semin. Cancer Biol.* 22, 234–249.
- Srivastava, R.K., 2001. TRAIL/Apo-2L: mechanisms and clinical applications in cancer. *Neoplasia* 3, 535–546.
- Stewart, A.F., Schütz, G., 1987. Camptothecin-induced *in vivo* topoisomerase I cleavages in the transcriptionally active tyrosine aminotransferase gene. *Cell* 50, 1109–1117.
- Stolz, A., Ertych, N., Bastians, H., 2011. Tumor suppressor CHK2: regulator of DNA damage response and mediator of chromosomal stability. *Clin Cancer Res* 17, 401–405.
- Stanford, J.S., Ruderman, J.V., 2005. Changes in regulatory phosphorylation of Cdc25C Ser287 and Wee1 Ser549 during normal cell cycle progression and checkpoint arrests. *Mol. Biol. Cell.* 16, 5749–5760.

- Strumberg, D., Pilon, A.A., Smith, M., Hickey, R., Malkas, L., Pommier, Y., 2000. Conversion of topoisomerase I cleavage complexes on the leading strand of ribosomal DNA into 5'-phosphorylated DNA double-strand breaks by replication runoff. *Mol. Cell. Biol.* 20, 3977–3987.
- Sui, X., Chen, R., Wang, Z., Huang, Z., Kong, N., 2013. Autophagy and chemotherapy resistance: a promising therapeutic target for cancer treatment. *Cell death dis.* 4, e838.
- Sun, M., Zhang, J., Liu, S., Liu, Y., Zheng, D., 2008. Sp1 is involved in 8-chloro-adenosine-upregulated death receptor 5 expression in human hepatoma cells. *Oncol. Rep.* 19, 177–185.
- Swift, L.H., Golsteyn, R.M., 2014. Genotoxic anti-cancer agents and their relationship to DNA damage, mitosis, and checkpoint adaptation in proliferating cancer cells. *Int. J. Mol. Sci.* 15, 3403–3431.
- Tabas, I., Ron, D., 2011. Integrating the mechanisms of apoptosis induced by endoplasmic reticulum stress. *Nat. Cell Biol.*, 13, 184–190.
- Teske, B.F., Wek, S.A., Bunpo, P., Cundiff, J.K., McClintick, J.N., Anthony, T.G., Wek, R.C., 2011. The eIF2 kinase PERK and the integrated stress response facilitate activation of ATF6 during endoplasmic reticulum stress. *Mol. Biol. Cell* 22, 4390–4405.
- Tian, W., Li, B., Warrington, R., Tomchick, D.R., Yu, H., Luo, X., 2012. Structural analysis of human Cdc20 supports multisite degron recognition by APC/C. *Proc. Natl. Acad. Sci. U S A* 109, 18419–18424.
- Tischer, E., Mitchell, R., Hartman, T., Silva, M., Gospodarowicz, D., Fiddes, J.C., Abraham, J.A., 1991. The human gene for vascular endothelial growth factor. Multiple protein forms are encoded through alternative exon splicing. *J. Biol. Chem.* 266, 11947–11854.
- Tomlinson, R.L., Ziegler, T.D., Supakorndej, T., Terns, R.M., Terns, M.P., 2006. Cell cycle-regulated trafficking of human telomerase to telomeres. *MolBiol Cell* 17, 955–965.
- Truneh, A., Sharma, S., Silverman, C., Khandekar, S., Reddy, M.P., Deen, K.C., McLaughlin, M.M., Srinvasula, S.M., Livi, G.P., Marshall, L.A., Alnemri, E.S., Williams, W.V., Doyle, M.L., 2000. Temperature-sensitive differential affinity of TRAIL for its receptors. DR5 is the highest affinity receptor. *J. Biol. Chem.* 275, 23319–23325.
- Tsimberidou, A.M., Takimoto C.H., Moulder, S., Uehara, C., Mita, M., Mita, A., Urban, P., Tan, E., Wang, Y., Vining, D., Kurzrock, R., 2011. Effects of patupilone on the pharmacokinetics and pharmacodynamics of warfarin in patients with advanced malignancies: a phase I clinical trial. *Mol. Cancer Ther.* 10, 209–217.
- Tyagi, A., Singh, R.P., Agarwal, C., Siriwardana, S., Sclafani, R.A., Agarwal, R., 2005. Resveratrol causes Cdc2-tyr15 phosphorylation via ATM/ATR-Chk1/2-Cdc25C pathways as a central mechanism for S phase arrest in human ovarian carcinoma Ovar-3 cells. *Carcinogenesis* 26, 1978–1987.
- Tufekci, K.U., Bayin, E.C., Genc. S., Genc. K., 2011. The Nrf2/ARE pathway: A promising target to counteract mitochondrial dysfunction in Parkinson's disease. *Parkinsons Dis.* 2011, 314082.

- Uttara, B., Singh, A.V., Zamboni, P., Mahajan, R.T., 2009. Oxidative stress and neurodegenerative diseases: a review of upstream and downstream antioxidant antioxidant therapeutic options. *Curr. Neuropharmacol.* 7, 65–74.
- Vafa, O., Wade, M., Kern, S., Beeche, M., Pandita, T.K., Hampton, G.M., Wahl, G.M., 2002. c-Myc can induce DNA damage, increase reactive oxygen species, and mitigate p53 function: a mechanism for oncogene-induced genetic instability. *Mol. Cell* 9, 1031–1044.
- Vicente, A.M., Guillén, M.I., Habib, A., Alcaraz, M.J., 2003. Beneficial effects of heme oxygenase-1 up-regulation in the development of experimental inflammation induced by zymosan. *J. Pharmacol. Exp. Ther.*, 307, 1030–1037.
- Walczak, H., Miller, R.E., Ariail, K., Gliniak, B., Griffith, T.S., Kubin, M., Chin, W., Jones, J., Woodward, A., Le, T., Smith, C., Smolak, P., Goodwin, R.G., Rauch, C.T., Schuh, J.C., Lynch, D.H., 1999. Tumorcidal activity of tumor necrosis factor-related apoptosis-inducing ligand *in vivo*. *Nat. Med.* 5, 157–163.
- Wall, M. E., Wani, M.C., Natschke, S.M., Nicholas, A.W., 1986. Plant antitumor agents. 22. Isolation of 11-hydroxycamptothecin from *Camptotheca acuminata* Decne: total synthesis and biological activity. *Med. Chem.* 29, 1553–1555.
- Walter, P., Ron, D., 2011. The unfolded protein response: from stress pathway to homeostatic regulation. *Science* 334, 1081–1086.
- Wang, L.M., Li, Q.Y., Zu, Y.G., Fu, Y.J., Chen, L.Y., Lv, H.Y., Yao, L.P., Jiang, S.G., 2008. Anti-proliferative and pro-apoptotic effect of CPT13, a novel camptothecin analog, on human colon cancer HCT8 cell line. *Chem. Biol. Interact.*, 176, 165–172.
- Wang, Y., Jin, F., Higgins, R., McKnight, K., 2014. The current view for the silencing of the spindle assembly checkpoint. *Cell Cycle* 13, 1694–1701.
- Wang, Z., Wang, N., Han, S., Wang, D., Mo, S., Yu, L., Huang, H., Tsui, K., Shen, J., Chen, J., 2013. Dietary compound isoliquiritigenin inhibits breast cancer neoangiogenesis via VEGF/VEGFR-2 signaling pathway. *PLoS One* 8, e68566.
- Wang, J.C., 2002. Cellular roles of DNA topoisomerases: a molecular perspective. *Nat. Rev. Mol. Cell. Biol.* 3, 430–440.
- Wang, S.H., Shih, Y.L., Ko, W.C., Wei, Y.H., Shih, C.M., 2008. Cadmium-induced autophagy and apoptosis are mediated by a calcium signaling pathway. *Cell Mol. Life Sci.* 65, 3640–3652.
- West, R.J.H., Sweeney, S.T., 2012. Oxidative stress and autophagy: Mediators of synapse growth? *Autophagy* 8, 284–285.
- Wong, H.W., Shaukat, Z., Wang, J., Saint, R., Gregory, S.L., 2014. JNK signaling is needed to tolerate chromosomal instability. *Cell Cycle* 13, 622–631.
- Wojtyla, A., Gladych, M., Rubis, B., 2011. Human telomerase activity regulation. *Mol. Biol. Rep.* 38, 3339–3349.
- Wu, N., Wu, X.W., Agama, K., Pommier, Y., Du, J., Li, D., Gu, L.Q., Huang, Z.S., An, L.K.

2010. A novel DNA topoisomerase I inhibitor with different mechanism from camptothecin induces G<sub>2</sub>/M phase cell cycle arrest to K562 cells. *Biochemistry* 49, 10131–10136.
- Xiao, Z., Chen, Z., Gunasekara, A.H., Sowin, T.J., Rosenberg, S.H., Fesik, S., Zhang, H., 2003. Chk1 mediates S and G<sub>2</sub> arrests through Cdc25A degradation in response to DNA damaging agents. *J. Bio. Chem.* 278, 21767–21773.
- Xu, C., Bailly-Maitre, B., Reed, J.C., 2005. Endoplasmic reticulum stress: cell life and death decisions. *J. Clin. Invest.* 115, 2656–2664.
- Xue, Y., Li, L., Zhang, D., Wu, K., Guo, P., Zeng, J., Wang, X.Y., He, D., 2010. Telomerase suppression initiates PML-dependent p53 activation to inhibit bladder cancer cell growth. *Onco. Rep.* 24, 1551–1559.
- Yang, Z.J., Chee, C.E., Huang, S., Sinicrope, F.A., 2011. The Role of Autophagy in Cancer: Therapeutic Implications. *Mol. Cancer Ther.* 10, 1533–1541.
- Yin, X., Sun, H., Yu, D., Liang, Y., Yuan, Z., Ge, Y., 2013. Hydroxycamptothecin induces apoptosis of human tenon's capsule fibroblasts by activating the PERK signaling pathway. *Invest. Ophthalmol. Vis. Sci.* 54, 4749–4758.
- Yin, Y., Liu, Q., Wang, B., Chen, G., Xu, L., Zhou, H., 2012. Expression and function of heme oxygenase-1 in human gastric cancer. *Exp. Biol. Med.* 237, 362–371.
- Yu, H., Huang, J., Wang, S., Zhao, G., Jiao, X., Zhu, L., 2013. Overexpression of Smad7 suppressed ROS/MMP9-dependent collagen synthesis through regulation of heme oxygenase-1. *Mol. Biol. Rep.* 40, 5307–5314.
- Yun, M., Han, Y.H., Yoon, S.H., Kim, H.Y., Kim, B.Y., Ju, Y.J., Kang, C.M., Jang, S.H., 2009. p31comet Induces cellular senescence through p21 accumulation and Mad2 disruption. *Mol. Cancer Res.* 7, 371–382.
- Yu, S., Shen, G., Khor, T.O., Kim, J.H., Kong, A.N., 2008. Curcumin inhibits Akt/mTOR signaling through protein phosphatase-dependent mechanism. *Mol. Cancer Ther.* 7, 2609–2620.
- Zeng, X., Sigoillot, F., Gaur, S., Choi, S., Pfaff, K.L., Oh, D.C., Hathaway, N., Dimova, N., Cuny, G.D., King, R.W., 2010. Pharmacologic inhibition of the anaphase-promoting complex induces a spindle checkpoint-dependent mitotic arrest in the absence of spindle damage. *Cancer Cell* 18, 382–395.
- Zeng, C.W., Zhang, X.J., Lin, K.Y., Ye, H., Feng, S.Y., Zhang, H., Chen, Y.Q., 2012. Camptothecin induces apoptosis in cancer cells via microRNA-125b-mediated mitochondrial pathways. *Mol. Pharmacol.* 81, 578–586.
- Zhang, J., Chiu, J., Zhang, H., Qi, T., Tang, Q., Ma, K., Lu, H., Li, G., 2013. Autophagic cell death induced by resveratrol depends on the Ca<sup>2+</sup>/AMPK/mTOR pathway in A549 cells. *Biochem. Pharmacol.* 86, 317–328.
- Zhang, P.H., Zou, L., Tu, Z.G., 2006. RNAi-hTERT inhibition hepatocellular carcinoma cell proliferation via decreasing telomerase activity. *J. Surg. Res.* 131, 143–149.

- Zhang, J.W., Zhang, S.S., Song, J.R., Sun, K., Zong, C., Zhao, Q.D., Liu, W.T., Li, R., Wu M.C., Wei, L.X., 2014. Autophagy inhibition switches low-dose camptothecin-induced premature senescence to apoptosis in human colorectal cancer cells. *Biochem. Pharmacol.* 90, 265–275.
- Zhang, Z., Miao, L., Lv, C., Sun, H., Wei, S., Wang, B., Huang, C., Jiao, B., 2013. Wentilactone B induces G<sub>2</sub>/M phase arrest and apoptosis via the Ras/Raf/MAPK signaling pathway in human hepatoma SMMC-7721 cells. *Cell Death Dis.* 4, e657.
- Zhao, Y., Cheng, D., Wang, S., Zhu, J., 2014. Dual roles of c-Myc in the regulation of *hTERT* gene. *Nucleic Acids Res.* 42, 10385–10398.
- Zhou, J., Yao, J., Joshi, H.C., 2002. Attachment and tension in the spindle assembly checkpoint. *J. Cell Sci.* 115, 3547–3555.
- Zhou, L., Du, L., Chen, X., Li, X., Li, Z., Wen, Y., Li, Z., He, X., Wei, Y., Zhao, X., Qian, Z., 2010. The antitumor and antimetastatic effects of *N*-trimethyl chitosan-encapsulated camptothecin on ovarian cancer with minimal side effects. *Oncol. Rep.* 24, 941–948.
- Zhou, Y.Y., Li, Y., Jiang, W.Q., Zhou, L.F., 2015. MAPK/JNK signalling: a potential autophagy regulation pathway. *Biosci. Rep.* 35, e00199.
- Zhou, H., Shen, T., Shang, C., Luo, Y., Liu, L., Yan, J., Li, Y., Huang, S., 2014. Ciclopirox induces autophagy through reactive oxygen species-mediated activation of JNK signaling pathway. *Oncotarget* 5, 10140–10150.
- Zhu, H.Y., Chao, L., Bai, W.D., Su, L.L., Liu, J.Q., Li, Y., Shi, J.H., 2014. MicroRNA-21 regulates hTERT via PTEN in hypertrophic scar fibroblasts. *PLoS One* 9, e97114.
- Zucker, S., Vacirca, J., 2004. Role of matrix metalloproteinases (MMPs) in colorectal cancer. *Cancer Metastasis Rev.* 23, 101–117.
- Zuco, V., Benedetti, V., Zunino, F., 2010. ATM- and ATR-mediated response to DNA damage induced by a novel camptothecin, ST1968. *Cancer Lett.* 292, 186–196.